DEVELOPMENT OF CELL VOLUME-REGULATORY MECHANISMS DURING OOCYTE GROWTH AND MEIOTIC MATURATION

SAMANTHA RICHARD

This thesis is submitted to the Faculty of Graduate and Postdoctoral Studies as a partial fulfillment of the Ph.D. program in Cellular and Molecular Medicine.

Department of Cellular and Molecular Medicine
Faculty of Medicine
University of Ottawa

ABSTRACT

The ability of oocytes and early cleavage-stage embryos to regulate their volume is essential to avoid developmental arrests at *in vivo*-osmolarities. This is accomplished primarily via GLYT1-mediated glycine transport into the cells. GLYT1 activity has previously been shown to be absent in freshly isolated oocytes but becomes activated ~3-4 hours after oocyte maturation has been initiated either by isolation from ovarian follicles *in vitro* or following an ovulatory stimulus *in vivo*. GLYT1 activity then persists until the 4-cell stage of preimplantation embryo development. GLYT1 has been shown to spontaneously activate in oocytes that are isolated from follicles either as denuded oocytes or as cumulus-oocyte complexes (COCs), this implies that GLYT1 activity is suppressed in intact follicles in the ovary. However, it is not known how GLYT1 activity is suppressed within the ovarian follicle or how initial GLYT1 activation occurs. The activation of independent cell volume regulation in oocytes first involves the release of the strong adhesion between the oocyte and zona pellucida (ZP) followed by secondary GLYT1 activation. These two processes have been shown to occur spontaneously in fully grown oocytes following isolation from ovarian follicles, however, it is not known whether small growing oocytes within ovarian follicles already possess the ability to detach from the ZP and activate GLYT1.

An osmotic assay was used to determine when during oogenesis oocytes are first able to detach from the ZP while the ability to activate GLYT1 was determined by measuring [^{3}H]-glycine uptake into oocytes. I found that oocytes acquire the ability to detach from the ZP when they are nearly fully grown and similarly, that high levels of

GLYT1 activity first develop in isolated oocytes during the late stages of oogenesis. Furthermore, I showed that SLC6A9 protein (GLYT1 transporter protein) and *Slc6a9a* transcripts steadily increased during oogenesis with SLC6A9 protein becoming localized to the oocyte plasma membrane during oocyte growth with predominant membrane localization apparent in fully grown oocytes. Taken together, these results suggest that oocytes become able to detach from the ZP and fully activate GLYT1 towards the end of oogenesis but that these processes remain suppressed in the ovarian follicle.

Intact and punctured antral follicles were used as a model to examine the potential mechanism(s) mediating GLYT1 suppression before ovulation is triggered. Using these models, I found that GLYT1 activity remains suppressed within preovulatory antral follicles in contrast to the spontaneous GLYT1 activation that occurred in isolated denuded oocytes or within COCs. Recently, the mechanism mediating oocyte maintenance of prophase I arrest within the ovarian follicle was elucidated and was shown to depend on the release of Natriuretic Peptide Precursor C (NPPC) from mural granulosa cells (MGCs) into follicular fluid which binds to NPR2 guanylate cyclases on cumulus cells stimulating the production of cyclic GMP (cGMP) within these cells. Diffusion of cGMP from cumulus granulosa cells to the oocyte via gap junctions is required to maintain meiotic arrest. Although GLYT1 activation and meiotic resumption are both suppressed in antral follicles prior to the ovulatory trigger and these two processes occur simultaneously following oocyte isolation from ovaries, I have shown here that GLYT1 suppression within the preovulatory antral follicle is mediated by a mechanism distinct from the gap junction-dependent NPPC-cGMP pathway controlling meiotic arrest. I also showed for the first time a direct requirement for meiotic arrest of both gap junctions between granulosa cells

(composed of connexin-43) and between the inner layer of cumulus granulosa cells and the oocyte (composed of connexin-37).

Since I showed that GLYT1 was suppressed in isolated antral follicles but not COCs, I hypothesized that MGCs are required to maintain low GLYT1 activity in antral follicles. I showed here that MGCs isolated from preovulatory antral follicles were sufficient to maintain GLYT1 suppression in co-cultured COCs, but not denuded oocytes. Furthermore, I found that GLYT1 activity was suppressed in COCs cultured in conditioned medium from MGC cultures. Thus, GLYT1 activity appears to be suppressed within the ovary prior to the ovulatory LH-stimulus likely by an unidentified inhibitory signal within the ovarian follicle originating from the MGCs and propagated by a gap junction-independent mechanism involving multiple cell types in the follicle.

TABLE OF CONTENTS

LIST OF FIGURES

LIST OF TABLES

LIST OF ABBREVIATIONS

AC: Adenylyl Cyclase

ADB: Antibody Dilution Buffer

ADI: Alpha Diagnostics

AGA: 18α-Glycyrrhetinic Acid

ANOVA: Analysis of Variance

AR: Aldose Reductase

ART: Assisted Reproductive Technologies

ATP: Adenosine Triphosphate

BGT1: Betaine Transporter

BMP15: Bone Morphogenetic Protein 15

BSA: Bovine Serum Albumin

cAMP: Cyclic Adenosine Monophosphate

CDK: cyclin-dependent kinase

cDNA: Complementary Deoxyribonucleic Acid

CFCS: Consensus Furin Cleavage Site

cGMP: Cyclic Guanosine Monophosphate

CHDH: Choline Dehydrogenase

CMP: Connexin-Mimetic Peptide

CNS: Central Nervous System

COC: Cumulus-Oocyte-Complex

CPM: Counts per Minute

CTP: C-Terminal Propeptide

Cx: Connexin

dbcAMP: dibutyryl cyclic Adenosine Monophosphate

DMSO: Dimethyl Sulfoxide

DNA: Deoxyribonucleic Acid

DNAse: Deoxyribonuclease

E_2: Estradiol

eCG: Equine Chorionic Gonadotropin

ECM: Extracellular Matrix

EDTA: Ethylenediaminetetraacetic Acid

EGF: Epidermal Growth Factor

EGFR: Epidermal Growth Factor Receptor

EHP: External Hydrophobic Patch

EHS Matrix: Matrix isolated from Engelbreth-Holm-Swarm (EHS) mouse tumor

EM: Extracellular Matrix Components

FBS: Fetal Bovine Serum

FGF: Fibroblast Growth Factor

fmole: Femtomole

FRET: Forster Resonance Energy Transfer

FSH: Follicle Stimulating Hormone

G: Gauge

GAPDH: Glyceraldehyde 3-Phosphate Dehydrogenase

GC: Granulosa Cells

GDF9: Growth Differentiation Factor 9

GFR: Growth Factor Reduced

GLYT1: Glycine Transporter 1

GLYT2: Glycine Transporter 2

GMP: Guanosine Monophosphate

GPR: G-Protein Coupled Receptor

GTP: Guanosine Triphosphate

GV: Germinal Vesicle

GVBD: Germinal Vesicle Breakdown

HA: Hyaluronic Acid

hCG: Human Chorionic Gonadotropin

HEPES: 4-(2-hydroxyethyl)-1-piperazineethane-sulfonic acid

ICM: Inner Cell Mass

IGF-1:Insulin-Like Growth Factor 1

IgG: Immunoglobulin G

IHP: Internal Hydrophobic Patch

IMP: Inosine Monophosphate

i.p.: Intraperitoneally

IU: International Units

IVF: In Vitro Fertilization

IVM: In Vitro Maturation

JAK2: Janus Kinase 2

KCC: K^+/Cl^- Co-Transporters

KITLG: KIT Ligand

KRB: Krebs-Ringer Bicarbonate

KSOM = K^+-Supplemented Optimized Medium

LH: Luteinizing Hormone

MAPK: Mitogen-Activated Protein Kinase

MEM: Minimum Essential Medium

MGC(s): Mural Granulosa Cell(s)

MI: Meiosis I

MII: Meiosis II

mKSOM: Modified K^+-Supplemented Optimized Medium

MPF: Maturation (M-phase) Promoting Factor

NGS: Normal Goat Serum

NHE: Na^+/H^+ Exchanger

NKCC: $Na^+/K^+/2Cl^-$ Co-Transporters

NMDA: N-Methyl-D-Aspartate

NMDAR: N-Methyl-D-Aspartate Receptor

NPPC (or CNP): Natriuretic Peptide Precursor C

NPR2: Natriuretic Peptide Receptor 2

NTS: N-Terminal Subdomain

NTT: Neurotransmitter Transporter

OHSS: Ovarian Hyperstimulation Syndrome

OOX: oocytectomized COC

OSF: Oocyte-Secreted Factor

P5-P21: Post-Natal Day 5-21

PBS: Phosphate-Buffered Saline

PCOS: Polycystic Ovarian Syndrome

PDE: Phosphodiesterase

PDGF: Platelet-Derived Growth Factor

PFA: Paraformaldehyde

PFK: Phosphofructokinase

PI3K: Phosphoinositide 3-Kinase

PKA: Protein Kinase A

PKC: Protein Kinase C

PMSF: Phenylmethylsulphonyl Fluoride

PN: Pronucleus or Pronuclei

PVA: Polyvinyl Alcohol

PVS: Pervitelline Space

RIPA Buffer: Radioimmunoprecipitation Assay Buffer

RNA: Ribonucleic Acid

RTK: Receptor Tyrosine Kinase

RT-PCR: Reverse-Transcribed Polymerase Chain Reaction

RVD: Regulatory Volume Decrease

RVI: Regulatory Volume Increase

ScrCMP: Scrambled Connexin-Mimetic Peptide

SDS: Sodium Dodecyl Sulfate

SDS-PAGE: Sodium Dodecyl Sulfate Polyacrylamide Gel Electrophoresis

SEM: Standard Error of the Mean

SMIT: Na+/Myo-Inositol Transporter

SNARE: Soluble NSF Attachment Protein

TAUT: Taurine/β-Amino Acid Transporter

TBS: Tris-Buffered Saline

TEM: Transmission Electron Microscopy

TGFβ: Transforming Growth Factor β

TMD: Transmembrane Domain

TonE: Tonicity-Responsive Enhancer

TonEBP: Tonicity Enhancer Binding Protein

TZPs: Transzonal Processes

UV: Ultraviolet

VRAC: Volume-Regulated Anion Channel

VSOAC: Volume-Sensitive Organic Osmolyte and Anion Channels

WGA: Wheat Germ Agglutinin

ZP: Zona Pellucida

ZPD: Zona Pellucida Domain

ACKNOWLEDGEMENTS

The work presented in this thesis was performed under the supervision of Dr. Jay M Baltz (Department of Cellular and Molecular Medicine, University of Ottawa, Ottawa Hospital Research Institute, Chronic Disease Program, Obstetrics and Gynecology). I would like to sincerely thank Dr. Baltz for his continued support during the course of my PhD and for always encouraging me to strive for academic excellence. Dr. Baltz has been an exceptional mentor throughout my graduate studies and I could not have completed this graduate degree without his endless patience, immense knowledge, and general support during both high and low points of academic study. I am so grateful for his guidance during the writing of this thesis and hope to have the pleasure of working with him sometime in my future career.

I would also like to thank the members of my Thesis Advisory Committee: Dr. Barbara Vanderhyden (Department of Cellular and Molecular Medicine, University of Ottawa, Ottawa Hospital Research Institute, Cancer Therapeutics Program), Dr. Christopher Kennedy (Department of Cellular and Molecular Medicine, University of Ottawa, Ottawa Hospital Research Institute, Chronic Disease Program), and Dr. Johnny Ngsee (Department of Cellular and Molecular Medicine, University of Ottawa, Ottawa Hospital Research Institute, Neuroscience Program). These brilliant scientists have helped me to strengthen my research by their insightful comments and questions and by challenging me to examine my results within a wider scientific context.

I would further like to thank past and present colleagues in the Baltz lab for their advice and moral support, especially trying to develop particularly difficult experimental systems. I would like to first acknowledge our talented lab technician, Mrs. Megan

Meredith, who taught me technical laboratory skills and the basics of oocyte and embryo culture. I will forever consider Megan a friend and am appreciative of her advice and encouragement both inside and outside the laboratory. I would also like to especially thank Mrs. Hannah Gray and Ms. Taylor McClatchie for their continued support and friendship over the course of my graduate studies. Additionally, I would like to thank all the members of the Baltz lab that I was fortunate enough to meet or work with including Dr. Alina Tartia, Dr. Chenxi Zhou, Dr. Violetta Syanov, Dr. Boahua Zhang, Dr. Jane Fenelon, and Dr. Baozeng Xu.

Finally, I would like to thank my family and friends, especially my husband, for their endless love and support throughout this graduate program. I could not imagine completing this academic journey without them and am deeply grateful to have them in my life.

This thesis work was supported by the Canadian Institutes of Health Research (CIHR) (Contract grant number:MOP115102) obtained by Dr. Baltz and the CIHR Training Program in Reproduction, Early Development, and the Impact on Health (studentship) (Contract grant number: TGF96122). I also acknowledge the financial support of the University of Ottawa Graduate and Postdoctoral Studies admission scholarship programs.

INTRODUCTION

1. Follicle, oocyte, and preimplantation embryo development

1.1 Folliculogenesis and oogenesis

Oocytes develop in the mammalian ovary during growth of the female fetus. In mammals, primordial follicles consisting of an oocyte arrested in the first meiotic prophase (dictyate stage) surrounded by flattened granulosa cells have developed within the first few days after birth [Da Silva-Buttkus et al. 2008; Solc et al. 2010]. Over time, cohorts of follicles are stimulated to grow in the ovaries which are initially independent of gonadotropin regulation [Abel et al. 2000]. As primordial follicles are initiated to grow, the flattened granulosa cells become cuboidal in shape and completely surround the oocyte to form a primary follicle. During this growth phase, the oocyte begins to synthesize and secrete glycoproteins which form an extracellular coat termed the zona pellucida (ZP). The ZP increases in thickness as the oocyte grows and transzonal processes extend through this coat ending in gap junction channels thus maintaining contact between the oocyte and surrounding granulosa cells during folliculogenesis [Simon et al. 1997; Da Silva-Buttkus et al. 2008; Wassarman & Litscher 2013].

The proliferation rate of granulosa cells increases as they transition from a flattened to cuboidal morphology and more layers of granulosa cells develop around the growing oocyte to produce a secondary follicle (2-3 layers of granulosa cells) [Da Silva-Buttkus et al. 2008]. Late secondary follicles are characterized by the formation of a clear layer of theca cells separated from granulosa cells by a basement membrane (basal lamina) and the

beginning of fluid accumulation between granulosa cells that will become the antrum [Hirshfield 1991; Young & McNeilly 2010]. These events mark the transitional period from pre-antral to early antral follicles at which time a limited number of follicles become sensitive to follicle stimulating hormone (FSH) to induce granulosa cell proliferation and differentiation [Richards et al. 2002; Sirard et al. 2007; Demeestere et al. 2012]. It is at the early antral stage of follicle development that the oocyte acquires the competence to resume meiosis following the ovulatory luteinizing hormone (LH) signal [Eppig & Schroeder 1989; Eppig et al. 2000].

Following stimulation by FSH from the pituitary, antral follicles develop which consist of granulosa cells that are differentiated into either outer mural granulosa cells (lining the antral basement membrane) or inner cumulus granulosa cells (surrounding the oocyte) which are separated by the fluid-filled antral cavity [Kreeger et al. 2005; Hunzicker-Dunn & Maizels 2006]. At this stage, the oocyte has reached its maximal size (~75-85μm in diameter in mouse) and is developmentally competent [Wassarman et al. 1979; Demeestere et al. 2012; Franciosi et al. 2016]. Typically, in humans one follicle will become the dominant follicle (preovulatory/Graafian follicle) that will be ovulated following the LH surge while the rest of the developing follicles undergo atresia [Richards 1980; Hirshfield et al. 1989; Spears et al. 1996]. Throughout folliculogenesis bidirectional communication between the granulosa cells and oocyte are mediated by paracrine and gap junctional signalling to enable development of a competent oocyte capable of being fertilized and undergoing preimplantation embryo development [Simon et al. 1997; Carabatsos et al. 2000; Ackert et al. 2001] (Figure 1).

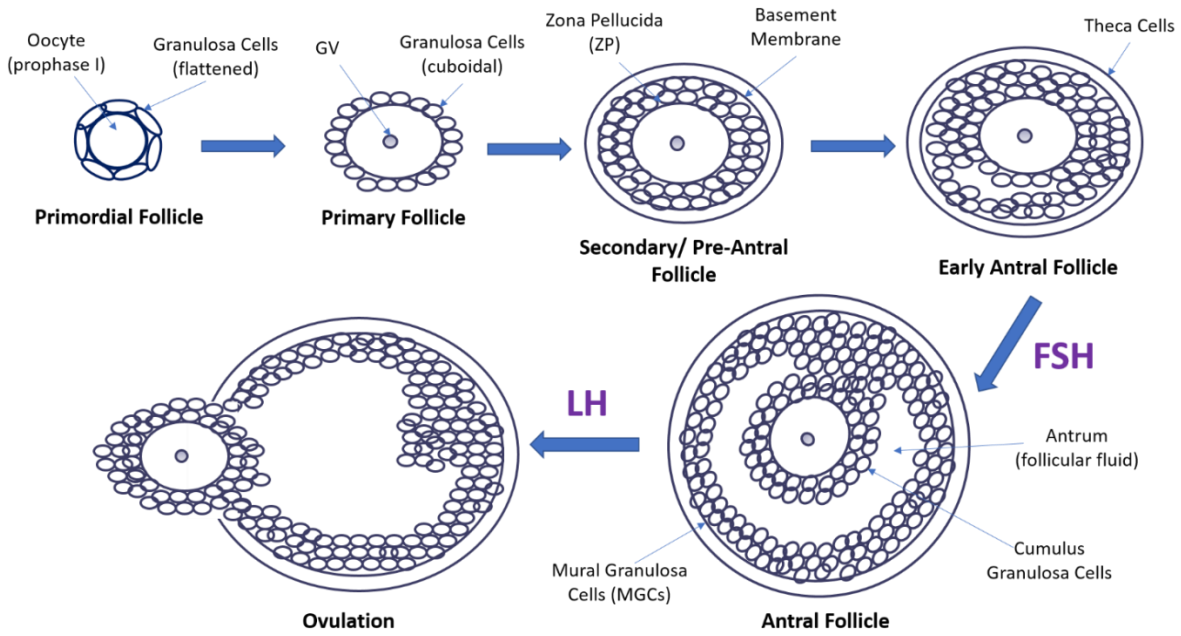

Figure 1. Folliculogenesis and oogenesis. Folliculogenesis begins at the primordial follicle stage which consists of a meiotically-arrested oocyte surrounded by a single layer of flattened granulosa cells. Cohorts of primordial follicles are stimulated to grow in the ovary to produce primary follicles in which formation of the ZP begins and the flattened granulosa cells become cuboidal and completely surround the oocyte [Da Silva-Buttkus et al. 2008; Abel et al. 2000; Solc et al. 2010]. Further follicle growth to the secondary follicle stage is characterized by an increase in the number of granulosa cell layers surrounding the growing oocyte. During the transition from the late secondary follicle stage to the pre-antral follicle stage a theca cell layer is distinguished from the granulosa cells by a basement membrane and fluid accumulation begins between granulosa cells [Hirshfield 1991; Young & McNeilly 2010]. In response to FSH, some follicles progress to the antral follicle stage with the formation of the fluid-filled antrum separating the outer mural granulosa cells from the inner cumulus granulosa cells. In humans, a single dominant

follicle containing a fully grown and competent oocyte will be ovulated in response to LH and released into the oviduct to be fertilized by sperm [Wassarman et al. 1979; Demeestere et al. 2012; Franciosi et al. 2016].

1.2 Ovulation

Ovulation of the cumulus-oocyte-complex (COC) is a complex process which occurs in response to a surge in LH (and FSH) from the pituitary resulting in activation of multiple signalling cascades and affecting all cell types comprising the ovarian follicle. LH receptors are most abundant in the mural granulosa cells therefore the ovulatory signal is initially received in the outermost layers of the follicle and is transmitted through granulosa cell layers to finally reach the oocyte. Binding of LH to receptors (G-protein coupled receptors) on mural granulosa cells stimulates multiple intracellular signalling pathways in these cells ultimately leading to significant changes in transcription factor expression and gene transcription to increase the synthesis of gene products directly required for ovulation. Cumulus granulosa cells do not express detectable levels of LH receptors and thus rely on signals from the LH-responsive mural granulosa cells to induce ovulatory responses. One major signalling pathway involves the release of epidermal growth factor (EGF)-like ligands from mural granulosa cells which bind cumulus granulosa cell EGF receptors leading to increased intracellular signalling in cumulus cells (discussed below) [Magnusson et al. 1982; Peng et al. 1991; Park et al. 2004].

Ovulatory signals relayed from mural granulosa cells stimulate gene expression in cumulus granulosa cells for the synthesis of products required for cumulus expansion and meiotic resumption [Buccione et al. 1990a; Russell & Robker 2007]. Expansion of the cumulus cells (mucification) is essential for successful ovulation, capture by oviductal fimbria, and fertilization and involves the deposition of an extracellular matrix composed of hyaluronic acid (HA) secreted by cumulus cells and mural granulosa cells located promixal to the antrum [Salustri et al. 1992; Chen et al. 1993; Fulop et al. 2003]. In addition

to substrates secreted by mural granulosa cells, oocyte-secreted factors (OSFs) have also been implicated in promoting cumulus expansion and thus ovulation. The role of OSFs in cumulus expansion is highlighted *in vitro* since cumulus granulosa cells cultured with FSH but without oocytes fail to secrete HA and do not expand [Salustri et al. 1990; Buccione et al. 1990a]. Recently, it has been proposed that several proteins are secreted from the oocyte in response to signalling from the cumulus granulosa cells stimulated by the ovulatory LH-induced signalling from mural granulosa cells [Cakmak et al. 2016]. This hypothesis illustrates a complex feedback mechanism within the ovarian follicle to facilitate successful ovulation of an expanded cumulus matrix and MII egg primed for fertilization.

1.3 Fertilization and preimplantation embryo development

The coordinated events of cumulus expansion and structural remodeling and rupture of the follicular wall enable extrusion of the expanded COC into the oviduct where ciliated cells of the oviductal epithelium transport the COC to the ampulla for fertilization [Lam et al. 2000; Russell & Robker 2007]. At this point, the oocyte has rearrested at metaphase of meiosis II (MII egg) and is "activated" by sperm binding and penetration of the egg plasma membrane resulting in the release of the second polar body and production of a fertilized diploid zygote. Maternal and paternal chromosomes are then surrounded by nuclear membranes, forming the male and female pronuclei (PN) which then travel to the center of the embryo while undergoing DNA replication. The first embryo cleavage from the 1-cell to the 2-cell stage occurs following mitotic spindle formation and chromosome segregation [Hogan et al. 1994; Evans & Robinson 2011]. The embryo then undergoes a series of cleavages (mitotic divisions) without an overall increase in cytoplasmic volume

from the 2-cell stage until the 8-cell stage. An increase in cell adhesion begins during the 8-cell stage and the embryo is compacted into a morula (16 – to 32-cell stage) with cell polarity developing for the first time. Tight junctions are formed between the outer cells of the morula to form an epithelium termed the trophoblast and these cells mediate extracellular fluid-accumulation in the embryo to produce a fluid-filled cavity which increases in size. This is now called an expanded blastocyst which will go on to hatch from the ZP and implant on the uterine wall. Formation of the blastocyst characterizes the final stage of preimplantation embryo development with the outer trophectoderm cells destined to become the placenta and the inner cell mass programmed to become the fetus (Figure 2) [Johnson & Ziomek 1981; Hogan et al. 1994; Cockburn & Rossant 2010].

2. Meiotic arrest and resumption in the antral follicle

2.1 Meiosis during folliculogenesis, ovulation, and fertilization

Meiosis is a specific type of cell division that occurs in germ cells which reduces by half the number of chromosomes from diploid to haploid. In oocytes, this process is required to prepare an egg for fertilization by the sperm to produce a viable diploid embryo for implantation in the uterus [Melhmann et al. 2004]. In the fetal mammalian ovary, meiosis I begins in oocytes during oogenesis but is then arrested at the diplotene stage of the first meiotic prophase until the ovulatory LH signal [Melhmann et al. 2005; Norris et al. 2010].

Following the LH surge, competent oocytes resume meiosis and re-arrest at metaphase of meiosis II until fertilization [Sorensen & Wassarman 1976; Park et al. 2004;

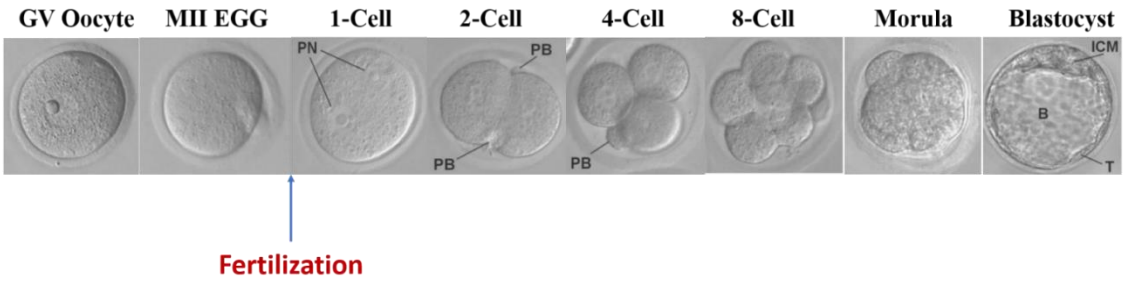

Figure 2. Preimplantation embryo development. Prior to ovulation, the oocyte is arrested at the first meiotic prophase which is characterized by an intact germinal vesicle (GV). In response to the ovulatory LH signal, the oocyte resumes meiosis and re-arrests at metaphase of meiosis II (MII egg) as germinal vesicle breakdown (GVBD) occurs and the first polar body is extruded. Fertilization of the haploid MII egg following sperm binding and penetration of the oocyte plasma membrane leads to the completion of meiosis and second polar body release and production of a fertilized diploid zygote. The 1-cell embryo is characterized by the presence of a maternal and paternal pronucleus (PN) and cleavage to the 2-cell stage occurs following mitotic spindle formation and chromosome segregation [Hogan et al. 1994]. Multiple cleavages occur after the 2-cell stage to eventually produce an 8-cell embryo after which compaction of the embryo begins to form the morula stage embryo. The final stage in preimplantation embryo development is the blastocyst stage with an outer trophectoderm destined to become the placenta, an inner cell mass which will become the fetus, and a fluid-filled blastocoel. At this final stage, the expanded blastocyst hatches from the ZP and implants on the uterine wall [Johnson & Ziomek 1981; Hogan et al. 1994; Cockburn & Rossant 2010].

Shuhaibar et al. 2015]. These coordinated "stops and starts" [Mehlmann, 2005] in meiosis are essential for normal fertilization, embryo development and for fertility preservation. Knockout mouse models of the G-protein coupled receptor 3 (GPR3) necessary for production of cyclic adenosine monophosphate (cAMP) (see below), and therefore maintenance of prophase I arrest, yield oocytes that undergo premature meiotic resumption as well as meiotically incompetent oocytes and results in decreased embryo development to the 2-cell stage and accelerated age-related reproductive failure [Ledent et al. 2005].

2.2 Maintenance of prophase I arrest in the antral follicle

Meiotic resumption following ovulation essentially depends on the activation of the heterodimer Maturation (M-phase) Promoting Factor (MPF) which is composed of the regulatory subunit Cyclin B1 and the active cyclin-dependent kinase, CDK1. In meiotically arrested oocytes, MPF is inactive (pre-MPF) due to inhibitory phosphorylation of CDK1 at Thr14 and Tyr15 [Adhikari et al. 2012; Gautier et al. 1989; Mueller et al. 1995]. In oocytes, it has been shown that prophase I arrest is maintained by a high intra-oocyte concentration of cAMP which is produced by adenylyl cyclase (AC) that is maintained in an active state by constitutively active G_s-linked G-protein coupled receptors (GPR3 and GPR12 in mice) at the oocyte plasma membrane [Cho et al. 1974; Melhmann et al. 2004; Hinckley et al. 2005; Horner et al. 2003; DiLuigi et al. 2008; Vaccari et al. 2008]. The high cAMP in the oocyte activates protein kinase A (PKA), which in turn phosphorylates and activates its substrates, WEE1 and MYT kinases. Activated WEE1 and MYT negatively regulate CDK1 by phosphorylation. PKA also phosphorylates CDC25A/B phosphatases which inactivates them. CDC25 A/B phosphatases must remain inactive to prevent

dephosphorylation, and therefore activation, of CDK1 and therefore maintain prophase I arrest (Figure 3) [Mueller et al. 1995a,b; Lincoln et al. 2002; Solc et al. 2008].

Inhibition of the phosphodiesterase that degrades cAMP in the oocytes is necessary for maintaining high intra-oocyte cAMP levels and therefore meiotic arrest. Using knockout models and pharmacological inhibitors *in vitro*, PDE3A was identified as the primary phosphodiesterase in the mouse oocyte required for cAMP degradation and meiotic resumption following ovulation [Tsafriri et al.1996; Masciarelli et al. 2004; Vaccari et al. 2008]. PDE3A is maintained in an inactive state until ovulation is triggered. It is the release of inhibition of PDE3A and consequent degradation of cAMP that triggers the resumption of meiosis.

The ability of the oocyte to resume meiosis is acquired during growth [Szybek 1972; Wassarman et al., 1979; Erdogan et al. 2005]. Prophase I arrest is maintained indefinitely in oocytes removed from follicles if the oocytes are less than ~80% fully grown (i.e., <60μm in diameter in mouse) likely due to insufficient amounts of CDK1and a decreased ability of CDK1 and Cyclin B1 to dimerize and form active MPF [Kanatsu-Shinohara et al. 2000; de Vantery et al. 1997; Sorensen & Wassarman 1976]. In fully grown oocytes (~80μm in diameter) or oocytes that have reached the size where they have become meiotically competent (>~60μm), however, meiosis was found to resume spontaneously when oocytes or COCs were removed from the fully grown Graafian follicle independent of gonadotropin signalling [Pincus & Enzmann 1935; Wassarman et al., 1979]. This observation prompted the hypothesis that inhibitory signalling from the somatic cells of the follicle (granulosa cells) maintains prophase I arrest prior to ovulation [Eppig & Telfer 1993; Conti et al. 2002].

Recently, the mechanism responsible for maintaining meiotic arrest in fully grown oocytes was elucidated and found to involve multiple cell compartments of the ovarian follicle. Natriuretic peptide precursor C (NPPC or CNP) secreted by the outer mural granulosa cells into the follicular fluid was shown to bind its cognate receptor, Natriuretic Peptide Receptor 2 (NPR2), which is a guanylate cyclase that is located on cumulus granulosa cells (surrounding the oocyte) as well as periantral mural granulosa cells (directly adjacent to the antral space) [Zhang et al. 2010; Zhang et al. 2011]. This binding stimulates the production of cGMP by NPR2 in cumulus granulosa cells which is transported to the oocyte via gap junctions. In the oocyte, cGMP directly inhibits PDE3A activity thus sustaining a high concentration of cAMP within the oocyte (Figure 3) [Tsafriri et al. 1996; Norris et al. 2009; Richard & Baltz 2014; Shuhaibar et al. 2015].

Therefore, spontaneous resumption of meiosis following removal of oocytes or COCs from the follicle *in vitro* results from a loss of the inhibitory signalling mechanism in the intact follicle. In the absence of NPPC secreted by mural granulosa cells, NPPC-stimulated production of cGMP in the isolated oocyte or COC is lost, PDE3A is activated, and cAMP levels decrease in the oocyte. Consistent with this model, isolated COCs cultured *in vitro* can be maintained in meiotic arrest for extended culture periods when NPPC is added to the medium (and estradiol is present to maintain NPR2 expression and hence sufficient cGMP production in cumulus granulosa cells) (Figure 3) [Zhang et al. 2010; Zhang et al. 2011; Richard & Baltz 2014].

In addition to the requirement of the somatic cells of the follicle to support oocyte development and regulate meiotic progression, the oocyte is actively involved in granulosa cell growth and differentiation which is achieved by oocyte-secreted growth factors,

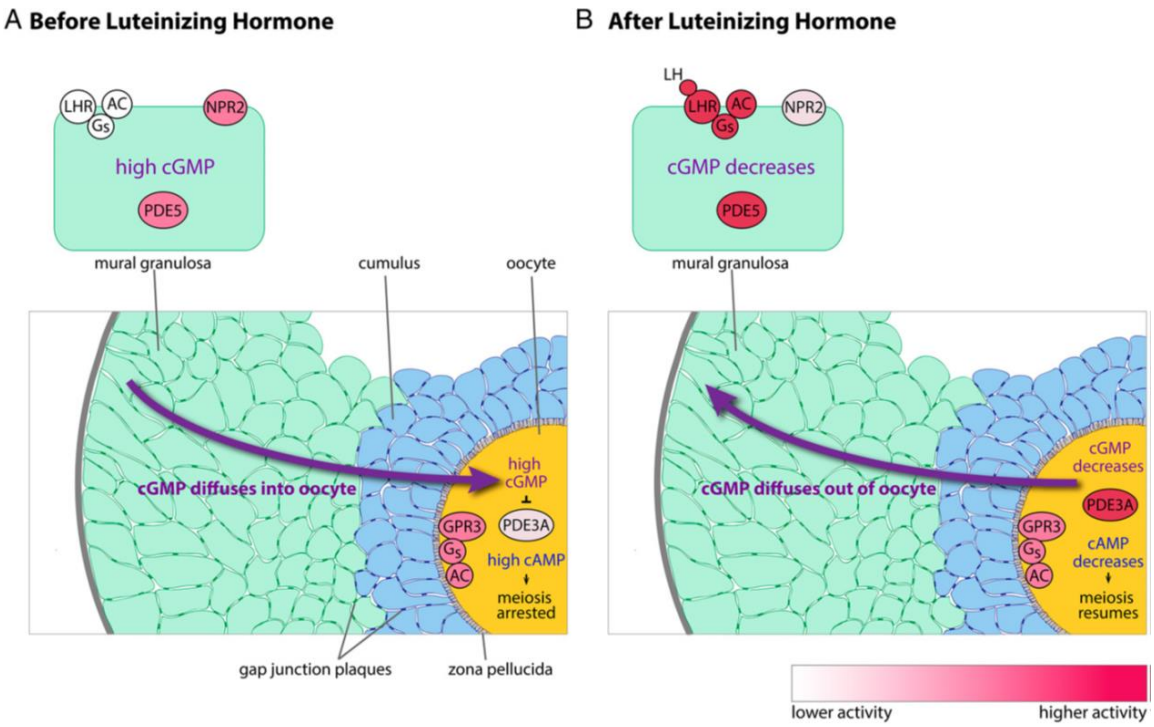

Figure 3. Meiotic arrest and resumption. (**a**) Prior to the ovulatory LH-surge, meiotic arrest is maintained within the oocyte by high intra-oocyte concentrations of cAMP produced as a result of the constitutively active oocyte-specific GPR3. The high level of cAMP within the oocyte is maintained by cGMP-mediated suppression of the cAMP phosphodiesterase PDE3A. NPPC released from the mural granulosa cells diffuses into the extracellular fluid to cumulus granulosa cells (upper panel) which binds to its cognate NPR2 receptor leading to the production of cGMP. Diffusion of cGMP through gap junctions to the oocytes establishes a uniformly high concentration of follicular cGMP thus maintaining meiotic arrest in the oocyte. (**b**) In response to LH-binding to mural granulosa cells, cGMP levels are decreased in the outer mural granulosa cells by both a decrease in NPR2 activity and an increase in cGMP phosphodiesterase (PDE5) activity (upper panel). This decrease in cGMP within the outer granulosa cells causes an outward diffusion of cGMP from cumulus granulosa cells and eventually the oocyte via gap junctions until

finally cGMP levels are uniformly lower within the entire follicle. The decrease in intra-oocyte cGMP leads to a release of PDE3A inhibition and therefore a decrease in oocyte cAMP levels causing meiotic resumption to occur [Zhang et al. 2010; Shuhaibar et al. 2015; Jaffe & Egbert 2016]. This image was obtained with permission from the following publication: Shuhaibar L.C., Egbert J.R., Norris, R.P., Lampe P.D., Nikolaev V.O., Thunemann M., Wen L., Feil R., and Jaffe L.A. (2015). Intercellular signaling via cyclic GMP diffusion through gap junctions restarts meiosis in mouse ovarian follicles. *PNAS*; 112:5527-5532.

cell growth and differentiation which is achieved by oocyte-secreted growth factors, especially from the transforming growth factor β (TGFβ) family of growth factors [Buccione et al. 1990a,b; Vanderhyden et al. 1990; Eppig 2001; Kidder & Vanderhyden 2010; Emori & Sugiura 2014]. The oocyte and its secreted growth factors have also been shown to play a role in maintenance of prophase I arrest in the ovarian follicle. Using oocytectomized COCs (OOX) and co-culture experiments it was demonstrated that oocyte-derived paracrine factors significantly promoted *Npr2* expression in cumulus cells contributing to meiotic arrest in the follicle [Zhang et al. 2010].

2.3 Luteinizing hormone-stimulated and spontaneous meiotic resumption

Meiotic resumption is stimulated *in vivo* at ovulation initially by LH binding to its receptors, which are located exclusively on mural granulosa cells. This causes the release of epidermal growth factor receptor (EGFR) ligands epiregulin and amphiregulin from the surface of mural granulosa cells [Park et al. 2004; Norris et al. 2010]. Binding of these ligands to EGFRs on cumulus and mural granulosa cells increases activity of EGFR kinase and contributes to meiotic resumption through gap junction closure and decreased follicular cGMP concentrations [Downs et al. 1988; Panigone et al. 2008; Norris et al. 2010].

LH-stimulated meiotic resumption is accomplished by the activation of multiple signalling mechanisms leading to both rapid and delayed responses involving multiple compartments of the ovarian follicle. As discussed above, meiotic arrest is maintained by NPPC-mediated cGMP production in granulosa cells which is transferred to the oocyte via gap junctions to suppress PDE3A and maintain high intra-oocyte cAMP levels. Within 1

minute after LH binding to LH receptors on mural granulosa cells, the concentration of cGMP is decreased in mural granulosa cells which is followed by a similar decrease in cGMP in the cumulus granulosa cells (~5 minutes), and finally in the oocyte (~7 minutes). Experiments using mouse follicles expressing a cGMP FRET (Förster resonance energy transfer or fluorescence resonance energy transfer) sensor and gap junction inhibitors have revealed that cGMP diffuses out of the oocyte and cumulus granulosa cells through gap junctions following the initial cGMP decrease in the mural granulosa cells [Shuhaibar et al. 2015; Jaffe & Egbert 2016]. The rapid decrease in the outer mural granulosa cells following LH stimulation has recently been shown to occur due to a decrease in NPR2 activity and an increase in the activity of the cGMP phosphodiesterase PDE5. Interestingly, inactivation of NPR2 by dephosphorylation has been found to depend on EGFR signalling while phosphorylation, and therefore activation, of PDE5 appears to occur independently of EGFR signalling suggesting that redundant mechanisms exist within the ovarian follicle to stimulate meiotic resumption [Robinson et al. 2012; Egbert et al. 2014; Egbert et al. 2016].

Following the rapid reduction in follicle cGMP, a slower response to LH stimulation also occurs involving a decrease in the levels of follicular NPPC which occurs ~2 hours following LH stimulation and likely contributes to the maintenance of low cGMP concentrations within the follicle. Although the mechanism mediating the LH-induced reduction in NPPC is incompletely understood, it seems that a reduction in *Nppc* expression could be responsible which may occur in response to EGFR activation [Kawamura et al. 2011; Robinson et al. 2012; Liu et al. 2014; Jaffe & Egbert 2016]. The role of gap junctions for maintenance of meiotic arrest has been well established, however, the contribution of

specific gap junctions to meiotic resumption is less clear. Functional gap junctions permeable to cGMP seem to be required for the rapid reduction in cGMP concentrations throughout the ovarian follicle immediately following LH-stimulation since gap junction inhibition prevented the fast cGMP decrease from occurring in cumulus granulosa cells and the oocyte, which do not have LH receptors [Shuhaibar et al. 2015]. After cGMP concentrations are uniformly low throughout the follicle (~20 minutes following LH stimulation), gap junction permeability between granulosa cells (connexin-43; GJA1 gap junctions) decreases due to connexin-43 phosphorylation with the lowest permeability at 1 hour after LH stimulation, after which gap junction permeability is restored to normal levels by 5 hours post-LH stimulation. Interestingly, this temporary permeability decrease is restricted to gap junctions between granulosa cells with no apparent decrease in the permeability of connexin-37 gap junctions located between the oocyte and innermost cumulus granulosa cells [Norris et al. 2008; Jaffe & Egbert 2016]. The reason for the phosphorylation, and therefore decreased permeability, of specifically connexin-43 gap junctions is unknown and does not seem to be necessary for meiotic resumption. It has been hypothesized that phosphorylation could lead to changes in the permeability of these gap junctions to cAMP or cGMP but this remains to be determined [Norris et al. 2008; Shuhaibar et al. 2016; Jaffe & Egbert 2016].

Thus, meiotic resumption in the ovary is a complex process with seemingly redundant mechanisms to ensure that meiotic progression occurs in response to LH stimulation. Further research is needed to elucidate the many components of the signalling pathways mediating this nuclear maturation, however the current literature does indicate that it is the removal of NPPC-cGMP inhibitory signalling (either by LH stimulation in

follicles or isolation of oocytes and COCs *in vitro*) that is ultimately responsible for the decrease in intra-oocyte levels of cAMP and therefore release of prophase I arrest (Figure 3) [Richard & Baltz 2014; Zhang et al. 2010].

3. Intercellular communication in the ovarian follicle

3.1 Paracrine signalling in the ovarian follicle

Throughout folliculogenesis, intercellular communication between the oocyte and somatic cell types within the ovarian follicle is essential for the growth and survival of a healthy and competent oocyte capable of being fertilized. This bi-directional communication between the oocyte and granulosa cells is accomplished by two main types of signalling mechanisms within the follicle: paracrine signalling and intercellular signalling through gap junctions.

Granulosa cell-derived paracrine signalling is required to support oocyte growth and acquisition of meiotic competence [Kidder & Vanderhyden 2010] as well as to mediate maintenance of prophase I arrest prior to ovulation (above). KIT ligand (KITLG) secreted by granulosa cells has been shown to be sufficient to stimulate oocyte growth in the mouse while KITLG knockout mouse models are infertile with arrested follicular development [Packer et al. 1994; Thomas et al. 2005; Huang et al. 1993]. KITLG binds to its receptor, the transmembrane tyrosine kinase KIT, on the oocyte which activates multiple intracellular signalling cascades in the oocyte including MAPK and PI3K signalling to stimulate growth and survival [Kidder & Vanderhyden 2010; Morita et al. 1999; Reddy et al. 2008; Jagarlamudi et al. 2009].

Experiments involving the removal of oocytes from follicles and COCs (oocytectomy, OOX) have conversely highlighted the importance of the oocyte in regulating vital processes in follicular somatic cells, including granulosa cell proliferation, suppression of luteinisation, and cumulus expansion [Buccione et al. 1990a,b; Eppig et al. 2002; Vanderhyden et al. 2003]. The ability of the oocyte to regulate granulosa cells is largely accomplished by oocyte-derived paracrine factors from the transforming growth factor β (TGFβ) family, especially growth-differentiation factor 9 (GDF9) and bone morphogenetic protein 15 (BMP15) [el-Fouly et al. 1970; Dong et al. 1996; Galloway et al. 2000; Persani et al. 2014]. These oocyte-derived factors were also shown to stimulate *Npr2* expression in cumulus granulosa cells thus contributing to maintenance of meiotic arrest [Zhang et al. 2010, 2011].

Although limited oocyte growth is possible in the presence of granulosa-derived paracrine factors (e.g., KIT ligand) in culture, secretion of paracrine factors alone cannot support follicular and oocyte growth and development [Cecconi & Colonna 1996]. Vital processes such as granulosa cell differentiation and maintenance of prophase I arrest depend on direct communication between adjacent cells through gap junctional channels [Vanderhyden et al. 1990; Zhang et al. 2010].

3.2 Gap junctions: structure and function

Gap junctions are transmembrane channels which allow the selective passage of ions and molecules between adjacent cells based on molecular charge and size (less than ~1 KDa). Each gap junction is formed by the end-to-end docking of two hemi-channels or

connexons spanning the plasma membranes of two adjacent cells [Goodenough 1975; Makowski et al. 1977]. These hemi-channels are composed of six connexin proteins arranged to form a pore. There are at least 20 known connexin isoforms in humans and mice [Unwin & Zampighi 1980; Beyer 1990; Gershon, Plaks, & Dekel 2008; Harris et al. 2001]. Each connexin protein contains four hydrophobic transmembrane regions which are connected by two extracellular loop domains and one cytoplasmic loop with cytoplasmic carboxy- (C) and amino- (N) terminal domains [Yeager et al. 1998].

Sequence homology is most highly conserved between connexins at the transmembrane and extracellular loop regions as well as the cytoplasmic N-terminus. The large majority of sequence differences among connexin proteins occur in the cytoplasmic loop and C-terminus domain which is thought to contribute to the differential gating properties of gap junctions [Zimmer et al. 1987; Verselis 1994; Yeager & Gilula 1992; Harris 2001]. Much is still unknown regarding the complex regulation of gap junction permeability although phosphorylation, binding of accessory proteins at the C-terminal tail, and intracellular pH appear to play a role, especially in connexin-43 proteins (GJA1) [Lampe et al. 2000; Giepmans et al. 2001; Evans & Martin 2002]. Gap junctions are found in nearly every tissue in the body and therefore must confer a high degree of selectivity for the passage of ions and molecules to avoid disrupting bodily systems. This selective ability of gap junctions is largely accomplished by their ability to form hemi-channels (connexons) made up of six of the same or different connexins (homomeric or heteromeric), thus making possible a very wide range of different combinations, each potentially having different permeabilities. In addition, these homomeric or heteromeric hemi-channels can dock with hemi-channels on adjacent cells composed of the same

connexins (homotypic) or different connexins (heterotypic) [He et al. 1999; Harris 2001; Veitch et al. 2004].

3.3 Gap junctional communication in the ovarian follicle

In the ovarian follicle, gap junctions are essential for oogenesis, folliculogenesis and meiotic arrest and resumption. From the start of folliculogenesis, the oocyte and surrounding granulosa cells are connected by gap junctions [Simon et al. 1997; Carabatsos et al. 2000; Ackert et al. 2001]. The developing oocyte depends on this mechanism of communication to receive ions, metabolites and signalling molecules from granulosa cells for growth and acquisition of meiotic competency while the granulosa cells depend on gap junctional communication with the oocyte to receive signals for differentiation, proliferation and to prevent premature luteinisation [Goodenough, Simon & Paul 1999; Simon 1997; Kidder & Vanderhyden 2010; Eppig et al. 2005]. Oocyte maintenance of meiotic arrest and resumption in fully grown antral follicles is also dependent on gap junctional communication as discussed above but it is unclear exactly which connexin proteins are essential.

Several connexins have been identified in the mouse ovary but only two isoforms have been shown to be vital for oogenesis: GJA1 (connexin-43) and GJA4 (connexin-37). Connexin-43 homotypic gap junctions have been detected as early as day 11.5 in fetal mice and are present between all granulosa cells during folliculogenesis with increasing expression as the follicle approaches a fully-grown size (Graafian follicle) [Perez-Armendariz et al. 2003; Wright et al. 2001; Gershon et al. 2008]. Knocking out *Gja1* is

lethal in mice due to cardiac malformation, however, when perinatal *Gja1* knockout ovaries were transplanted onto kidney capsules of wild-type mice folliculogenesis was impaired producing abnormal, meiotically incompetent oocytes which could not be fertilized [Reaume et al. 1995; Ackert et al. 2001]. Connexin-37 gap junctions are primarily localized at the oocyte surface where the granulosa cell projections through the zona pellucida (transzonal processes) come into contact with the oocyte. Folliculogenesis progresses normally until the preantral stage in *Gja4* knockout mice but Graafian follicles never develop in the absence of connexin-37 gap junctions. Ovaries in these mice also showed signs of premature corpus luteum formation and oocytes isolated from these ovaries were growth restricted, meiotically incompetent, and were not ovulated [Simon et al. 1997; Carabatsos et al. 2000].

To further examine the respective roles of connexin-43 and connexin-37 in granulosa cells and the oocyte throughout folliculogenesis, Kidder and colleagues constructed chimeric reaggregated ovaries with various combinations of wild-type and connexin knockout oocytes and granulosa cells [Gittens & Kidder 2005]. They found that impaired folliculogenesis and oocyte development observed in *Gja1* knockout mice was due to a lack of connexin-43 specifically in the granulosa cells since reaggregated ovaries with granulosa cells deficient in connexin-43 with wild-type oocytes contained only follicles at very early stages of development (single layer of granulosa cells) compared to ovaries with oocytes deficient in connexin-43 with wild-type granulosa cells. They also found that the inability of follicles to progress to the antral or Graafian stage and restricted oocyte growth and competence observed in *Gja4* knockout mice was a result of oocyte-specific knockout of connexin-37 since reaggregated ovaries with connexin-37 deficient

oocytes and wild-type granulosa cells failed to develop Graafian follicles (follicles contained three or fewer layers of granulosa cells) compared to normal ovaries with connexin-37 deficient granulosa cells and wild-type oocytes [Gittens & Kidder 2005]. It remains unclear whether the gap junctions at the oocyte-granulosa interface are composed of homotypic connexin-37 gap junctions or heterotypic gap junctions composed of both connexin-37 and connexin-43. Connexin-37 has been identified in gap junctions between the oocyte and innermost granulosa cell layer (homotypic junctions) using confocal immunofluorescence [Veitch et al. 2004; Simon et al. 2006] however, chimeric reaggregated ovaries containing granulosa cells deficient in connexin-37 were able to produce fully grown Graafian follicles with oocytes maintained in meiotic arrest suggesting the existence of functional heterotypic gap junctions connecting the oocyte with the surrounding granulosa cells [Gittens & Kidder 2005].

It is clear that gap junctions are required for maintenance of prophase I arrest since disrupting gap junctions in ovarian follicles causes meiotic resumption due to decreased cGMP transfer into the oocyte, as discussed previously [Sela-Abramovich et al. 2006; Norris et al. 2009]. Exactly which gap junction isoforms are required to maintain meiotic arrest could not be determined from the knockout or reaggregated ovary models since connexin deficiency led to either impaired folliculogenesis without fully grown Graafian follicles developing or a normal phenotype with oocytes maintained in meiotic arrest. The only study that addresses this is one by Norris et al. [2008] who showed that decreased connexin-37 protein causes meiotic resumption in intact Graafian follicles microinjected with connexin isoform-specific antisera. As discussed above, gap junctions have also been implicated in meiotic resumption following LH stimulation. Since functional gap junctions

are required to enable the diffusion of cGMP between granulosa cells and the oocyte for the inhibition of PDE3A and therefore maintenance of meiotic arrest, the complete inhibition of gap junctional communication has been shown to be sufficient to cause meiotic resumption in intact mouse follicles. However, in response to LH, gap junction permeability is diminished due to MAPK-mediated phosphorylation of connexin-43 but not abolished entirely in intact mouse follicles and this effect is transient. In addition, meiotic maturation proceeded in intact follicles cultured with LH even when MAPK-mediated connexin phosphorylation was inhibited, suggesting that although gap junction inhibition is sufficient to cause meiotic resumption, LH-stimulated meiotic resumption is not dependent on gap junction inhibition [Norris et al. 2008]. Furthermore, studies have shown that immediately following LH stimulation, cGMP levels are substantially decreased in mural granulosa cells which is followed by a sequential reduction in cGMP in the cumulus cells and oocyte due to outward diffusion of cGMP which is dependent on gap junctions [Shuhaibar et al. 2015] (Figure 3). Thus, it appears that in response to LH, gap junctional communication between granulosa cells and the oocyte is involved in mediating meiotic resumption, however, as discussed above, other redundant mechanisms exist within the follicle to facilitate meiotic resumption in the absence of gap junctional communication [Jaffe & Egbert 2016].

In addition to their role in the maintenance of meiotic arrest and resumption, gap junctions have also been implicated in the transfer of various metabolites, nutrients, and amino acids from follicular granulosa cells to the oocyte to facilitate oocyte growth and competence acquisition during oogenesis. The large volume of the oocyte results in a relatively small surface area which limits the ability of the oocyte to take up these

compounds, therefore, the presence of granulosa cells surrounding the oocyte provides a mechanism to increase the uptake of various metabolites and nutrients into the oocyte by diffusion through gap junctions. Compared to denuded oocytes, uptake of the ribonucleosides uridine, guanosine, and cytidine but not adenosine, was increased as well as choline into COCs which is thought to diffuse from granulosa cells to the oocyte through gap junctions [Heller & Shultz 1980; Heller et al. 1981]. Gap junctions have also been shown to facilitate the transport of energy substrates such as pyruvate from granulosa cells to the oocyte since granulosa cells, but not oocytes, are able to metabolize glucose, as discussed in more detail in the following section [Biggers et al. 1967; Downs 2002].

Although oocytes themselves are capable of transporting amino acids, some amino acid transport mechanisms are inactive or have limited transport abilities at different stages of oocyte growth. The presence of granulosa cells has been shown to enhance the overall rate of transport of specific amino acids into both growing and fully-grown oocytes, including increases in the uptake of taurine, alanine, and lysine. Additionally, the uptake of glutamine and arginine was enhanced in fully-grown COCs compared to denuded GV oocytes while the uptake of leucine was actually diminished by the presence of cumulus granulosa cells [Pelland et al. 2009]. Interestingly, glycine uptake into oocyte was increased by granulosa cells in preantral follicles (growing oocytes) but not antral follicles (fully grown oocytes) possibly due to differing roles of glycine at various stages of oocyte development. Gap junction inhibitors were shown to abrogate the effect of increased amino acid uptake by granulosa cells suggesting that amino acids taken up by granulosa cells diffuse to the oocyte via gap junctions [Haghighat & Van Winkle 1990].

Gap junctions also seem to play a role in pH regulation in growing oocytes. Although fully grown oocytes are capable of regulating pH by the combined actions of Na^+/H^+ and Cl^-/HCO_3^-exchangers (discussed below), denuded growing oocytes display minimal activity of these exchangers and thus are unable to effectively regulate their pH [FitzHarris & Baltz 2006]. Cultured follicle-enclosed growing oocytes, however, were able to regulate pH in response to induced alkalosis or acidosis which was attributed to Na^+/H^+ and Cl^-/HCO_3^-exchanger activity in granulosa cells. Gap junctions seemed to play a vital role in this granulosa cell-derived pH regulatory mechanism since gap junction inhibitors abrogated the effects of granulosa cells on the ability of growing oocytes to regulate their pH [FitzHarris & Baltz 2006; FitzHarris et al. 2007]. This "metabolic cooperativity" between oocytes and granulosa cells is essential for the development of a healthy and competent oocyte and is discussed further below.

Recently metabolic cooperativity was also demonstrated in meiotically arrested COCs which were shown to have an increased rate of betaine uptake compared to denuded GV oocytes. It was proposed that betaine is accumulated in granulosa cells largely via the y+LAT2 (*Slc6a7*) transporter and transported through gap junctions to the oocyte; which transport betaine directly via SIT1 [Pelland et al. 2009; Corbett et al. 2014].

Clearly, successful folliculogenesis and oogenesis depend on complex paracrine and gap junctional intercellular communication to produce a healthy, fertilizable oocyte. These signalling mechanisms can be utilized in combination to achieve a common end result, as is the case for maintenance of meiotic arrest.

4. Oocyte and preimplantation embryo culture

4.1 Oocyte and embryo metabolic requirements

Significant work has been done in the past to develop culture medium suitable to support embryo culture from the zygote to blastocyst stage considering the differing biochemical requirements. The availability of the necessary energy substrates to satisfy the distinct metabolic demands of growing oocytes and preimplantation embryo development is an important consideration required when formulating appropriate culture media [Biggers et al. 1967; Sutton-McDowall et al 2010].

Glucose is the preferred energy substrate utilized during and after compaction of the embryo (morulae and blastocysts) which satisfies the high demand for energy during these developmental stages as cell polarity, transporting epithelium, and the blastocoel is formed [Biggers et al. 1988]. Although the presence of glucose in culture medium is beneficial to late stages of embryo development, too high concentrations (>10mM) and too low concentrations (<2.3mM) of glucose were previously shown to be detrimental to cultured oocytes and early cleavage-stage embryos resulting in a reduced ability to undergo cytoplasmic and meiotic maturation with poor embryo development [Biggers et al. 1967; Rose-Hellekant et al. 1998; Downs et al. 1998; Eppig et al. 2000; Ali et al. 2003]. Oocytes are unable to utilize glucose as an energy substrate due to their lack of high-affinity glucose transporters and low activity of the glycolytic rate-limiting enzyme phosphofructokinase [Saito et al. 1994; Downs et al. 1996; Cetica et al. 2002; Harris et al. 2007]. These combined conditions result in an overall reduced glycolytic rate in the oocyte which then must depend on “metabolic cooperativity” with surrounding granulosa cells to acquire metabolites (via gap junctions) which can be used by the oocyte [Sugiura et al. 2005].

Since the oocyte is unable to utilize glucose, it relies on the cumulus cells to metabolize glucose to its preferred energy substrate, pyruvate [Biggers et al. 1967; Conaghan et al. 1993]. Cumulus cells express high-affinity glucose transporters and contain active enzymes involved in glucose metabolism which produces pyruvate, among other metabolites, which is then transported to the oocyte via gap junctions [Downs 2002]. In the oocyte, pyruvate (and lactate) is readily metabolized by the tricarboxylic acid cycle to produce ATP [Steeves & Gardner 1999]. The presence of amino acids in culture medium is also able to greatly impact the success of embryo development *in vitro* with requirements varying depending on the developmental stage.

4.2 Amino acids and amino acid derivatives: requirements and functions during oocyte and embryo development

It was shown previously that the addition of specific amino acids to embryo culture medium increased the number of *in vitro* cultured embryos developing to the blastocyst stage, the rate of development, and implantation success rates. This beneficial effect of amino acids was found to be stage-specific with non-essential amino acids being preferable during the early stages of embryo development (up to the 8-cell stage) and both non-essential and essential amino acids conferring beneficial effects during later stages of development (8-cell to blastocyst stage) [Gardner & Lane 1993; Lane & Gardner 1994]. Various amino acids and amino acid derivatives have been found to support early preimplantation embryo development *in vitro* at osmolarities similar to that found in oviductal fluid (~300mOsM) including glycine, betaine, β-alanine, proline, and glutamine, as discussed below.

Glycine is readily transported during the cleavage-stages of preimplantation embryo development corresponding to the expression of System Gly (specifically GLYT1), a transport mechanism which is absent by the blastocyst stage [Van Winkle & Campione 1996; Richard et al. 2016]. In mice, GLYT1, a Na^+/Cl^--dependent transporter of the neurotransmitter transporter (NTT) family encoded by the *Slc6a9* gene, is responsible for nearly all glycine accumulation in mouse oocytes and cleavage-stage embryos before compaction [Van Winkle et al. 1988a; Steeves et al. 2003; Tartia et al. 2009]. Although glycine is the preferred substrate for the GLYT1 transporter, glutamine can also be transported but with much lower affinity [Lewis & Kaye 1992]. The taurine/β-amino acid transporter (TAUT) is expressed throughout preimplantation embryo development and has been shown to transport both β-alanine and taurine in embryos with intracellular concentrations increasing from the 2-cell stage to blastocysts [Van Winkle et al. 1994; Van Winkle & Dickinson 1995; Hammer & Baltz 2003]. Betaine and proline transport in preimplantation embryos was found to be mediated by the SIT1 transporter (*Slc6a20a*) which is only active after fertilization and persists in 1- and 2-cells embryos until the 4-cell stage; although proline transport has also previously been shown to occur in 1-cell embryos by additional mechanisms which exclude betaine [Hammer & Baltz 2002; Anas et al. 2007, 2008]. Other amino acid transporters show stage-specific activity including system x_c^- at the 1-cell stage (glutamine and cystine), system $b^{0,+}$(arginine, lysine, and glutamine) during oocyte maturation until the blastocyst stage, and system L which is present from the 1-cell stage to blastocyst stage (branched chain amino acids such as leucine) [Pelland et al. 2009; Van Winkle 2001]. In addition to direct transport by specific transporters at the plasma

membrane, amino acids can be transferred to oocytes from cumulus granulosa cells which are coupled by gap junctions, as discussed above.

The addition of specific amino acids to culture medium was shown to significantly affect the number of embryos developing to the blastocyst stage, the overall number of trophectoderm and inner cell mass cells, and implantation and fetal development [Lane & Gardner 1997]. It was found that optimal embryo development and implantation was achieved when embryos were cultured in the presence of non-essential amino acids for the first 48 hours (up to the 8-cell stage) followed by culture in the presence of all 20 amino acids and glutamine for the second 48 hours (8-cell stage and later). This suggests that the amino acid requirements of the embryo changes as development progresses and the need for an overall greater concentration of intracellular amino acids increases since culture of blastocysts from day 4 to 5 was accompanied by an increase of essential amino acids by 170% and non-essential amino acids by 30% within blastocysts [Lane & Gardner 1997]. Expression of amino acid transporters specific to later stages of embryo development has been described and include the Na^+/Cl^--dependent system $B^{0,+}$ (zwitterionic substrates), system A (zwitterionic substrates) in the ICM, and a significant increase in the activity of the Na^+-independent system $b^{0,+}$ (cationic and zwitterionic substrates) in blastocysts [Van Winkle et al. 1985; Van Winkle et al. 1988b; Van Winkle et al. 1990a; Van Winkle et al. 1990b; Jamshidi & Kaye 1995; Van Winkle et al. 2001].

The specific metabolite and amino acid requirements of developing preimplantation embryos is reflected in the composition of oviduct fluid. When compared to blood plasma, amino acid concentrations are much higher in oviduct fluid highlighting their protective role in preimplantation embryo development especially prior to compaction

[Harris et al. 2005]. Depending on the stage of embryo development, amino acids may differ in their roles in embryos which may include protein synthesis, utilization as an energy source, protection from oxidative stress, cell signalling and/or maintenance of cell volume [Lane & Gardner 1997; Van Winkle 2001; Houghton 2012].

4.3 Culture medium in early and late-stage preimplantation embryo culture

As discussed above, successful embryo culture depends on the presence of stage-specific substrates in the medium to support development from 1-cell embryos to blastocysts which are capable of implanting and producing healthy offspring. Initial attempts to culture embryos *in vitro* dating back to 1912 were performed in undefined biological fluids such as blood serum which were unable to support preimplantation embryo development in the majority of mammals through more than a few cleavages [Brachet 1912; Lewis & Hartmann 1933; Alexandre 2001; Baltz 2012]. Defined culture medium capable of supporting embryo development from the 8-cell to blastocyst stage was developed in 1956 by Whitten. This medium was based on Krebs's and Henseleit's Krebs-Ringer Bicarbonate (KRB) that is simply saline solution buffered with bicarbonate/CO_2 which cannot support embryo development at any stage [Krebs & Henseleit 1932; Whitten 1956]. Whitten's medium differs from KRB simply in that bovine serum albumin and glucose were added allowing development of viable blastocysts from 8-cell embryos that were capable of producing live young, though culture at stages earlier than 8-cell was still not possible [Whitten 1956; McLaren & Biggers 1958]. This defined medium contained essentially the same six inorganic ions as culture medium used today including Na^+, K^+, Cl^-, Ca^{2+}, Mg^{2+}, and SO_4^{2-} [Baltz 2012].

As mentioned previously, embryos prefer different primary energy substrates depending on the stage of development with earlier stages preferring pyruvate (and lactate) and later stages (during and post-compaction) preferring glucose [Biggers et al. 1988; Steeves & Gardner 1999]. The inability of Whitten's initial culture medium, which contained only glucose as the energy substrate, to support early embryo development was likely due to the unavailability of pyruvate or lactate as an energy substrate for early cleavage-stage embryos. This inability to support embryo culture from early stages to the blastocyst *in vitro* was overcome shortly after the development of Whitten's first defined culture medium by the addition of lactate to Whitten's medium which enabled development from the 2-cell to blastocyst stage, though not from the fertilized zygote to the 2-cell stage [Whitten 1957; Baltz 2012]. The addition of pyruvate to this medium in 1967 finally permitted development of embryos from the fertilized zygote to the 2-cell stage, although embryos could still not be cultured from the zygote all the way to the blastocyst stage *in vitro* [Biggers et al. 1967; Whittingham & Biggers 1967]. Since mouse embryos could develop to the 2-cell stage but then became arrested *in vitro*, this phenomenon was referred to as the "2-cell block". Optimization of the concentrations of these energy substrates resulted in the development of widely used defined culture mediums such as M16 which were used as the standard in mouse embryo culture for many years, although the 2-cell block could still not be avoided with these medium [Whittingham 1971; Hogan et al. 1994; Biggers 1998; Baltz & Tartia 2010].

The 2-cell block occurred in standard culture media (e.g., M16) in embryos from mice of most strains (with the exception of embryos derived from some F1 hybrid females) as well as in rats while other mammalian species were also susceptible to developmental

blocks at various stages of development including the 8-cell block in bovine, 2- to 4-cell block in hamster, and 4- to 8-cell block in humans [Camous et al. 1984; Bolton et al. 1989; Schini & Bavister 1988; Kishi et al. 1991; Biggers 1998; Baltz 2012]. Medium capable of supporting embryo development from a fertilized zygote to the blastocyst stage was first produced in the late 1980s and early 1990s under a targeted "National Cooperative Program" funded by the US National Institute of Child Health and Human Development of the National Institutes of Health. Two types of medium were developed within this program: CZB by Chatot, Ziomek, and Bavister and KSOM by the Biggers group. Both types of medium improved upon the widely-used M16 medium with the addition of glutamine and EDTA and further optimization of inorganic ion and energy substrate concentrations [Baltz 2012]. CZB could support embryo development from the fertilized zygote to blastocyst stage but required a two-step culture protocol with glucose absent for the first two days of culture which was then added to medium during the 4- to 8-cell stage [Chatot et al. 1989]. KSOM was able to support embryo development in a single medium from the zygote to blastocyst stage with salt concentrations differing from CZB and is now commonly used for mouse embryo culture due to the ability to support growth beyond the 2-cell block and the high rate of blastocyst yields in mice [Lawitts & Biggers 1992; Lawitts & Biggers 1993; Erbach et al. 1994; Baltz & Tartia 2010]. Human embryo culture media today seems to be largely based on culture media refined by mouse and hamster embryo culture in the laboratory likely without major differences in overall inorganic ion, amino acid, and energy substrate concentrations [Baltz 2012].

Shortly following the development of these new culture media capable of overcoming the 2-cell block, it was discovered that this developmental block could be

reproduced using KSOM if the osmolarity was increased using either NaCl or the inert trisaccharide raffinose [Lawitts & Biggers 1992; Biggers et al. 1993; Dawson & Baltz 1997; Hadi et al., 2005]. Earlier culture media such as M16 which caused the 2-cell block to occur had osmolarities around 290 mOsM while CZB had an osmolarity of ~275 mOsM and KSOM of ~250 mOsM. The decreased osmolarity of the newly developed culture media proved to be the solution to overcoming the 2-cell block *in vitro* [Baltz & Tartia 2010]. Since the osmolarity of oviductal fluid has been measured at ~300mOsM, it is unlikely that the decreased osmolarities more accurately reflect the *in vivo* environment of the developing embryo, but rather earlier culture media likely lacked a vital component which was essential for embryo development at osmolarities similar to that found *in vivo* [Borland et al. 1977; Collins & Baltz 1999; Fiorenza et al., 2004].

One of the major adjustments of these media from previous culture media such as M16 was the addition of the amino acid glutamine. None of the earlier culture media contained any amino acids which we now know are beneficial for embryo development as discussed above. Interestingly, Lawitts and Biggers discovered that the addition of glutamine to media could rescue embryo development past the 2-cell block in KSOM culture media when the osmolarity was increased with NaCl [Lawitts & Biggers 1992]. It was also found by Van Winkle et al. that glycine could act similarly to glutamine and support embryo development from the 2-cell stage at these high osmolarities [Van Winkle et al. 1990c]. As discussed above, amino acids are important for many processes in the developing embryo. However, the ability of these single amino acids to support development through the 2-cell block at *in vivo* osmolarities is due specifically to their action as organic osmolytes in volume regulation.

5. Cell volume regulation

5.1 Donnan equilibrium and osmoregulation in somatic cells

The mammalian cell membrane is highly permeable to water due to the presence of aquaporin water channels that are present in most cell types [King & Agre 1996; Borgnia et al. 1999]. This passive influx and efflux of water is dependent on the osmotic pressure gradient across the cell membrane. Cells are known to contain a high concentration of plasma membrane-impermeable, large molecular weight anionic colloids such as proteins and organic phosphates which exhibit a net negative charge at physiological pH [Hoffmann et al. 2009]. In contrast, the extracellular fluid contains a low non-diffusible anion concentration (fewer proteins) in comparison to the intracellular environment resulting in a net positive charge extracellularly and thus establishment of electroneutrality across the plasma membrane at equilibrium; this is referred to as Gibbs-Donnan equilibrium. Under these conditions, the osmolarity inside the cell would be higher than the extracellular fluid due to the higher concentration of intracellular charged macromolecules leading to the development of an osmotic pressure gradient, water influx into the cell, and subsequent cell swelling. Cell swelling would increase until the cell eventually burst by colloid osmotic lysis. Therefore, a mechanism exists in cells to maintain steady state volume which relies on the activity of the plasma membrane Na^+/K^+-ATPase [Hoffmann 2001; Hoffmann et al. 2009].

The cell plasma membrane has a very low permeability to Na^+ and this property combined with the activity of the Na^+/K^+-ATPase which pumps Na^+ out of the cell essentially makes the cell impermeable to Na^+. This produces a “double Donnan equilibrium” as the impermeable intracellular anion concentration is balanced by the

extracellular impermeable cation concentration thus allowing osmotic equilibrium and cell volume maintenance; this mechanism is referred to as the "pump-and-leak" concept [Tosteson & Hoffmann 1960; Baltz 2001; Kaplan 2002; Hoffmann et al. 2009; Lang 2007]. The Na^+/K^+-ATPase is also responsible for maintaining the ion gradient across the plasma membrane of cells, and therefore cell membrane potential. Cell membrane potential is established by a high intracellular concentration of K^+ and low intracellular concentrations of Na^+ and Cl^- thus providing an energy source for membrane transporters such as organic osmolyte transporters which depend on this ion gradient as discussed below [Kaplan 2002; Baltz 2012].

5.2 Osmolarity, osmolality, tonicity, and molarity

Osmolarity is a measure of the solute concentration per liter in a given solution which is described as osmoles/L (OsM). This is different from osmolality which measures the solute concentration in a solution per kilogram with units of osmoles/kg [Baltz 2012]. Most physiological fluids are dilute at ~300mOsM where the difference between osmolarity and osmolality is very small and therefore these terms are commonly used interchangeably for biological fluids [Caon 2008; Baltz 2012]. For simplicity and convenience of units, osmolarity will be used as a measure of osmotic pressure in the following sections. Tonicity is similar to osmolarity since it is a measure of the osmotic pressure exerted on a semi-permeable membrane. However, tonicity only accounts for the non-penetrable solute concentration (solutes unable to cross the plasma membrane) in a solution. Therefore, a solution can be isotonic but not iso-osmotic when the concentration of non-penetrable solutes is equivalent across the membrane but a difference exists in the

concentration of penetrable solutes across the membrane. It is also important to keep in mind that osmolarity and molarity are often not equal in solutions since osmolarity takes into account the dissociation of solutes in solution while molarity does not. For example, 1 mole of NaCl when dissolved in water is actually equal to ~2 osmoles since the NaCl dissociates almost entirely into two individual Na^+ and Cl^-ions. The molarity and osmolarity are equivalent in solutions with solutes that do not dissociate such as non-ionic solutes [Baltz 2001; Baltz 2012]. Measures of osmolarity (and osmolality) can be used to determine the osmotic pressure of a solution and thus the direction of flow of water and penetrable solutes across the cell plasma membrane.

5.3 Cell volume regulation: response to osmotic perturbations

The osmotic equilibrium achieved under the conditions described above can be disrupted when a shift in the intracellular or extracellular osmolarity occurs and the cell must be able to adapt to these fluctuations to maintain a steady-state volume; even cells in an isotonic environment need to utilize volume regulatory mechanisms to respond to the diffusion of ions and water or changes in intracellular concentrations due to metabolism [Hoffmann et al. 2009]. Cells which have shrunk in a hypertonic extracellular environment respond by activating cell volume regulatory mechanisms, such as increasing inorganic ion transport into the cell, to increase water influx and therefore increase cell volume. The ability of the cell to restore cell volume under these conditions is termed “regulatory volume increase” (RVI). Osmotically swollen cells in a hypotonic extracellular environment will also activate volume regulatory mechanisms including the release of nonessential organic osmolytes which causes water efflux out of the cell thus

accomplishing “regulatory volume decrease” (RVD) [Hoffmann & Dunham 1995; Lang 2007; Hoffmann et al. 2009]. Cells utilize different volume regulatory mechanisms depending on whether the change in osmolarity is acute or chronically altered.

The function and survival of a cell is dependent on its ability to regulate its volume. Changes in cell volume can occur under normal or pathological conditions and has been shown to regulate a number of physiological processes including cell migration, proliferation, and death [Lang et al. 1998; Lambert et al. 2008; Hoffmann et al. 2009]. These cell functions are essentially influenced by changes in cell volume as a result of macromolecular crowding, alterations in intracellular ionic strength, and changes in the mechanical and chemical properties of the lipid plasma membrane [Strange et al. 1996; Okada 1997; Burg 2000; Hoffmann et al. 2009]. If cells were unable to regulate their volume, cell functioning would be disrupted leading to an increase in the osmotic pressure across the plasma membrane causing cell stress and eventually necrotic or apoptotic cell death [Bortner & Cidlowski 1996; Maeno et al. 2000; Okada 2001].

Much remains to be determined regarding the mechanisms involved in the ability of the cell to detect volume changes and the signalling pathways mediating RVI and RVD. This process can essentially be broken down into three main components: sensors, transducers, and effectors [Pederson et al. 2011]. “Sensors” initially detect changes in cell volume leading to “transduction” of the signal causing activation of “effectors” which regulates osmotic adaptation of the cell. Effectors in osmoregulation, such as ion and organic osmolyte transporters and channels, have been extensively studied but less is known regarding the location and identity of sensors and transducers [Jentsch 2016]. Understanding this process is complicated by the fact that some components of the osmotic

response perform more than one role. For example, effectors of volume regulation may also act as sensors such as volume-regulated anion channels (VRACs, discussed below) which detect changes in intracellular ionic strength causing these channels to increase or decrease permeability to anions and/or organic osmolytes [Emma et al. 1997; Voets et al. 1999; Syeda et al. 2016].

As mentioned above, cells generally sense changes in osmotic pressure by macromolecular crowding, alterations in intracellular ionic strength, or mechanical and chemical changes in the plasma membrane lipid bilayer or extracellular matrix (ECM) [Hoffmann et al. 2009]. Macromolecular crowding occurs when cell shrinkage leads to an increased intracellular concentration of nucleic acids, polysaccharides, and proteins in specific cell compartments [Burg 2000; Hoffmann et al. 2009]. This crowding leads to alterations in the function, structure, and stability of proteins and macromolecules within cells. The degree of macromolecular crowding can thus influence sensing of osmotic perturbations in cells by affecting the activity of macromolecules leading to activation or inhibition of sensors, transducers, and/or effectors, although the exact pathways mediating these processes are not well known in various cell types [Garner & Burg 1994; Burg 2000; Al-Habori 2001; Mittal et al. 2015]. Changes in ionic strength and ion concentrations within cells have been shown to stimulate ion and organic osmolyte influx/efflux in response to volume perturbations. Recently, VRACs incorporated into lipid bilayers were shown to be able to detect changes in cytoplasmic ionic strength directly and respond by increasing their permeability to and outward conductance of anions [Voets et al. 1999; Syeda et al. 2016]. Sensors can also utilize the outer membrane and ECM to detect cell volume perturbations by sensing changes in membrane curvature due to mechanical forces

or membrane composition, direct stretching of the membrane, changes in cytoskeletal organization and F-actin content, and interaction with integrins within the membrane which can be activated or inhibited in response to osmotic stress [Hoffmann et al. 2009; Pederson et al. 2011].

Transduction of the volume perturbation signal is mediated by a variety of signalling mechanisms including receptor tyrosine-kinases (RTKs) which have been shown to be activated in response to hypotonic swelling and inhibited by hypertonic shrinkage in some but not all cell types [Reinehr et al. 2004; Copp et al. 2005; Lezama et al. 2005; Pasantes-Morales et al. 2006; Nielsen et al. 2008]. Activation and inhibition of RTKs as well as additional signalling mechanisms regarding osmoregulation creates a complex interaction of transducers with many converging factors making it difficult to understand the physiological role of these signals in osmotic adaptation. Osmotic stress "effectors" including membrane transporters and channels and their role in RVI and RVD is more completely understood and is discussed in more detail below [Okada et al. 2004; Browe & Baumgarten 2006; Hoffmann et al. 2009; Pederson et al. 2011].

5.4 Regulatory volume increase (RVI): acute and chronic mechanisms

The most rapid and efficient mechanism of volume regulation in mammalian somatic cells is the transport of ions into and out of the cell via plasma membrane transporters. Following a decrease in volume, cells will initially activate inorganic ion transporters to facilitate the transport of primarily Na^+ and Cl^- into the cell cytoplasm thus increasing water diffusion into the cell (osmosis) and restoring cell volume [Lang et al.

1998; Hoffmann et al. 2009]. Cell shrinkage first activates plasma membrane Na^+/H^+ exchangers (NHEs, *Slc9* family) causing an increase in cytoplasmic Na^+ and an efflux of H^+ increasing the intracellular pH [Orlowski & Grinstein 2004; Alexander & Grinstein 2006; Baltz & Zhou 2012]. In mammals NHE1, NHE2, and NHE4 have been shown to be activated by cell shrinkage while NHE3 is activated by cell swelling and inactivated by shrinkage; NHE1 is the most ubiquitously expressed exchanger and likely the major isoform involved in RVI [Orlowski & Grinstein 2004; Hoffmann et al. 2009].

The intracellular alkalinisation due to H^+ efflux leads to activation of the Cl^-/HCO_3^- exchanger causing Cl^- influx and HCO_3^- efflux which then decreases intracellular pH, countering the Na^+/H^+ exchange-induced increase. AE2 (*Slc4* family) has been identified as the most widely expressed Cl^-/HCO_3^- exchanger in mammals and has been shown to contribute to RVI while AE1 is predominately expressed in erythrocytes and cells of the renal collecting duct and is not involved in RVI [Jiang et al. 1997; Lang et al. 1998; Alper 2006]. This influx of Na^+ and Cl^- via these functionally coupled cation and anion exchangers brings with it osmotically obliged water thus rapidly restoring cell volume with no net effect on pH when both exchangers are active.

RVI can also be accomplished by the activation of $Na^+/K^+/2Cl^-$ co-transporters (NKCCs, *Slc12* gene family) [Moore-Hoon & Turner 2000; Hebert et al. 2004]. As the name implies, this mechanism of volume regulation involves the coupled uptake of Na^+, K^+ and $2Cl^-$ into the cell along the ion gradient established by the low intracellular concentration of Na^+ and Cl^-. In response to a cell volume decrease the ubiquitously expressed NKCC1 transporter is activated via phosphorylation to facilitate the influx of these ions into the cell along with water to counteract osmotic cell shrinkage [Markadieu

& Delpire 2014; Hebert et al. 2004]. In many cell types both NKCC and coupled Na^+/H^+ and Cl^-/HCO_3^-exchangers (NHE1 and AE2) are co-expressed and work in combination to restore cell volume often with NHE and AE transporters contributing most significantly to acute regulatory volume increases (Figure 4) [Pedersen et al. 2006; Hoffmann 2009].

The influx of inorganic ions such as Na^+ and Cl^- is appropriate as a rapid and acute response to osmotic perturbations. However, the increased accumulation of these ions leads to an increased intracellular ionic strength which over time disrupts ion gradients across the plasma membrane, interferes with metabolic and macromolecular function, and can alter protein structure [Yancey et al. 1982; Garcia-Perez & Burg 1991; Lang et al. 1998; Baltz & Zhou 2012]. Thus, cells exposed to chronically (more than several hours) hypertonic extracellular osmolarities (such as kidney medullary cells) actively transport small neutral organic solutes termed "osmolytes" into the cytoplasm to replace the inorganic ions. This mechanism allows for volume regulation even at very high osmolarities since these electroneutral osmolytes do not disrupt cell functioning since intracellular ionic strength remains unchanged [Garcia-Perez & Burg 1991; Kwon & Handler 1995; Yancey 2005; Baltz 2012].

Organic osmolytes comprise a diverse group of solutes including small carbohydrates, polyols, methylamines, methylsulfonium solutes, and amino acids which have been shown to be used interchangeably in certain cells for volume regulation and likely varies depending on osmolyte availability in natural environments [Yancey 2005]. Some organic osmolytes can be synthesized within cells including sorbitol and GPC but the replacement of inorganic ions with organic osmolytes is largely accomplished through the intracellular accumulation of osmolytes from the extracellular environment via specific

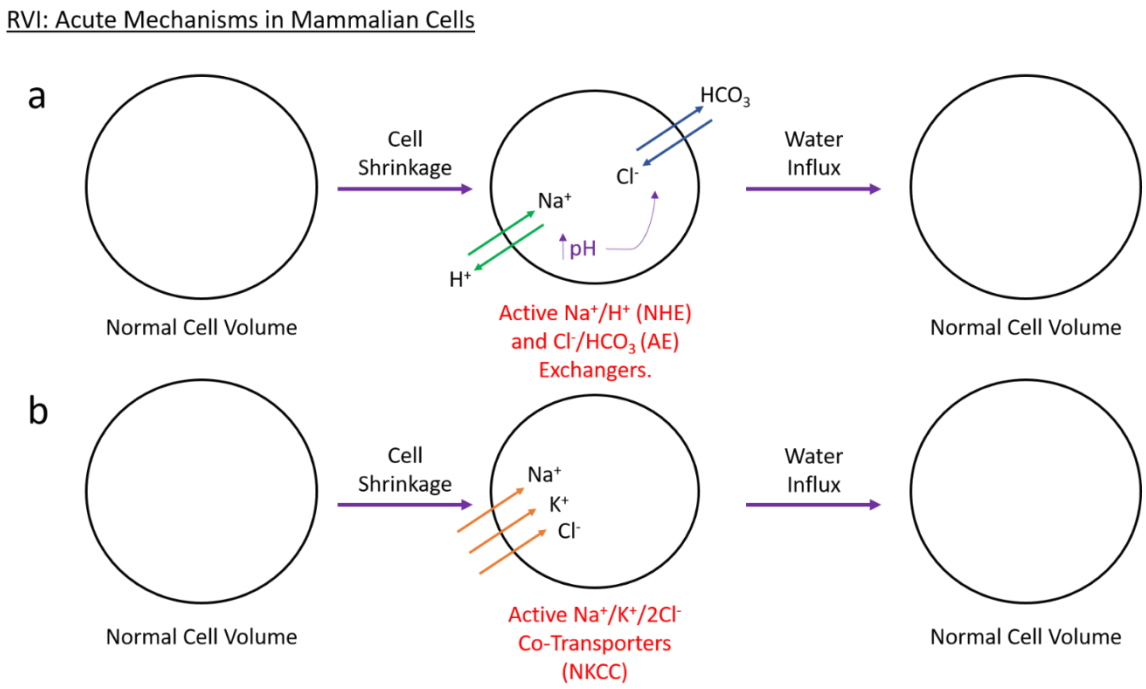

Figure 4. Acute mechanisms of regulatory volume increase (RVI) in mammalian somatic cells. (**a**) Following a decrease in cell volume, plasma membrane Na^+/H^+ exchangers (NHEs, *Slc9* family) are initially activated causing an increase in cytoplasmic Na^+ and an efflux of H^+ increasing the intracellular pH [Orlowski & Grinstein 2004; Alexander & Grinstein 2006; Baltz & Zhou 2012]. The intracellular alkalinisation due to H^+ efflux leads to activation of the Cl^-/HCO_3^- exchanger (AE2, *Slc4* family) causing Cl^- influx and HCO_3^- efflux which then decreases intracellular pH, countering the Na^+/H^+ exchange-induced increase [Jiang et al. 1997; Lang et al. 1998; Alper 2006]. This influx of Na^+ and Cl^- brings with it osmotically obliged water thus rapidly restoring cell volume with no net effect on pH when both exchangers are active. (**b**) Another mechanism of acute RVI involves the activation of $Na^+/K^+/2Cl^-$ co-transporters (NKCCs, *Slc12* gene family) and involves the coupled uptake of Na^+, K^+ and $2Cl^-$ into the cell along the ion gradient established by the low intracellular concentration of Na^+ and Cl^- [Moore-Hoon & Turner

2000; Hebert et al. 2004]. In response to a cell volume decrease the ubiquitously expressed NKCC1 transporter is activated via phosphorylation to facilitate the influx of these ions into the cell along with water to counteract osmotic cell shrinkage [Markadieu & Delpire 2014; Hebert et al. 2004].

plasma membrane transporters [Baltz 2001]. In mammalian somatic cells, there are four main organic osmolyte transporters that have been identified: the Na^+/myo-inositol transporter (SMIT), betaine/GABA transporter (BGT1), taurine/β-amino acid transporter (TAUT), and System A amino acid transporter [Garcia-Perez & Burg 1991; Kwon & Handler 1995]. SMIT (SLC5A3) is a Na^+-coupled transporter responsible for the transport of inositol into cells while BGT1 (SLC6A12) is a Na^+/Cl^--dependent transporter required to transport betaine into cells in response to cell shrinkage [Handler & Kwon 1996; Kwon & Handler 1995; Burg & Ferraris 2008]. TAUT (SLC6A6) is another Na^+/Cl^--dependent transporter which transports taurine and other β-amino acids such as β-alanine and hypotaurine into cells under hypertonic conditions [Baltz 2001; Burg et al. 2007]. The Na^+-dependent transporter System A has a large range of substrates including alanine, serine, glutamine, asparagine, threonine, and branched side chain amino acids which are all increased in response to hypertonic shrinkage but glutamine has been shown to be accumulated to the greatest levels by this transporter for volume regulation [Dall'Asta et al. 1999; Bussolati et al. 2001].

Acute inorganic ion accumulation through coupled Na^+/H^+ and Cl^-/HCO_3^- exchangers and/or NKCCs is a rapid response to cell shrinkage which is regulated by cell signalling including phosphorylation and is independent of protein synthesis [Okada 2004]. In contrast, organic osmolyte transport into somatic cells for volume regulation is a slow process (hours to days in duration) which requires an increase in transcription and synthesis of organic osmolyte transporters [Garcia-Perez & Burg 1991; Kwon & Handler 1995; Wehner et al. 2003]. In the kidney, this increase in organic osmolyte transport synthesis is regulated by the Tonicity Enhancer Binding Protein (TonEBP/NFAT5) which is active

under isotonic conditions but dramatically increases under hypertonic conditions. A prolonged increase in extracellular osmolarity stimulates a rapid (within 30 minutes) increase in the phosphorylation of existing TonEBP in the cell at serine and tyrosine residues and increased translocation to the nucleus. A slower (~12 hours) hypertonicity-induced increase in TonEBP transcription and synthesis also occurs to increase the overall amount of nuclear TonEBP [Ferraris et al. 2002; Woo et al. 2002]. TonEBP translocated to the nucleus forms dimers and binds to the tonicity-responsive enhancer (TonE) which drives transcription of osmoprotective genes including those for osmolyte transporters such as SMIT, BGT and TAUT as well as enzymes required for organic osmolyte synthesis such as aldose reductase which catalyzes the conversion of glucose to sorbitol [Miyakawa et al. 1999; Woo et al. 2002]. TonEBP is also negatively regulated under hypotonic conditions which causes a decrease in TonEBP transcription and synthesis as well as a decrease in the nuclear localization of TonEBP leading to a decrease in transcription of osmoprotective genes [Cha et al. 2001; Woo et al. 2002]. Thus, the osmoprotective effect of TonEBP in response to hypertonic conditions is dependent on two distinct regulatory mechanisms: the rate of TonEBP transcription and protein synthesis and the cellular distribution of TonEBP, with nuclear localization of TonEBP shown to be the greater regulator of activity (Figure 5) [Cha et al. 2001].

TonEBP has also been shown to increase the expression of genes involved in the adaptation of kidney medullary cells to hypertonic stress which acts independently of organic osmolyte accumulation. These genes include Hsp70, asporin, IGFBP5,7 and Enpp2 which, when knocked down, individually result in a decreased ability of cells to adapt to

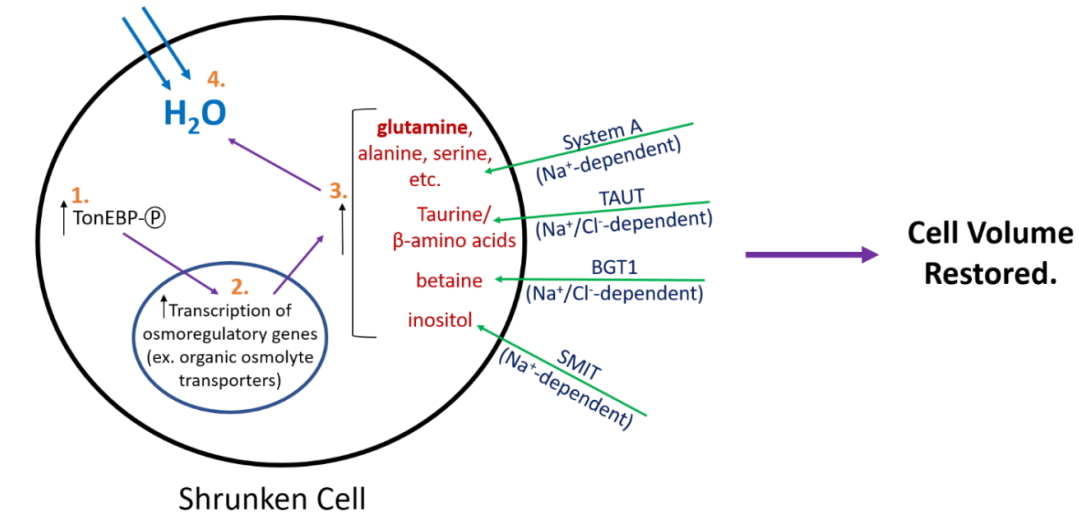

Figure 5. Chronic mechanisms of regulatory volume increase (RVI) in mammalian somatic cells. Cells exposed to chronically hypertonic extracellular osmolarities actively transport small neutral organic solutes termed "osmolytes" into the cytoplasm to replace inorganic ions allowing for volume regulation even at very high osmolarities [Garcia-Perez & Burg 1991; Kwon & Handler 1995; Yancey 2005; Baltz 2012]. A prolonged increase in extracellular osmolarity stimulates a rapid increase in the phosphorylation of existing TonEBP and increased translocation to the nucleus (**1.**). TonEBP translocated to the nucleus forms dimers and binds to the tonicity-responsive enhancer (TonE) which drives transcription of osmoprotective genes including those for osmolyte transporters such as SMIT, BGT and TAUT as well as enzymes required for organic osmolyte synthesis such as aldose reductase (AR) which catalyzes the conversion of glucose to sorbitol (2.) [Miyakawa et al. 1999; Woo et al. 2002]. An increase in the synthesis of organic osmolyte transporters (SMIT, TAUT, BGT1, System A) increases the influx of organic osmolytes (**3.**) and thus osmotically obliged water to restore set-point cell volume (**4.**).

hypertonic stress without decreasing the accumulation of organic osmolytes [Lee et al. 2011].

Although TonEBP is vital for osmotic adaptation in the hypertonic renal medulla, this transcription factor is also active under isotonic conditions in a variety of other tissues. TonEBP is largely expressed in brain, liver, thymus, heart, and placenta among other tissues suggesting that it may act as a "house-keeping" transcription factor regulating a range of functions in these cell types, not limited to increasing the intracellular organic osmolyte concentration [Miyakawaet al. 1999; Trama et al. 2000; Maouyo et al. 2001]. Although TonEBP has been extensively studied in the kidney, little is known regarding its role in osmoregulation and hypertonic adaptation in other mammalian tissues. TonEBP is most abundantly expressed in the human placenta, specifically in trophoblast cells, where its function in osmoregulation is unknown [Miyakawa et al. 1999; Shin et al. 2012]. A recent study involving the isolation and culture of human trophoblast cells (BeWo cells) from normal and pre-eclamptic placentas showed an increase in TonEBP expression as well as increased SMIT and AR under hypertonic culture conditions suggesting a role for TonEBP in increasing organic osmolyte concentrations in the placenta [Lee et al. 2014]. In addition to placental trophoblast cells, TonEBP was found to mediate the expression of genes encoding organic osmolyte transporters in various other tissues in response to changes in osmolarity. Decreases in osmolarity were found to decrease overall TonEBP expression in the thymus and liver while decreases in the expression of TonEBP-regulated genes such as SMIT and TAUT were tissue-specific; hypotonicity decreased SMIT expression in rat liver and muscle while TAUT was decreased in rat brain and thymus and both were increased by hypertonicity in the rat intervertebral disc cells [Zhang et al. 2003;

Tsai et al. 2006; Johnson et al. 2014]. From these data, it is clear that in non-renal tissues, TonEBP does appear to play a role in osmoregulation. However, the involvement of this mechanism specifically for volume regulation is largely unknown.

5.5 Regulatory volume decrease (RVD)

RVD occurs very differently from RVI in mammalian cells. Cell swelling under hypotonic conditions stimulates the efflux of ions and organic osmolytes from the cell through anion channels and transporters causing diffusion of osmotically obliged water out of the cell to restore the cell's "set-point" cell volume [Grunder et al. 1992; Strange et al. 1996]. In mammalian cells, RVD is accomplished mainly by efflux of Cl^-, K^+, and organic osmolytes which is accomplished by either electroneutral K^+/Cl^- co-transporters (KCCs) or passive release through coupled K^+ and Cl^- channels.

KCCs (SLC12A4-7) are expressed in many cell types and utilize the established K^+ gradient across the cell plasma membrane to transport Cl^- out of cells in a 1:1 ratio. KCC1 is the most ubiquitously expressed KCC transporter and seems to be primarily involved in volume regulation in cells [Hebert et al. 2004; Hoffmann 2009]. KCCs are activated in response to cell swelling to facilitate K^+ and Cl^- release. However, much still remains to be determined regarding regulation of the activity of these co-transporters. Kinetic studies mostly performed on red blood cells suggest that the same kinase which increases activity of NKCCs via phosphorylation in response to cell shrinkage also mediates KCC activity. First demonstrated in Xenopus oocytes, WNK (With No lysine = K) serine/threonine kinases have been identified as kinases that are involved in the regulation of NKCCs and

KCCs in response to osmotic perturbations through interaction with Ste20-type kinases (SPAK and OSR1) [Piechotta et al. 2002; Gagnon et al. 2006; Kahle et al. 2010]. Activation of volume-sensitive kinases (such as WNKs) following cell shrinkage causes phosphorylation of NKCCs and KCCs which leads to increased activation of NKCCs and inactivation of KCCs. The opposite effect occurs in response to cell swelling where these volume-sensitive kinases are inactivated leading to net dephosphorylation and inactivation of NKCCs and activation of KCCs [Hoffmann et al. 2009; Kahle et al. 2010; Jentsch 2016].

A more widely utilized mechanism of RVD involves the passive efflux of Cl^-, K^+, and organic osmolytes through coupled Cl^- and K^+ channels. The nearly ubiquitously expressed canonical Cl^- channels, which also allow passive diffusion of organic osmolytes out of the cell, are also referred to as "volume-sensitive organic osmolyte and anion channels" (VSOACs) [Nilius et al. 1994; Strange et al. 1996; Hoffmann et al. 2009]. Patch-clamp studies detecting outwardly rectifying anion currents have shown that VRACs permit increased passive Cl^- and organic osmolyte efflux in response to hypotonic cell swelling within minutes to restore cell set point volume [Nilius et al. 1994; Jentsch 2016]. Coupled cation efflux is required during anion release through VRACs in order to maintain electroneutrality in cells. This is accomplished by passive K^+ efflux through swell-activated K^+ channels which accompanies Cl^- release during cell swelling thus mediating KCl and uncharged organic osmolyte release along with osmotically obliged water to decrease cell volume [Hoffmann et al. 2009; Baltz 2012]. Recently, the molecular identity of VRACs was determined and LRRC8 proteins were identified as critical components of these channels required for Cl^- efflux and RVD based on knockdown studies [Voss et al. 2014; Qiu et al. 2014; Jentsch et al. 2016]. It was found that LRRC8A forms heteromers

with other LRRC8 isoforms which may alter Cl^- and organic osmolyte conduction depending on which isoform is present. Differences in subunit composition of LRCC8 proteins could indicate a role of these proteins in anion and organic osmolyte efflux selectivity and account for observed differences among VRACs in their ability to enable organic osmolyte diffusion out the cell [Planells-Cases et al. 2015; Syeda et al. 2016].

6. Cell volume regulation in oocytes and preimplantation embryos

6.1 Volume regulation in oocytes prior to ovulation: the zona pellucida (ZP)

The zona pellucida (ZP) is a thick and porous extracellular matrix composed primarily of glycoproteins which surrounds the mammalian oocyte. The mouse, porcine, and bovine ZP consist of three ZP glycoproteins called ZP1, ZP2, and ZP3 while in humans, hamsters, rats, monkeys, and rabbits an additional fourth ZP protein is present called ZP4 [Bleil & Wassarman 1980a; Wassarman 1988; Stetson et al. 2012; Yonezawa 2014]. The ZP accounts for ~10% of the total protein content of the mouse egg with mouse ZP2 (mZP2) and mouse ZP3 (mZP3) comprising ~80% of total ZP protein and mouse ZP1(mZP1) comprising ~20%.These mZP glyocoproteins are heterogeneously glycosylated with complex-type asparagine-linked (N-) and serine/threonine-linked (O-) oligosaccharides [Boja et al. 2003].N-linked oligosaccharides have previously been shown to be required for the secretion and assembly of mZP2 but not mZP3 and these N- and O-linked chains seem to be required for sperm-ZP binding during fertilization although this process is still incompletely understood [Roller & Wassarman 1983; Evans 2002; Wassarman & Litscher 2013; Yonezawa 2014].

The structure of ZP glycoproteins is relatively well conserved among mammals and consists of several regions that are common to the various ZP polypeptides. Mouse and human ZP glycoproteins are synthesized as precursor polypeptides composed of an N-terminal signal sequence, a ZP domain (ZPD), a C-terminal propeptide (CTP), and a transmembrane domain each of which has been shown to participate in various ways to the secretion and assembly of ZP glycoproteins (Figure 6) [Wassarman 2008].

ZP glycoprotein synthesis, secretion, and assembly in the mouse

Several lines of evidence have conclusively shown that mouse ZP glycoproteins are exclusively synthesized by the oocyte within the ovarian follicle and that the ZP increases in thickness concomitantly with growth of the oocyte during oogenesis [Haddad & Nagai 1977; Bleil & Wassarman 1980b; Roller & Wassarman 1983; Shimizu et al. 1983; Lira et al. 1990]. The ZP is absent in small non-growing oocytes within primordial follicles, increases in thickness substantially as the oocyte increases in diameter, and is completely formed by the time the oocyte is fully grown (~80 μm in diameter). During oocyte growth, the number of mZP3 mRNA transcripts increases from undetectable levels in non-growing oocytes to ~300,000 transcripts when oocytes are mid-growth and then decreases back to undetectable levels in MII eggs illustrating the dramatic increase in mZP protein synthesis which occurs during oogenesis [Roller et al. 1989; Epifano et al.1995; Liang et al. 1990;Wassarman & Litscher 2013].The fully formed ZP appears as a fibrillar porous structure in which mZP2 and mZP3 polymerize to form long fibrils which are connected by mZP1 dimers [Wassarman & Mortillo 1991; Jovine et al. 2002; Wassarman 2008].

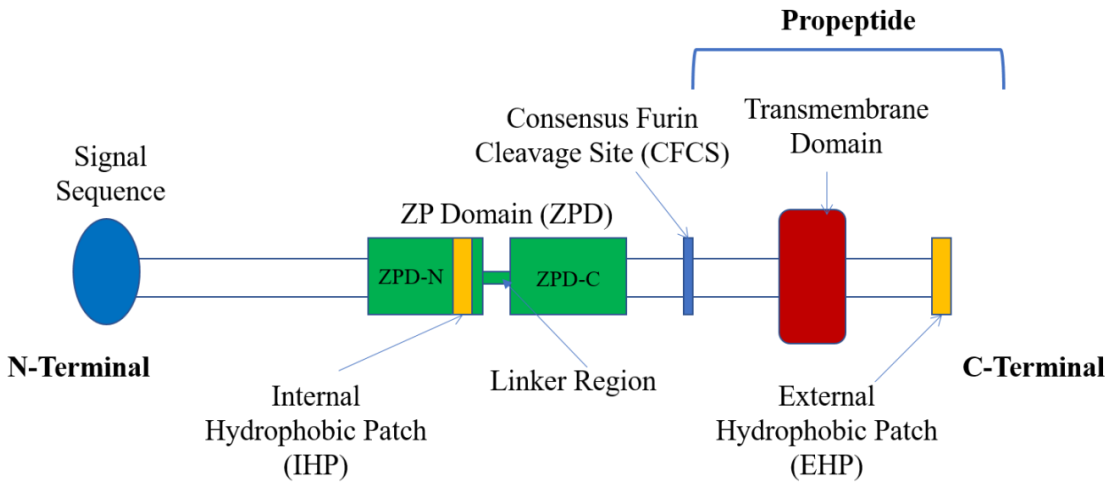

Figure 6. Zona pellucida (ZP) glycoprotein structure. The structure of ZP glycoproteins is relatively well conserved among mammals and consists of several regions that are common to the various ZP polypeptides. Mouse and human ZP glycoproteins are synthesized as precursor polypeptides composed of an N-terminal signal sequence, a bipartite ZP domain (ZPD), a C-terminal propeptide (CTP), and a transmembrane domain each of which has been shown to participate in various ways to the secretion and assembly of ZP glycoproteins [Wassarman 2008].

Assembly of the mouse ZP was previously demonstrated to occur from the innermost surface (adjacent to the oocyte) outward as ZP glycoproteins are incorporated following secretion from the oocyte [Qi et al. 2002]. Studies using heterozygous and homozygous null mutant female mice have shed light on the importance of each mZP glycoprotein for ZP synthesis. Abolishment of either mZP2 or mZP3 synthesis prevented ZP formation resulting in infertility while the absence of mZP1 synthesis produced a highly porous ZP causing sub-fertility in mice [Liu et al. 1996; Rankin et al. 1996, 1999, 2001]. These results suggest that although synthesized independently, mZP2 and mZP3 must both be present for assembly into the ZP [Wassarman & Litscher 2013]. As mentioned above, ZP glycoproteins contain several regions which are common among mammals and further examination into these regions has provided insight into the mechanism of mZP1-3 secretion and assembly into the ZP.

Polymerization of mZP glycoproteins is accomplished at the zona pellucida domain (ZPD) which is located close to the C-terminus of the ZP glycoprotein and is composed of ~260 amino acids and eight cysteine residues. This region is present in many eukaryotic extracellular proteins where it serves a variety of functions depending on the expressed protein [Bork & Sander 1992; Jovine et al. 2005]. The ZPD is a bipartite structure containing an N-terminal subdomain (NTS) and a C-terminal subdomain (CTS) which are connected by a protease-sensitive linker region [Han et al. 2010; Jovine et al. 2004; Llorca et al. 2007; Wassarman & Litscher 2013]. The NTS has previously been shown to be required for polymerization of ZPDs into fibrils and contains the internal hydrophobic patch (IHP) which is associated with the external hydrophobic patch (EHP) located downstream of the consensus furin cleavage site (CFCS, Figure 6).

Prior to secretion and assembly, mZP glycoproteins are synthesized within the oocyte as precursor polypeptides and transported to the plasma membrane in large vesicles originating from the trans-Golgi [Qi et al. 2002; Hoodbhoy et al. 2006; Jiminez-Movilla& Dean 2011]. Both mZP2 and mZP3 were shown to be co-localized within these vesicles but do not polymerize until after processing at a CFCS and after they are secreted from the oocyte plasma membrane. The prevention of mZP2 and mZP3 interaction within secretory vesicles prior to CFCS proteolytic processing is thought to depend on the association of the internal hydrophobic patch (IHP; located within the ZPD upstream of the CFCS) and the external hydrophobic patch (EHP; located near the C-terminus downstream of the CFCS) [Jovine et al. 2004, 2005; Han et al. 2010; Wassarman & Litscher 2013].Cleavage at the CFCS by a member of the furin family of serine proteases is proposed to disrupt the interaction of the IHC and EHC thus allowing polymerization of mZP glycoproteins to occur [Zhao et al. 2003]. Processing at the CFCS may also be required for secretion of mZP glycoproteins. However, conflicting results have been obtained using transgenic mice with a mutated CFCS and it is possible that other proteases other than furin proteases may be able to cleave mZP glycoproteins at or near this site [Williams & Wassarman 2001; Qi et al. 2002; Zhao et al. 2002]. Future studies are required to further elucidate the mechanism of ZP glycoprotein secretion and assembly into the ZP.

The role of the ZP in oocyte volume regulation prior to ovulation

Prior to ovulation and throughout oogenesis, the oocyte is tightly adhered to the ZP matrix by microvilli [Tartia et al. 2009]. This intimate interaction between the ZP and oocyte plasma membrane is vital to oocyte development and viability since processes

spanning the ZP (transzonal processes) facilitate bi-directional communication between the oocyte and surrounding granulosa cells via gap junctions [Anderson & Albertini 1976; Simon et al. 1997; Tartia et al. 2009]. The tight association of the oocyte to the rigid ZP has also been demonstrated to be required for cell volume regulation in fully grown oocytes before ovulation within the ovarian follicle.

After the ovulatory stimulus, fully grown GV oocytes resume meiosis and re-arrest at metaphase of meiosis II as discussed above. During this transition to MII eggs, the first polar body is released from the oocytes and the oocyte detaches from the ZP forming a space termed the "perivitelline space" (PVS) located between the oocyte and ZP [Talbot & Dandekar 2003]. Initially, the development of the PVS was thought to occur as a result of oocyte cell volume decrease due to the first polar body release, however, Tartia et al. demonstrated that the majority of the observed cell volume decrease occurs by the MI stage before the first polar body is emitted. It was also shown that this decrease in oocyte cell volume and PVS formation occurs *in vitro* in GV oocytes isolated from ovaries and maintained in meiotic arrest in which polar body release is prevented [Tartia et al. 2009].

GV oocytes freshly isolated from ovarian follicles are tightly adhered to the ZP prior to ovulation and lose this association ~2-3 hours after ovulation or removal from the ovarian follicle, although the stage in development when oocytes first acquire the ability to detach from the ZP is unknown. This oocyte-ZP detachment in fully grown oocytes occurs concomitantly with the activation of independent volume regulation involving the transport of organic osmolytes, especially glycine, into the oocyte (discussed below) [Steeves et al. 2003; Tartia et al. 2009]. Prior to ovulation therefore, oocyte volume appears to be maintained through a passive mechanism dependent on firm contact with the rigid ZP

matrix which is lost following ovulation leading to the activation of independent volume regulatory mechanisms to maintain oocyte volume.

6.2 Volume regulation in oocytes and preimplantation embryos

Acute volume regulation in oocytes and preimplantation embryos

As discussed previously, mammalian somatic cells initially respond to acute decrease in cell volume primarily through the increased intracellular accumulation of Na^+ and Cl^- by the coupled activation of the Na^+/H^+ exchanger and the Cl^-/HCO_3^- exchanger. The increase of NaCl and osmotically obliged water within the cell increases cell volume thereby restoring the cell set-point volume without disrupting intracellular pH [Lang et al. 1998; Hoffman et al. 2009]. This acute volume regulatory mechanism is also present in mouse preimplantation embryos and is primarily accomplished by the NHE1 isoform of the Na^+/H^+ exchanger and the AE2 Cl^-/HCO_3^- exchanger (Harding et al. 2002; Zhou et al. 2009; Erdogan et al. 2011; Siyanov & Baltz 2013).

NHE1 activity and subsequent Cl^-/HCO_3^- exchanger activation was clearly shown by our laboratory to be elicited in response to a cell volume decrease in preimplantation embryos exposed to hypertonic conditions, an ability which was greatest at the 2-cell stage and began to decrease during compaction [Zhou & Baltz 2013]. The mechanisms regulating NHE1 activation in response to volume changes is still incompletely understood in somatic cells and appears to vary between cell types. However, it is known that cell volume-mediated NHE1 activation is accompanied by increased protein phosphorylation although not phosphorylation of NHE1 directly [Grinstein et al. 1992]. In early mouse

preimplantation embryos, phosphorylation of the non-receptor tyrosine kinase Janus kinase 2 (JAK2) was shown to be increased when embryo volume was decreased and the presence of JAK2 inhibitors prevented NHE1 activation under hypertonic conditions [Zhou & Baltz 2013]. JAK2-mediated NHE1 activation was previously found to involve the phosphorylation and activation of Calmodulin (CaM) in Chinese Hamster Ovary (CHO) cells with CaM directly binding and activating NHE1 [Gatsios et al. 1998; Garnovskaya et al. 2003]. Similarly, in early preimplantation embryos CaM inhibition prevented NHE1 activation in response to a decrease in cell volume suggesting that acute RVI in preimplantation embryos relies on inorganic ion uptake via NHE1 (and AE2) mediated by JAK2-CaM signalling [Zhou et al. 2009; Zhou & Baltz 2013].

Interestingly, NHE1 activity is increased in response to an increase in intracellular acidosis in freshly isolated GV oocytes but is not activated when they are exposed to hypertonic conditions. Thus, NHE1 is present and can be activated by a decrease in intracellular pH, but is nonetheless unable to respond to a cell volume decrease. From 2-6 hours following removal from the follicle however, NHE1 is able to respond to decreased cell volume as well as decreased intracellular pH, until ~8 hours. After this NHE1 becomes quiescent and cannot be activated by either stimulus until after fertilization [Zhou et al. 2013]. This downregulation in NHE1 (and also AE2) activity coincides with oocyte meiotic progression although NHE1 was also inactivated in cultured oocytes maintained in meiotic arrest using cell-permeant synthetic cAMP. The timing of this decrease in inorganic ion transport into oocytes occurs while the oocyte is adhered to the ZP and immediately following oocyte-ZP detachment and the decrease in oocyte volume of ~20%. After this significant decrease in oocyte volume, the intracellular accumulation of the organic

osmolyte glycine is greatly increasing in oocytes through the GLYT1 transporter (discussed below). It appears that the NHE1/AE2 activity increase in response to volume decrease is inhibited in GV oocytes prior to ovulation since the oocyte is tightly adhered to the ZP and thus does not require independent volume regulatory mechanisms to be active and increased external osmolarity cannot decrease oocyte cell volume. Activation of NHE1/AE2 may need to be suppressed immediately following oocyte-ZP detachment since a massive influx of inorganic ions could occur to correct for the ~20% decrease in oocyte volume which follows oocyte-ZP detachment. This would be detrimental to cell functioning due to an increase in intracellular ionic strength, implying that organic osmolyte uptake would be the preferred mechanism of volume regulation at this stage (discussed in detail below) [Zhou & Baltz 2013; Tartia et al. 2009].

Longer-term volume regulation in oocytes and preimplantation embryos: organic osmolytes

Volume regulation by increased organic osmolyte transport into somatic cells via the four known organic osmolyte transporters SMIT, BGT1, TAUT, and System A was discussed above. This mechanism of volume regulation is employed within cells of tissues such as the kidney which are exposed to sustained hypertonic environments and thus replace intracellular inorganic ions with neutral organic osmolytes to maintain set-point cell volume without perturbing cell functioning as a result of increased intracellular ionic strength [Garcia-Perez &Burg 1991; Hoffmann et al. 2009]. In these cells, the increased uptake of organic osmolytes is regulated by the TonEBP transcription factor which increases expression of organic osmolyte transporters under hypertonic conditions (Figure

5). This process can vary from hours to days in duration since new organic osmolyte transporters must be synthesized [Cha et al. 2001; Ferraris et al. 2002; Woo et al. 2002].

In contrast to the cells of the kidney, preimplantation embryos are exposed to a relatively constant osmolarity within the oviduct (~300 mOsM [Collins and Baltz, 1999; Fiorenza et al., 2004]). However, as mentioned above, embryos of various mammalian species underwent developmental arrests when cultured at oviductal osmolarities (~300 mOsM) in the absence of specific amino acids or their derivatives. Since volume regulation under these conditions would occur primarily by an increase in intracellular inorganic ions, it was hypothesized that preimplantation embryos also utilize organic osmolytes for volume regulation to prevent high intracellular ionic strength which can cause developmental arrests in cleavage-stage embryos [Lawitts & Biggers 1992; Biggers et al. 1993; Dawson & Baltz 1997].

As predicted, the addition of amino acids to culture medium abrogated the effects of "high" osmolarity on embryo development. The most effective osmoprotective substrates for mouse preimplantation embryos were found to be glycine, glutamine, proline, and betaine; β-alanine and hypotaurine also acted as osmoprotectants but only at much higher concentrations [Dawson & Baltz 1997]. Interestingly, the four organic osmolyte transporters identified in somatic cells do not appear to be responsible for transporting these osmolytes in preimplantation embryos. TAUT is expressed throughout preimplantation embryo development and is able to transport β-amino acids into embryos. However, among β-amino acids tested, only β-alanine was shown to be able to act as an osmoprotectant in early embryos and then only when insufficient glycine was available [Van Winkle et al. 1994; Dawson & Baltz 1997; Hammer & Baltz 2003]. Based on this, it

is likely that accumulated β-amino acids perform alternative functions to support preimplantation embryo development possibly by functioning as an antioxidant [Liu et al., 1995; Devreker et al., 1999; Hammer & Baltz 2003]. System A is able to transport all of the organic osmolytes shown to be osmoprotective in early embryos but is not expressed until the blastocyst stage and thus cannot be responsible for organic osmolyte transport in cleavage stage embryos [Jamshidi & Kaye 1995]. The absence of typical organic osmolyte transporter expression in early preimplantation embryos summons the question of how these osmoprotective substrates are transported into oocytes, eggs, and embryos.

The SIT1 Na^+/Cl^--dependent transporter (*Slc6a20a*) was shown to be responsible for betaine and proline transport into embryos. SIT1 is activated following fertilization and persists until the 2-cell stage and is inactive by the 4-cell stage [Anas et al. 2007, 2008; Hammer & Baltz 2002]. Prior to fertilization, no measurable betaine transport occurs in oocytes and eggs however, MII eggs were shown to contain high levels of betaine despite this lack of transport [Baltz& Zhou 2012; Corbett et al. 2014]. Since betaine is not transported into embryos until after fertilization, betaine accumulation in oocytes and eggs may occur by two possible mechanisms: betaine transport from cumulus granulosa cells and/or betaine synthesis directly within oocytes. Recently, Corbett et al. demonstrated that cumulus granulosa cells were shown to express the y+L-type transporter SLC7A6 which can transport betaine while no expression was detected in denuded GV oocytes. This suggests that betaine accumulation in oocytes before fertilization may partly depend on diffusion of betaine through gap junctions from the cumulus granulosa cells to the oocyte [Corbett et al. 2014]. Additionally, our lab has recently shown that betaine may be synthesized from choline by choline dehydrogenase (CHDH) within oocytes during

meiotic maturation [McClatchie et al. 2017]. The contribution of betaine and proline accumulation to cell volume regulation in early embryos still remains to be determined, but a clear role for glycine in volume homeostasis within oocytes and early embryos has been well established.

Glycine has been shown to be extremely effective for osmoprotection of embryos when cultured at osmolarities similar to those found in the oviduct (~300 mOsM). The addition of 1mM glycine to culture medium at an osmolarity of ~310mOsM significantly rescued development of zygote embryos to the blastocyst stage, an effect which was also possible with glutamine [Van Winkle et al. 1990c; Dawson & Baltz 1997; Hadi et al. 2005]. The half-maximally effective concentration of glycine was shown to be 50μM [Hammer & Baltz, 2002], a concentration well below that found in mouse oviductal fluid (0.5-3.0mM) indicating that substantial glycine is available for osmoprotection of early embryos *in vivo* [Harris et al. 2005]. Consistent with this, freely soluble glycine is accumulated to high levels in MII eggs, 1-cell, and 2-cell embryos (~4-10 pmoles) isolated from mouse oviducts which is decreased by the morula stage (0.1-0.3 pmoles). Levels of endogenous glycine are low in GV oocytes and MI eggs reflecting the stage when glycine transport is first activated as discussed below [Van Winkle & Dickinson 1995; Steeves et al. 2003; Steeves & Baltz 2005]. Glycine accumulation into oocytes, eggs, and early cleavage-stage embryos was also shown to occur *in vitro*. Glycine accumulation was first detected at the MII stage and persisted until the 2-cell stage while glycine accumulation was low in freshly isolated GV oocytes, MI eggs, and 4-cell embryos [Tartia et al. 2009]. Thus, glycine-dependent volume regulation becomes activated in oocytes after their removal from the ovarian follicle coincident with meiotic maturation and persists until the 4-cell stage and is

nearly absent by the morula stage. Glycine transport into oocytes, eggs, and embryos has been shown to occur exclusively by the Na^+/Cl^--dependent GLYT1 transporter in its seemingly unique role as an organic osmolyte transporter [Van Winkle et al. 1988a; Steeves et al. 2003]. See Figure 7 below for a summary of active organic osmolyte transporters during early preimplantation embryo development.

7. The GLYT1 glycine transporter

7.1 GLYT1 gene and protein expression and function

GLYT1 (SLC6A9) is a member of the Na^+/Cl^--dependent neurotransmitter transporter (NTT) or *Slc6*family of transporters that also includes transporters for GABA, serotonin, dopamine, norepinephrine, proline, betaine (SIT1), taurine (TAUT) and some orphan transporters [Chen et al. 2004; Zafra & Giménez 2008]. GLYT1 as well as GLYT2 (*Slc6a5*) have been identified as high-affinity glycine transporters that are encoded by different genes, both of which have previously been cloned [Guastella et al., 1992; Liu et al., 1992, 1993; Smith et al., 1992]. These glycine transporters differ in their sensitivities to sarcosine (N-methylglycine) and also display differences in their cellular distribution, transport mechanisms, and function which has been most extensively studied in the central nervous system (CNS) where these transporters are involved in the regulation of synaptic glycine concentrations involved in neurotransmission (discussed below) [Supplisson & Bergman 1997]. The following sections will focus on the GLYT1 transporter which is of primary interest for this research project since expression of the GLYT2 transporter is restricted to the central nervous system and not found in oocytes or preimplantation

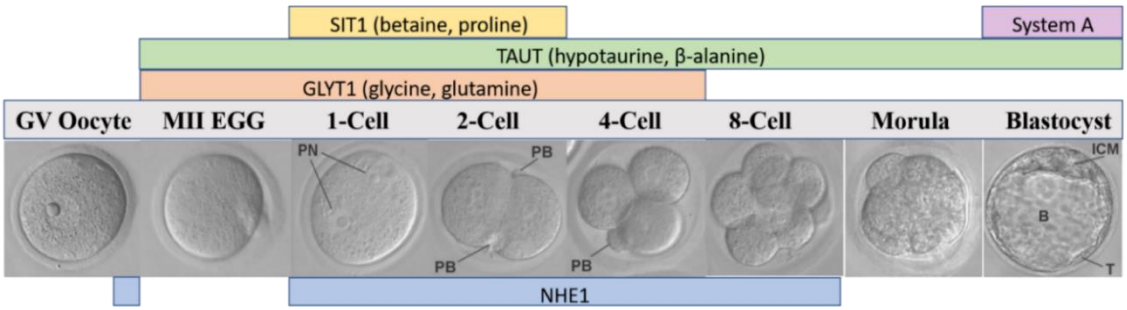

Figure 7. Organic osmolyte transporters during preimplantation embryo development. Organic osmolyte transporter activity varies throughout preimplantation embryo development with certain organic osmolytes acting more effectively for volume regulation. TAUT is expressed throughout preimplantation embryo development and is able to transport β-amino acids into embryos [Van Winkle et al. 1994; Dawson & Baltz 1997; Hammer & Baltz 2003]. The SIT1 Na^+/Cl^--dependent transporter (*Slc6a20a*) was shown to be responsible for betaine and proline transport into embryos which is activated following fertilization and persists until the 2-cell stage and is inactive by the 4-cell stage [Anas et al. 2007, 2008; Hammer & Baltz 2002]. System A is able to transport all of the organic osmolytes shown to be osmoprotective in early embryos but is not expressed until the blastocyst stage and thus cannot be responsible for glycine uptake in cleavage stage embryos [Jamshidi & Kaye 1995]. Glycine is the most effective organic osmolyte in early cleavage stage embryos and is transported exclusively by the GLYT1 transporter. GLYT1 activation coincides with meiotic maturation and persists until the 4-cell stage and is absent by the morula stage [Steeves et al. 2003; Tartia et al. 2009]. Interestingly, the ability of the Na^+/H^+ exchanger (NHE1) coupled with the Cl^-/HCO_3 exchanger (AE2) to acutely restore cell volume is only possible during a short window of time following removal from the

ovarian follicle (from 2-6 hours until ~8 hours), after this NHE1 becomes quiescent and cannot be activated by either stimulus until after fertilization [Zhou et al. 2013].

embryos; a brief discussion will be presented where major differences in expression or function exist between GLYT1 and GLYT2.

GLYT1 isoform expression and cellular distribution

GLYT1 expression has been detected to varying degrees within most tissues but is most highly expressed in glial processes within the brain and spinal cord. In contrast, GLYT2 expression was found to be more restricted to glycinergic neurons in the spinal cord, brainstem, and cerebellum [Borowsky et al. 1993; Zafra et al. 1995a; Zafra et al. 1995b; Jursky & Nelson 1996; Spike et al. 1997]. Although historically GLYT1 was thought to be exclusively expressed in glial cells, low levels of GLYT1 have more recently been detected in neurons primarily at glutamatergic pre- and post-synaptic membranes indicative of a role for GLYT1 in regulating glycine binding to NMDA receptors as discussed briefly below [Smith et al. 1992; Supplisson & Bergman 1997; Cubelos et al. 2005a; Zafra & Giménez 2008]. Multiple variants of the GLYT1 transporter have also been identified including GLYT1a, GLYT1b, GLYT1c, GLYT1e, and GLYT1f.

GLYT1a and GLYT1b are the most well characterized GLYT1 isoforms and are expressed in numerous species including human, mouse, rat, and bovine [Guastella et al. 1992; Borowsky et al. 1993; Kim et al. 1994; Hanley et al. 2000]. These GLYT1 isoforms are produced by the use of alternative promoters and differ only by 19 amino acids in the N-terminal region with GLYT1b containing an additional fourteen residues at the proximal end of the N-terminus [Borowsky & Hoffman 1998; Howard & Hirst 2011]. Despite this sequence variation, both GLYT1a and GLYT1b display similar substrate specificity,

transport kinetics, and function but differ in their respective expression sites [Smith et al. 1992; Durkin et al. 2011]. For instance, GLYT1a is expressed throughout the central nervous system and peripheral tissues while GLYT1b expression is limited to brain and spinal cord tissues [Borowsky et al. 1993; Liu et al. 1993]. GLYT1c is expressed in human brain and at low levels in kidney (but not in mouse) and is generated as a result of alternative splicing. This isoform shares a nearly identical sequence similarity to GLYT1b and does not differ in function or transport mechanisms from either GLYT1a or GLYT1b isoforms [Kim et al. 1994; Durkin et al. 2011; Howard & Hirst 2011]. The final GLYT1 isoforms, GLYT1e and GLYT1f, have been identified only in bovine retina and contain a novel C-terminus which was shown to alter transport kinetics but not ion dependence or pharmacological properties. Interestingly, GLYT1e and GLYT1f isoforms were shown to uniquely interact with the GABA receptor however the purpose of this interaction and whether this occurs in other species has yet to be investigated [Hanley et al. 2000].

GLYT1 structure, transport mechanisms, and pharmacology

Similar to other members of the NTT family, the structure of the GLYT1 (and GLYT2) transporter is predicted to consist of twelve transmembrane domains with the amino (N-) and carboxyl (C-) terminal tails located intracellularly [Olivares et al. 1994; Nelson et al. 1998]. Four N-glycosylation sites have been identified on the large second extracellular loop between transmembrane domain (TMD) three and four which are glycosylated during transit of GLYT1 through the Golgi apparatus. Studies using site-directed mutagenesis of these glycosylation sites have revealed that glycosylation is likely required for appropriate targeting of GLYT1 to the plasma membrane resulting in an

overall decreased glycine transport into cells when this glycosylation is disrupted [Olivares et al. 1995; Olivares et al. 1997; Zafra & Giménez 2008]. In addition, GLYT1a was shown to contain two putative C-terminal phosphorylation sites while GLYT1b also contains two additional N-terminal phosphorylation sites indicating possible regulation by protein kinases (Figure 8) [Guastella et al. 1992; Liu et al. 1993].

The GLYT1 transporter depends on the co-transport of Na^+ and Cl^- along their ion gradient to transport substrate into or out of the cell [Nelson 1998; Rudnick 1998]. Briefly, initial Na^+ and Cl^- binding to the extracellular-facing transporter induces a conformational change in the transporter which allows substrate (glycine) binding to occur. Following substrate binding, the transporter changes from an outward facing position to an inward facing position exposed to the cytoplasm of the cell. Na^+ ions are first released from the transporter into the intracellular space followed by glycine and then Cl^- after which the transporter spontaneously returns to the outward facing position (facing the extracellular space) [Aragón et al. 1987; Nelson 1998; Eulenberg et al. 2005].

The requirement for Na^+ and Cl^- ions for glycine transport is true for both GLYT1 and GLYT2 however, the thermodynamic coupling to the Na^+ gradient differs between these two transporters with GLYT1 requiring two Na^+ ions for glycine binding while GLYT2 requires three Na^+ ions; a distinction which is significant for the differing roles of these two glycine transporters in the CNS as discussed briefly below [Aragón et al. 1987; Roux & Supplisson 2000; Zafra & Giménez 2008]. The mechanism of ion and substrate transport across the plasma membrane by members of the SLC transporter family has largely been inferred from the known three-dimensional structure of the related leucine bacterial transporter, LeuTAa. Briefly, a region containing the residues thought to be

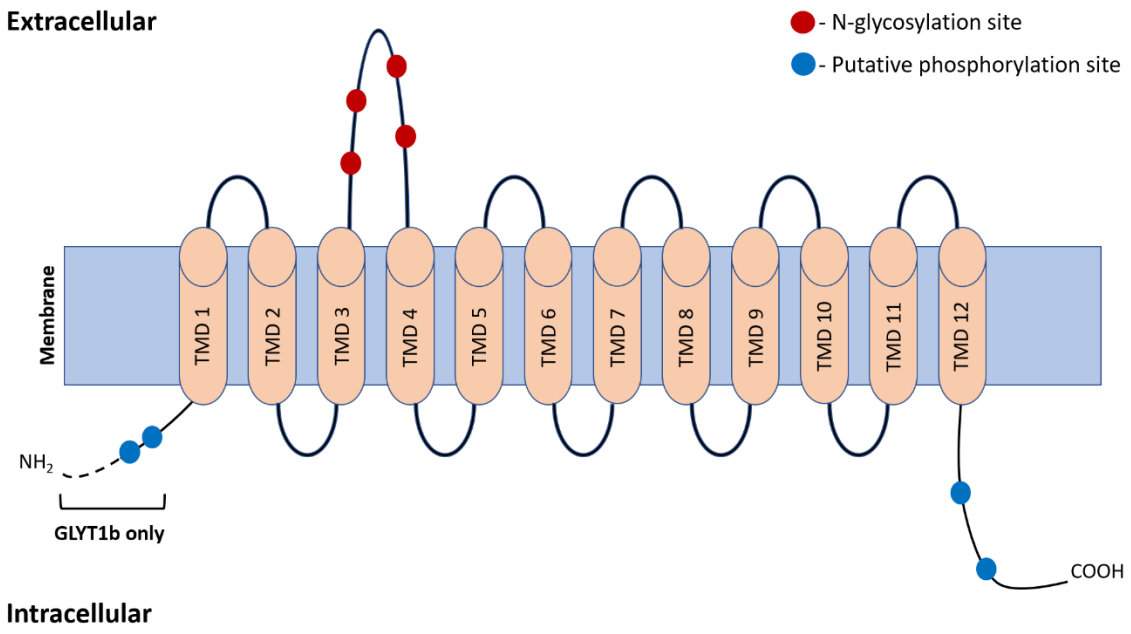

Figure 8. GLYT1 transporter structure. The GLYT1 (and GLYT2) transporter is predicted to consist of twelve transmembrane domains with the amino (N-) and carboxyl (C-) terminal tails located intracellularly [Olivares et al. 1994; Nelson et al. 1998]. Four N-glycosylation sites have been identified on the large second extracellular loop between transmembrane domain (TMD) three and four which are glycosylated during transit of GLYT1 through the Golgi apparatus [Olivares et al. 1995; Olivares et al. 1997; Zafra & Giménez 2008]. In addition, GLYT1a was shown to contain two putative C-terminal phosphorylation sites while GLYT1b contains two additional phosphorylation sites and 14 additional amino acids in the N-terminus [Guastella et al. 1992; Liu et al. 1993].

involved in ion and substrate binding associates the TMD 1-5 part of the transporter with TMD 6-10 part. This axis provides a junction where specific aromatic residues act as gates to regulate ion and substrate binding on both the extracellular and cytoplasmic faces of the transporter. Thus, binding of ions and substrates on the extracellular side of the transporter is thought to occur when the extracellular gates are open and the cytoplasmic gates are closed. Upon binding of these ions and substrates, it has been proposed that a conformational change is induced in the transporter which enables release of the bound ions and substrate into the cell as the extracellular gates are closed and cytoplasmic gates are open [Zafra & Giménez 2008; Yamashita et al. 2005; Vandenberg et al. 2007].

The pharmacology of GLYT1and GLYT2 has been a focus of research due largely to the implications in the treatment of schizophrenia. As discussed below, GLY transporters are involved in the regulation of glycine concentrations at both glycinergic synapses where glycine acts as an inhibitory neurotransmitter and glutamatergic synapses where glycine is a co-agonist of NMDA receptors (NMDARs) [Zafra & Giménez 2008]. Schizophrenia has been linked to hypofunction of NMDARs and thus various classes of GLYT1 inhibitors have been developed which elevate synaptic glycine concentrations in order to treat the symptoms of schizophrenia [Johnson & Asher 1987; Millan 2005; Coyle 2006; Lechner 2006]. Since GLYT1, rather than GLYT2, has been shown to be expressed at glutamatergic terminals and post-synaptic glutamatergic synapses, this specific transporter is the primary target to inhibit glycine uptake at these sites [Cubelos et al. 2005a; Roux et al. 2001]. GLYT1 can be distinguished pharmacologically from GLYT2 by the sarcosine sensitivity of each transporter. GLYT1 is able to transport both glycine and sarcosine (N-methylglycine) while GLYT2 can only transport glycine, a specificity

which was found to depend on the difference of a single amino acid on TMD 6 within the substrate binding axis. This was demonstrated in *Xenopus laevis* oocytes injected with human cRNA in which Ser-481 in GLYT2, corresponding to Gly-305 in GLYT1, was substituted for a Gly residue enabling GLYT2 to transport sarcosine [Vandenberg et al. 2007]. Two main classes of potent GLYT1 inhibitors are used to specifically inhibit this transporter and include sarcosine-based and non-sarcosine-based inhibitors. Sarcosine-based inhibitors such as NFPS (N-[3-(4'-fluorophenyl)-3-(4'phenylphenoxy) propyl] sarcosine) and ORG24598 (R,S)-(±)N-methyl-N-[(4-trifluoromethyl)phenoxy-3-phenyl-propylglycine) were found to be non-competitive inhibitors which inhibit GLYT1 regardless of the concentration of glycine and appear to be irreversible. In contrast, non-sarcosine-based inhibitors such as SSR504734(2-chloro-N[(S)-phenyl[(2S)-piperidin-2-yl]methyl]-3trifluoromethylbenzamine, monohydrochloride) and N-methyl-SSR504734 reversibly inhibit GLYT1 and are glycine-competitive. The use of these inhibitors for therapeutic purposes would therefore need to be considered carefully to avoid irreversible GLYT1 inhibition potentially increasing glycine concentrations to undesirable levels in specific areas of the central nervous system [Mezler et al. 2008]. The GLYT1 inhibitor ORG23798 (bis(4-fluorophenyl)methylenepiperidineacetic acid, lithium salt) has previously been demonstrated to be a potent and specific inhibitor of GLYT1 in preimplantation mouse embryos which eliminated the osmoprotective effect of glycine on early embryos cultured at physiological osmolarities [Steeves et al. 2003].

7.2 GLYT1 function in the nervous system

As mentioned above, GLYT1 and GLYT2 have been extensively studied in the central nervous system (CNS) where glycine has been shown to participate in both excitatory and inhibitory neurotransmission. Glycine is a major inhibitory neurotransmitter within the CNS which is exocytosed from glycinergic nerve terminals through a calcium-dependent mechanism following depolarization and binds to glycine receptors on the postsynaptic membrane to result in hyperpolarization of post-synaptic glycinergic neurons [Zafra & Giménez 2008]. The high expression of GLYT2 at presynaptic glycinergic nerve terminals and the requirement to bind three Na^+ ions to transport glycine is consistent with a role for GLYT2 in replenishing the stores of pre-synaptic glycine into vesicles following depolarization of the membrane [Poyatos et al. 1997; Roux et al. 2001]. In contrast, GLYT1 has been shown to be highly expressed in glial elements in glycinergic regions in the CNS where it most likely is required for depleting the extracellular synaptic glycine concentration; although the lower thermodynamic coupling to the Na^+ gradient characteristic of GLYT1 also enables reverse transport of glycine into the synaptic cleft, which may be relevant for glycine-mediated inhibition of neurotransmission at glycinergic neurons or activation of NMDARs [Cubelos et al. 2005a; Eulenberg et al. 2005]. Studies using *Glyt1* and *Glyt2* knockout mice support these respective roles for GLYT1 and GLYT2 [Gomeza 2003a,b].

In addition to its role as an inhibitory neurotransmitter, glycine has also been shown to act as a co-agonist with the excitatory neurotransmitter glutamate to activate NMDARs [Johnson & Ascher 1987]. GLYT1 has been detected at glutamatergic neurons in nerve terminals as well as post-synaptic membranes suggesting that this transporter is involved

in NMDAR neurotransmission through the regulation of extracellular synaptic glycine concentrations at glutamatergic synapses [Cubelos et al. 2005a]. The involvement of GLYT1 for NMDAR function has been demonstrated using *Glyt1* conditional knockout mice and pharmacological inhibitors which lead to increased NMDAR activation manifesting as pro-cognitive and antipsychotic phenotypes [Yee et al. 2006; Singer et al. 2007; Zafra & Giménez 2008]. Taken together, differences in expression patterns and thermodynamic transport properties suggest that GLYT1 and GLYT2 perform complimentary but distinct functions within the CNS.

The regulation of GLYT1 expression and function in the CNS is still incompletely understood. GLYT1 trafficking and plasma membrane insertion has previously been shown to depend on posttranslational modifications including glycosylation in the second extracellular loop. The glycosylation status of GLYT1 and the identification of specific trafficking proteins which interact with GLYT1 such as SNARE protein and syntaxin 1A suggest that levels of GLYT1 at the plasma membrane and thus the activity of GLYT1 is regulated by vesicular transport and exo- and endocytosis [Olivares et al. 1995; Martinez-Maza et al. 2001; Geerlings et al. 2000, 2001; Cubelos et al. 2005b]. Internalization of GLYT1 transporters leads to a reduction in GLYT1-mediated glycine transport into cells which has been shown to be largely regulated by protein kinase C (PKC) signalling. Stimulation of PKC signalling by phorbol ester (PMA) was shown to enhance GLYT1 phosphorylation and ubiquitination ultimately leading to internalization of the transporter and an overall decrease in glycine uptake into cells [Geerlings et al. 2000; Sung et al. 2003; Vargas-Medrano et al. 2011]. This regulatory mechanism has not been fully elucidated however and is further complicated by additional interacting signalling molecules which

influence the trafficking of this transporter to and from the plasma membrane [Zafra et al. 1997; Barrera et al. 2015].

In an attempt to establish whether GLYT1 is regulated by these same mechanisms in oocytes, our lab tested the effects of various inhibitors and activators of factors thought to potentially be involved in this regulatory network of GLYT1 activation. GLYT1 activity was unimpeded by PKC agonists, general kinase inhibitors, or serine-threonine kinase inhibitors [Tartia 2009]. Our lab also investigated the possibility that GLYT1 activation in oocytes following ovulation (or removal from the ovarian follicle) depends on SNARE proteins for vesicular transport of GLYT1 to the plasma membrane as demonstrated in brain tissue and other cell lines. Oocytes were exposed to Botulinum or Tetanus neurotoxins which perturb SNARE-complexes. However, no effect on GLYT1 activity was observed [Tartia 2009]. Taken together, these results suggest that the mechanisms of GLYT1 regulation found to be active in the CNS are not shared by oocytes and preimplantation embryos.

7.3 GLYT1 as a unique organic osmolyte transporter in oocytes and preimplantation embryos

As discussed above, glycine has been shown to be an effective organic osmolyte in oocytes, eggs, and early preimplantation embryos. Our lab has previously determined that all osmoregulatory glycine uptake in preimplantation embryos occurs via the GLYT1 transporter using the potent, specific and reversible GLYT1 inhibitor ORG23798 and through its competitive inhibiton profile [Dawson et al., 1998; Steeves et al. 2003].

Inhibition of GLYT1 abrogated the osmoprotective effects of glycine on development of embryo culture to the blastocyst stage and disrupted the ability of oocytes and embryos to utilize glycine for the maintenance of cell volume [Steeves et al. 2003, 2005; Tartia et al. 2009].

GLYT1 is spontaneously activated following removal of oocytes from the ovarian follicle *in vitro* (or following ovulation *in vivo*) and the rate of GLYT1-mediated glycine uptake into oocytes steadily increases until ~3-4 hours in culture. Early cleavage stage embryos were found to increase GLYT1-mediated glycine uptake and initiate increased glycine accumulation without any apparent lag time when transferred from 250 mOsM culture medium to 350 mOsM culture medium suggesting that the increase in GLYT1 activity occurs independent of protein synthesis, a conclusion which was further confirmed by the observation that glycine accumulation occurs normally in 1-cell embryos cultured in the presence of cycloheximide, an inhibitor of protein synthesis [Steeves et al. 2003]. The activation of GLYT1 independent of protein synthesis is a unique phenomenon different from other known organic osmolyte transporters in somatic cells which rely on activation of the TonEBP transcription factor and transporter synthesis over several hours to days (discussed above). Although preimplantation embryos are exposed to relatively constant osmolarities compared to somatic cells of the kidney, this rapid volume-regulatory response is likely necessary since preimplantation embryos are highly sensitive to even slight changes in cell volume which can lead to developmental arrests [Baltz & Zhou 2012].

Spontaneous GLYT1 activation *in vitro* occurs independent of meiotic maturation and develops similarly in both denuded oocytes and COCs [Tartia et al. 2009]. The mechanism(s) regulating GLYT1 suppression prior to ovulation and GLYT1 activation

following ovulation are currently unknown but appear to be unique to oocytes and preimplantation embryos since GLYT1 is not known to be utilized as an organic osmolyte transporter in other mammalian cell types [Baltz & Zhou 2012].

8. Unanswered questions, significance, and specific aims and hypotheses

8.1 Unanswered questions

The ability of oocytes and early preimplantation embryos to regulate their volume is of critical importance to the development of a healthy blastocyst capable of implantation and successful fetal development. Significant progress has been made to identify the various volume regulatory mechanisms utilized by oocytes and cleavage stage embryos including the stage in which various organic osmolyte transporters are expressed and their relative contribution to volume regulation [Baltz & Zhou 2012]. The timing of the development of GLYT1 activity following removal from the ovarian follicle *in vitro* or ovulation *in vivo* has been characterized and the necessity for GLYT1 activity during early preimplantation embryo development to avoid developmental arrests has previously been demonstrated [Steeves et al. 2003; Tartia et al. 2009].

Although much is known regarding substrate specificity, transport kinetics, and the activity profile of GLYT1 during oocyte maturation and preimplantation embryo development, little is known regarding the mechanism(s) regulating GLYT1 suppression in the ovarian follicle prior to ovulation or the mechanism(s) involved in GLYT1 activation following ovulation or removal of the oocyte from the ovarian follicle. Furthermore, it is not known when during oogenesis that GLYT1 is first expressed or whether GLYT1

activation can occur in small growing oocytes prior to the stage in which oocytes become meiotically competent. It is also unclear when during oogenesis that oocytes are first able to detach from the ZP and therefore depend on the activity of independent volume regulatory processes, such as GLYT1-mediated glycine uptake, for volume maintenance. Although previous work has shown that spontaneous GLYT1 activation occurs in oocytes even when they are maintained in meiotic arrest with synthetic cAMP [Tartia et al. 2009], it is not known whether the physiological pathway mediating meiotic arrest (NPPC-cGMP signalling) is involved in GLYT1 suppression or activation. Throughout the course of my thesis I have explored these questions and have come to conclusions which have shed light on the process(es) mediating the activity of the GLYT1 transporter within the ovarian follicle and following ovulation (or removal from the ovarian follicle) which provide the basis for future work aimed at identifying the signalling network that regulates this critical component of early preimplantation embryo volume regulation.

8.2 Significance and overall objective

The importance of cell volume regulatory mechanisms involving the uptake of organic osmolytes has previously been demonstrated in cleavage stage embryos which undergo developmental arrests at osmolarities similar to that found *in vivo* in the absence of available organic osmolytes or active organic osmolyte transporters [Baltz & Zhou 2012]. As discussed above, volume regulation during oocyte maturation and early preimplantation embryo development is accomplished by GLYT1-mediated glycine uptake, a mechanism which becomes activated immediately following an ovulatory

stimulus *in vivo* or removal from the ovarian follicle *in vitro* [Steeves et al. 2003; Tartia et al. 2009].

Interest in the study of preimplantation embryo development has increased over the last several decades with the development of human assisted reproductive technologies (ARTs) and the use of *in vitro* fertilization (IVF) for commercial uses such as livestock production in the agricultural industry [Coticchio et al. 2012]. The success of ARTs depends on the ability to obtain competent and fertilizable oocytes and successfully culture healthy preimplantation embryos to the blastocyst stage, which hopefully will implant on a receptive endometrium to produce offspring. Therefore, the development of culture medium capable of supporting preimplantation embryo development *in vitro* has been essential to the advancement of ARTs. The osmoregulatory mechanisms found to be present in mouse preimplantation embryos have also been shown to occur in human embryos allowing for advancements in culture medium used for mouse embryos to also be applied to human embryo culture [Hammer et al. 2000]. Since early cleavage stage embryo development under *in vivo*-like conditions depends on the activity of the GLYT1 transporter for osmoregulation, the addition of glutamine (and glycine) to culture medium has enabled the continued development of preimplantation embryos *in vitro* without the occurrence of developmental arrests [Van Winkle et al. 1990c; Lawitts & Biggers 1992; Baltz & Tartia 2010].

Typical human IVF treatments involve the administration of high doses of gonadotrophins including FSH and LH/hCG to stimulate growth of a large cohort of follicles and to trigger oocyte maturation *in vivo*. These types of controlled ovarian stimulation protocols can lead to the development of ovarian hyperstimulation syndrome

(OHSS), a potentially lethal condition in the most severe cases which occurs in response to a rise in LH or hCG and is characterized by an increase in vascular permeability leading to fluid accumulation in the peritoneal and thoracic cavities [Shmorgun et al. 2011; Coticchio et al. 2012; Corbett et al. 2014]. Certain populations of patients are more susceptible to the development of OHSS even with the administration of low doses of gonadotrophins including patients diagnosed with polycystic ovarian syndrome (PCOS) since often a large number of antral follicles develop in response to hormonal stimulation. Furthermore, patients diagnosed with cancer (especially estrogen-sensitive cancers) and requiring immediate treatment may not be able to undergo a full gonadotrophin stimulation protocol due to the urgency for chemotherapy or radiation therapy. In these cases, typical ovarian stimulation protocols are not ideal and the availability of alternative IVF methodologies is desirable.

Although the majority of IVF treatments involve stimulating oocyte maturation *in vivo*, *in vitro* maturation (IVM) methods have been practiced for human ART since 1994 in which IVM was first utilized for PCOS patients and eventually further applied to normovulatory women with high ovarian reserves. The use of IVM generally involves tracking follicle growth in the ovary without gonadotrophin stimulation and retrieving oocytes prior to the development of a dominant follicle [Trounson et al. 1994; Fadini et al. 2009, 2011]. At the time of recovery, essentially all retrieved oocytes are immature (GV stage oocytes) and COCs are cultured for an additional 30-48 hours and then maturation status is assessed following the removal of cumulus granulosa cells [Conticchio et al. 2012]. Despite the advantage of this ART method in eliminating gonadotrophin stimulation, drawbacks of this technique have been identified when compared to typical

ovarian stimulation protocols including a decreased number of oocytes which undergo meiotic maturation to MII eggs (~50-55% with IVM compared to ~80% with standard gonadrotrophin stimulation) [Mikkelsen & Lindenberg 2001; Fandini et al. 2009], the requirement for an earlier date of transfer (often on day 2) which does not allow for the selection of high quality embryos on culture day 5, and an overall lower implantation rate requiring transfer of a greater number of embryos into the uterus [Coticchio et al. 2015].

The poorer development of preimplantation embryos derived from IVM protocols compared to *in vivo*-matured protocols (gonadotrophin stimulation) could be explained by the use of maturation culture conditions which have remained relatively unchanged in the past 20 years with medium composition derived rather empirically and with few human studies examining effective culture vessels or even the appropriate number of COCs which can be cultured in a defined volume of medium to achieve maximal oocyte maturation [Coticchio et al. 2012]. In the last decades, significant advances have been made in our understanding of the mechanisms mediating oocyte and follicle health prior to ovulation and during maturation in response to an ovulatory stimulus (discussed above). During oocyte maturation, many processes must occur to produce a healthy and fertilizable oocyte including nuclear maturation involving the release of cGMP-mediated prophase I arrest as well as cytoplasmic maturation involving cytoskeletal reorganization, organelle redistribution, and chromatin remodelling [Coticchio et al. 2015]. The successful completion of these processes depends on intercellular signalling mechanisms between the oocyte and follicular granulosa cells which mediate the acquisition of oocyte competence during oogenesis to ensure that the oocyte is capable of undergoing nuclear and cytoplasmic maturation, and which also mediate these maturation events themselves in

response to an ovulatory stimulus. In human IVM, COCs are removed from the *in vivo* environment and exposed to *in vitro* culture conditions for the duration of these vital maturation processes which can influence the overall health and developmental ability of preimplantation embryos.

As discussed, the ability of oocytes and early cleavage-stage embryos to regulate their volume is essential to avoid developmental arrests at *in vivo*-osmolarities which is accomplished primarily via GLYT1-mediated glycine transport into the cells [Baltz & Zhou 2012]. Prior to ovulation, however, GLYT1 remains suppressed and oocyte volume is maintained through a tight adherence of the oocyte to the rigid ZP. It is possible that independent cell volume regulation is inhibited within the follicle in order to maintain intact oocyte-cumulus cell interactions via TZPs and gap junctions and therefore regulate the acquisition of oocyte competence and ensure effective oocyte maturation [Tartia et al. 2009]. For human IVM to be improved and widely used as an alternative to typical ovarian stimulation requiring high doses of gonadrotrophins, knowledge previously acquired regarding the complex processes mediating oocyte maturation must be integrated into IVM culture systems. In regard to volume regulation, the culture conditions of small, immature, incompetent oocytes in IVM systems will need to support the maintenance of GLYT1 suppression to ensure that oocytes can become fully competent to undergo both nuclear and cytoplasmic maturation which requires maintenance of intact oocyte-cumulus cell communication.

The mechanism(s) mediating GLYT1 suppression prior to ovulation or GLYT1 activation following removal from the ovarian follicle is currently unknown. In addition, the stage in oogenesis when oocytes can first detach from the ZP and activate GLYT1 for

independent volume regulation is unknown. **Thus, the overall objective of my thesis was to determine how GLYT1 suppression is maintained within the ovarian follicle prior to ovulation.** Using a number of culture methodologies, pharmacological manipulations, and molecular biology techniques I have identified the cell types involved within the ovarian follicle required for GLYT1 suppression and I have identified possible mechanisms mediating this suppression. Furthermore, although I found that the ability of oocytes to detach from the ZP and activate GLYT1 is acquired at a similar stage during oogenesis and that these processes occur nearly simultaneously following removal from the follicle, I found that GLYT1 activity is mediated by an entirely different signalling mechanism from meiotic arrest and resumption. These findings have revealed the existence of another major intra-follicular signalling mechanism involving multiple cell types within the follicle which is distinct from signalling involved in the maintenance of meiotic arrest. The identification of the exact components of the GLYT1-inhibitory signalling mechanism within the antral follicle could help to refine human IVM culture conditions to facilitate complete oocyte competence acquisition and maturation *in vitro*.

8.3 Specific aims and hypotheses

Specific aim 1: **Determine when during oogenesis oocytes first acquire the ability to detach from the ZP and activate GLYT1 and examine the expression and localization of GLYT1 protein during oogenesis and preimplantation embryo development.** Detachment of the oocyte from the ZP and GLYT1 activation were previously shown to occur spontaneously in fully grown oocytes after isolation from ovaries that was independent of meiotic maturation [Tartia et al. 2009]. However, when during oogenesis

these abilities are first acquired or the localization of the GLYT1 transporter throughout oogenesis and preimplantation embryo development is unknown. I sought to determine the GLYT1 expression pattern and activity profile during oogenesis as well as transporter localization throughout oogenesis and preimplantation embryo development to reveal the potential mechanism(s) of GLYT1 activation, and therefore suppression.

Since GLYT1-mediated glycine uptake begins immediately when oocytes are exposed to hypertonic medium [Steeves et al. 2003], I hypothesized that GLYT1 transporters are present at the oocyte plasma membrane throughout oogenesis and in the fully grown GV oocyte prior to removal from the ovarian follicle and during maturation and preimplantation embryo development until compaction at the morula stage.

Specific aim 2: **Develop an antral follicle culture methodology capable of maintaining healthy follicle-enclosed oocytes and use this methodology to determine which cell types are required to maintain GLYT1 suppression in the antral follicle prior to ovulation.** Since efforts to suppress GLYT1 activation in isolated denuded oocytes and COCs have previously failed [Tartia 2009], I sought to develop an antral follicle culture methodology capable of supporting healthy follicles in culture for at least 4 hours. This would provide an experimental system which could be used to examine the requirement of mural granulosa cells and/or follicular fluid in the maintenance of suppressed GLYT1 activity prior to ovulation.

Since spontaneous GLYT1 activation occurs in isolated denuded oocytes and COCs, I hypothesized that the mural granulosa cells (MGCs) are at least required to

maintain GLYT1 suppression within the ovarian follicle. I further hypothesized that an inhibitory signal originating from the MGCs is propagated to the oocyte and removal of this inhibitory signal following removal from the ovarian follicle, or an ovulatory signal *in vivo*, results in GLYT1 activation, not unlike the mechanism involved in meiotic arrest and resumption [Zhang et al. 2010, 2011].

Specific aim 3: **Determine the signalling mechanism within the ovarian follicle required to maintain GLYT1 suppression before ovulation and examine whether the physiological signalling pathway mediating meiotic arrest (NPPC-cGMP) is involved in GLYT1 suppression.** Recently, meiotic arrest within the ovarian follicle was found to be mediated by NPPC from MGCs that stimulates cGMP production in cumulus granulosa cells which is transferred to the oocyte via gap junctions to maintain prophase I arrest (discussed above) [Norris et al. 2008; Zhang et al. 2010; Norris et al. 2008; Shuhaibar et al. 2015; Jaffe & Egbert 2016]. Although it has previously been demonstrated that GLYT1 will spontaneously activate in denuded oocytes even when maintained in meiotic arrest by dbcAMP [Tartia et al. 2009], the physiological meiosis-inhibitory mechanism identified within the ovarian follicle exhibits similarities to the above hypothesis that GLYT1 is suppressed by inhibitory signalling within the ovarian follicle prior to ovulation.

Therefore, I hypothesized that GLYT1 suppression within the antral follicle is mediated by signalling that resembles NPPC-cGMP-mediated inhibition of meiotic maturation, including the requirement for gap junctional communication and multiple cell types within the follicle. I further hypothesized that a component of this signalling

mechanism may directly participate in the maintenance of GLYT1 suppression in the antral follicle.

MATERIALS & METHODS

1.Chemicals and pharmaceutical agents

All chemicals and solutions used for culture were embryo tested or cell culture grade. Chemicals and compounds were obtained from the sources listed below in Table 1 and Table 2.

2. Culture medium

2.1 Oocyte, COC, preimplantation embryo, and antral follicle culture medium

Unless stated otherwise, denuded oocytes and cumulus-oocyte-complexes (COCs) were cultured in minimum essential medium alpha modification (MEMα) with no added nucleosides (12561-049; Life Technologies, Burlington, CA) and with 1mg/ml of polyvinyl alcohol added (PVA; cold-water soluble, molecular weight: 30 000 – 70 000). This same medium was used for the culture of both growing and fully-grown oocytes.

Preimplantation embryos from the 1-cell stage to blastocyst stage were cultured in modified potassium simplex optimized medium (mKSOM) which was modified from classical (unmodified) KSOM by omitting glutamine, since it can be transported by GLYT1, and substituting PVA for bovine serum albumin (BSA) [Lewis & Kaye 1992; Lawitts & Biggers 1993]. mKSOM contained 95 mM NaCl, 2.5 mM KCl, 0.35 mM KH_2PO_4, 0.2 mM $MgSO_4$, 10 mM sodium lactate, 0.2 mM glucose, 0.2 mM sodium pyruvate, 25 mM $NaHCO_3$, 1.7 mM $CaCl_2$, 0.01 mM tetrasodium ethylenediaminetetra-acetic acid (EDTA), 0.03 mM streptomycin sulfate, 0.16 mM penicillin G, and 1 mg/ml polyvinyl alcohol (PVA). The medium used for oocyte and preimplantation embryo

Table 1: Summary of chemicals and compounds used.

Name of Chemical or Compound	Source
4-(2-hydroxyethyl)-1-piperazineethane-sulfonic acid (HEPES)	Sigma Aldrich (St. Louis, MO, USA)
[^{3}H]-glycine ([2-^{3}H]-glycine; ~47 Ci/mmol)	Perkin Elmer (Boston, MA, USA)
β-mercaptoethanol	Sigma Aldrich (St. Louis, MO, USA)
Antifade mounting solution	Life Technologies (Burlington, ON, Canada)
Aprotinin	Sigma Aldrich (St. Louis, MO, USA)
Ascorbic acid	Sigma Aldrich (St. Louis, MO, USA)
Bovine serum albumin (BSA)	Sigma Aldrich (St. Louis, MO, USA)
BSA standard	Bio-Rad Laboratories (Mississauga, ON, Canada)
$CaCl_2$	Sigma Aldrich (St. Louis, MO, USA)
Dimethyl sulfoxide (DMSO)	Calbiochem (La Jolla, CA, USA)
Ethanol	Sigma Aldrich (St. Louis, MO, USA)
Fetal bovine serum (FBS)	Life Technologies (Burlington, ON, Canada)
Glucose	Sigma Aldrich (St. Louis, MO, USA)
Glycine	Sigma Aldrich (St. Louis, MO, USA)
Guanosine	Sigma Aldrich (St. Louis, MO, USA)
KCl	Sigma Aldrich (St. Louis, MO, USA)
KH_2PO_4	Sigma Aldrich (St. Louis, MO, USA)
L-glutamine	Sigma Aldrich (St. Louis, MO, USA)
Laemmli buffer (2X)	Bio-Rad Laboratories (Mississauga, ON, Canada)
Leupeptin	Sigma Aldrich (St. Louis, MO, USA)
Methanol	Sigma Aldrich (St. Louis, MO, USA)
$MgSO_4$	Sigma Aldrich (St. Louis, MO, USA)
NaCl	Sigma Aldrich (St. Louis, MO, USA)
$NaHCO_3$	Sigma Aldrich (St. Louis, MO, USA)
Na lactate	Sigma Aldrich (St. Louis, MO, USA)
Na pyruvate	Sigma Aldrich (St. Louis, MO, USA)
Normal goat serum (NGS)	Jackson ImmunoResearch (West Grove, PA, USA)
Paraformaldehyde (PFA, 20%)	Fisher Scientific (Toronto, ON, Canada)
Penicillin G	Sigma Aldrich (St. Louis, MO, USA)
Phenylmethylsulphonyl fluoride (PMSF)	Sigma Aldrich (St. Louis, MO, USA)
Phosphate-buffered saline (PBS; pH 7.4)	Life Technologies (Burlington, ON, Canada)
Polyvinyl alcohol	Sigma Aldrich (St. Louis, MO, USA)

Ponseau S solution	Sigma Aldrich (St. Louis, MO, USA)
Scintillation fluid	Scintiverse BD, Fisher Scientific (Pittsburgh, PA, USA)
Sodium azide	Sigma Aldrich (St. Louis, MO, USA)
Sodium deoxycholate	Sigma Aldrich (St. Louis, MO, USA)
Sodium dodecyl sulfate (SDS)	Sigma Aldrich (St. Louis, MO, USA)
Streptomycin sulfate	Sigma Aldrich (St. Louis, MO, USA)
Tetrasodium ethylenediaminetetra-acetic acid (EDTA)	Sigma Aldrich (St. Louis, MO, USA)
Tris	Sigma Aldrich (St. Louis, MO, USA)
Tris-buffered saline (TBS, pH 7.4)	Bio-Rad Laboratories (Mississauga, ON, Canada)
Tris-HCl (pH 7.4)	Sigma Aldrich (St. Louis, MO, USA)
Triton X-100	Sigma Aldrich (St. Louis, MO, USA)
Tween 20	Sigma Aldrich (St. Louis, MO, USA)

Table 2: Summary of pharmaceutical agents used.

Pharmaceutical Agent	Source	Action
18α-glycyrrhetinic acid (AGA)	Sigma Aldrich (St. Louis, MO, USA)	General gap junction inhibition.
Acidic Tyrode's solution (pH 2.5)	Sigma Aldrich (St. Louis, MO, USA)	Zona pellucida (ZP) removal.
BAY 73-6691	Sigma Aldrich (St. Louis, MO, USA)	Potent and selective inhibitor of phosphodiesterase 9 used for the maintenance of meiotic arrest (PDE9).
Collagenase type I	Worthington Biochemical Corp. (Lakewood, NJ, USA)	Enzyme used for neonatal ovary digestion.
Cx37/40 (Cx2601-P-1; connexin 37/40 hemi-channel blocking peptide, Gap 26 domain)	Alpha Diagnostics (San Antonio, TX, USA)	Specific inhibition of GJA4 (connexin-37) gap junctions.
Cx37 scrambled peptide (Cx2602-PS-1; connexin 37/40 hemi-channel scrambled peptide, Gap26 domain)	Alpha Diagnostics (San Antonio, TX, USA)	Scrambled peptide control for Cx37/40 gap junction inhibition.
Cx43 CMP (Cx2605-P-1; connexin 43 hemichannel blocking peptide, Gap 26 domain)	Alpha Diagnostics (San Antonio, TX, USA)	Specific inhibition of GJA1 (connexin-43) gap junctions.
Cx43 scrambled peptide (Cx2606-PS-1; connexin 43 hemi-channel scrambled peptide, Gap 26 domain)	Alpha Diagnostics (San Antonio, TX, USA)	Scrambled peptide control for Cx43 gap junction inhibition.
Deoxyribonuclease Type IV (DNAse)	Sigma Aldrich (St. Louis, MO, USA)	Enzyme used for neonatal ovary digestion.
eCG (equine chorionic gonadotropin)	Sigma Aldrich (St. Louis, MO, USA)	Stimulation of ovarian follicle growth *in vivo* (hormone).
Estradiol (E_2)	Sigma Aldrich (St. Louis, MO, USA)	Maintenance of functional NPR2 expression on cumulus granulosa cells *in vitro*.
Follicle stimulating hormone (FSH)	National Hormone and Pituitary Program of National Institute of Diabetes and Digestive	Antral follicle culture support (hormone).

	and Kidney Diseases (Bethesda, MD, USA)	
hCG (human chorionic gonadotropin)	Sigma Aldrich (St. Louis, MO, USA)	Ovulation stimulation in mice *in vivo* (hormone).
Hypoxanthine	Sigma Aldrich (St. Louis, MO, USA)	Maintenance of meiotic arrest (purine).
Lindane	Sigma Aldrich (St. Louis, MO, USA)	General gap junction inhibition.
Luteinizing hormone (LH)	National Hormone and Pituitary Program of National Institute of Diabetes and Digestive and Kidney Diseases (Bethesda, MD, USA)	Ovulation stimulation of antral follicles *in vitro*.
Natriuretic peptide C (NPPC)	Sigma Aldrich (St. Louis, MO, USA)	Maintenance of meiotic arrest in COCs.

collection and handling was identical to mKSOM except with 21 mM Hepes added (pH ~7.3) and NaOH reduced to 4 mM; this medium was designated as Hepes-mKSOM.

Antral follicle culture medium was based on the medium developed by Downs [Downs 2000]. Culture medium for both intact and punctured antral follicles was MEMα with essential amino acids and without glutamine (10370-021; Life Technologies, Burlington, CA) with fetal bovine serum (FBS, 10%; Life Technologies), 0.16 mM penicillin G, EDTA (0.01 mM), ascorbic acid (50 µg/ml), and follicle stimulating hormone (FSH, 100 ng/ml; National Hormone and Pituitary Program of National Institute of Diabetes and Digestive and Kidney Diseases, Bethesda, MD) added. Hepes-mKSOM was used for the isolation and handling of antral follicles.

2.2 Mural granulosa cell (MGC) culture medium

Mural granulosa cell culture medium was developed based on the method by Lee and colleagues which was shown to support MGC expression of *Nppc* [Lee et al. 2013]. MGC medium was minimum essential medium (MEMα) (M4526) with L-glutamine (0.292 g/L), penicillin (75 µg/ml), streptomycin sulfate (50 µg/ml), bovine serum albumin (BSA, 3 mg/ml), follicle stimulating hormone (FSH, 5 ng/ml; National Hormone and Pituitary Program of National Institute of Diabetes and Digestive and Kidney Diseases, Bethesda, MD), and estradiol (E_2; 100 nM) added. See Table 3 for a summary of all commercial medium used.

Table 3: Summary of commercial medium used.

Type of Medium	Source
Oocyte and COC **MEMα**	Life Technologies (Burlington, ON, Canada) Cat# **12561-049**
Antral follicle **MEMα**	Life Technologies (Burlington, ON, Canada) Cat# **10370-021**
Mural granulosa cell (MGC) **MEMα**	Sigma Aldrich (St. Louis, MO, USA) Cat# **M4526**

3. Oocyte, COC, preimplantation embryo, and antral follicle isolation and culture

3.1 Superovulation and timing of oocyte, embryo, and antral follicle collection

The Animal Care Committee of the Ottawa Hospital Research Institute or University of Ottawa Faculty of Medicine approved all animal protocols. To obtain sufficient numbers of oocytes and embryos, adult female CF1 mice (Crl:CF1, Charles River Laboratories, Saint-Constant, QC) that were ~4 weeks old were intraperitoneally (i.p.) injected with either equine chorionic gonadotropin (eCG, 5 IU) or eCG (5 IU) followed by an i.p. injection with human chorionic gonadotropin (hCG, 5 IU) [Hogan et al. 1994; Dawson & Baltz 1997]. eCG displays FSH-like activity and stimulates the growth of follicles in the mouse ovary while hCG acts like LH thus stimulating ovulation.

To obtain fully grown denuded GV oocytes and COCs, adult CF1 female mice were i.p. injected with eCG (5 IU) and then oocytes and COCs were isolated from ovaries by mincing with a razor blade 43-45 hrs post-eCG injection. Denuded GV oocytes are oocytes devoid of any cumulus cells (Figure 9) while COCs are oocytes surrounded by cumulus granulosa cells (Figure 9). Antral follicles in which an oocyte and antrum were visible (Figure 9) were mechanically isolated from ovaries of adult CF1 female mice 43-45 hours post-eCG injection.

To obtain mature MII eggs and preimplantation embryos, adult CF1 female mice were first injected with eCG (5 IU i.p.) and then injected with hCG (5 IU i.p.) 47.5 hours post-eCG injection. MII eggs were isolated 15 hours post-hCG injection by oviductal flushing (described below). To obtain preimplantation embryos, adult CF1 female mice

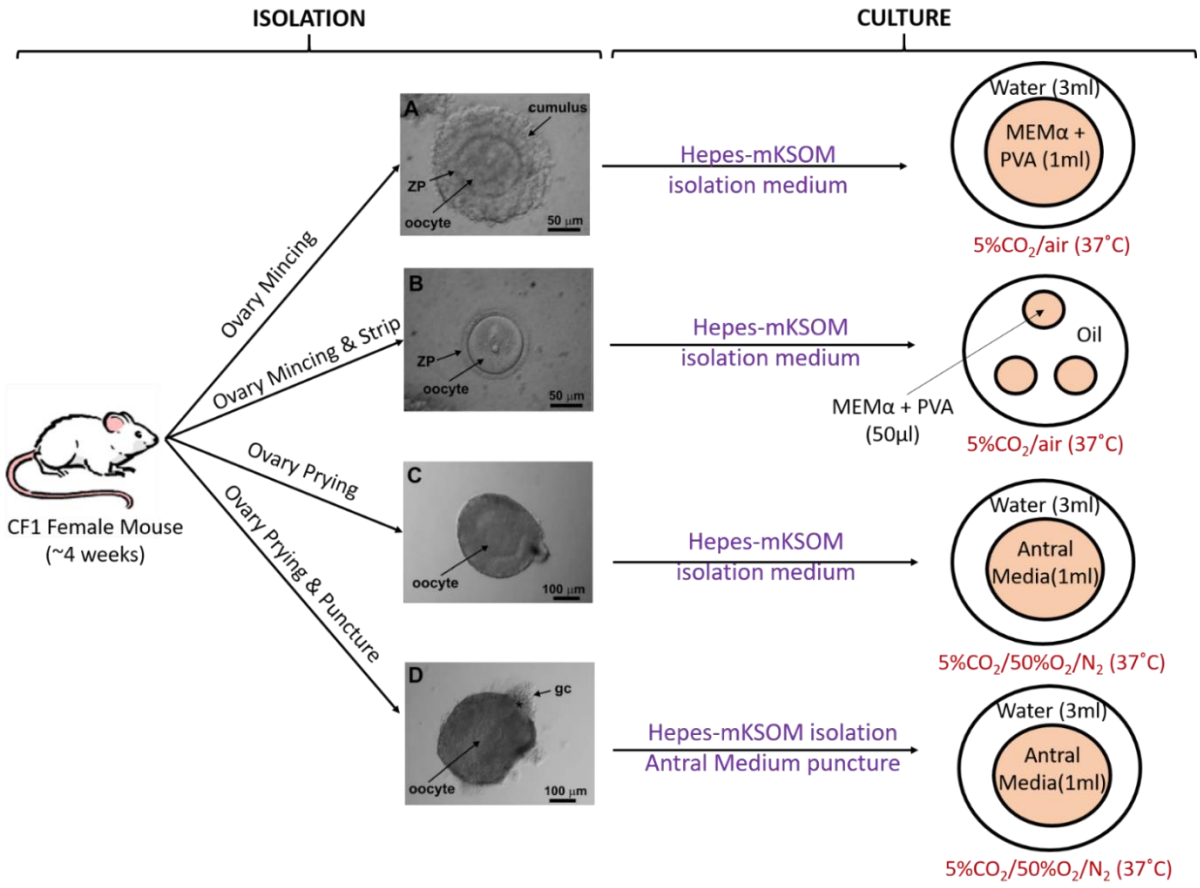

Figure 9. Denuded oocyte, COC, and antral follicle isolation and culture. Fully grown COCs, denuded oocytes, intact and punctured antral follicles were isolated from adult CF1 female mice 43-45 hrs post-eCG injection. (**a**) COCs were isolated by mincing ovaries with a razor blade and collected using Hepes-mKSOM medium. COCs were cultured in 1 ml of MEMα (+PVA) in organ culture dishes with filter sterilized water added to the outer well and cultured at 5%CO_2/air at 37˚C. (**b**) Denuded GV oocytes were isolated by mincing ovaries with a razor blade and then cumulus granulosa cells were removed by repeated pipetting with a flame-pulled Pasteur pipette and collected using Hepes-mKSOM medium. Denuded oocytes were cultured in 50µl drops of MEMα (+PVA) under an oil overlay at

5%CO_2/air and 37˚C. (**c**) Intact antral follicles were isolated by gently prying apart ovarian tissue with tweezers using Hepes-mKSOM for collections and handling. Intact antral follicles were cultured in 1 ml of antral follicle culture medium in organ dishes with filter sterilized water added to the outer well and cultured at 5%CO_2/50%O_2/45%N_2 and 37˚C. (**d**) Punctured antral follicles were isolated the same as intact antral follicles except that a small puncture was made in the wall of the follicle using a 25-G needle which could be visualized by the release of a small number of granulosa cells (gc) from the puncture site. Collection and handling of punctured antral follicles was performed using Hepes-mKSOM while puncturing was performed using antral follicle culture medium. Punctured antral follicles were cultured in 1 ml of antral follicle culture medium in organ dishes with filter sterilized water added to the outer well and cultured at 5%CO_2/50%O_2/45%N_2 and 37˚C.

were immediately caged overnight with BDF1 (B6D2F1/Crl) male mice (Charles River) for mating following i.p. injection with hCG. Preimplantation embryos were isolated by oviductal flushing and blastocyst stage embryos were isolated by oviductal and uterine flushing at various times following hCG injection and mating: 1-cell, ~21 hours; 2-cell, ~44 hours; 8-cell (uncompacted), ~67 hours; and blastocysts, ~94 hours [Hogan et al. 1994].

3.2 Growing and fully-grown oocyte and COC isolation and culture

Growing oocytes were isolated from non-hormonally stimulated post-natal day 5-21 (P5-P21) CF1 neonatal mice or adult CF1 female mice 24 hours following i.p. injection with eCG (5 IU). Hepes-mKSOM was used for the collection and handling of growing oocytes. Growing oocytes >55 μm in diameter were isolated mechanically from eCG-stimulated (24 hours post- injection) CF1 adult female mice or from unstimulated P14-P21 neonatal CF1 female mice. Growing oocytes were mechanically isolated from ovaries excised from neonatal or adult female mice by first thoroughly mincing ovaries with a razor blade to release growing follicles and/or COCs. Denuded growing oocytes >55 μm in diameter contained within follicles after ovary mincing were isolated by puncturing one side of the follicle with a flame-pulled Pasteur pipette and gently pushing the oocyte out of the follicle with the Pasteur pipette; cumulus cells become stripped from the oocytes during this isolation procedure. Larger growing oocytes that were released as COCs following mincing were denuded by repeated pipetting with a flame-pulled Pasteur pipette until all cumulus cells were removed.

Growing oocytes <55 µm in diameter were too small to be isolated mechanically and therefore were isolated using an enzymatic digestion protocol using only ovaries isolated from P5-P13 neonatal mice. Enzymatic isolation of growing oocytes was not possible in neonatal mice older than P13 due to the greater amount of ovarian tissue which would need to be digested and its resistance to digestion. Ovaries were excised from P5-P13 neonatal mice and transferred to organ dishes containing 1 ml of pre-equilibrated (5% CO_2/air; 37ºC) mKSOM with $MgSO_4$ and $CaCl_2$ omitted and with 2 mg/ml collagenase type I (Worthington Biochemical Corp., Lakewood, NJ, USA) and 0.01 mg/ml of deoxyribonuclease Type IV added. Ovaries were incubated in the digesting solution for 30 minutes (5% CO_2/air and 37ºC) and then ovaries were vigorously pried apart using tweezers to release denuded GV oocytes. Denuded oocytes were immediately washed through 5 drops of Hepes-mKSOM following ovary digestion. To ensure that the enzymatic isolation method did not influence GLYT1 activity or the ability of oocytes to resume meiosis, oocytes isolated either enzymatically or mechanically were cultured 4 hours following isolation and GLYT1 activity was measured and oocytes were examined for meiotic resumption (GVBD). No difference in GLYT1 activation (Figure 14B, see Results section) or meiotic resumption (data not shown) was found.

To determine the size of oocytes, growing denuded GV oocytes were immediately imaged after isolation using a Nikon Coolpix 4500 digital camera on a Zeiss IM35 microscope fitted with Hoffman optics and two orthogonal measures were taken. Oocytes were assumed to be spherical and thus the mean of the orthogonal measures was taken to represent the diameter of oocytes which was converted to µm using calibrations obtained with a stage micrometer.

Fully grown denuded GV oocytes and COCs were isolated from ovaries excised from adult female CF1 mice 43-45 hours post-eCG injection. Ovaries were minced using a razor blade to release COCs. To obtain denuded GV oocytes, COCs released from ovaries by mincing were stripped of cumulus cells by repeated pipetting with a flame-pulled Pasteur pipette. All collections and handling steps were performed using Hepes-mKSOM. Where indicated, denuded growing and fully grown GV oocytes were maintained in meiotic arrest with dbcAMP (300 µM) added to isolation (Hepes-mKSOM) and culture medium while COCs were maintained in meiotic arrest with NPPC (100 nM) and estradiol (E_2, 100 nM). Unless stated otherwise, denuded oocytes were cultured in 50 µl drops of oocyte culture medium (MEMα + PVA) under an overlay of filter-sterilized embryo culture-grade mineral oil while COCs were cultured in organ dishes containing 1 ml of COC culture medium (MEMα + PVA) with filter-sterilized water added to the outer well; both culture methods involved pre-equilibration of medium at 5% CO_2/air and 37ºC for at least 2 hours before adding oocytes or COCs (Figure 9).

3.3 MII egg and preimplantation embryo isolation and culture

Mature MII eggs and preimplantation embryos were isolated from oviducts excised from adult female CF1 mice i.p. injected with eGC (5 I.U) followed by hCG (5 I.U). MII eggs, 1-cell, 2-cell, and 8-cell embryos (pre-compaction) were flushed with Hepes-mKSOM from oviducts using tweezers and a blunted needle and syringe. MII eggs and 1-cell embryos were briefly immersed in Hepes-mKSOM containing 300 µg/ml hyaluronidase to release eggs and embryos from the expanded cumulus matrix. Fertilization of 1-cell embryos was confirmed by the presence of two PN.

To obtain blastocyst stage embryos, oviducts and uterine horns were excised from adult CF1 female mice and flushed with Hepes-mKSOM using tweezers and a blunted needle and syringe. Flushing was performed at the infundibulum of the oviduct so that blastocysts were flushed out the end of the uterine horn. Only blastocyst stage embryos with a clear expanded blastocoel and visible inner cell mass were used for experiments. Unless stated otherwise, preimplantation embryos were cultured in 50 µl drops of mKSOM under an overlay of filter-sterilized embryo culture-grade mineral oil and pre-equilibrated at 5% CO_2/air and 37ºC for at least 2 hours prior to the addition of embryos.

3.4 Antral follicle isolation and culture

Based on the method by Downs [2000], intact antral follicles were isolated from excised ovaries using tweezers 43-45 hours following eCG (5 I.U) i.p. injection of adult CF1 female mice. Tweezers were used to mechanically pry apart ovarian tissue to obtain antral follicles which displayed a visible oocyte and antrum and were devoid of excess ovarian tissue (Figure 9). Intact antral follicle isolation was performed in Hepes-mKSOM and then follicles were transferred using tweezers to antral follicle culture medium that was pre-equilibrated in modular chambers (Billups-Rothenburg, Inc., Del March, CA) gassed with 5%CO_2/50%O_2/45%N_2 and incubated at 37ºC for at least 2 hours prior to adding antral follicles.

Punctured antral follicle isolation was performed identically to intact antral follicle isolation except that a small hole was made in the outer wall of the follicle opposite the oocyte (through the theca, basement membrane, and mural granulosa cell layers) using a

25-G needle. The follicular wall puncture was confirmed by visualization of the release of a small amount of antral fluid and a few granulosa cells from the follicle through the puncture site (Figure 9). Only punctured antral follicles within which the oocyte was clearly visible were used for experiments. Punctured antral follicles were transferred to pre-equilibrated (5%CO_2/50%O_2/45%N_2 at 37ºC) culture medium using tweezers and the puncture was performed once follicles were in the final culture medium to avoid additional loss of antral fluid and/or cells during transfer between isolation medium (Hepes-mKSOM) and culture medium (antral follicle medium). Where specified, meiotic arrest was maintained during extended culture periods by the addition of NPPC (100 nM) and E_2 (100 nM) to culture medium.

Intact and punctured antral follicles were cultured in 1 ml of antral follicle culture medium in organ dishes with filter-sterilized water added to the outer well, unless stated otherwise, at 5%CO_2/50%O_2/45%N_2 and 37ºC in modular chambers (Billups-Rothenburg, Inc., Del March, CA) (Figure 9). After the desired antral follicle culture period, COCs were isolated from follicles by further puncturing the follicular outer wall with a 25-G needle and gently pushing on the follicle to release the COC. Denuded oocytes were obtained by stripping off cumulus cells by repeated pipetting with a flame-pulled Pasteur pipette as described above.

3.5 Mural granulosa cell (MGC) isolation and culture

Mural granulosa cells were isolated and cultured based on the methods of Lee and colleagues and Pepin and colleagues [Lee et al. 2013; Pepin et al. 2013]. Intact antral

follicles (~50 from the ovaries of 4 eCG-injected adult CF1 mice) were first isolated as described above and cleaned of excess ovarian tissue. A small hole was made in the follicular wall through the theca, basement membrane, and mural granulosa cell layers using a 25-G needle, like the puncture site in a punctured antral follicle (described above). COCs were gently popped out of punctured follicles by pressing gently on the follicles with tweezers. Once COCs were removed from antral follicles, tweezers were used to further depress the punctured follicles to expel the mural granulosa cells. The mural granulosa cells were expelled from the follicle in sheets which were then separated and dispersed within MGC culture medium using a flame-pulled Pasteur pipette. Isolation of intact antral follicles was performed in Hepes-mKSOM and MGC culture was performed in MGC culture medium.

Immediately following MGC isolation and dispersion in MGC culture medium, MGCs were transferred in a cell suspension (~50 µl) to individual wells in a 96-well culture dish (Thermo Scientific; coated or uncoated) and cultured overnight (~18-20 hours) in MGC culture medium to allow adherence of the MGC to bottom of the culture well. After the initial overnight culture period, MGC monolayers were visually examined and COCs were added to the MGCs and cultured under the various conditions described for each experiment. Where COCs were maintained in meiotic arrest with NPPC (100nM) and E_2 (100nM), only oocytes with an intact GV, to signify that meiotic arrest was maintained, were used for measuring GLYT1 activity.

3.6 Extracellular matrix components (EMs) culture

Multiple extracellular matrix components were used as a coating surface for culture wells upon which MGCs and/or COCs were cultured for a specified amount of time. For

all EHS Matrix brands and purified extracellular matrix components (EMs) used, a final concentration of 50 µg/ml was prepared and 50 µl of the coating material was added to individual wells of a 96-well culture dish. Culture wells containing the EHS Matrix or EM solutions were incubated for 2 hours at 5%CO_2/air and at 37ºC and then the 50 µl solutions were removed using a pipette resulting in a thin layer of coating matrix on the surface of the culture well. Poly-lysine was additionally washed twice with water to remove all excess unattached poly-lysine. Immediately after the coating matrix solution was removed from culture wells, 50 µl of MGC culture medium was added to the wells (with or without a MGC suspension) and cultured either overnight or for an additional 4 hours depending on the desired experiment. Each coating matrix solution was prepared per the manufacturer's instructions and is summarized in Table 4.

4. Micromanipulations and ZP staining

4.1 Oocyte-ZP adhesion: a hypertonic assay

An assay was developed based on the method by Tartia and colleagues where oocytes are exposed to a hypertonic solution to cause oocyte shrinkage and to determine whether the oocyte is adhered to the ZP [Tartia et al. 2009]. This original protocol was modified by increasing the hypertonicity of the assay (from 450 mOsM to 1000 mOsM) to more clearly identify the degree of oocyte-ZP adhesion in denuded oocytes. Denuded oocytes were isolated as described and exposed to mKSOM, made hypertonic (1000 mOsM) by the addition of NaCl, either immediately following isolation from ovaries or

Table 4: Summary of EHS Matrix and extracellular matrix components (EMs) used.

Coating Matrix Type	Source	Preparation
ECL Cell Attachment Matrix isolated from Engelbreth-Holm-Swarm (EHS) mouse tumor.	EMD Millipore (Etobicoke, ON, CA) **Cat# 08-110**. Supplied as a frozen solution of 5 mg in 5 ml of 0.05 M Tris-HCl, pH 7.4, 0.15 M NaCl.	The frozen solution was thawed at 4ºC and then kept on ice during dilutions. The thawed solution was diluted directly in MGC culture medium to obtain a final concentration of 50 µg/ml and aliquots were stored at -20ºC until use.
Matrigel© Basement Membrane Matrix from Engelbreth-Holm-Swarm (EHS) mouse tumor.	Corning (New York, NY, USA) Cat# **356234**. Supplied as a frozen 5 ml solution in Dulbecco's Modified Eagle's Medium with 50 µg/mL gentamycin. Protein concentration was determined by the manufacturer and indicated for each vial received.	The frozen solution was thawed on ice at 4ºC overnight and gently swirled to evenly disperse. The thawed solution was kept on ice during dilutions and handling. Stock solutions were prepared by diluting directly into Minimum Essential Medium (Sigma Cat# M4526) to obtain a 1mg/ml concentration and aliquots were stored at -20ºC. Prior to use, aliquots were further diluted in MGC culture medium to obtain a final concentration of 50 µg/ml.
Matrigel© Growth Factor Reduced (GFR) Basement Membrane Matrix from Engelbreth-Holm-Swarm (EHS) mouse tumor.	Corning (New York, NY, USA) Cat# **356230**. Supplied as a frozen 5 ml solution in Dulbecco's Modified Eagle's Medium with 50 µg/mL gentamycin. Protein concentration was determined by the manufacturer and indicated for each vial received.	The preparation method was identical to Corning Matrigel© Basement Membrane Matrix (non-GFR; cat# 356234).

Collagen IV from human placenta.	Sigma Aldrich (St. Louis, MO, USA) Cat# **C5533**. Supplied as 5 mg of a lyophilized powder stored at -20ºC.	The lyophilized powder was reconstituted in 1X PBS to obtain a 1 mg/ml stock solution. As per the manufacturer's instructions, the collagen IV solution was dissolved over several hours at 4ºC with occasional swirling until completely dissolved. Aliquots of the stock solution were stored at -20ºC. Prior to use, aliquots were further diluted in MGC culture medium to obtain a final concentration of 50 µg/ml.
Laminin isolated from Engelbreth-Holm-Swarm (EHS) mouse tumor.	Sigma Aldrich (St. Louis, MO, USA) Cat# **L2020**. Supplied as a frozen solution at a concentration of 1 mg/mL in 50 mM Tris-HCl, pH 7.5, with 150 mM NaCl.	The frozen 1 mg/ml solution was thawed at 4ºC and aliquots were prepared and stored at -20ºC. Prior to use, aliquots were further diluted in MGC culture medium to obtain a final concentration of 50 µg/ml.
Fibronectin from human fibroblasts.	Sigma Aldrich (St. Louis, MO, USA) Cat# **F0556**. Supplied as a frozen solution at a concentration of 0.5 mg/ml in a CAPS saline buffer.	The frozen 0.5 mg/ml solution was thawed at 4ºC and aliquots were prepared and stored at -20ºC. Prior to use, aliquots were further diluted in MGC culture medium to obtain a final concentration of 50 µg/ml.
Collagen I from rat tail.	Sigma Aldrich (St. Louis, MO, USA) Cat# **C7661**. Supplied as a powder at room temperature.	The powder was solubilized in 0.1 M acetic acid for three hours at room temperature on a rotator to obtain a 1 mg/ml stock solution. Aliquots of the stock solution were stored at -20ºC. Prior to use, aliquots were further diluted in MGC culture

		medium to obtain a final concentration of 50 µg/ml.
Poly-L-Lysine	Sigma Aldrich (St. Louis, MO, USA) Cat# **P8920**. Supplied as a 0.10 % solution in water at room temperature with 0.01% thimerosal, added as a preservative.	As per the manufacturer's instructions, the 0.1% poly-l-lysine solution was diluted 1:10 with MilliQ water and was stored at 4ºC. The diluted 0.01% poly-l-lysine solution was used for coating culture wells.

after a desired culture period. Osmolarity was measured with a Vapro 5520 osmometer (Wescor, Logan, UT) and was within ± 5 mOsM of the nominal value.

The resultant appearance of denuded oocytes following exposure to the hypertonic solution was examined and a classification system was devised to assess whether oocytes were fully adhered to the ZP, partially adhered to the ZP, or fully detached from the ZP. Oocytes were classified as fully attached to the ZP if the oocyte formed a concave disc shape when exposed to hypertonic solution (Figure 10 A, B, see Results section). Oocytes were classified as completely detached from the ZP if the oocyte shrunk into a tight sphere with a clear visible space surrounding the oocyte from the ZP (Figure 10 A, E, see Results section). Oocytes were classified as partially attached to the ZP if the oocyte deformed into an intermediate of attached and detached with some areas of adhesion to the ZP and other areas containing a space (Figure 10 A, C, D, see Results section). Immediately following exposure to the hypertonic solution, oocytes were examined visually and were scored as attached, partially attached, or detached from the ZP. For some experiments, oocytes were also imaged using a Nikon E4500 camera mounted on a Zeiss Axiovert microscope immediately following hypertonic shock treatment.

Confocal imaging was used to confirm the morphologies of denuded oocytes which were visually classified attached, partially attached, or completely detached from the ZP after exposure to the hypertonic mKSOM. Immediately after exposure to the hypertonic solution, oocytes were fixed in phosphate-buffered saline (PBS, pH 7.4) containing 2% paraformaldehyde (PFA) and 0.02% Triton X-100 for 30 minutes in a benchtop warming box set at 37ºC. After fixation, oocytes were washed through blocking solution which was 2% BSA, 2% FBS, 0.1M glycine, 0.01% Triton X-100 in Tris-buffered saline (TBS) three

times for 10 minutes per wash. Following washing, oocytes were transferred to staining solution which was TBS with 1% BSA and 0.5% Triton X-100 supplemented with Alexa 488-conjugated wheat germ agglutinin (WGA; W11261; Life Technologies; 5µg/ml) and Alexa 594-phalloidin (A12381; Life Technologies, Burlington, ON, Canada; 1:40). WGA was used to label ZP glycoproteins as green and phalloidin was used to label oocyte actin as red. Oocytes were incubated in the staining solution overnight (~16-18 hours) at 4ºC. All fixation, staining, and washing steps were performed in a 96-well culture dish with filter-sterilized water added to the outer empty wells to limit evaporation of solutions during heated exposures. Oocytes were moved between solutions using flame-pulled glass Pasteur pipettes. For the overnight incubation in staining solution at 4ºC, 96-well culture dishes were additionally incubated within a small dark box on top of two culture dish lids placed upon a dampened KimWipe to maintain humidity. After the overnight culture in staining solutions, oocytes were washed briefly (~30 seconds) through a single culture well containing TBS and then through a single culture well containing filter-sterilized water and mounted on glass slides in 4 µl of 50% Antifade mounting solution (Life Technologies, Burlington, ON, Canada). Oocytes were imaged using a Zeiss LSM 510 META with a 40x oil-immersion objective to obtain confocal images and ImageJ 1.48v (Rasband, W.S., U. S. National Institutes of Health, Bethesda, Maryland, USA) was used to optimize contrast and brightness equally for all oocytes and the Orthogonal Views function of ImageJ was used to construct XZ and YZ sections.

4.2 Alexa 488-conjugated wheat germ agglutinin (WGA) staining of denuded oocytes and COCs

To determine whether the presence of cumulus granulosa cells hinder the ability of larger molecules in culture medium to access the oocyte, denuded oocytes and COCs were cultured in the presence of Alexa 488-conjugated wheat germ agglutinin (WGA; W11261; Life Technologies) and ZP fluorescence was examined. Denuded GV oocytes and COCs were isolated as described above (Figure 9) and cultured 2 hours in 1 ml of culture medium in organ dishes with filter-sterilized water added to the outer culture well and with 5 µg/ml WGA added at 5%CO_2/air and 37ºC. After the 2-hour culture period, COCs were denuded by repeated pipetting using a flame-pulled glass Pasteur pipette to remove all cumulus granulosa cells. The oocytes cultured as COCs in the presence of WGA were kept separate from oocytes which were denuded for the culture with WGA so that the staining intensity of the ZP could be compared between the two culture conditions (denuded oocytes versus COCs). Denuded oocytes from each culture group were mounted on glass slides in 4 µl of 50% Antifade mounting solution (Life Technologies, Burlington, ON, Canada). Confocal images of oocytes were taken using a Zeiss LSM 510 META with a 40x oil-immersion objective and ImageJ 1.48v (Rasband, W.S., U. S. National Institutes of Health, Bethesda, Maryland, USA) was used to optimize contrast and brightness equally for all oocytes.

4.3 COC microinjection

Two different microinjection protocols were utilized to examine the role of GJA4 (connexin-37) gap junctions in the maintenance of meiotic arrest: microinjection of GJA4

antiserum into oocytes within COCs and microinjection of Cx37 connexin mimetic peptides (CMPs) directly at the oocyte surface of COCs. CMPs are short peptide sequences which bind to a specific amino acid sequence on the gap junction extracellular loop domains thus blocking gap junctional communication in an isoform-specific manner (see section below) [Evans & Leybaert 2007; Evans et al. 2012].

Microinjection into oocytes within COCs was performed in drops of Hepes-mKSOM plated on the lid of a 60mm x 15mm culture dish under an overlay of filter-sterilized embryo culture-grade mineral oil. Holding and injection pipettes were controlled using a Medical Systems PLI-100 microinjection apparatus (Harvard Apparatus, Holliston, MA) with Narishige MMN-I micromanipulators mounted on a Zeiss Axiovert microscope. COCs were held in place using holding pipettes (Humagen Fertility Diagnostics, Charlottesville, VA) which immobilize the COC during microinjection by suction controlled by the microinjection apparatus. Microinjection into the oocyte was achieved using microinjection needles preloaded with antiserum and inserted into oocytes using the micromanipulators. Using the microinjection apparatus and pressure-pulse, ~10 picolitres was injected into oocytes representing ~5-10% of the total oocyte volume. Confirmation of successful oocyte microinjection was determined based on the observed displacement of oocyte cytoplasm upon injection.

Microinjection at the oocyte surface of COCs was performed similarly to microinjection into oocytes except that the microinjection needle was not directly inserted into the oocyte but instead the tip of the injection needle was placed directly at the oocyte surface and just beneath the ZP. Using the micromanipulators, the injection needle preloaded with Cx37 CMP was advanced toward the oocyte until the slightest deformation

of the oocyte surface was observed microscopically at which point no further movement of the microinjection needle was performed. Microinjection at the oocyte surface was assessed by visible detection of lateral injection fluid movement along the surface of the oocyte below the ZP. COCs were excluded if any displacement of oocyte cytoplasm (swelling) was observed to indicate that intra-oocyte microinjection had occurred.

4.4 Antral follicle culture in small volumes of culture medium

To determine whether increasing the number of follicles within a specified volume of culture medium could prevent significant antral fluid dilution during culture, intact antral follicles were cultured in small drops of culture medium varying from 10-500 µl. NPPC (100 nM) and E_2 (100 nM) were used to maintain meiotic arrest throughout the culture period. To prevent E_2 loss into the oil overlay, culture drops were plated on 35mm x 10mm culture dishes and enclosed within 100mm x 15mm petri dishes containing a KimWipe moistened with antral follicle culture medium to maintain humidity and prevent evaporation of the small drops of culture medium. Antral follicles were added to culture drops using tweezers to minimize the transfer of additional culture medium to drops and drops containing antral follicles were cultured at 5%CO_2/air and 37ºC. Prior to plating culture drops, medium was pre-equilibrated in organ dishes with filter-sterilized water added to outer wells at 5%CO_2/air and 37ºC. No increase in osmolarity was detected using a Vapro 5520 osmometer (Wescor, Logan, UT) in the smallest culture drops (10 µl) indicating that significant evaporation did not occur during the culture period.

5. Pharmacological manipulations

5.1 NPPC-cGMP signalling and maintenance of meiotic arrest

In most experiments, NPPC (100 nM) and E_2 (100 nM) were added to culture medium to maintain meiotic arrest in COCs and during prolonged punctured antral follicle culture. Meiotic arrest was maintained in the absence of additional NPPC and E_2 for cultured intact antral follicles and denuded GV oocytes were maintained in meiotic arrest with dbcAMP (300 µM).

To further examine a possible role for NPPC-cGMP signalling in the maintenance of GLYT1 suppression, COCs were cultured 4 hours in the presence of various agonists of the NPPC-cGMP signalling pathway known to mediate meiotic arrest [Zhang et al. 2010]. COC culture medium was supplemented with various combinations of NPPC (100 nM), E_2 (100 nM), guanosine (50 µM), hypoxanthine (4 mM), and the oocytes-specific PDE9 inhibitor BAY 73-6691 (100 µM). COC culture medium containing the additional components was pre-equilibrated for 2 hours at 5%CO_2/air and 37ºC in organ dishes with filter-sterilized water added to the outer well. COCs were isolated as described above and added directly to the organ dishes and cultured at 5%CO_2/air and 37ºC. Freshly isolated COCs were used as a control with an intact GV found to be present in all COCs.

5.2 General and specific gap junction inhibition

General gap junction inhibition was performed in COCs, intact antral follicles, and punctured antral follicles. The primary inhibitor used to non-selectively block all gap junctional communication in COCs and antral follicles was 18α-glycyrrhetinic acid (AGA)

at a final working concentration of 150 µM. This inhibitor was previously shown to block the diffusion of fluorescein that was microinjected into oocytes to the surrounding granulosa cells indicating that gap junctions had effectively been inhibited [FitzHarris & Baltz 2006]. Lindane was also used in some experiments to confirm the effect of general gap junction inhibition on the maintenance of meiotic arrest and was used at a final working concentration of 10 µM. COCs were cultured in 1 ml of COC culture medium with or without general gap junction inhibitors in organ dishes with filter-sterilized water in the outer well at 5%CO_2/air and 37ºC. Intact and punctured antral follicles were cultured in 1 ml of antral follicle culture medium with or without general gap junction inhibitors in organ dishes with filter-sterilized water in the outer well at 5%CO_2/50%O_2/45%N_2 and 37ºC in modular chambers (Billups-Rothenburg, Inc., Del March, CA). NPPC (100 nM) and E_2 (100 nM) were added to culture medium for COC and punctured antral follicle culture to maintain meiotic arrest.

Connexin-mimetic peptides (CMPs; Alpha Diagnostics, San Antonio, TX) directed against GJA1 (connexin-43) and GJA4 (connexin-37) gap junctions were used to inhibit specific gap junction isoforms in COCs and punctured antral follicles. A scrambled version of each CMP (ScrCMP; Alpha Diagnostics, San Antonio, TX) was used as a control for each experiment as described in the results section of this thesis. To conserve peptide, COCs were cultured in 20 µl drops of COC culture medium with or without CMPs or ScrCMPs added on 35mm x 10mm culture dishes enclosed within 100mm x 15mm petri dishes containing a KimWipe moistened with COC culture medium. An additional CMP (CHI Scientific, supplied by Dr. Laurinda Jaffe) and corresponding scrambled CMP were also used to specifically inhibit GJA1 (connexin-43) gap junctions in COCs. For both CMP

brands, COCs were cultured at 5%CO_2/air and 37ºC with NPPC (100 nM) and E_2 (100 nM) added to maintain meiotic arrest.

Since we showed that the maintenance of healthy intact antral follicles in culture requires a minimum of 100 µl per follicle (Figure 20), punctured antral follicles were cultured in 1 ml of antral follicle culture medium with or without CMPs or ScrCMPs in organ dishes with filter-sterilized water added to the outer well. Punctured antral follicles were cultured at 5%CO_2/50%O_2/45%N_2 and 37ºC in modular chambers (Billups-Rothenburg, Inc., Del Mar, CA) with NPPC (100 nM) and E_2 (100 nM) added to maintain meiotic arrest. Specific inhibition of gap junctions using CMPs was performed using punctured antral follicles, and not intact antral follicles, since gap junction inhibition was shown to be more effective when antral follicles were punctured to allow peptides to access the follicle interior rapidly (Figure 24, see Results section).

5.3 Luteinizing hormone (LH) stimulation in antral follicles

To examine the effect of LH stimulation on meiotic resumption and GLYT1 activation, intact antral follicles from neonatal mice (unstimulated) were cultured based on the method by Norris and colleagues [Norris et al. 2008]. Follicles from neonatal (prepubertal) mice were used to obtain a uniform population of follicles at the same developmental stage in which LH-responsiveness could be stimulated simultaneously with FSH treatment *in vitro*; the use of intact antral follicles from neonatal mice has previously been validated and follicles from neonatal mice were shown to be able to resume meiosis in response to LH treatment [Norris et al. 2008]. Intact antral follicles were isolated

mechanically from postnatal day 21 (P21) CF1 mice by gently prying apart ovarian tissue to obtain intact antral follicles devoid of excess ovarian tissue with a clear visible antrum and oocyte. Intact antral follicle isolations were performed in Hepes-mKSOM medium. Following isolation, intact antral follicles were transferred using tweezers to antral follicle culture medium pre-equilibrated at 5%CO_2/50%O_2/45%N_2 and 37ºC. Follicles were cultured ~20 hours in 1 ml of antral follicle culture medium in organ dishes with filter-sterilized water in the outer well at 5%CO_2/50%O_2/45%N_2 and 37ºC. Antral follicle culture medium contains 100 ng/ml of FSH which increases the LH-responsiveness of the antral follicles. After the initial 20-hour culture period, antral follicles were transferred, using tweezers, to organ dishes containing 1 ml of antral follicle culture medium pre-equilibrated at 5%CO_2/50%O_2/45%N_2 and 37ºC either with or without 350 nM of LH added (National Hormone and Pituitary Program of National Institute of Diabetes and Digestive and Kidney Diseases, Bethesda, MD). Antral follicles were cultured in the presence or absence of LH in modular chambers at 5%CO_2/50%O_2/45%N_2 at 37ºC.

5.4 COC-laminin binding inhibition: anti-laminin antibody

An anti-laminin antibody (rabbit polyclonal, affinity purified, Cat# L9393) directed specifically against laminin-111 isolated from Engelbreth-Holm-Swarm (EHS) mouse tumor was added to culture medium to block COCs from binding to laminin during culture. This specific antibody has previously been used to successfully block the ability of laminin to maintain pericytes in an undifferentiated state leading to differentiation of primary pericyte cultures plated on laminin [Yao et al. 2014]. The anti-laminin antibody was supplied in a solution of 0.01M phosphate buffered saline (PBS, pH 7.4) with 1% BSA and

15 mM sodium azide with an antibody concentration of 0.5 mg/ml. Sodium azide is toxic to cells in culture and was therefore removed from the antibody solution prior to use by dialysis with D-Tube Dialyzers (EMD Millipore, Etobicoke, ON) to enable diffusion of the sodium azide out of solution while retaining antibody and proteins. This method utilizes a semi-permeable membrane with pore sizes through which small components may pass resulting in the removal of these components from the solution. The molecular weight of sodium azide is small (~65 Da) relative to IgG (~150 kDa) which allows sodium azide to easily diffuse through the membrane pores and out of the antibody solution while the resulting solution in the D-tube Dialyzers retains the antibody.

Mini D-tube Dialyzers (EMD Millipore, Etobicoke, ON) with a volume capacity of 10-250 µl were used for the dialysis of the laminin antibody solution containing 15 mM of sodium azide. In accordance with the manufacturer's instruction, D-tube Dialyzer caps were removed and 250 µl of filter-sterilized water was added to the membrane and allowed to set for at least 5 minutes at room temperature with the cap screwed on. After the 5-minute incubation, the filter-sterilized water was removed using a pipette with care taken to ensure that the membrane was not punctured. The laminin antibody solution was then added to the D-tube dialyzer (20 µl) using a pipette and the cap was screwed onto the tube securely. The D-tube Dialyzer was placed into a floating rack provided by the manufacturer. The dialysis buffer was Hepes-mKSOM and ~200 mL was added to a beaker with a stir bar in the bottom and the D-tube dialyzer in the floating rack was placed into the beaker with the entire membrane surface submerged in Hepes-mKSOM. The beaker was placed on a magnetic stirrer and equilibration of the antibody solution and buffer was performed overnight at 4ºC to ensure adequate removal of the sodium azide from the

antibody solution. After the overnight equilibration, the antibody solution was gently removed from the D-tube Dialyzer using a pipette. The volume of the removed antibody solution was verified to be the same as the volume originally added to the D-tube Dialyzer to ensure that the antibody concentration had not changed. Purified rabbit IgG was used as a control and a solution containing 1% BSA and 15 mM sodium azide was prepared in PBS (pH 7.4) with a final concentration of 0.5 mg/ml rabbit IgG (the same as the laminin antibody concentration). Sodium azide removal from the rabbit IgG solution was identical to the removal method used for the laminin antibody solution.

To examine the effect of anti-laminin antibody on the ability of laminin to suppress GLYT1 activity in COCs, the minimum concentration of the sodium azide-free laminin antibody solution needed to prevent adhesion of COCs to the laminin coating was determined. Preliminary experiments revealed that at least 50 µg/ml of the laminin antibody solution was needed to fully block laminin-COC binding. Purified laminin was plated on culture wells of a 96-well culture dish as described above and 50 µg/ml of laminin antibody or rabbit IgG solution (without sodium azide) was added to MGC culture medium. Medium supplemented with anti-laminin antibody or rabbit IgG control was added to the laminin-coated culture wells and incubated overnight (~18 hours) at 5%CO_2/air and 37ºC to facilitate binding to the purified laminin coating. Uncoated culture wells (plastic only) and laminin-coated culture wells covered with MGC medium without laminin antibody or rabbit IgG were used as controls. After the overnight incubation period, COCs were added to culture wells and cultured 4 hours at 5%CO_2/air and 37ºC and then cumulus cells were removed using a flame-pulled Pasteur pipette and GLYT1 activity was measured.

6. Radiolabelled glycine experiments

A detailed protocol has been published by our laboratory which describes how to measure the transport and accumulation of radiolabelled substrates in oocytes and embryos:

Baltz JM, Corbett HE, & Richard S. (2013) Measuring transport and accumulation of radiolabeled substrates in oocytes and embryos. *Meth Molec Biol*; 957:163-78.

The utilization of [^{3}H]-glycine ([2-^{3}H]-glycine; ~47 Ci/mmol; Perkin Elmer, Boston, MA, USA) as a method for measuring the rate of GLYT1-specific glycine transport into oocytes and embryos has been previously demonstrated in our laboratory [Dawson et al. 1998; Steeves et al. 2003; Steeves et al. 2005; Tartia et al. 2009]. Based on the results of previous experiments which showed that [^{3}H]-glycine accumulation occurs rapidly when GLYT1 is active and reaches a plateau by ~3-4 hours, oocytes were first cultured 4 hours and then incubated in the presence of [^{3}H]-glycine (1µM) and the total molar amount of accumulated [^{3}H]-glycine was measured following a 10-minute incubation period [Steeves et al. 2003; Tartia et al. 2009].

To determine the total molar amount of [^{3}H]-glycine in oocytes following the 10-minute incubation period, a standard curve was prepared weekly. The serial dilutions used in the construction of the standard curve were previously validated so that the radioactive measurements in oocytes incubated for 10 minutes with 1 µM [^{3}H]-glycine uptake fall within the range of points of the standard curve. Two 15 ml tubes were filled with 5 ml or 7.5 ml of filter-sterilized water and 1 µl of the stock solution of [^{3}H]-glycine (~21 µM) was added to each tube and vortexed. Thus, one tube contained a 1:5,000 dilution and the other tube contained a 1:7,500 dilution relative to the stock solution of [^{3}H]-glycine. Five serial

twofold dilutions were performed from each tube producing a range of dilutions including: 1:5,000, 1:7,500, 1:10,000, 1:15,000, 1:20,000, 1:30,000, 1:40,000, 1:60,000, 1:80,000, 1:120,000, 1:160,000, and 1:240,000. Thirteen polyethylene scintillation vials with screw caps were labelled with the appropriate dilution and 5 µl from each dilution tube was added to the vials with a final vial containing 5 µl of filter-sterilized water which was used as a background measure. Scintillation fluid (4 ml; Scintiverse BD, Fisher Scientific, Pittsburgh, PA, USA) was added to each scintillation vial, caps were securely screwed on, and vortexed. The radioactivity was measured using a scintillation counter (2200CA TriCarb, Packard Instrument Co., Downer's Grove, IL, USA) and each sample was counted for 5 minutes [Dawson et al. 1998].

Isolation of oocytes was performed as described above for the [^{3}H]-glycine uptakes and washed through 3 drops of Hepes-mKSOM before incubation with [^{3}H]-glycine. [^{3}H]-glycine incubation drops were prepared using a concentrated mKSOM (70mKSOM) which was identical to mKSOM except that only 70% of the normal amount of filter-sterilized water was added to the medium. This concentrated 70mKSOM was used to enable the addition of the stock concentration of radiolabelled compound directly and the amount of filter-sterilized water added was adjusted to obtain normal strength medium for the final incubation drop. Immediately prior to incubation with [^{3}H]-glycine, oocytes were quickly washed through three 50 µl drops of pre-equilibrated (5%CO_2/air; 37ºC) mKSOM under an oil overlay using a flame-pulled Pasteur pipette. Oocytes were then incubated for 10 minutes at 5%CO_2/air and 37ºC in a 50 µl drop of pre-equilibrated (5%CO2/air; 37ºC) 70mKSOM containing [^{3}H]-glycine (1 µM) and added filter-sterilized water to produce an osmolarity of 250 mOsM (± 5 mOsM) in the incubation drop. Immediately after the 10-

minute incubation, oocytes (5-10 pooled) were washed quickly through 6 drops of ice-cold Hepes-mKSOM and expelled with a minimal amount of medium into a scintillation vial. The same amount of medium from the final wash drop (without oocytes) was expelled into another scintillation vial to be used as a measure for background. Scintillation fluid (4 ml; Scintiverse BD, Fisher Scientific, Pittsburgh, PA, USA) was added to each scintillation vial, caps were securely screwed on, and vortexed. The radioactivity was measured using a scintillation counter (2200CA TriCarb, Packard Instrument Co., Downer's Grove, IL, USA) and each sample was counted for 5 minutes [Dawson et al. 1998]. For small growing oocytes (< 75 µm in diameter), the concentration of [^{3}H]-glycine in the incubation drops was increased to 3 µM to ensure that adequate glycine was accumulated for detection by the scintillation counter and the rate was later normalized by dividing by 3 [Baltz et al. 2013].

The standard curve was plotted and a line was fit by linear least squares regression in which the r^2 value was not less than 0.98 and all points did not significantly deviate from the fitted line. Using the parameters of the regression in a linear equation, the total molar amount (fmoles) of [^{3}H]-glycine in the pooled oocytes in scintillation vials was measured based on the average counts per minute as determined by the scintillation counter. To determine the rate of [^{3}H]-glycine uptake into oocytes, the total molar amount of [^{3}H]-glycine in oocytes was divided by the number of oocytes and this value was divided by 10 to obtain a rate of uptake per oocyte per minute expressed in fmoles/oocyte/min.

7. GLYT1 gene and protein expression analysis

7.1 Immunofluorescence

Immunofluorescence detection of GLYT1 in oocytes and embryos was performed using a polyclonal rabbit IgG anti-SLC6A9 (GLYT1) antibody raised against a 19-amino acid sequence (AQIPIVGSNGSSRFQDSRI) in the C-terminus of mouse GLYT1 [Gabernet et al. 2005]. This antibody has been previously validated in the dorsal telencephalon of conditional knockout mice homozygous null for a forebrain-selective deletion of GLYT1 in which GLYT1 immunoreactivity was absent compared to wildtype mice, and in mice heterozygous null for GLYT1 in brain where western blot band intensity was reduced compared to wildtype mice; furthermore, an immunogenic peptide targeted to the same peptide sequence eliminated all GLYT1-specific staining [Gabernet et al. 2005; Mohler et al. 2011].

Oocytes and embryos were isolated as described above and washed through 3 drops of Hepes-mKSOM. Immediately following isolations, oocytes and embryos were transferred to acidic Tyrode's solution (stored at -20ºC) pre-warmed for ~30 minutes at 37ºC and incubated for 10-15 seconds at room temperature to remove the ZP. ZP removal was visually monitored on a stereoscope and oocyte and embryos were removed from the Tyrode's solution as soon as the ZP could no longer be seen. Oocytes and embryos were immediately washed through 3 drops of Hepes-mKSOM and then transferred to 300 µl of fixation solution (2% PFA in PBS) in a 24-well culture dish (Thermo Scientific) with ~15 oocytes or embryos per well. ZP-free oocytes and embryos were incubated for 20 minutes in fixation solution at room temperature and then washed through 3 wells containing 300 µl of washing solution (0.05% Tween 20 in PBS) for 5 minutes per wash. When a

developmental series of embryo stages was required for immunofluorescence, embryos were kept in the final wash solution well for up to 1 day (24 hours) in a humidified box at 4ºC. After fixation and washing, oocytes and embryos were permeabilized in 100 µl of blocking solution (5% normal goat serum (NGS), 0.01% Triton X-100 in PBS) in a 96-well culture dish for 1 hour at room temperature and then transferred to a well containing 50 µl of antibody dilution buffer (ADB; 1% NGS, 0.005% Triton X-100 in PBS) containing the previously validated anti-SLC6A9 primary antibody (1:100) and incubated overnight (16-18 hours) at 4°C in a humidified box. After the overnight incubation, oocytes and embryos were washed through 4 culture wells containing 100 µl of ADB for 15 minutes per wash and then transferred to a well containing 100 µl of ADB with goat anti-rabbit-Alexa 594 secondary antibody (1:200, Life Technologies, Burlington, ON, Canada) and incubated overnight (16-18 hours) at 4°C in a humidified box. After the overnight incubation with secondary antibody, oocyte and embryos were washed through 3 wells containing 100 µl ADB and were mounted onto glass slides in 4 µl of Antifade mounting solution (Life Technologies, Burlington, ON, Canada). Imaging was performed using confocal microscopy on a Zeiss LSM 510 META Confocal Microscope using a 40x oil-immersion objective.

A peptide (Selleck Chemicals, Houston, TX) identical to the 19 amino acid sequence used to produce the anti-GLYT1 (SLC6A9) primary antibody (AQIPIVGSNGSSRFQDSRI) was used as a competitive inhibitor. Where specified, the competitive peptide (1:10) was added to the GLYT1 primary antibody solution for the overnight incubation period.

7.2 Western blot

The same SLC6A9 antibody used for the detection of GLYT1 by immunofluorescence was also used to detect GLYT1 protein by western blot analysis [Gabernet et al. 2005; Mohler et al. 2011]. GAPDH was used as the loading control and was detected using sc-25778 antibody (rabbit IgG; Santa Cruz, Dallas, Texas, USA). RIPA lysis buffer was used for protein extraction which was 20 mM Tris-HCl (pH 7.4), 150 mM NaCl, 1 mM EDTA, 1% Triton X-100, 1% sodium deoxycholate, 0.1% SDS, 1 mM PMSF, 5 µg/ml aprotinin, and 5 µg/ml leupeptin. Oocytes and embryos were isolated as described above, washed through 3 drops of Hepes-mKSOM, and expelled into 3 µl of RIPA lysis buffer in 1.5 ml microcentrifuge tubes using a flame-pulled Pasteur pipette. Tubes containing lysed oocytes and embryos in RIPA buffer were incubated on ice for 5 minutes and then stored at -20ºC until use. Preliminary experiments showed that GLYT1 could be detected by western blot when ~120 oocytes were present in each lane, therefore, oocytes and embryos were pooled from 2-3 microcentrifuge tubes to yield 120 oocytes or embryos per lane and considered to be one independent repeat.

Brain tissue from the hippocampus and cortical regions was used as a positive control and for testing the antibody specificity using western blot analysis. Brain tissue was isolated from a CF1 female mouse and transferred to a 1.5 ml microcentrifuge tube and 1 ml of RIPA lysis buffer was immediately added. The tissue was frozen and thawed 3 times using liquid nitrogen and warm water and then transferred to a hand-held glass homogenizer tube and incubated 10 minutes on ice. After 10 minutes, the tissue was completely homogenized by a glass plunger, transferred to a 1.5 ml microcentrifuge tube, and centrifuged at 11,000xg for 10 minutes at room temperature. Supernatant was collected

and stored at -80ºC until use. The amount of isolated brain protein lysate was measured by Lowry assay using a BSA standard curve (1.38 mg/ml stock; Bio-Rad Laboratories, Mississauga, ON) and spectrophotometer at an absorbance of 750 nm. Western blots were performed using 5 µg of brain protein per lane.

Laemmli buffer (2X; Bio-Rad Laboratories, Mississauga, ON) was added in equal volume to samples in RIPA lysis buffer (10µl sample + 10µl 2X Laemmli buffer) and β-mercaptoethanol added to make up 5% of the final volume. Samples were centrifuged briefly and boiled in a water bath for 5 minutes. Samples were loaded into wells of 10% SDS-PAGE gels and run in SDS-PAGE buffer (25 mM Tris, 190 mM glycine, 0.1% SDS in filter-sterilized water) for 1 hour at ~70V. Empty wells were filled with an equal volume of 1X Laemmli buffer and pre-stained protein ladders (Rio-Rad Laboratories, Mississauga, ON) were run as markers for molecular weight and as a reference for appropriate band separation. Proteins separated on SDS-PAGE gels were transferred onto nitrocellulose membranes for 70 minutes at ~100V in transfer buffer (25 mM Tris, 190 mM glycine, 20 % methanol in filter-sterilized water) at 4ºC.

After transfer, protein transfer was visualized by Ponseau S solution and membranes were cut for blocking and primary antibody exposure. Membranes were blocked for 1 hour at room temperature with 5% milk powder dissolved in TBST buffer (20 mM Tris pH 7.5, 150 mM NaCl, 0.1% Tween 20 in filter-sterilized water) and then incubated overnight at 4ºC with SLC6A9 primary antibody (1:1000) in 5% milk powder. For some experiments, the same competitive SLC6A9 peptide used for immunofluorescence was also used to determine the specificity of bands visualized by western blot. For these experiments, competitive peptide was added to the primary

antibody incubation (1:1000) at a final concentration of 2-10 µg/ml. Membranes were then incubated with 1:2000 goat anti-rabbit HRP-conjugated IgG (Bio-Rad Laboratories, Mississauga, ON) for 1 hour at room temperature. For GAPDH, membranes were incubated overnight with anti-GAPDH primary antibody (1:200) and then incubated for 1 hour at room temperature with 1:5000 goat anti-rabbit HRP-conjugated IgG. After the secondary antibody incubation, membranes were washed three times with TBST buffer for 10 minutes per wash at room temperature.

Chemiluminescent detection of GLYT1 was performed using the Amersham ECL Prime kit (RPN2232, GE Healthcare, Mississauga, ON) and the Thermo Scientific Pierce ECL kit (32209, ThermoFisher Scientific, Burlington, ON) was used for GAPDH detection.

7.3 Reverse transcription-polymerase chain reaction

RT-PCR and qRT-PCR were used to identify and quantify *Glyt1a* expression throughout oogenesis and preimplantation embryo development. RNA was extracted from 30 oocytes or embryos, liver was used as a positive control tissue, and water was used as a negative control. Samples were frozen-thawed three times in 1.5 ml microcentrifuge tubes using liquid nitrogen and warm water to lyse samples completely. RNA extraction was performed as per manufacturer's instructions using the RNeasy Micro Kit (Qiagen, Mississauga, Ontario, Canada) and immediately reverse-transcribed using the Retroscript Kit (Ambion, Austin, TX). RNA was extracted from three independent sets of oocytes and embryos. Reverse transcription of RNA was performed as per manufacturer's instructions

using the Retroscript Kit with the RNA template first heated at 70ºC for 3 minutes with water and random decamers added. After the initial heating, the remaining RT components provided with the Retroscript Kit were added and samples were incubated at 42ºC for 1 hour and then the temperature raised to 92ºC for 10 minutes to terminate the reverse transcription reaction. Following reverse transcription, cDNA was stored at -20ºC until use for PCR reactions.

Primers (Invitrogen/Thermo Fisher, Waltham, MA) were designed to detect the *Slc6a9a (Glyt1a)* variant reported in rodents for RT-PCR [Liu et al. 1993]. For *Slc6a9a*, the forward, sense primer was 5'-AAAAGGTGCCAAAGGGATGTT-3'(nucleotides 316-335 of mouse *Slc6a9a*, NM_008135.4) and the reverse, antisense primer was 5'-GTCAGTACAAACTCGATCTGGTT-3' (nucleotides 401-423), producing a 108 bp amplicon. Peptidylprolyl isomerase A (*Ppia*), whose expression throughout preimplantation embryo development has previously been validated in mouse preimplantation embryos [Mamo et al. 2007], was used to confirm the expected mRNA expression pattern. For *Ppia*, the forward, sense primer was 5'-CGCGTCTCCTTCGAGCTGTTTG-3' and the reverse, antisense primer was 5'TGTAAAGTCACCACCCTGGCACAT-3' (mouse Ppia, NM_008907) producing a 150 bp amplicon.

Conventional PCR reactions (Hotstar Taq polymerase, Qiagen; Mastercycler thermocycler, Eppendorf, Hamburg, Germany) contained 1 (*Slc6a9a* and *Ppia*) oocyte or embryo equivalent of cDNA in a 20 µl reaction volume or 100 ng of liver cDNA in a 20 µl reaction volume. For *Glyt1a*, PCR cycles were 95ºC for 15 minutes then 35 cycles at 94ºC for 60 seconds, 60ºC for 30 seconds, and 72ºC for 60 seconds then a final 72ºC for

10 minutes. For *Ppia*, PCR cycles were 95ºC for 2 minutes then 40 cycles at 95ºC for 15 seconds, 60ºC for 20 seconds, and 72ºC for 30 seconds and then a final 72ºC for 5 minutes. DNA amplicons were visualized by gel electrophoresis on a 1.4% agarose gel with 0.6 µg/ml ethidium bromide which was run for 1 hour at 105V. DNA fragments were visualized by UV light after electrophoresis, agarose gel extraction was performed (QIAquick gel extraction kit, Qiagen), and confirmed to be *Glyt1a* by direct sequencing.

Quantification of *Glyt1a* cDNA was performed using FastStart DNA MasterPLUS SYBRGreen I (Roche Applied Science, Laval, QC) on a LightCycler 480 System. The primers and thermocycle temperatures were identical to those used for conventional PCR but the cycle times were 60, 10, and 15 sec. Six serial dilutions of liver cDNA were used to prepare standard curves for *Glyt1a* and *Ppia* beginning with a concentration of 1 pg/µl. The PCR product concentration of the dilution series was determined by absorbance and the resulting standard curve was used to quantify the amount of cDNA in oocyte or embryo samples for quantitative PCR. The specificity of the PCR products was confirmed by a melting curve analysis.

8. Data analysis

Graphs were prepared using GraphPad Prism 5.00 (GraphPad Software, San Diego, CA). Data for continuous variables were expressed as mean ±SEM. Statistical analysis of the data was performed by ANOVA followed by the Tukey multiple comparison test (when three or more groups were compared) or by Student two-tailed t-test (to compare two groups) using Prism.

For oocyte-ZP attachment experiments, data were grouped into two outcome categories, attached and not attached, the latter taken to be the sum of the detached and partially attached categories. In each case where Chi-square for trend was used, a standard Chi-square was first performed (using all 3 outcome categories in the case of oocyte-ZP attachment) and confirmed to have at least the same level of significance as the trend test.

SUMMARY OF PUBLICATIONS

Portions of the results and methodology reported here have been published as follows:

Chapter 1:

Baltz J.M., Corbett H.E., & **Richard S.** (2013). Measuring transport and accumulation of radiolabeled substrates in oocytes and embryos. *Meth Molec Biol*; 957:163-78. Ch. 11, In: Mammalian Oocyte Regulation: Methods and Protocols (ed. HA Homer), Springer, NY.

Chapter 1:

Richard S., Tartia A.P., Boison D., & Baltz J.M. (2016). Mouse oocytes acquire mechanisms that permit independent cell volume regulation at the end of oogenesis. *J. Cell Physiol*; 232(9):2436-2446.

Chapter 2:

Richard S. & Baltz J.M. (2014). Prophase I arrest of mouse oocytes mediated by natriuretic peptide precursor C requires GJA1 (connexin-43) and GJA4 (connexin-37) gap junctions in the antral follicle and cumulus-oocyte complex. *Biol. Reprod;* 90: 137, 1-10.

Chapter 3, 4, & 5:

Richard S. & Baltz J.M. (2017). Preovulatory suppression of oocyte cell volume regulatory mechanisms is via signaling distinct from meiotic arrest. *Sci. Rep;*7(1):702.

RESULTS

1. The abilities to activate GLYT1 and to release oocyte-zona pellucida (ZP) adhesion are acquired during oogenesis

Detachment of the oocyte from the ZP and GLYT1 activation were previously shown to occur spontaneously when fully grown oocytes were isolated from ovarian follicles [Tartia et al. 2009]. GLYT1 activation was independent of meiotic maturation [Tartia et al. 2009]. However, when during oogenesis these abilities are first acquired is unknown. Therefore, I sought to determine the stage in oocyte development that oocytes are first able to detach from the ZP and activate GLYT1 and compare this to the stage in oogenesis that oocytes become meiotically competent. I also investigated when during oocyte growth that *Glyt1* (*Slc6a9*) transcripts and GLYT1 (SLC6A9) protein first appear to gain insight into how GLYT1 is activated after ovulation is triggered *in vivo* or following removal of oocytes from ovaries *in vitro*.

1.1 A hypertonic shock assay enables rapid determination of the extent of oocyte-ZP attachment

Our lab has previously shown that GLYT1 activation begins immediately following isolation of oocytes from follicles and is essentially complete by ~4 hours in fully grown oocytes [Tartia et al. 2009]. To examine whether oocyte-ZP detachment follows a similar time-course to GLYT1 activation, a simple osmotic shock assay was first developed and validated to rapidly assess the extent of oocyte-ZP adhesion at various times following the removal of oocytes from the ovarian follicle.

After the specified period in culture, oocytes were transferred to the hypertonic assay medium (1000 mOsM mKSOM) to induce hypertonic shock and oocyte shrinkage. They were then imaged immediately using a Nikon E4500 camera mounted on a Zeiss Axiovert microscope. Oocytes that were completely adhering to the ZP formed a structure resembling a concave disc, oocytes that were completely detached from the ZP shrank into a small sphere with a clear space between the oocyte and ZP, while oocytes that were partially attached to the ZP resembled an intermediate of the attached and detached state (Figure 10A).

Confocal microscopy with Z-series stacks were used to confirm the geometries of oocyte-ZP adhesion following hypertonic shock treatment. This was particularly needed to confirm that the ZP was completely adhering to the oocyte membrane in the proposed concave disc configuration. Alexa 488-conjugated WGA stained the ZP (green) while Alexa 594-phalloidin strongly stained subcortical actin within oocytes (red). Control oocytes in 250 mOsM culture medium (no hypertonic shock treatment) were spherical with a distinct ring shape for both the oocyte and ZP (Figure 10B). Oocytes which were completely adhering to the ZP and exposed to hypertonic shock treatment (1000 mOsM mKSOM) showed identical deformation of the oocyte plasma membrane and ZP into a concave disc shape (Figure 10C). Hypertonically shocked oocytes which were partially adhered to the ZP showed multiple areas of the oocyte plasma membrane which shrunk away from the ZP while other areas remained adhered to the ZP (Figure 10D). Oocytes which completely detached from the ZP during culture shrunk away from the ZP with a clear spherical oocyte contained with a spherical ZP separated nearly completely by an extensive space (Figure 10E).

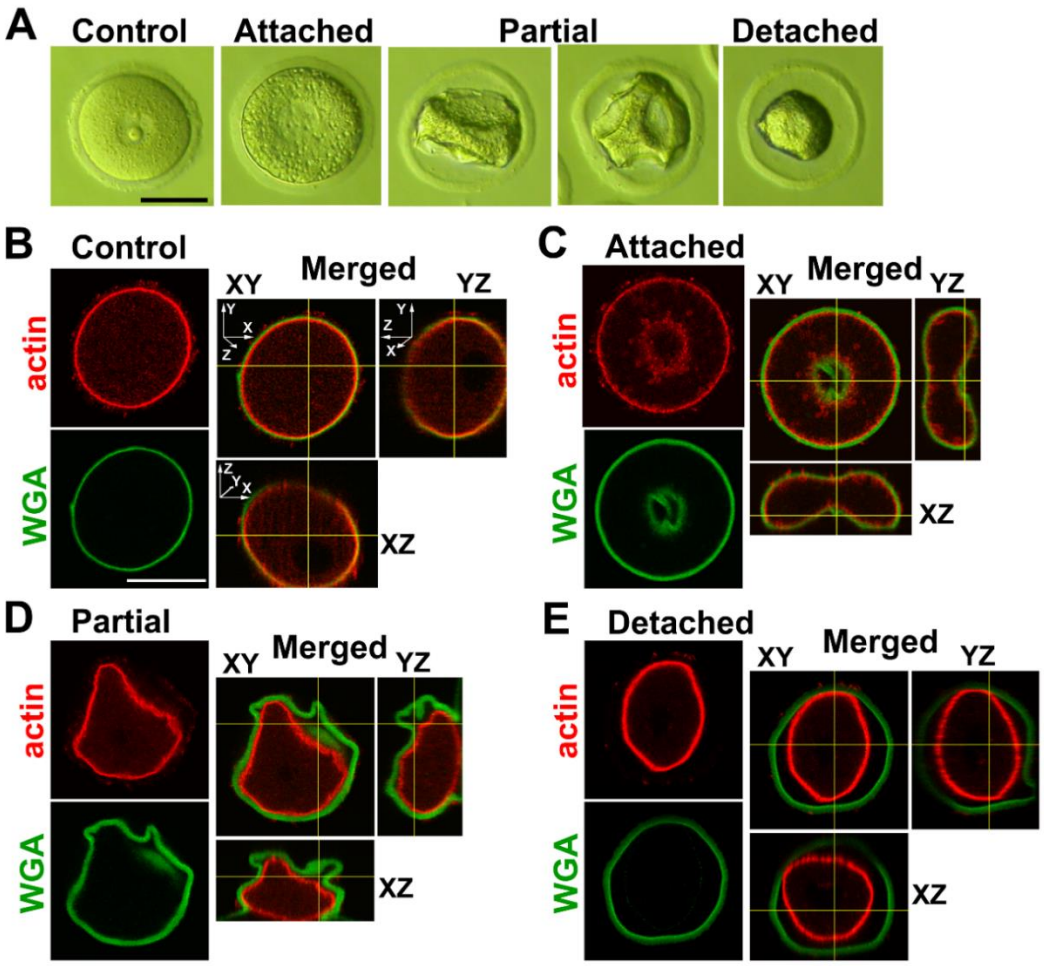

Figure 10. Oocyte-ZP hypertonic shock assay. (**A**) Images of oocytes exposed to our hypertonic shock assay at various times following isolation from ovarian follicles. Oocyte images were captured immediately after hypertonic shock (1000 mOsM mKSOM) using a Nikon E4500 camera mounted on a Zeiss Axiovert microscope. A control oocyte is shown without exposure to the hypertonic assay at 250 mOsM. Attached oocytes are completely adhered to the ZP, this image was taken immediately after isolation from the ovary. Partially attached oocytes are attached to the ZP in some but not all areas, two images are shown with the first taken at 1 hour after isolation from the ovary and the second taken at

1.5 hours after isolation from the ovary. Detached oocytes are completely detached from the ZP with a clear space visible, this image was taken 2 hours after isolation from the ovary. The scale bar in the first image represents 50 μm and is applicable to all images shown in panel **A**. For **B-E** Representative slices are shown of Z-series stacks of oocytes exposed to hypertonic shock (1000 mOsM mKSOM), stained for actin (red; oocyte plasma membrane) and wheat germ agglutinin (WGA; green; zona pellucida) and imaged with a Zeiss LSM 510 META Confocal Microscope. Merged images in three planes of view are shown (XYZ) to better visualize the geometry of oocytes which were not exposed to hypertonic shock (**B**) or were exposed to hypertonic shock at various times after removal from ovarian follicles and which were scored as attached (**C**), partially attached (**D**), or completely detached (**E**) from the ZP. Images of each plane (XY, YZ, and XZ) were constructed from Z stacks using Image J. The scale bar represents 50 μm and is applicable to all images shown in panel **B** through **E**. Visualization was optimized individually for each image by adjusting the contrast and brightness of the confocal images to enhance visualization of the oocyte and ZP, and not to allow direct comparison of staining intensities between images. This figure was reproduced with permission from WILEY & Journal of Cellular Physiology. Richard S. et al. (2016). Mouse oocytes acquire mechanisms that permit independent cell volume regulation at the end of oogenesis. *J Cell Physiol*; 232(9): 2436-2446.

1.2 Oocyte-ZP detachment occurs spontaneously following removal from the ovarian follicle and is complete by 2.5 hours

Tartia et al. [2009] previously used transmission electron microscopy to infer that oocyte plasma membrane microvilli gradually lose association with the ZP *in vivo* during the interval 0-3 hours after hCG administration. To examine the timing of functional oocyte-ZP detachment *in vitro* following removal of oocytes from the ovarian follicle, fully grown GV oocytes were isolated from eCG-primed adult female mice and cultured 0-2.5 hours *in vitro* with cohorts of oocytes exposed to hypertonic shock treatment at half hour intervals. Oocytes were maintained in meiotic arrest during the culture period by adding dbcAMP to culture medium. Oocytes all completely adhered to the ZP immediately after removal from ovarian follicles (0 hours). This had decreased to ~40% by 1 hour and no oocytes were still fully adhering to the ZP by 2.5 hours in culture (Figure 11A). During the transition from complete oocyte-ZP adhesion to complete oocyte-ZP detachment, a population of oocytes transiently appeared that were partially attached to the ZP (as described in section 1.1) which was maximal at ~1 hour with ~60% of oocytes partially attached to the ZP; by the end of the culture period (2.5 hours), no oocytes remained that were scored as partially attached to the ZP (Figure 11B). Oocytes that were completely detached from the ZP were first observed at ~1.5 hours which steadily increased until all oocytes were scored as completely detached from the ZP by 2.5 hours (Figure 11C).

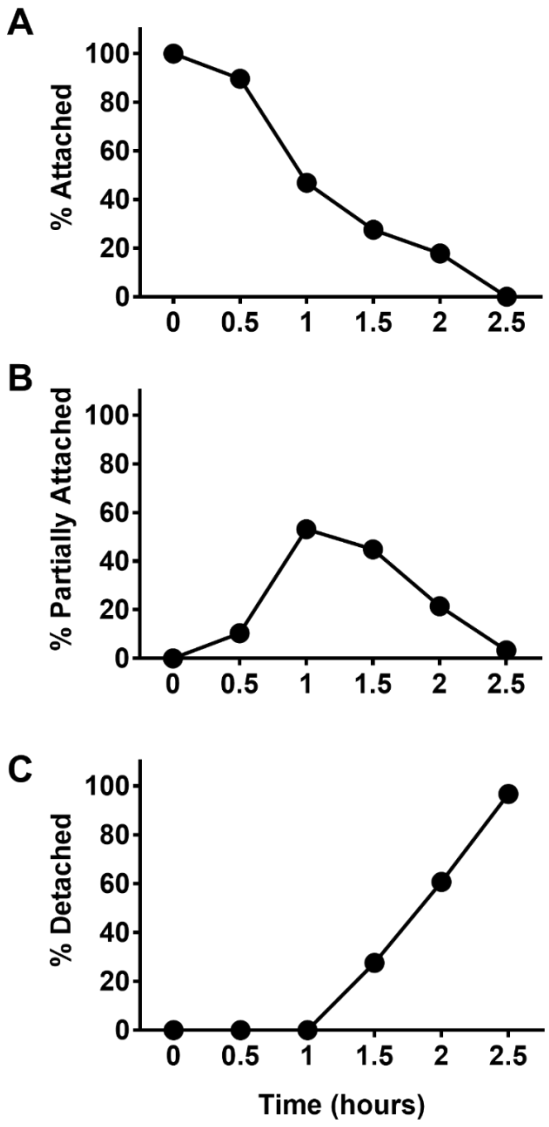

Figure 11. Timing of oocyte-ZP detachment in GV oocytes following removal from the ovarian follicle. Fully grown GV oocytes were isolated from adult female mice 43-45 hrs post-eCG injection and cultured 0-2.5 hours *in vitro* and then cohorts of oocytes were exposed to hypertonic shock treatment and scored as attached, partially attached, or detached from the ZP. (**A**) The percentage of oocytes that were scored as completely attached to the ZP following hypertonic shock. (**B**) The percentage of oocytes that were scored as partially attached to the ZP following hypertonic shock. (**C**) The percentage of

oocytes that were scored as detached from the ZP after hypertonic shock. For **A-C**, each point represents the total percentage of oocytes that were scored as attached, partially attached, or detached at each time point with 27-30 oocytes per group which were pooled from 5 independent replicates. The effect of time on oocyte-ZP detachment was found to be significant ($P < 0.0001$ by Chi-square test for trend). This figure was reproduced with permission from WILEY & Journal of Cellular Physiology. Richard S. et al. (2016). Mouse oocytes acquire mechanisms that permit independent cell volume regulation at the end of oogenesis. *J Cell Physiol*; 232(9): 2436-2446.

1.3 The ability of oocytes to detach from the ZP is acquired during oogenesis when the oocyte is nearly fully grown

It is unknown when oocytes first acquire the ability to detach from the ZP and activate GLYT1 during development. To determine the stage in oogenesis that oocytes are first able to detach from the ZP, denuded growing oocytes ranging in diameter from ≤65 µm to ≥80 µm were mechanically isolated from adult female mice and cultured in cohorts of 5 µm diameter bins. Growing oocytes were isolated 24 hours post-eCG injection while fully-grown oocytes were isolated 43-45 hours post-eCG injection. Since all fully-grown oocytes were able to detach from the ZP by 2.5 hours in culture, growing oocytes were cultured for 3 hours and then subjected to the hypertonic assay (1000 mOsM mKSOM) for rapid assessment of oocyte-ZP adhesion status.

All oocytes from adult ovaries <70 µm in diameter remained completely attached to the ZP while few fully-grown oocytes ≥80 µm in diameter remained attached to the ZP throughout the 3-hour culture period (Figure 12A). Some oocytes that were~70 – 80 µm in diameter only partially detached from the ZP during culture which likely represents an intermediate stage during oogenesis when oocytes are starting to acquire the ability to detach from the ZP (Figure 12B). Complete oocyte-ZP detachment was first observed in oocytes 75-79 µm in diameter while nearly all oocytes≥80 µm in diameter completely detached from the ZP during culture (Figure 12C). Thus, oocytes acquire the ability to detach from the ZP during oogenesis when the oocyte is nearly fully grown.

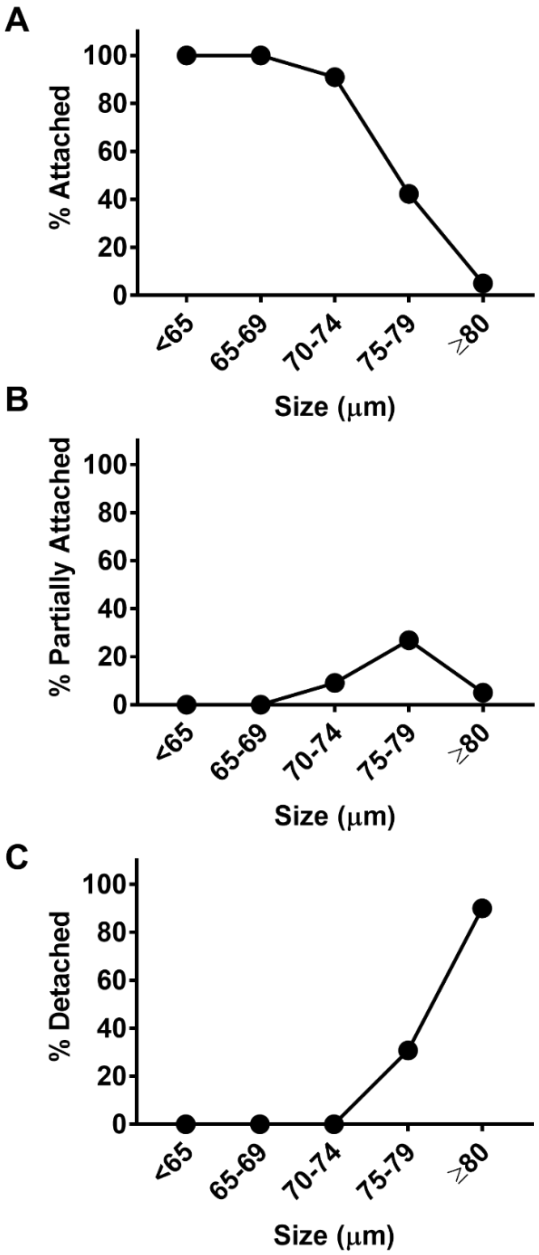

Figure 12. Acquisition of oocyte-ZP detachment ability during oogenesis. Growing oocytes were isolated from adult female mice 24 hours post-eCG and fully grown GV oocytes were isolated from adult female mice 43-45 hours post-eCG. Oocytes were grouped into 5 μm cohorts according to diameter, cultured for 3 hours, and then exposed to hypertonic shock treatment. (**A**) Percentage of oocytes which were completely attached

to the ZP. (**B**) Percentage of oocytes which were partially attached to the ZP. (**C**) Percentage of oocytes which were completely detached from the ZP. For **A-C**, each point represents the percentage of total oocytes that were scored as either attached, partially attached, or detached for each time point examined. A total of 12-25 oocytes were pooled together from ≥ 3 independent replicates for each size cohort. The effect of oocyte size on oocyte-ZP detachment was found to be significant ($P < 0.0001$ by Chi-square test for trend). This figure was modified with permission from WILEY & Journal of Cellular Physiology. Richard S. et al. (2016). Mouse oocytes acquire mechanisms that permit independent cell volume regulation at the end of oogenesis. *J Cell Physiol*; 232(9): 2436-2446.

1.4 The ability of oocytes to activate GLYT1 is acquired during oogenesis when the oocyte is nearly fully grown

Tartia et al. [2009] previously showed that maximal GLYT1 activity developed in freshly isolated GV oocytes cultured ~3-4 hours *in vitro* and in oocytes isolated from excised ovaries ~3-4 hours following hCG administration *in vivo* [Tartia et al. 2009]. However, it is unknown when during oocyte development oocytes first become capable of activating GLYT1. To determine when oocytes become able to activate GLYT1 during oogenesis, growing GV oocytes ranging from 55 μm to >80 μm in diameter were isolated from adult female mice 24 hours following eCG-stimulation and fully-grown GV oocytes were isolated from adult female mice 43-45 hours post-eCG. Oocytes were grouped into 5 μm diameter bins, cultured 4 hours *in vitro*, and then GLYT1 activity was measured by [^{3}H]-glycine uptake. Although oocyte-ZP detachment was found to occur only in oocytes ≥70 μm in diameter, oocytes as small as 55 μm in diameter were examined for GLYT1 activity to determine the earliest stage in oogenesis that GLYT1 activation can occur. Oocytes were cultured for 4 hours since this was previously shown to be sufficient time for GLYT1 activity to develop in oocytes isolated from ovaries [Tartia et al. 2009].

The majority of growing oocytes (55-79 μm in diameter) developed only low levels of GLYT1 activity following isolation from ovarian follicles. The ability to activate GLYT1 to levels similar to those measured in fully-grown oocytes was only acquired by oocytes ≥80 μm in diameter (Figure 13). This significant increase in the ability of oocytes to activate high levels of GLYT1 activity following isolation from ovaries is comparable to when oocytes first acquire the ability to completely detach from the ZP.

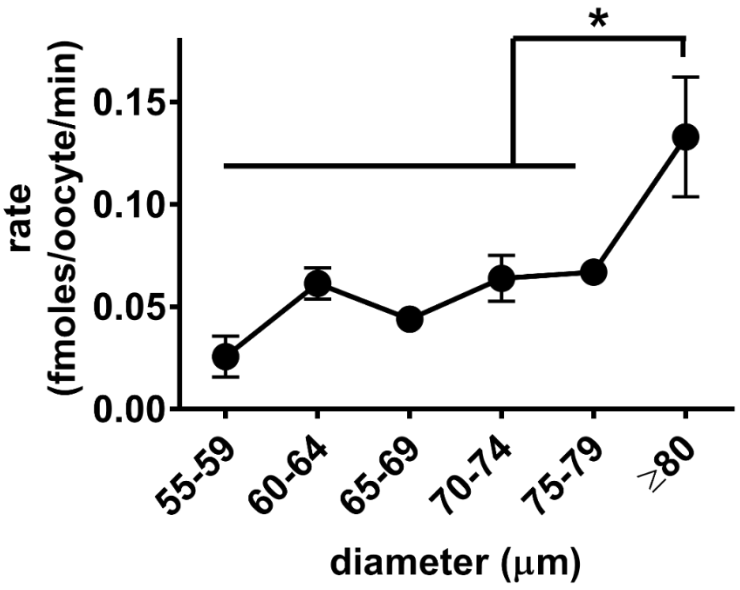

Figure 13. GLYT1 activation in growing oocytes from adult mice. Oocytes ranging from 55 µm to >80 µm in diameter were isolated from eCG-stimulated adult female mice, cultured 4 hours *in vitro* and then GLYT1 activity was measured by a [^{3}H]-glycine uptake experiment. Growing oocytes were isolated 24 hours post-eCG while fully grown oocytes were isolated 43-45 hours post-eCG. GLYT1 activity is shown as the rate of glycine uptake in femtomoles per oocyte per minute (fmoles/oocyte/min). Circles represent the rate of glycine uptake for each cohort of growing oocytes (mean ± SEM, n=3). Differences between means for each size cohort were analyzed by ANOVA with Tukey test. Only oocytes ≥80 µm in diameter were significantly different from all other oocyte sizes (*$P < 0.05$). This figure was reproduced with permission from WILEY & Journal of Cellular Physiology. Richard S. et al. (2016). Mouse oocytes acquire mechanisms that permit independent cell volume regulation at the end of oogenesis. *J Cell Physiol*; 232(9): 2436-2446.

1.5 The ovarian follicle possesses the ability to suppress GLYT1 activity and oocyte-ZP detachment throughout oogenesis

To extend the range of oocyte sizes that could be obtained, oocytes ranging from 30 μm to ≥80 μm in diameter were isolated from neonatal (P5-P21) female mice (not stimulated with eCG) and grouped by size into 5 μm diameter bins. Neonatal mice were used to isolate this wide range of growing oocytes since a larger number of small growing oocytes could be collected during the initial wave of oogenesis that occurs in neonatal mice compared to adult mice in which oocytes at many different stages of development are present. Oocytes were then cultured 4 hours *in vitro* and then GLYT1 activity was measured by [^{3}H]-glycine uptake. Growing oocytes <60 μm in diameter were isolated using an enzymatic method while oocytes ≥60 μm in diameter were isolated mechanically.

Similar to results with oocytes isolated from adult mouse ovaries, a low level of GLYT1 activity was detected in small growing oocytes ranging from 30 μm to ~74 μm in diameter following the 4-hour culture period and was significantly increased in oocytes ≥ 75 μm in diameter (Figure 14A). The highest rate of [^{3}H]-glycine uptake was measured in oocytes which were nearly fully grown (≥ 80 μm in diameter). To confirm that the isolation method (enzymatic vs mechanical) did not have an effect on GLYT1 activation, oocytes ~55-60 μm in diameter were isolated either enzymatically or mechanically, cultured 4 hours, and then GLYT1 activity assessed by measuring the rate of [^{3}H]-glycine uptake into oocytes. No significant difference in [^{3}H]-glycine uptake was detected using either enzymatic or mechanical isolation indicating that enzymatic isolation did not result in a loss of GLYT1 activity that would otherwise have been detected (Figure 14B).

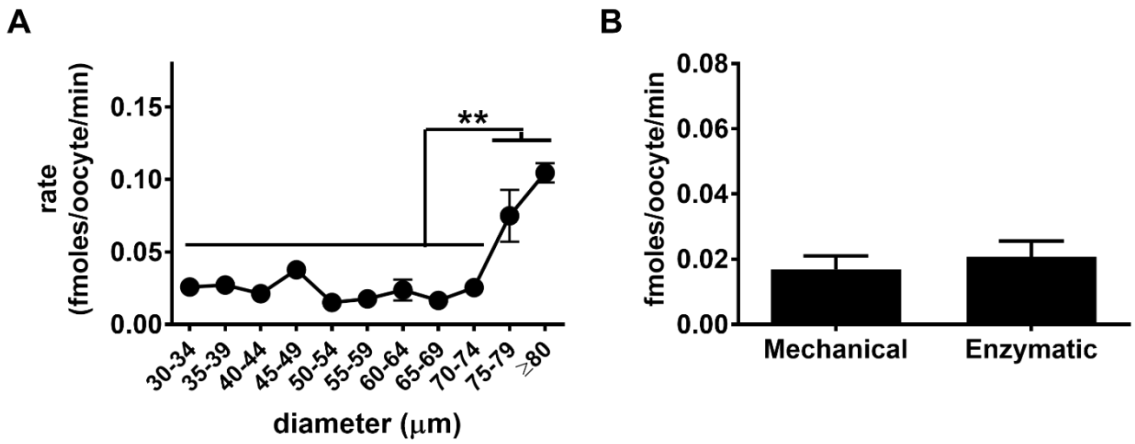

Figure 14. GLYT1 activation in growing oocytes isolated from neonatal mice. Oocytes ranging from 30 to ≥80 μm in diameter were isolated mechanically or enzymatically from neonatal female mice (not stimulated with eCG), cultured 4 hours *in vitro*, and GLYT1 activity was measured by [^{3}H]-glycine uptake. GLYT1 activity is shown as the rate of glycine uptake in fmoles/oocyte/min. (**A**) The rate of [^{3}H]-glycine uptake in growing and fully-grown oocytes is represented by circles (mean ± SEM, n=3). Differences between means for each size cohort were analyzed by ANOVA with Tukey test. Only oocytes ≥75 μm in diameter were significantly different from all other oocyte sizes (**P < 0.01). (**B**) GLYT1 activity in oocytes ~55-60 μm in diameter isolated by a mechanical or enzymatic method and cultured 4 hours *in vitro* (mean ± SEM, n=4). Differences between means of GLYT1 activation in mechanically- and enzymatically-isolated oocytes were analyzed by Student *t*-test and were not found to be significantly different (P=0.4285). Panel A of this figure was reproduced with permission from WILEY & Journal of Cellular Physiology. Richard S. et al. (2016). Mouse oocytes acquire mechanisms that permit independent cell volume regulation at the end of oogenesis. *J Cell Physiol*; 232(9): 2436-2446.

The development of even the small level of GLYT1 activity present in growing oocytes following the 4-hour culture period *in vitro* is normally suppressed within the ovarian follicle as shown by data obtained from Dr. Alina Tartia and included in our recent publication [Richard et al. 2016]. Briefly, GLYT1 activity was essentially absent in growing oocytes isolated from P9 mice (~40-45 μm in diameter) immediately following isolation from ovaries with no significant difference when the GLYT1-specific inhibitor ORG23798 was present or absent from culture medium**.** In contrast, GLYT1 activity was significantly increased in these growing oocytes in the absence of ORG23798 during a 4-hour culture period, compared to oocytes that were cultured in the presence of ORG23798 [Richard et al. 2016]. Thus, the low level of GLYT1 activity I observed in growing oocytes developed during the culture period and was not already present in oocytes within ovaries suggesting that GLYT1 activity is suppressed within the ovarian follicle throughout oogenesis.

Oocytes have previously been shown to become meiotically competent at ~65-70 μm in diameter [Erdogan et al. 2005]. I sought to directly compare when during development oocytes acquire the ability to resume meiosis to when oocytes become able to fully activate GLYT1 and detach from the ZP following isolation from the ovary. To determine the stage in oogenesis when oocytes develop meiotic competence, oocytes ranging from ≤65 μm in diameter to >80 μm in diameter were mechanically isolated from eCG-primed adult female mice either 24 (growing oocytes) or 43-45 (fully grown) hours following eCG administration and grouped into 5 μm diameter cohorts. Growing oocytes were cultured for 4 hours and meiotic competency was determined by the presence of GVBD. All fully grown oocytes from eCG-primed adult female mice resumed meiosis by

3 hours *in vitro* and therefore GVBD in growing oocytes was assessed at 4 hr, after GVBD in all oocytes should have been completed (Figure 15A). As expected, growing oocytes <70 µm in diameter did not resume meiosis and only ~20% of growing oocytes 70–74 µm in diameter resumed meiosis during the 4-hour culture period. This suggests that some oocytes start to become meiotically competent within the range of 70 – 74 µm in diameter. Approximately 60% of oocytes ranging from 75-79 µm in diameter resumed meiosis *in vitro* while all oocytes ≥ 80 µm in diameter resumed meiosis (Figure 15B).

The ability of oocytes to both detach from the ZP and to substantially activate GLYT1 is acquired when oocytes are nearly fully grown and after they become meiotically competent. It appears that the ovarian follicle prevents oocyte-ZP detachment from occurring in the final stages of oogenesis and suppresses even low levels of GLYT1 activity from developing in oocytes throughout oogenesis.

1.6 *Glyt1* (*Slc6a9*) mRNA expression increases during oogenesis and is present until the 8-cell embryo stage

Since GLYT1 becomes activated in GV oocytes after ovulation is triggered, we sought to determine when *Slc6a9* transcripts and SLC6A9 protein first appear during oogenesis. Our lab previously determined using conventional RT-PCR that only *Glyt1a* (*Slc6a9a*) transcripts are expressed in oocytes and preimplantation embryos with no *Glyt1b* (*Slc6a9b*) expression detected at any stage of embryo development [Richard et al. 2016]. To determine when during oogenesis *Glyt1a* transcripts are first expressed, conventional RT-PCR was performed using oocytes isolated at various stages of growth from P5-P21

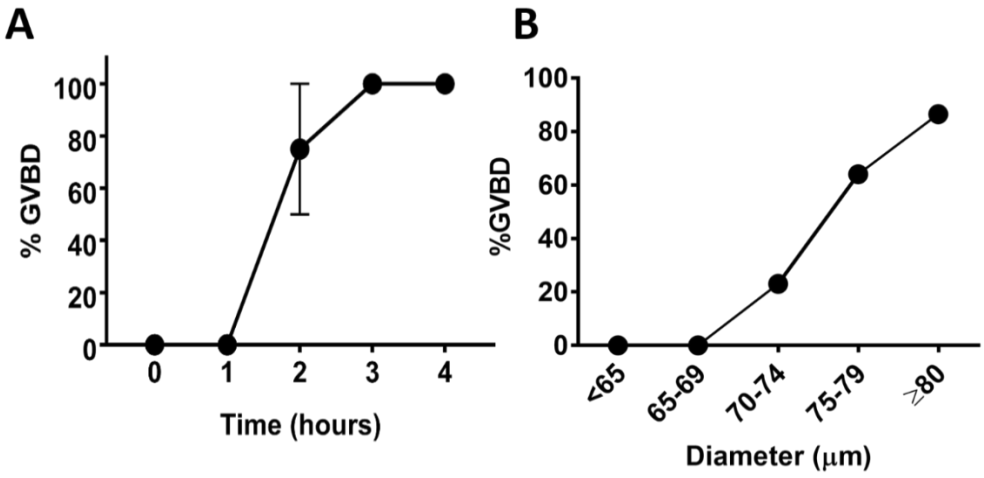

Figure 15. Timing of oocyte meiotic resumption *in vitro* and meiotic competency during oogenesis. (**A**) Fully grown GV oocytes were isolated from eCG-primed adult female mice, cultured 0-4 hours, and then were scored for meiotic resumption (% GVBD). Circles represent the percentage of oocytes which underwent GVBD at each time point indicated (mean ± SEM, n=3). (**B**) Growing oocytes were mechanically isolated from eCG-primed adult female mice, cultured 4 hours, and then scored for meiotic resumption. Each point represents the percentage of total oocytes that resumed meiosis with 12-25 total oocytes pooled from 3 independent replicates for each size cohort. The effect of diameter on GVBD was found to be significant ($P < 0.0001$ by Chi-square test for trend). This figure was modified with permission from WILEY & Journal of Cellular Physiology. Richard S. et al. (2016). Mouse oocytes acquire mechanisms that permit independent cell volume regulation at the end of oogenesis. *J Cell Physiol*; 232(9): 2436-2446.

female mice. Q-RT-PCR was performed to quantify *Glyt1a* transcript levels throughout oogenesis. *Glyt1a* mRNA expression was detected at all stages of oogenesis, in fully grown GV oocytes, eggs, and 1-cell embryos while no expression above background was detected in 8-cell embryos (Figure 16A). *Glyt1a* expression was shown to increase throughout oogenesis and was highest in fully grown GV oocytes, comparable to transcript levels detected in eggs and 1-cell embryos. Consistent with conventional RT-PCR results, no measurable *Glyt1a* expression above background levels was detected at the 8-cell embryo stage (Figure 16B). Liver was used as a positive control for both RT-PCR and Q-RT-PCR.

1.7 GLYT1 (SLC6A9) expression increases during oogenesis and becomes localized to the oocyte plasma membrane during oocyte growth

I next sought to examine the location and amount of GLYT1 protein present throughout oogenesis and preimplantation embryo development. To first confirm that the GLYT1 antibody donated to our laboratory by Dr. Detlev Boison and colleagues functioned as expected in our hands, western blots were performed using brain protein lysate from the hippocampus and cortex region as a positive control, since this antibody was previously validated in tissue from these brain regions [Gabernet et al. 2005]. As expected, several diffuse bands appeared in brain tissue with the most prominent band at ~70 kDa consistent with previous descriptions by other laboratories [Olivares et al. 1995; Gabernet et al. 2005; Cubelos et al. 2005a] (Figure 17A, 0). To confirm that the band near 70 kDa was specific to GLYT1 (SLC6A9), membranes were incubated with primary GLYT1 antibody and increasing concentrations of a C-terminal binding peptide identical

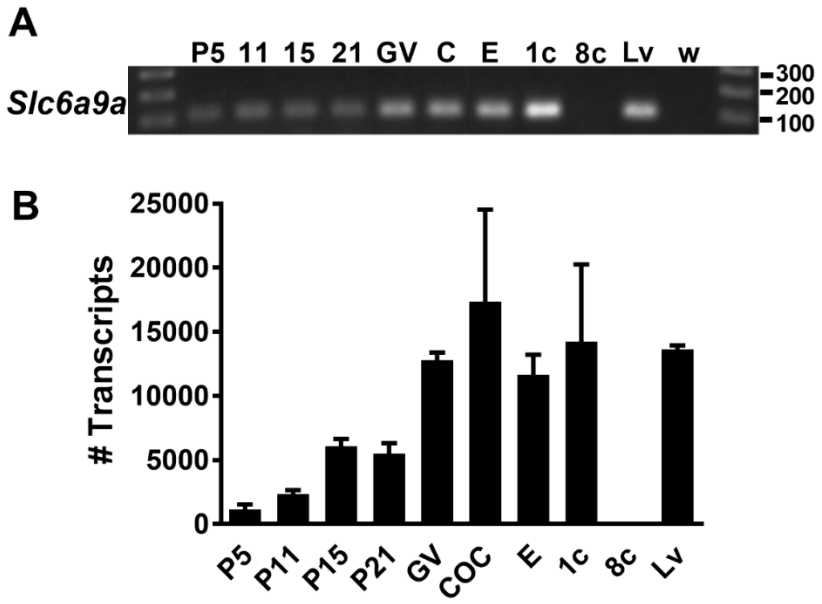

Figure 16. *Glyt1a* (*Slc6a9a*) expression during oogenesis and preimplantation embryo development. (**A**) *Glyt1a* (*Slc6a9a*) mRNA expression in growing oocytes (P5-P21), fully grown GV oocytes (GV), cumulus-oocyte-complexes (C), MII eggs (E), 1-cell embryos (1c), and 8-cell embryos (8c) using RT-PCR. Liver (Lv) was used as a positive control and water (w) was used as a negative control (n=3). (**B**) Q-RT-PCR was performed to detect *Glyt1a* (*Slc6a9a*) expression in growing oocytes (P5-P21), fully grown GV oocytes (GV), cumulus-oocyte-complexes (C), MII eggs (E), 1-cell embryos (1c), and 8-cell embryos (8c) with liver(Lv) used as a positive control (100ng). *Glyt1a* transcript numbers are represented by black bars (mean ± SEM, n=3). The significance of changes between stages of oocytes (P5 through GV only) was assessed by ANOVA with Tukey test, which indicated that all stages differed significantly ($P<0.01$) except P11 vs P21 ($P<0.05$) and P5 vs. P11 and P15 vs. P21, which were not significantly different. This figure was reproduced with permission from WILEY & Journal of Cellular Physiology. Richard S. et al. (2016). Mouse oocytes acquire mechanisms that permit independent cell volume regulation at the end of

oogenesis. *J Cell Physiol*; 232(9): 2436-2446.

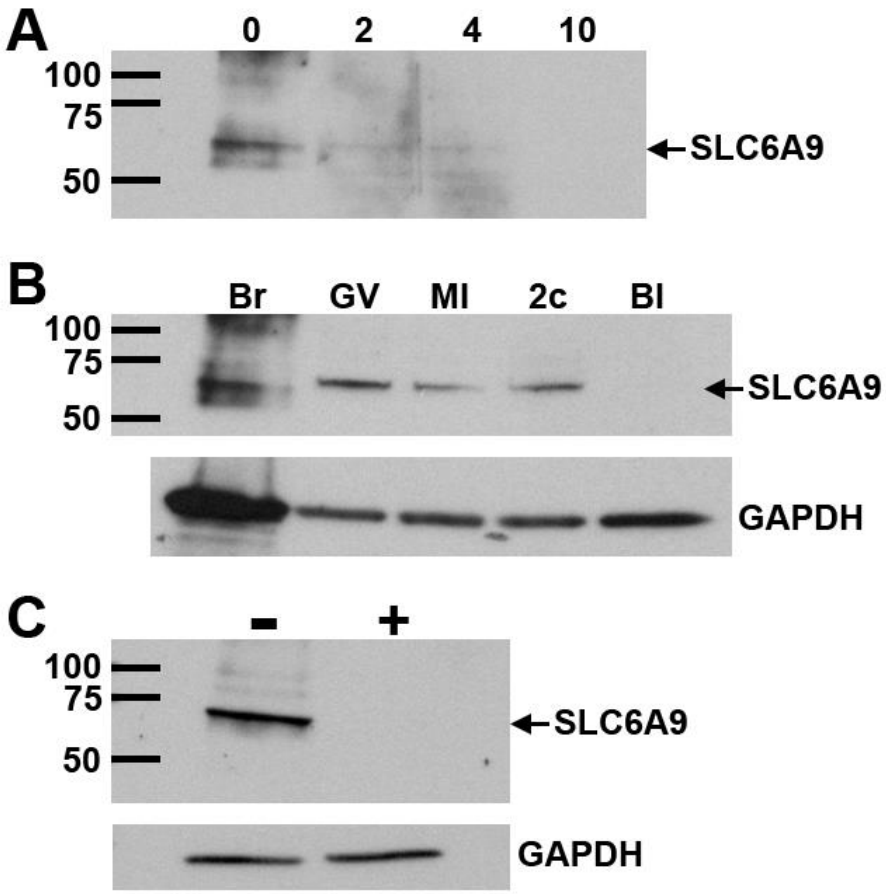

Figure 17. GLYT1 (SLC6A9) expression in oocytes and preimplantation embryos. (**A**) GLYT1 (SLC6A9) primary antibody was first tested using brain protein (5µg, 0) and specificity was confirmed by adding increasing concentrations of a competitive C-terminal peptide at 2µg/ml (2), 4µg/ml (4), and 10µg/ml (10). The band corresponding to GLYT1 (SLC6A9) is labelled with an arrow and molecular weight markers (kDa) are indicated on the left. This western blot with competitive peptide was only performed one time with brain since it has previously been validated and to conserve antibody. Membranes were cut to perform the blot and then reassembled for the final exposure. (**B**) GLYT1 (SLC6A9) expression in brain protein (5µg), GV oocytes (GV, 120 per lane), MI oocytes (MI, 120 per lane), 2-cell embryos (2c, 120 per lane), and blastocysts (Bl, 120 per lane). The band

corresponding to GLYT1 (SLC6A9) is indicated with an arrow and GAPDH expression is shown in the lower pane (n=2). Molecular weight markers (kDa) are shown on the left. An additional replicate was performed with only GV and MI oocytes and brain lysate which gave similar results. (**C**) GLYT1 protein expression in fully grown GV oocytes with primary GLYT1 antibody only (-) or with primary antibody and C-terminal peptide (10µg/ml) (+). GLYT1 (SL6A9) is indicated with an arrow and GAPDH expression is shown in the lower pane (n=2). Molecular weight markers (kDa) are shown on the left. This figure was reproduced with permission from WILEY & Journal of Cellular Physiology. Richard S. et al. (2016). Mouse oocytes acquire mechanisms that permit independent cell volume regulation at the end of oogenesis. *J Cell Physiol*; 232(9): 2436-2446.

to the peptide sequence used as the immunogen for the primary antibody. Bands became faint in the presence of 2 µg/ml and 4 µg/ml of peptide while no bands were seen when membranes were incubated with 10 µg/ml of peptide suggesting that the observed bands represent specific binding (Figure 17A).

GLYT1 protein expression was next examined by western blots in oocytes and preimplantation embryos. In fully grown GV oocytes, MI oocytes (oocytes cultured 4 hours *in vitro*), and 2-cell embryos a single band was detected at ~70 kDa while no bands were present in blastocysts (consistent with the lack of GLYT1 activity at the blastocyst stage), although GAPDH expression appeared similar across all embryo stages (Figure 17B). No major difference in GLYT1 protein expression levels was observed between oocytes, MI oocytes, or 2-cell embryos. To confirm that the single ~70 kDa band likely corresponded to GLYT1, competitive C-terminal peptide (10 µg/ml) was added to the primary antibody incubation period which caused the band to disappear in fully grown GV oocytes (Figure 17C). Whole mount immunofluorescence was performed to quantify GLYT1 protein expression during oogenesis since accurate protein normalization is very difficult when examining cells of dramatically different sizes and developmental stages by western blot analysis. By immunofluorescence analysis, GLYT1 expression increased during oogenesis in growing oocytes isolated from P11-P21 neonatal mice and appeared to become primarily localized to the oocyte plasma membrane by P15. GLYT1 staining was faint in oocytes isolated from P11 neonatal mice without any apparent membrane localization, however, the majority of oocytes isolated from P15 neonatal mice showed distinct GLYT1 plasma membrane staining (Figure 18A**)**. Prominent GLYT1 plasma membrane staining was observed in all oocytes isolated from P21 neonatal mice which are nearly fully grown, and

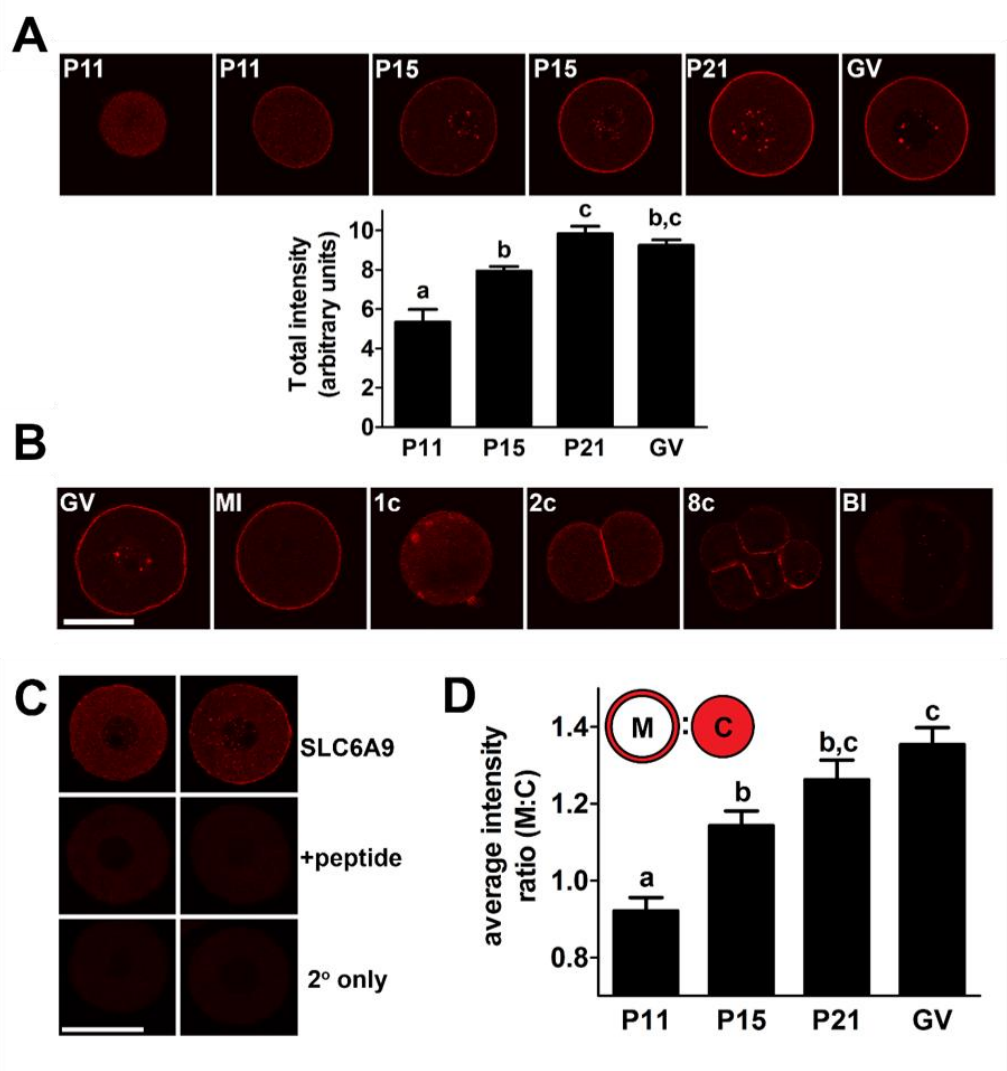

Figure 18. GLYT1 (SLC6A9) expression during oogenesis and preimplantation embryo development. GLYT1 expression and localization using immunofluorescence analysis. (**A**) GLYT1 expression in growing and fully grown GV oocytes isolated from P11-P21 female mice and adult female mice (~4 weeks) (n=3). The total fluorescence intensity was quantified using ImageJ analysis and graphed in arbitrary units. Black bars represent the total fluorescence intensity of a total of 15-18 oocytes pooled for each size which were derived from 3 independent replicates (mean ± SEM, n=3). Bars that do not share letters have significantly different means (P <0.01 by ANOVA with Tukey test).

(**B**)GLYT1 expression in fully grown GV oocytes (GV), MI oocytes (MI), 1-cell embryos (1c), 2-cell embryos (2c), 8-cell embryos (8c), and blastocysts (Bl) (n=3). (**C**) GLYT1 primary antibody immunofluorescence expression in fully grown GV oocytes (SLC6A9), GLYT1 expression in fully grown GV oocytes incubated in the presence of primary antibody and with 10 µg/ml C-terminal peptide (+peptide), and GLYT1 expression in fully grown GV oocytes incubated with only secondary antibody (2º only) (n=3). (**D**) The average intensity ratio of GLYT1 immunofluorescence in the oocyte plasma membrane (M) compared to the cytoplasm (C) was quantified between growing GV oocytes from P11-P21 neonatal mice and fully grown GV oocytes from adult mice (GV). The total fluorescence intensity was first measured using ImageJ (integrated density measure) and was then normalized to the calculated area of the plasma membrane (M). The equation $I_R = IntDen_R/A_R$ was used where I_R is the average intensity of M, $IntDen_R$ is the total fluorescence intensity of M, and A_R is the total area of M; the same formula was used to calculate the average fluorescence intensity of the cytoplasm (C). Black bars represent the average fluorescence intensity ratio of the plasma membrane (M) to the cytoplasm (C) (mean ± SEM for the same oocytes as in **A**). Bars that do not share letters have significantly different means ($P < 0.0001$ by ANOVA and Tukey test). The scale bars in panel **B** and **C** represent 50 µm and also apply to panel **A**. Visualization was optimized by adjusting the contrast and brightness equally for the confocal images in **A**-**D**. This figure was reproduced with permission from WILEY & Journal of Cellular Physiology. Richard S. et al. (2016). Mouse oocytes acquire mechanisms that permit independent cell volume regulation at the end of oogenesis. *J Cell Physiol*; 232(9): 2436-2446.

this staining pattern did not appear different from GLYT1 staining in fully grown GV oocytes isolated from adult mice (~4 weeks) (Figure 18A). GLYT1 plasma membrane staining in growing oocytes was quantified by measuring average fluorescence intensity and was plotted as the ratio of average fluorescence intensity in the region of the plasma membrane to the average fluorescence intensity in the cytoplasm for oocytes isolated from P11-P15 neonatal mice and adult mice. Using this method of quantification, GLYT1 plasma membrane staining intensity (relative to cytoplasmic staining) was significantly increased in oocytes isolated from P15 neonatal mice compared to smaller oocytes isolated from P11 neonatal mice. GLYT1 plasma membrane staining was increased in oocytes from P21 neonatal mice but was not significantly different from oocytes from P15 neonatal mice and did not differ from fully grown oocytes isolated from adult mice (Figure 18D). Quantification of total fluorescence intensity in growing oocytes showed a similar increase in GLYT1 expression during oocyte growth (Figure 18A). Increasing GLYT1 protein at the oocyte plasma membrane is clearly visible with the highest expression and membrane localization occurring when oocytes are nearly fully grown, but prior to GLYT1 activation.

GLYT1 (SLC6A9) protein expression was also examined at various stages throughout preimplantation embryo development by immunofluorescence. GLYT1 plasma membrane staining was present in GV oocytes, MI oocytes (oocytes cultured 4 hours *in vitro*), 1-cell embryos, 2-cell embryos, and 8-cell embryos (prior to compaction) while no staining was detected in blastocysts stage embryos, as expected since no GLYT1 activity has been measured at this stage (Figure 18B). To confirm that the observed immunofluorescence was specific to GLYT1, fully grown GV oocytes were incubated with primary GLYT1 antibody alone, with primary antibody and the C-terminal binding peptide

(10µg/ml), or with secondary antibody only. As shown in the previous experiment, GLYT1 staining was clearly visible in oocytes incubated with GLYT1 primary antibody alone. In contrast, oocytes incubated with primary antibody and peptide or with secondary antibody alone did not show any obvious fluorescence suggesting that the observed plasma membrane (and cytoplasmic) immunofluorescence is specific to GLYT1 (Figure 18C).

2. Development of an antral follicle culture methodology and the requirement for functional connexin-43 (GJA1) and connexin-37 (GJA4) gap junctions to maintain prophase I arrest

Since efforts to suppress GLYT1 activation in isolated denuded oocytes and COCs have previously failed [Tartia 2009], I sought to develop an antral follicle culture methodology capable of supporting healthy follicles in culture and to develop a preparation that would allow the introduction of reagents into the interior of the follicle. This would provide an experimental system which could be used to examine the requirement of mural granulosa cells and/or follicular fluid in the maintenance of suppressed GLYT1 activity prior to ovulation. Since maintenance of prophase I arrest was previously shown to depend on a multi-cell signalling mechanism involving mural granulosa cells, follicular fluid, cumulus granulosa cells, and functional gap junctions, I used oocyte maintenance of meiotic arrest as a marker for follicle viability.

The specific requirements for connexin-43 gap junctions (GJA1; between mural granulosa cells) and connexin-37 gap junctions (GJA4; between the oocyte and innermost cumulus granulosa cells) in the maintenance of meiotic arrest is unclear. Although it is

known that both gap junction isoforms are vital to mouse oocyte and follicle growth, conflicting results have been produced regarding the necessity of both GJA1 and GJA4 for prophase I arrest [Reaume et al. 1995; Simon et al. 1997; Ackert et al. 2001; Kidder & Mhawi 2002; Gittens & Kidder 2005; Kidder 2005; Li et al. 2007; Gershon et al. 2008]. Therefore, using my *in vitro* antral follicle methodology, I used specific peptides (connexin-mimetic peptides, CMPs) designed against GJA1 and GJA4 to inhibit each type of gap junction in cultured antral follicles and COCs to determine which gap junctions are required for the maintenance of meiotic arrest. To enable these CMPs to access their target gap junctions within antral follicles, I developed a punctured antral follicle methodology consisting of an antral follicle with a hole in the outer wall of the follicle. To allow sufficient time for gap junction inhibitors to block gap junctional communication, I sought to maintain healthy intact and punctured antral follicles in culture for at least 20 hours.

2.1 Successful mouse antral follicle culture requires a minimum of 100 µl of medium per follicle to maintain meiotically-arrested GV oocytes

The antral follicle culture methodology was developed based on the method developed by Downs [2000] who was able to maintain meiotically-arrested GV oocytes within cultured intact antral follicles for up to 20 hours. The same culture conditions were used to determine whether viable antral follicles with a small hole in the outer wall (punctured follicles) could also maintain oocyte meiotic arrest for 20 hours. Although meiotic arrest was maintained in cultured intact antral follicles, oocytes resumed meiosis in punctured antral follicles for this length of culture (Figure 19). Since the punctured antral follicles had a hole in the wall of the follicle, it was possible that the follicular fluid was

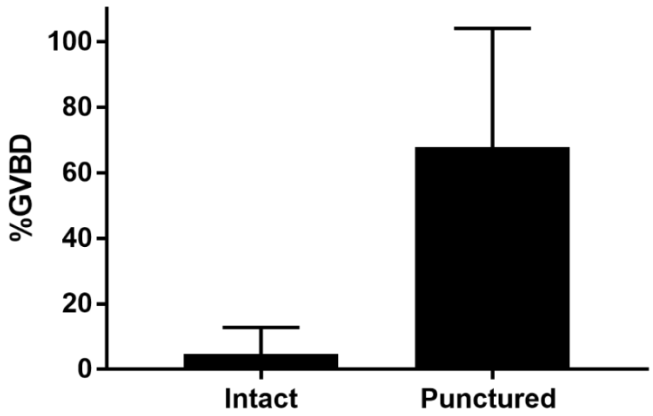

Figure 19. Meiotic resumption in cultured intact and punctured antral follicles. Intact and punctured antral follicles were cultured 20 hours and meiotic resumption was determined based on the percentage of oocytes which underwent GVBD (% GVBD). Black bars represent the percentage of oocytes isolated from antral follicles following culture which underwent GVBD (mean ± SEM, n=3). No significant difference was found between means as examined by Student *t*-test (P=0.0695).

diluted out of the follicle into the 1ml of antral follicle culture medium. Specifically, I hypothesized that NPPC from mural granulosa cells that is secreted into the extracellular fluid of the follicle was being diluted thus decreasing the production of cGMP and causing meiotic resumption [Zhang et al. 2010]. Therefore, smaller volumes of antral follicle culture medium were tested to determine whether it was possible to increase the follicle:medium ratio and thus prevent significant dilution of the follicular fluid.

To determine the minimum volume of medium required to culture viable antral follicles for up to 20 hours, for each experimental group three intact antral follicles were cultured in 10-500 µl of antral follicle medium for 20 hours and then oocytes were isolated and examined for the presence of an intact GV, which would indicate that meiotic arrest was maintained. In a culture medium volume of at least 300 µl, meiotic arrest was maintained in ~80% of oocytes while about half of oocytes were meiotically-arrested in a culture volume of 150 µl, and only ~20% of oocytes maintained meiotic arrest in volumes ≤ 50 µl (Figure 20). Groups of five intact antral follicles were also cultured for 20 hours in either 300 µl or 500 µl of antral follicle culture medium and oocytes were again examined for the presence of an intact GV. Meiotic arrest was maintained in ~80% of oocytes when five follicles were cultured in 500 µl of medium while only ~15% of oocytes maintained meiotic arrest when five follicles were cultured in 300 µl of medium. Taken together, these results suggest that at least 100 µl of antral follicle culture medium per follicle is necessary to sustain viable intact antral follicles in culture for at least 20 hours under these conditions (Figure 20). Thus, prevention of follicular fluid dilution from punctured antral follicles during culture, and therefore maintenance of meiotic arrest, would not likely be possible, given that such large volumes relative to the volume of antral fluid are required.

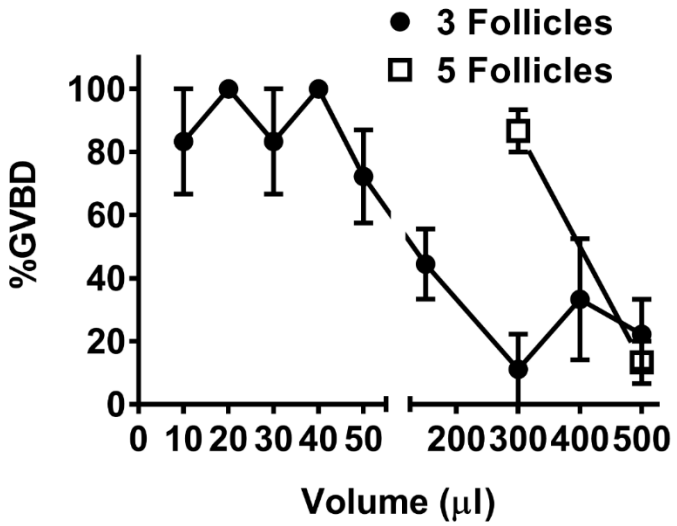

Figure 20. The minimum required volume of culture medium required to maintain meiotic arrest in cultured intact antral follicles. Three follicles (circles) were cultured in 10-500µl of antral follicle culture medium for 20 hours. After the culture period, oocytes were isolated from follicles and were examined for meiotic resumption (characterized by % GVBD). Five follicles (empty squares) were cultured in 300 or 500 µl of antral follicle culture medium for 20 hours and then isolated oocytes were examined for meiotic resumption (% GVBD) (mean ± SEM, n=3). This figure was reproduced with the permission of Oxford University Press, Society for the Study of Reproduction©. Richard S. & Baltz J.M. (2014). Prophase I arrest of mouse oocytes mediated by natriuretic peptide precursor C requires GJA1 (connexin-43) and GJA4 (connexin-37) gap junctions in the antral follicle and cumulus-oocyte complex. *Biol Reprod*; 90(6):137.

2.2 Intact and punctured antral follicles can sustain healthy, prophase I-arrested GV oocytes for at least 20 hours if NPPC is maintained

Since prophase-I arrest is dependent on the secretion of NPPC from mural granulosa cells into the follicular fluid and the subsequent binding of NPPC to its cognate NPR2 receptor on cumulus granulosa cells, I hypothesized that NPPC was being diluted from the punctured antral follicles (through the small hole in the follicular wall) during the culture period, therefore leading to meiotic resumption of oocytes (Figure 19). To determine whether the addition of NPPC to culture medium would maintain meiotic arrest in punctured antral follicles for up to 20 hours, punctured antral follicles were isolated and cultured in the presence or absence of NPPC for up to 20 hours and oocyte meiotic resumption was compared to intact antral follicles cultured for the same amount of time.

I first determined the minimum concentration of NPPC required to maintain meiotic arrest for 4 hours. This culture period was chosen to allow sufficient time for meiotic resumption (GVBD) to occur in denuded oocytes or COCs based on my experiments above that showed meiotic resumption had occurred in all denuded oocytes by 3 hours following isolation from ovarian follicles (Figure 15A). COCs were isolated and cultured in the presence of 0-1000 nM NPPC for 4 hours and then oocytes were examined for the presence of an intact GV to indicate maintenance of meiotic arrest. In the absence of NPPC, all oocytes resumed meiosis while ~85% of oocytes maintained meiotic arrest in the presence of 100-500 nM NPPC; however meiotic resumption occurred in ~60% of oocytes cultured with 1000 nM NPPC (Figure 21A). Thus, 100 nM NPPC was the minimum concentration required to most effectively maintain oocyte meiotic arrest in COCs cultured for 4 hours. To ensure that the exogenous NPPC could maintain meiotically-arrested COCs for the

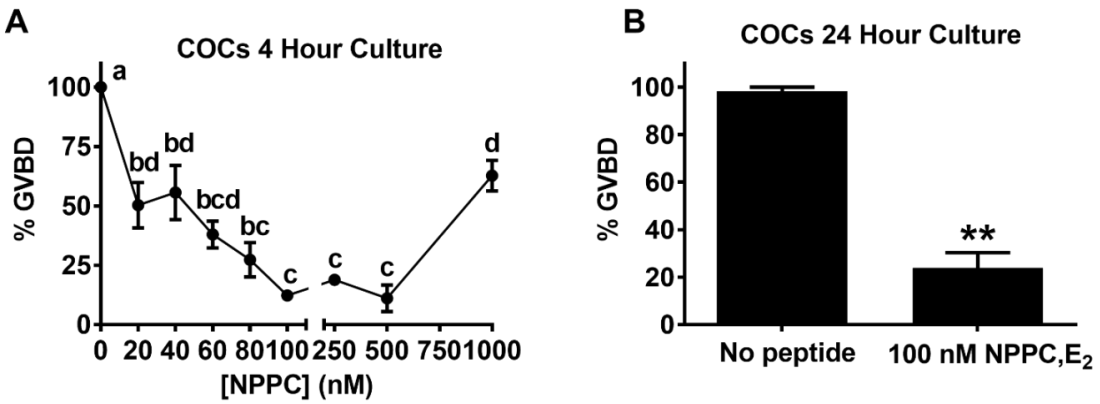

Figure 21. NPPC-mediated meiotic arrest in COCs. (**A**) COCs were cultured for 4 hours in culture medium with 0-1000 nM NPPC added. After the culture period, oocytes were examined for resumption of meiosis (characterized by GVBD). Circles represent the percentage of oocytes which underwent GVBD during culture (mean ± SEM, n=3). Circles which do not share letters are significantly different ($P < 0.05$ by ANOVA with Tukey test). (**B**) COCs were cultured for 24 hours in the presence or absence of 100 nM NPPC and estradiol (E_2) and then oocytes were examined for meiotic resumption (GVBD). Black bars represent the percentage of oocytes which underwent GVBD (mean ± SEM, n=4). Differences between means was examined by Student *t*-test (** $P< 0.01$). This figure was reproduced with the permission of Oxford University Press, Society for the Study of Reproduction©. Richard S. & Baltz J.M. (2014). Prophase I arrest of mouse oocytes mediated by natriuretic peptide precursor C requires GJA1 (connexin-43) and GJA4 (connexin-37) gap junctions in the antral follicle and cumulus-oocyte complex. *Biol Reprod*; 90(6):137.

desired 20-hour culture period, COCs were cultured for 24 hours in the presence or absence of 100 nM NPPC and estradiol (E_2, 100 nM); E_2 was previously shown to be required to maintain NPR2 expression in cumulus granulosa cells [Zhang et al. 2011]. After the culture period, oocytes were examined for the presence of GVBD to indicate meiotic resumption had occurred. In the absence of NPPC and E_2, meiotic resumption occurred in nearly all COCs while ~80% of COCs were maintained in meiotic arrest in the presence of NPPC and E_2 indicating that meiotic arrest could be effectively maintained in COCs cultured for at least 24 hours under these conditions (Figure 21B).

I next examined whether the addition of 100 nM exogenous NPPC (and E_2) to culture medium would be sufficient to maintain meiotic arrest in punctured antral follicles for extended culture (up to 20 hours). Both intact and punctured antral follicles were cultured for up to 20 hours with or without NPPC (100 nM) and E_2 (100 nM) added to culture medium. Experiments (above) had already established that intact antral follicles would maintain meiotic arrest for up to 20 hours in the absence of additional exogenous NPPC and thus were used as a positive control for the maintenance of meiotic arrest (Figure 19 & 20). After the desired culture period, oocytes were isolated from antral follicles and examined for the presence of GVBD to indicate that meiotic resumption had occurred. As expected, meiotic arrest was maintained in nearly all intact antral follicles throughout the culture period regardless of the presence of NPPC and E_2 (Figure 22A, B).

In the absence of NPPC and E_2, meiotic resumption occurred in ~20% of punctured antral follicles after 4 hours; however, ~60% of punctured antral follicles had resumed meiosis by 12 hours and ~80% had resumed meiosis by 20 hours in culture (Figure 22A). In contrast, when NPPC and E_2 were added to culture medium, meiotic arrest was

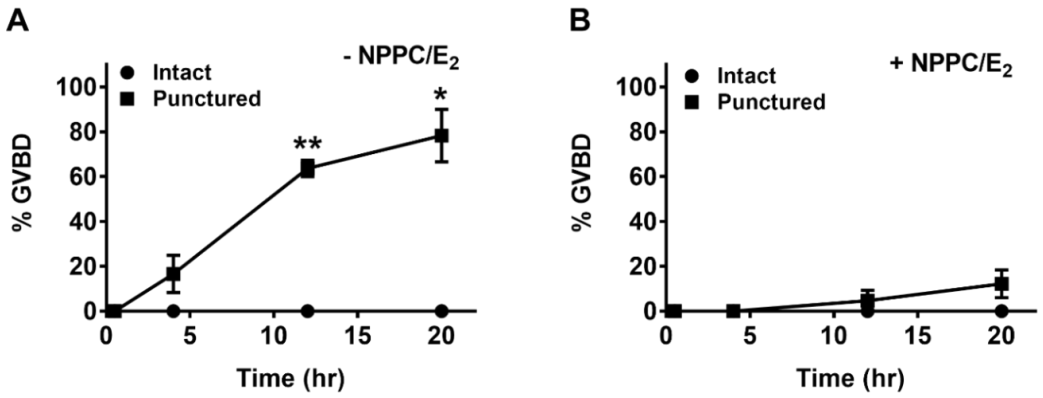

Figure 22. Meiotic arrest in intact and punctured antral follicles: the effect of NPPC and E_2 addition to culture medium. Intact and punctured antral follicles were isolated and cultured for 0-20 hours in the presence or absence of NPPC (100 nM) and E_2 (100 nM). (**A**) The percentage of oocytes which resumed meiosis is shown (% GVBD) in intact (circles) and punctured (squares) antral follicles which were cultured in the absence of NPPC/E_2 for up to 20 hours (mean ± SEM, n=3). (**B**) The percentage of oocytes which resumed meiosis is shown (% GVBD) in intact (circles) and punctured (squares) antral follicles which were cultured in the presence of NPPC/E_2 for up to 20 hours (mean ± SEM, n=3). For both **A** and **B**, follicles were cultured in 1 ml of culture medium. Differences between means of % GVBD in intact and punctured antral follicles at each time point were examined by Student *t*-test (*P< 0.05, **P < 0.01). This figure was reproduced with the permission of Oxford University Press, Society for the Study of Reproduction©. Richard S. & Baltz J.M. (2014). Prophase I arrest of mouse oocytes mediated by natriuretic peptide precursor C requires GJA1 (connexin-43) and GJA4 (connexin-37) gap junctions in the antral follicle and cumulus-oocyte complex. *Biol Reprod*; 90(6):137.

maintained in punctured antral follicles throughout the culture period, which was not significantly different from intact antral follicles (Figure 22B). Therefore, meiotically-arrested oocytes can be sustained within punctured antral follicles for at least 20 hours in culture when exogenous NPPC and E_2 are added to culture medium, an effect that is likely a result of counteracting dilution of endogenous NPPC into culture medium.

To examine whether oocytes remained meiotically competent following a 20-hour culture period within intact or punctured antral follicles, the progression of oocytes to MII eggs after removal from cultured antral follicles was assessed. Intact and punctured antral follicles were first cultured for 20 hours with exogenous NPPC and E_2 (100 nM) added to culture medium and then oocytes were isolated and examined for the presence of an intact GV to indicate maintenance of meiotic arrest. As expected, meiotic arrest was maintained in nearly all cultured intact and punctured antral follicles (Figure 23). To determine the meiotic competence of oocytes following the 20-hour culture period, oocytes isolated from intact and punctured antral follicles were additionally cultured overnight (~18 hours) in the absence of NPPC and E_2 to allow progression to MII eggs, characterized by release of the first polar body. Meiotic progression to MII eggs occurred in ~60% of oocytes which was not significantly different in oocytes isolated from intact or punctured antral follicles (Figure 23). Taken together, these results suggest that the intact and punctured antral follicle methodologies I developed can successfully sustain meiotically-competent GV oocytes in culture for up to 20 hours.

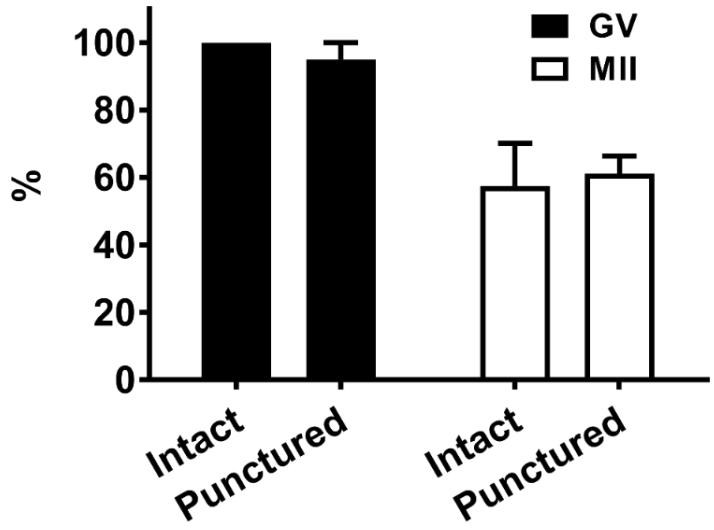

Figure 23. Maintenance of meiotic arrest and progression to MII eggs in cultured intact and punctured antral follicles. Intact and punctured antral follicles were isolated and cultured 20 hours in the presence of NPPC (100 nM) and E_2 (100 nM) and then oocytes were examined for the presence of an intact GV. After removal from follicles, oocytes were cultured overnight in the absence of NPPC and E_2 to enable progression to MII eggs. Black bars represent the percentage of oocytes which had an intact GV after the initial 20-hour culture in intact or punctured antral follicles. White bars represent the percentage of oocytes isolated from intact or punctured antral follicles which progressed to MII eggs during overnight culture (mean ± SEM, n=4). No significant differences were found between means of GV status (P=0.3910) or MII progression (P=0.8225) in intact or punctured antral follicles as determined by Student *t*-test. This figure was reproduced with the permission of Oxford University Press, Society for the Study of Reproduction©.

Richard S. & Baltz J.M. (2014). Prophase I arrest of mouse oocytes mediated by natriuretic peptide precursor C requires GJA1 (connexin-43) and GJA4 (connexin-37) gap junctions in the antral follicle and cumulus-oocyte complex. *Biol Reprod*; 90(6):137.

2.3 General gap junction inhibition causes meiotic resumption in intact and punctured antral follicles

Since the intact and punctured antral follicle culture systems that I developed maintained meiotically-arrested oocytes during culture, I next sought to determine whether the inhibition of gap junctional communication within the follicles would cause oocytes to resume meiosis under my conditions, as has been demonstrated previously by Sela-Abramovich et al. [2006]. I first determined the minimum amount of time required for gap junction inhibition to cause GVBD in my intact and punctured antral follicle culture systems. The general gap junction inhibitor 18α-glycyrrhetinic acid (AGA) was initially used to inhibit gap junctions since it has previously been shown to rapidly inhibit gap junctional communication in preantral mouse follicles [FitzHarris & Baltz 2006]. Intact and punctured antral follicles were isolated and cultured for 0-10 hours in the presence or absence of AGA (150 μM); NPPC and E_2 were added to punctured antral follicle culture medium as described above. After the desired culture period, oocytes were isolated from follicles and examined for the presence of GVBD to indicate meiotic resumption. In the presence of AGA, intact antral follicles resumed meiosis beginning at 8 hours (~70% of oocytes) with the most significant meiotic resumption occurring by 10 hours in culture (~80% of oocytes) compared to intact antral follicles cultured in the absence of inhibitor in which only ~20% of oocytes resumed meiosis at 10 hours (Figure 24A). Punctured follicles cultured in the presence of AGA significantly resumed meiosis by 4 hours with ~75% of oocytes resuming meiosis which increased to ~90% of oocytes that underwent GVBD by 10 hours (Figure 24B). In contrast, meiotic arrest was maintained in nearly all punctured antral follicles cultured in the absence of AGA for the entire culture period. It is

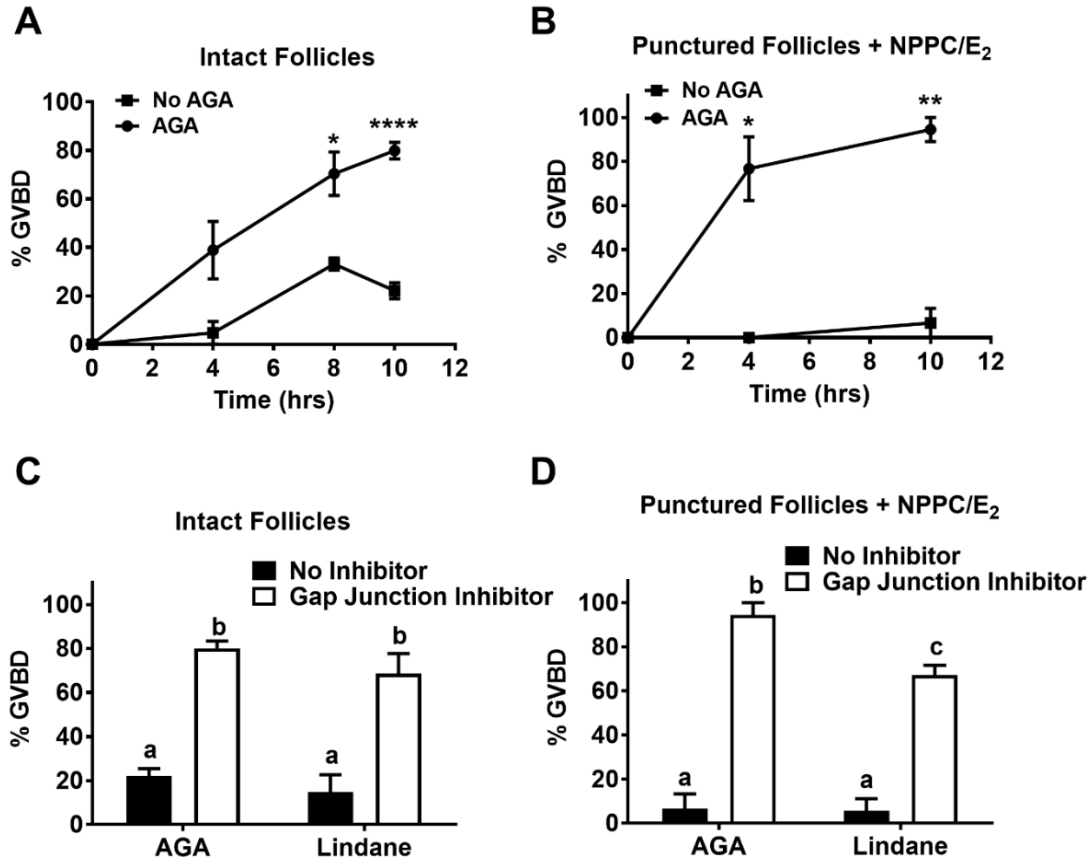

Figure 24. General gap junction inhibition in intact and punctured antral follicles. Intact (**A**) and punctured (**B**) antral follicles were cultured for 0-10 hours with or without AGA (150 µM) and then oocytes were examined for % GVBD. For both **A** and **B,** circles represent follicles cultured in the presence of AGA and squares represent follicles cultured without AGA (mean ± SEM, n=3-4). Differences between means of % GVBD in follicles cultured with or without AGA at each time point were examined by Student *t*-test (*P< 0.05, **P < 0.01, ***P < 0.0001). Intact (**C**) and punctured (**D**) antral follicles were cultured for 10 hours with or without the general gap junction inhibitors AGA (150 µM) or lindane (10 µM). After the culture period, oocytes were examined for the percentage that underwent GVBD. For both **C** and **D**, black bars represent the percentage of oocytes

which resumed meiosis (GVBD) in the absence of gap junction inhibitors (mean ± SEM, n=5) while white bars represent the percentage of oocytes which resumed meiosis (GVBD) in the presence of either AGA or lindane (mean ± SEM, n=3). Bars that do not share letters are significantly different ($P < 0.001$ by ANOVA with Tukey test, except **b** vs. **c** in panel **B**, $P < 0.05$). This figure was reproduced with the permission of Oxford University Press, Society for the Study of Reproduction©. Richard S. & Baltz J.M. (2014). Prophase I arrest of mouse oocytes mediated by natriuretic peptide precursor C requires GJA1 (connexin-43) and GJA4 (connexin-37) gap junctions in the antral follicle and cumulus-oocyte complex. *Biol Reprod*; 90(6):137.

likely that gap junctional inhibition was faster in punctured follicles compared to intact follicles due to the presence of a hole in the follicular wall allowing easier access to the follicle interior and thus to target gap junctions within the antral follicle.

Lindane, another general gap junction inhibitor previously confirmed to inhibit GJA1 (connexin-43) gap junctions in oocyte-granulosa cell primary cultures [Li & Mathur 1997], was also used to examine the ability of gap junction inhibition to cause GVBD. As expected, meiotic arrest was maintained in ~80-90% of intact and punctured antral follicles that were cultured 10 hours in the absence of either AGA or lindane (Figure 24C, D). Similar to the previous experimental results, the addition of AGA to culture medium of both intact and punctured antral follicles caused meiotic resumption to occur in ~80% of intact antral follicles and ~95% of punctured antral follicles over the 10-hour culture period. Lindane also resulted in an increase in meiotic resumption with ~70% of both intact and punctured antral follicles undergoing GVBD during the 10-hour culture, an effect which was somewhat less effective than AGA but significantly greater than control antral follicles cultured without gap junction inhibitors (Figure 24C, D). These results provide support for the importance of gap junctional communication in the maintenance of prophase-I arrest in antral follicles and further confirm the ability of these antral follicle culture methodologies to maintain healthy antral follicles with functional gap junctions in culture.

2.4 Cx43 CMPs cause meiotic resumption in cultured COCs

Although it has been well established that functional gap junctions are required to maintain meiotic arrest prior to ovulation, it is still unclear what specific gap junction isoforms are vital to this process. Since the general gap junction inhibitors AGA and

lindane exert their effects by indirectly disrupting gap junction function, they can have non-specific effects and do not selectively target specific gap junction isoforms [Juszczak & Swiergiel 2009; Brokamp et al. 2012]. To inhibit GJA1 (connexin-43) and GJA4 (connexin-37) gap junctions specifically, I used short peptides called connexin-mimetic peptides (CMPs) which bind to a specific amino acid sequence on the gap junction extracellular loop domains thus blocking gap junctional communication in an isoform-specific manner. These CMPs have been previously validated in other tissues and connexin-43 CMPs have previously been shown to inhibit gap junctions between rat granulosa cell primary cultures, although they have not previously been used to investigate the maintenance of meiotic arrest [Ke et al. 2005; Evans & Leybaert 2007; Evans et al. 2012].

The effect of specifically inhibiting GJA1 and GJA4 gap junctions on meiotic arrest was first examined in cultured COCs with NPPC and E_2 added to the medium to maintain meiotic arrest. CMPs obtained from Alpha Diagnostics (ADI) directed against GJA1 (Cx43 CMP) and GJA4 (Cx37 CMP) were added to COC culture medium at concentrations ranging from 0-600 µM and COCs were cultured for 20 hours in the presence of NPPC (100 nM) and E_2 (100 nM) to maintain meiotic arrest. After the 20-hour culture period, oocytes were examined for GVBD to indicate whether meiotic resumption had occurred. Meiotic resumption in COCs was significantly increased in the presence of 450 µM Cx43 CMP with ~60% of COCs resuming meiosis and was greatest in the presence of 600 µM Cx43 CMP with ~80% of oocytes resuming meiosis. COCs were also cultured in the presence of 600 µM of a scrambled Cx43 CMP (Scr43 CMP) which did not cause COCs to resume meiosis (Figure 25A). No significant difference in the percentage of COCs that

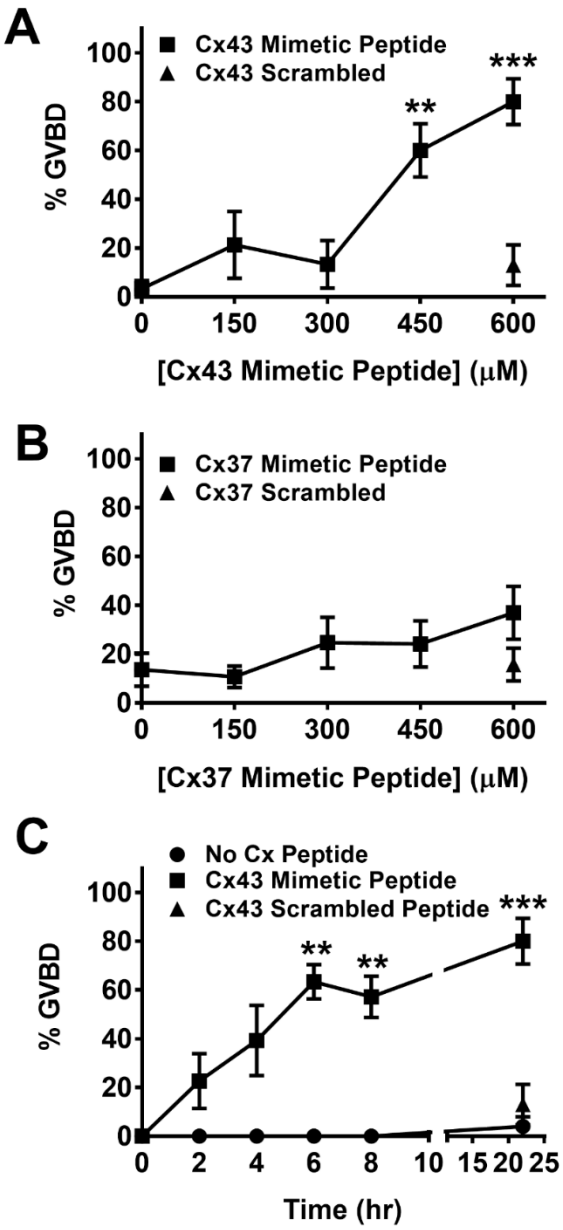

Figure 25. Gap junction inhibition in COCs: connexin-mimetic peptides (CMPs). (**A**) COCs were cultured 20 hours with 0-600 μM of connexin-43 CMP (squares, Cx43 CMP) or 600 μM of a scrambled control peptide (triangle, Scr Cx43) (mean ± SEM, n=5). Differences between means for each CMP concentration tested were measured compared to the % GVBD in COCs cultured in the presence of 0 μM CMP by ANOVA and Tukey

test (**P < 0.01, ***P < 0.001). (**B**) COCs were cultured 20 hours with 0-600 µM of connexin-37 CMP (squares, Cx37 CMP) or 600 µM of a scrambled control peptide (triangle, Scr Cx37) (mean ± SEM, n=5). No differences between means of % GVBD were detected between COCs cultured with 0-600 µM Cx37 CMP compared to COCs cultured in the absence of CMP (0 µM) by ANOVA and Tukey test (P=0.30). For both **A** and **B**, NPPC (100 nM) and E_2 (100 nM) were added to culture medium to maintain meiotic arrest in COCs. After culture, oocytes were examined for GVBD. (**C**) COCs were cultured for 0-22 hours with NPPC (100nM) and E_2 (100 nM) and with no Cx43 CMP (0 µM, circles), with 600 µM Cx43 CMP (squares), or with 600 µM Scr 43 CMP (triangles, 22 hours). After culture, oocytes were examined for meiotic resumption as indicted by the percentage of COCs that underwent GVBD (% GVBD) (mean ± SEM, n=5). Differences between means at each time point were determined by Student *t*-tests (**P< 0.01, ***P < 0.001). This figure was reproduced with the permission of Oxford University Press, Society for the Study of Reproduction©. Richard S. & Baltz J.M. (2014). Prophase I arrest of mouse oocytes mediated by natriuretic peptide precursor C requires GJA1 (connexin-43) and GJA4 (connexin-37) gap junctions in the antral follicle and cumulus-oocyte complex. *Biol Reprod*; 90(6):137.

resumed meiosis was observed when COCs were cultured with 0-600 µM Cx37 CMP, or with 600 µM scrambled Cx37 CMP (Scr37 CMP) (Figure 25B).

Since meiotic resumption was only observed in COCs cultured in the presence of Cx43 CMP, I next determined the minimum amount of time required for Cx43 CMP-induced gap junction inhibition to occur in COCs. COCs were cultured for 0-22 hours in the presence or absence of 600 µM Cx43 CMP and for 22 hours in the presence of Scr43 CMP. NPPC (100 nM) and E_2 (100 nM) were added to culture medium under all culture conditions described to maintain meiotic arrest in COCs. After the desired culture period, oocytes were examined for the presence of GVBD to indicate that meiotic resumption had occurred. In the absence of Cx43 CMP meiotic arrest was maintained in COCs throughout the culture period. COCs cultured in the presence of Cx43 CMP (600 µM) progressively began to resume meiosis from 0-6 hours with ~60% of COCs undergoing GVBD at 6 hours which increased to ~80% of COCs at 22 hours (Figure 25C). No significant difference in the percentage of COCs which resumed meiosis was detected between COCs cultured without Cx43 CMP or in the presence of Scr43 CMP for 22 hours.

The ability of Cx43 CMP to cause meiotic resumption in COCs cultured in the presence of NPPC and E_2 was further confirmed using an additional Cx43 CMP synthesized by CHI Scientific provided by Dr. Laurinda Jaffe and colleagues. COCs were cultured for 24 hours with no CMP (-Cx), with Cx43 CMP from Alpha Diagnostics (600 µM, +ADI), with Cx43 CMP from CHI Scientific (600 µM, +CHI), or with a scrambled peptide from CHI Scientific (600 µM, + CHIscr). After the 24-hour culture period, COCs were examined for the presence of GVBD (meiotic resumption). In the absence of CMP

and in the presence of scrambled CHI Scientific peptide, meiotic resumption occurred in ~20% of COCs (Figure 26). In the presence of Cx43 CMP from ADI, meiotic resumption occurred in ~60% of COCs while meiotic resumption occurred in ~40% of COCs cultured with Cx43 CMP from CHI Scientific (Figure 26). Thus, meiotic resumption was also significantly increased in COCs by Cx43 CMP from CHI Scientific, however, release of NPPC-mediated meiotic arrest by the CHI Scientific CMP was not as effective as the CMP from ADI.

2.5 Cx43 CMPs cause meiotic resumption in punctured antral follicles

I showed above that general gap junction inhibitors caused meiotic resumption in cultured intact and punctured antral follicles. To more specifically inhibit gap junctions in antral follicles, I sought to use CMPs to inhibit both GJA1 (connexin-43) and GJA4 (connexin-37) gap junctions. I hypothesized that punctured antral follicles would be required for this specific method of gap junction inhibition due to the increased access to the follicle interior, especially since GJA4 (connexin-37) gap junctions are located deep within the follicle at the interface between the oocyte and innermost cumulus granulosa cell layer. To first compare the effectiveness of gap junction inhibition by CMPs in both intact and punctured antral follicles, intact and punctured antral follicles were cultured for 20 hours in the presence of Cx43 CMPs (+Cx, 600 µM) or in the presence of the corresponding scrambled peptide (Scr, 600 µM); Cx43 CMP was used since meiotic resumption occurred in COCs when Cx43 CMP was added to culture medium but not when Cx37 CMP was added. After the culture period, oocytes were examined for meiotic

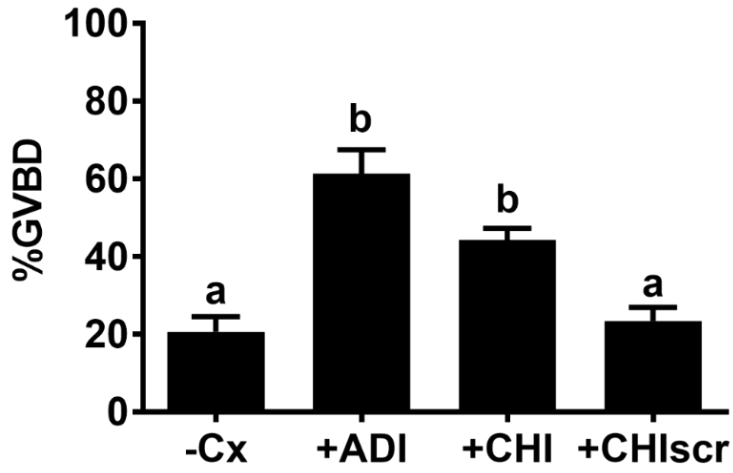

Figure 26. ADI and CHI Cx43 CMPs and meiotic resumption in COCs. COCs were cultured with NPPC (100 nM) and E_2 (100 nM) for 24 hours with no CMP (-Cx), with Cx43 CMP from Alpha Diagnostics (600 µM, +ADI), with Cx43 CMP from CHI Scientific (600 µM, +CHI), or with a scrambled peptide from CHI Scientific (600 µM, + CHIscr). Black bars represent the percentage of COCs that underwent GVBD (meiotic resumption) (mean ± SEM, n=3). Bars that do not share letters have significantly different means ($P < 0.05$ for **-Cx** vs **+CHI** and **+ CHI** vs **+ CHIscr**, $P < 0.01$ for **+ADI** vs **+CHIscr**, and $P < 0.001$ for **-Cx** vs **+ADI** by ANOVA with Tukey test).

resumption characterised by GVBD. In the presence of scrambled peptide, meiotic arrest was maintained in ~90% of oocytes in both intact and punctured antral follicles (Figure 27). In contrast, when Cx43 CMP was present in culture medium, meiotic resumption was significantly increased in both intact (~40% GVBD) and punctured (~70% GVBD) antral follicles with the greatest effect observed in punctured antral follicles.

Since the percentage of oocytes which resumed meiosis in the presence of Cx43 CMP was higher in punctured antral follicles (Figure 27) and general gap junction inhibition by AGA was faster in punctured antral follicles (Figure 24A, B) compared to intact antral follicles, punctured antral follicles were used for the following experiments. To determine whether meiotic resumption occurs in antral follicles when Cx43 CMP or Cx37 CMP is added to culture medium, punctured antral follicles were cultured 20 hours in the absence of CMPs (-Cx), in the presence of 600 µM Cx43 or Cx37 CMPs (+Cx), or with 600 µM of the corresponding scrambled peptide (Scr). After the culture period, oocytes were removed from follicles and examined for meiotic resumption (GVBD). Similar to the results with COCs, the presence of Cx37 CMP in culture medium did not cause meiotic resumption to occur in punctured antral follicles which was not significantly different from punctured antral follicles cultured without CMPs or with the scrambled peptide (Figure 28). In contrast, the presence of Cx43 CMP in culture medium significantly increased meiotic resumption in punctured follicles with ~85% of oocytes undergoing GVBD while meiotic arrest was maintained in the absence of CMP or with the scrambled peptide (5-10% GVBD) (Figure 28). Therefore, as with COCs, meiotic resumption only occurred in cultured antral follicles when Cx43 CMP was present in culture medium while meiotic arrest was maintained in the presence of Cx37 CMP.

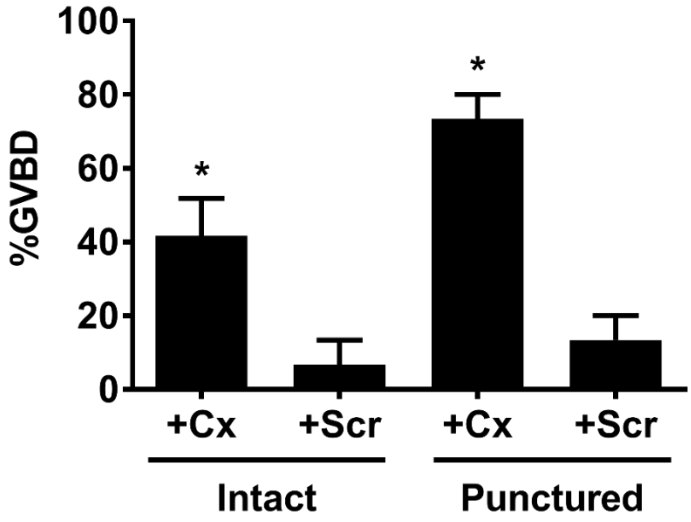

Figure 27. Cx43 CMP and meiotic resumption in intact and punctured antral follicles. Intact and punctured antral follicles were cultured 20 hours in the presence of Cx43 CMP (600 µM, +Cx) or in the presence of the corresponding scrambled peptide (600 µM, +Scr). After the culture period, oocytes were isolated from follicles and examined for meiotic resumption (mean ± SEM, n=3). Black bars represent the percentage of oocytes that resumed meiosis (% GVBD) after the culture period. Differences between means for +Cx and +Scr in intact and punctured follicles were measured by Student *t*-test (*P< 0.05).

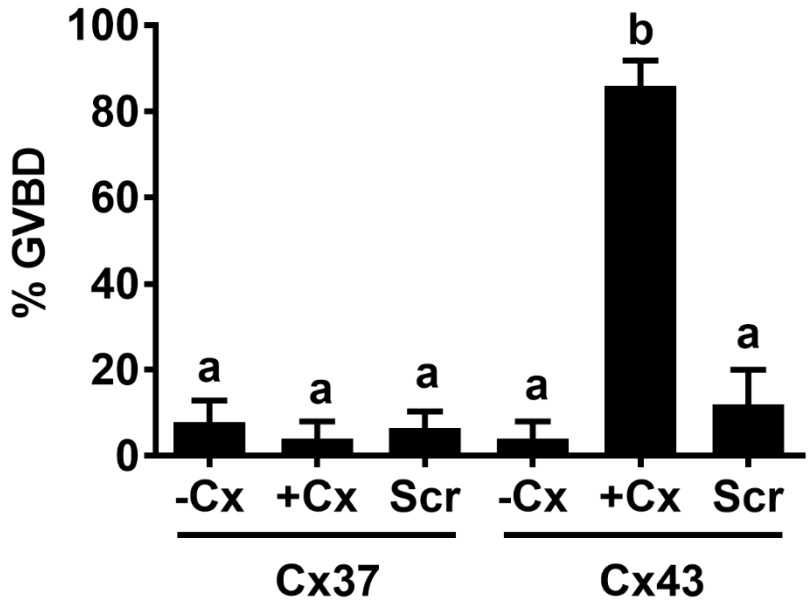

Figure 28. Cx43 and Cx37 CMPs and meiotic resumption in punctured antral follicles. Punctured antral follicles were cultured 20 hours without CMPs (-Cx), with CMPs (+Cx), or with scrambled peptide (Scr). Black bars represent the percentage of oocytes which resumed meiosis (% GVBD) (mean ± SEM, n=5). For each culture condition, the specific CMP examined is indicated by an underline and corresponding Cx label (Cx37 or Cx43). Bars that do not share letters have significantly different means ($P < 0.001$ by ANOVA and Tukey test). This figure was reproduced with the permission of Oxford University Press, Society for the Study of Reproduction©. Richard S. & Baltz J.M. (2014). Prophase I arrest of mouse oocytes mediated by natriuretic peptide precursor C requires GJA1 (connexin-43) and GJA4 (connexin-37) gap junctions in the antral follicle and cumulus-oocyte complex. *Biol Reprod*; 90(6):137.

2.6 Cx37 CMP cause meiotic resumption in COCs when deposited at the site of their target gap junctions

The ability of Cx43 CMPs, but not Cx37 CMPs, to cause meiotic resumption in COCs and punctured antral follicles when added to culture medium could indicate that only GJA1 gap junctions are necessary to maintain NPPC-mediated meiotic arrest. GJA4 gap junctions have been shown to be exclusively expressed between the oocyte and innermost cumulus granulosa cells under the ZP while GJA1 gap junctions are located between granulosa cells throughout the follicle. Therefore, it is alternatively possible that Cx37 CMPs were unable to reach their target gap junctions, thus preventing inhibition of GJA4 gap junctions and causing NPPC-mediated meiotic arrest to be maintained. To examine whether the presence of cumulus granulosa cells surrounding the oocyte might impede peptide access to the oocyte surface, COCs and denuded GV oocytes were incubated for 2 hours with fluorescently-labelled WGA which binds to ZP glycoproteins. After the incubation period, COCs were denuded and oocytes were imaged by confocal microscopy. ZP staining (green) was strong in oocytes which were already denuded (DO) for the duration of the incubation with WGA and staining was present through the entire width of the ZP (Figure 29A). In comparison, weaker ZP staining was observed when entire COCs were incubated with WGA with only the outermost edge of the ZP exhibiting fluorescence. Thus, the presence of cumulus granulosa cells appears to diminish the ability of WGA to penetrate through the ZP to the oocyte surface, possibly suggesting that Cx37 CMPs also could not access the gap junctions located nearest to the oocyte.

To determine whether the Cx37 CMPs failed to cause meiotic resumption because they were unable to reach the gap junctions at the oocyte surface, I microinjected

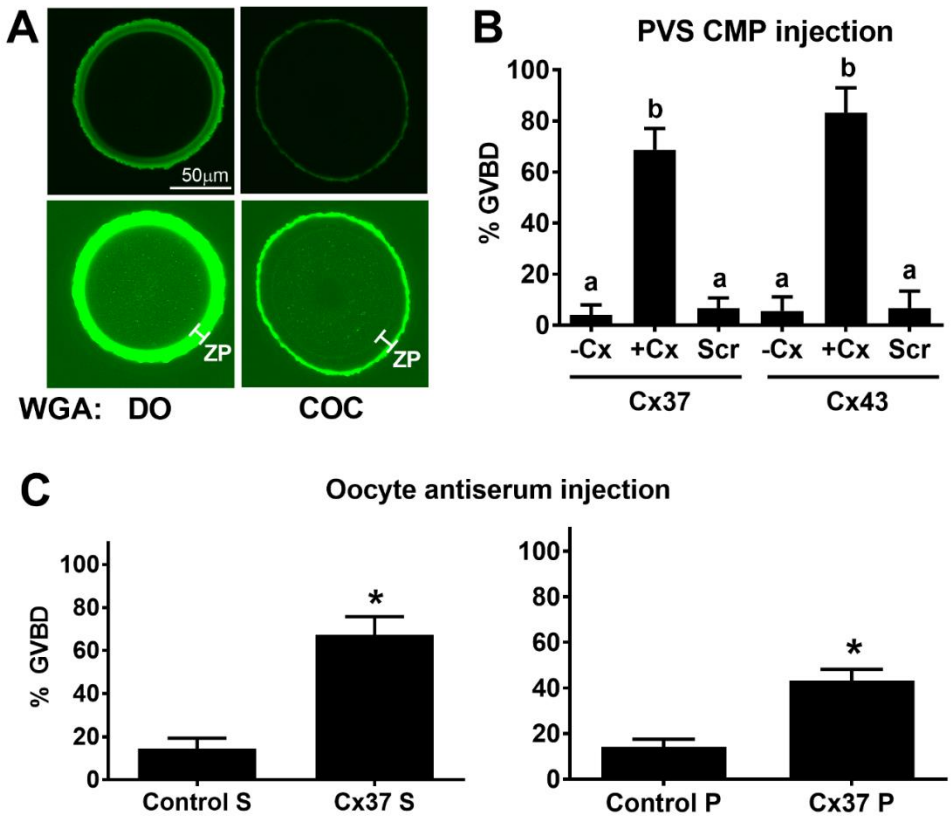

Figure 29. Meiotic resumption and inhibition of GJA4 gap junctions in COCs. (**A**) COCs or denuded GV oocytes (DO) were incubated with or without Alexa-488 conjugated WGA (5µg/ml) for 2 hours and then fluorescence (green) was observed by confocal microscopy in denuded oocytes and COCs after denudation. Images in the upper panel are original images while images in the lower panel were equally adjusted for brightness to indicate the location of the ZP as labelled in the lower panels. The scale bar in the DO upper panel image represents 50 µm and applies to all images. (**B**) Medium containing Cx37 CMPs (600 µM, +Cx), Cx37 scrambled peptide (600 µM, Scr), or no peptide (-Cx) was microinjected at the oocyte surface of COCs and cultured for 20 hours. Culture medium also contained CMPs or scrambled peptides and was supplemented with NPPC

(100 nM) and E_2 (100nM) to maintain meiotic arrest. Black bars represent the percentage of oocytes which resumed meiosis (% GVBD) (mean ± SEM, n=3). For each culture condition, the specific CMP examined (Cx37 or Cx43) is indicated by an underline and corresponding Cx label. Bars that do not share letters have significantly different means ($P < 0.001$ by ANOVA and Tukey test). (**C**) COCs were microinjected with previously validated anti-GJA4 (connexin-37) antibodies and cultured for 20 hours in the presence of NPPC (100 nM) and E_2 (100 nM). Meiotic resumption was assessed by the presence of GVBD (mean ± SEM, n=3). The left panel represents COCs that were microinjected with GJA4 antiserum (Cx37 S) developed by Dr. Alexander Simon or with a paired IgG control (Control S). The right panel represents COCs that were microinjected with GJA4 antiserum (Cx37 P) develop by Dr. David Paul or with a paired IgG control (Control P). Black bars represent the percentage of COCs that resumed meiosis (% GVBD) during the culture period. Differences between means were determined by Student *t*-test (*$P< 0.05$). This figure was reproduced with the permission of Oxford University Press, Society for the Study of Reproduction©. Richard S. & Baltz J.M. (2014). Prophase I arrest of mouse oocytes mediated by natriuretic peptide precursor C requires GJA1 (connexin-43) and GJA4 (connexin-37) gap junctions in the antral follicle and cumulus-oocyte complex. *Biol Reprod*; 90(6):137.

medium supplemented with Cx43 or Cx37 CMPs (600 μM) directly at the oocyte surface in COCs, cultured COCs for 20 hours, and then examined COCs for meiotic resumption. COCs microinjected with medium alone (-Cx) served as a control for the microinjection manipulation. The same medium used for the microinjection was used for COC culture medium (containing no additions, CMPs, or scrambled peptide) to maintain a concentration of 600 μM of CMPs or scrambled CMPs for the duration of culture. NPPC and E_2 were added to the medium to maintain meiotic arrest. The ability of CMPs to cause COCs to overcome NPPC-mediated meiotic arrest was assessed by the percentage of COCs which underwent GVBD. For both Cx37 and Cx43, meiotic arrest was maintained in COCs microinjected and cultured with medium containing the scrambled version of the peptide (Scr) or medium alone (-Cx) indicating that the microinjection manipulation itself did not cause meiotic resumption (Figure 29B). Microinjection of medium containing Cx43 CMP at the oocyte surface of COCs, and subsequent culture in medium containing Cx43 CMP (600 μM), caused meiotic resumption to occur in ~80% of COCs while microinjection of medium containing Cx37 CMP and culture in medium containing Cx37 CMP (600 μM) caused meiotic resumption in ~70% of COCs, a significantly higher percentage than for COCs microinjected with medium alone or scrambled peptide (Figure 29B). This suggests that the Cx37 CMPs were impeded from accessing the gap junctions located at the oocyte surface under my previous COC and punctured antral follicle culture conditions and that functional GJA4 (connexin-37) gap junctions are required to maintain NPPC-mediated meiotic arrest.

To further confirm the requirement for GJA4 gap junctions for NPPC-mediated meiotic arrest, two separate previously validated anti-GJA4 (connexin-37) antibodies were

microinjected into COCs (within the oocyte) and cultured for 20 hours in the presence of NPPC and E_2. These antibodies were previously shown to downregulate GJA4 (connexin-37) gap junctions when injected into oocytes within intact antral follicles [Norris et al. 2008]. For both anti-GJA4 antibodies tested, meiotic resumption was significantly increased in COCs microinjected with the antibodies compared to COCs microinjected with control IgG (Figure 29C). These results further support a vital role for GJA4 gap junctions in the maintenance of NPPC-mediated meiotic arrest.

3. Suppression of GLYT1 activity by antral follicles.

I showed in the above section that the intact and punctured antral follicle methodology was successful in maintaining healthy, prophase I-arrested oocytes with functional gap junctional communication throughout a 20-hour culture period. I next sought to determine whether GLYT1 suppression could also be maintained in cultured antral follicles. GLYT1 activity is low in oocytes immediately after isolation from ovaries but becomes spontaneously activated in isolated denuded oocytes and COCs during culture reaching a maximal rate of GLYT1-mediated glycine uptake by ~3-4 hours [Tartia et al. 2009]. I have also shown above that a low level of GLYT1 activity develops during a 4-hour culture period in denuded growing oocytes which is not present immediately following isolation from ovaries (Figure 14) [Richard et al. 2016]. Thus, GLYT1 activity appears to be suppressed within growing and fully-grown oocytes within the ovary prior to ovulation by an unknown mechanism. The following experiments were performed to determine whether GLYT1 could remain suppressed within cultured antral follicles compared to denuded oocytes and COCs in which GLYT1 activation normally occurs.

3.1 GLYT1 becomes spontaneously activated in denuded oocytes and COCs isolated from mouse ovaries but remains suppressed in cultured mouse antral follicles.

To determine whether GLYT1 suppression could be maintained in cultured antral follicles, intact antral follicles were cultured for 0-20 hours and then GLYT1 activity was examined by measuring the rate of [^{3}H]-glycine uptake into oocytes at various time points throughout culture. Denuded oocytes and COCs were simultaneously cultured to compare spontaneous GLYT1 activation with the GLYT1 activity measured in oocytes that were cultured within antral follicles. Since I previously showed that meiotic arrest is maintained in cultured intact antral follicles for up to 20 hours, meiotic arrest was also maintained throughout the culture period in denuded oocytes with dbcAMP (300 μM) and in COCs with NPPC (100 nM) and E_2 (100 nM). Prior to measuring GLYT1 activity, resumption of meiosis in oocytes, COCs, and antral follicles was examined by the presence of GVBD.

Meiotic arrest was maintained in denuded oocytes, COCs, and intact antral follicles and did not significantly differ at any time points throughout the culture period (Figure 30A). For denuded oocytes and COCs, GLYT1 activity was low immediately following isolation from ovaries but increased steadily during culture reaching maximal GLYT1 activity between 2-4 hours which did not continue to increase for up to 6 hours (Figure 30B). Similar to denuded oocytes and COCs, GLYT1 activity was essentially absent in freshly isolated intact antral follicles however, GLYT1 activity did not increase to the levels observed in denuded oocytes and COCs throughout the culture period. Although GLYT1 activity increased somewhat by 1 hour after isolation from ovaries, only this low level of activity remained for the entire duration of culture for up to 20 hours and was significantly lower than GLYT1 activity in denuded oocytes and COCs at all time

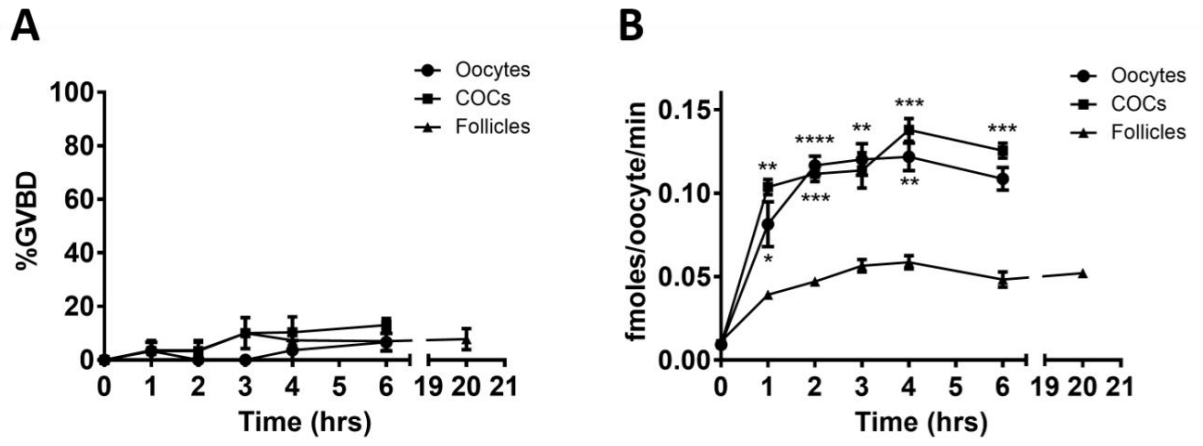

Figure 30. GLYT1 activation in denuded oocytes, COCs, and antral follicles. (**A**) Before GLYT1 activity was measured, meiotic resumption was examined. In denuded oocytes, meiotic arrest was maintained with dbcAMP (300 µM) while COCs were maintained in meiotic arrest with NPPC (100 nM) and E_2 (100 nM). For intact antral follicles, cultured medium was not supplemented with NPPC/E_2 or dbcAMP. Meiotic resumption is indicated by the percentage of oocytes that underwent GVBD (% GVBD) (mean ± SEM, n=3). No significant differences between means of denuded oocytes, COCs, or antral follicles was measured for % GVBD by Student *t*-test. (**B**) Denuded oocytes (circles), COCs (squares), and intact antral follicles (triangles) were cultured for 0-20 hours. GLYT1 activity is represented as the rate of [^{3}H]-glycine uptake into oocytes and shown in fmol/oocyte/min (mean ± SEM, n=3). At each time point examined, differences between means for GLYT1 activity in denuded oocytes, COCs, and intact antral follicles was measured by Student *t*-test (*P< 0.05, **P < 0.01, ***P < 0.001, ****P < 0.0001). This figure was reproduced from the following publication: Richard S. & Baltz J.M. (2017). Preovulatory suppression of mouse oocyte cell volume-regulatory mechanisms is

via signalling that is distinct from meiotic arrest. *Sci Rep*; 7(1):702.

points examined (Figure 30B). I hypothesize that the minimal GLYT1 activity detected in intact antral follicles represents a small number of oocytes that did not have effective GLYT1 suppression during culture and thus caused an apparent increase in GLYT1-mediated [^{3}H]-glycine uptake when pooled with oocytes from antral follicles with successful GLYT1 suppression, however this remains to be investigated. The ability of intact antral follicles, but not denuded oocytes or COCs, to maintain suppressed GLYT1 activity in culture suggests that GLYT1 suppression prior to ovulation (or removal from ovaries) depends on inhibitory mechanisms involving at least mural granulosa cells and/or follicular fluid.

3.2 GLYT1 activation occurs normally after oocytes are removed from cultured intact antral follicles.

To ensure that GLYT1 can be normally activated in oocytes after culture within intact antral follicles using this culture methodology, intact antral follicles were cultured for 4 or 24 hours and then denuded oocytes were isolated from the follicles. GLYT1 activity was measured in half of the isolated oocytes after each culture period immediately after removal from antral follicles while the other half of isolated oocytes were cultured for an additional 4 hours to determine whether GLYT1 activation could occur. As expected, GLYT1 activity was still suppressed in oocytes immediately following isolation from intact antral follicles when cultured for 4 or 24 hours (Figure 31). In denuded oocytes cultured for an additional 4 hours after isolation from antral follicles, however, the rate of GLYT1-mediated [^{3}H]-glycine uptake was significantly increased for both time points examined compared to GLYT1 activity in oocytes immediately after isolation from

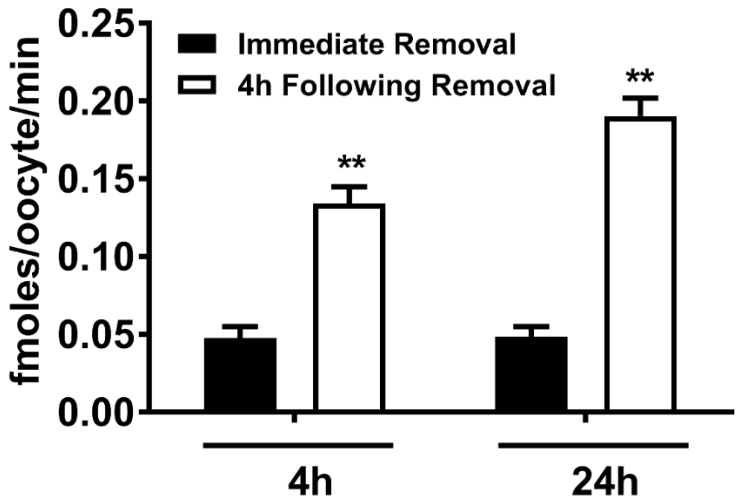

Figure 31. GLYT1 activation after removal of oocytes from cultured intact antral follicles. Intact antral follicles were cultured for 4 or 24 hours and then denuded oocytes were isolated from follicles. GLYT1 activity was measured in half of oocytes from each culture period immediately after isolation from follicles (black bars) while the other half of oocytes were cultured for an additional 4 hours and then GLYT1 activity measured (white bars) (mean ± SEM, n=5). The rate of [^{3}H]-glycine uptake (GLYT1 activity) is shown in fmoles/oocyte/min. Differences between means for each culture period was measured by Student *t*-test (**P< 0.01). This figure was modified from the following publication: Richard S. & Baltz J.M. (2017). Preovulatory suppression of mouse oocyte cell volume-regulatory mechanisms is via signalling that is distinct from meiotic arrest. *Sci Rep*; 7(1):702. This article is licensed under a Creative Commons Attribution 4.0 International License. © Richard S. & Baltz J.M. 2017.

cultured antral follicles. This indicates that the GLYT1 suppression observed in cultured intact antral follicles is not simply due to a loss of the oocyte's ability to activate GLYT1 and that normal GLYT1 activation can occur in these oocytes after removal from antral follicles.

3.3 Punctured antral follicles maintain GLYT1 suppression for 20 hours in culture when NPPC and E_2 are added to culture medium.

Since I showed that intact antral follicles could maintain suppressed GLYT1 activity within oocytes for up to 24 hours in culture, I next sought to determine whether GLYT1 suppression could also be maintained in punctured antral follicles. The ability to successfully maintain GLYT1 suppression within the punctured antral follicle culture system would allow for manipulations to be performed that may require the enhanced access to the follicle interior that would be provided by the hole in the outer follicular wall. For example, specific gap junction inhibition using Cx43 CMP was more effective in punctured antral follicles compared to intact antral follicles (Figure 27). To determine if GLYT1 suppression could also be maintained in punctured antral follicles, punctured follicles were cultured for 0-20 hours and then GLYT1 activity was assessed by measuring the rate of [^{3}H]-glycine uptake at various time points. Since I showed previously that GLYT1 remains suppressed in intact antral follicles for up to 20 hours, intact follicles were simultaneously cultured as a comparison for GLYT1 suppression at each time point examined. As expected, a low level of GLYT1 activity was measured in oocytes immediately after isolation from intact antral follicles for the duration of the culture. In contrast, GLYT1 suppression was only maintained for 4 hours in oocytes in punctured

antral follicles and then increased significantly by 12 hours and continued to steadily increase up until the final 20-hour culture period (Figure 32A).

Since I observed above that meiotic resumption also started to occur in punctured antral follicles by 12 hours in culture when NPPC and E_2 were not added to culture medium (Figure 22), I cultured intact and punctured antral follicles in the presence of NPPC (100 nM) and E_2 (100 nM) for 0-20 hours and then measured GLYT1 activity at various time points. I hypothesized that the follicular fluid was again being diluted into the culture medium causing meiotic resumption, and possibly GLYT1 activation, to occur during extended culture periods. Interestingly, when culture medium was supplemented with NPPC and E_2, GLYT1 suppression was maintained in both intact and punctured follicles without any significant difference at any time points examined (Figure 32B). Thus, GLYT1 suppression is maintained in punctured antral follicles for up to 20 hours only when NPPC and E_2 are added to culture medium, possibly suggesting that NPPC signalling is partly involved in GLYT1 suppression prior to ovulation.

3.4 GLYT1 activation is stimulated by luteinizing hormone (LH) in intact antral follicles.

It has previously been shown that meiotic resumption is stimulated in cultured intact antral follicles by LH via EGFR kinase signalling [Norris et al. 2010]. To determine whether this signalling mechanism may also cause GLYT1 activation to occur in cultured antral follicles, I adapted the protocol developed by Norris and colleagues wherein antral follicles from post-natal day 21 (P21) neonates are cultured first in the presence of FSH

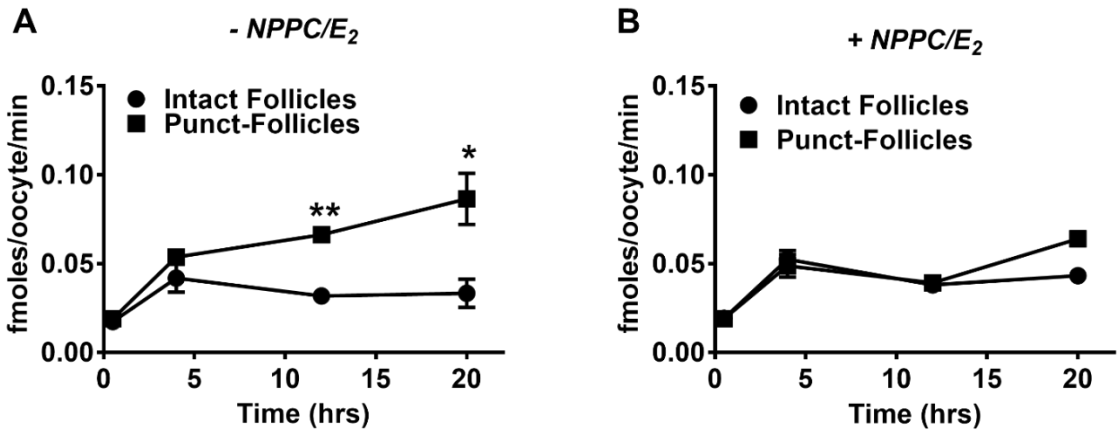

Figure 32. GLYT1 suppression in intact and punctured antral follicles cultured with or without NPPC and E_2. Intact and punctured antral follicles were cultured for 0-20 hours in the absence (**A**) or presence (**B**) of NPPC (100 nM) and estradiol (E_2, 100 nM) and then GLYT1 activity was measured at various time points throughout culture (mean ± SEM, n=3). For both **A** and **B**, GLYT1 activity in intact (circles) and punctured (squares) antral follicles is shown as the rate of [^{3}H]-glycine uptake in fmoles/oocyte/min. Differences between means in intact and punctured follicles at each time point was measured by Student *t*-test (*P< 0.05, **P < 0.01). When NPPC and E_2 were present in culture medium (**B**), no significant differences between means were detected at any time points.

and then secondarily cultured with or without LH [Norris et al. 2010]. More specifically, I isolated intact antral follicles from P21 neonatal mice and cultured them overnight (20 hours) in antral follicle culture medium which contains 100 ng/ml FSH. After the overnight culture, follicles were transferred to fresh antral follicle culture medium with or without LH (350 nM) added and then oocytes from these follicles were examined for meiotic resumption (GVBD) and GLYT1 activation.

Similar to previous results obtained by Norris and colleagues [2008], meiotic resumption occurred in significantly more antral follicles cultured in the presence of LH compared to antral follicles cultured without LH. In the presence of LH, ~55% of oocytes had resumed meiosis by 3 hours which increased to ~70% of oocytes by 5 hours in culture (Figure 33A). As expected, in the absence of LH, GLYT1 suppression was successfully maintained in intact antral follicles for the entire culture period. However, when intact antral follicles were cultured with LH GLYT1 activity was somewhat increased compared to follicles cultured without LH (Figure 33B). The observed increase in GLYT1-mediated glycine uptake in response to LH suggests that LH-induced signalling at ovulation may disrupt the putative inhibitory signalling mechanism responsible for GLYT1 suppression prior to ovulation.

4. GLYT1 suppression is mediated by signalling distinct from the signalling mechanism involved in the maintenance of prophase I arrest.

It has previously been demonstrated that GLYT1 will become spontaneously activated in denuded oocytes even when maintained in meiotic arrest by dbcAMP or

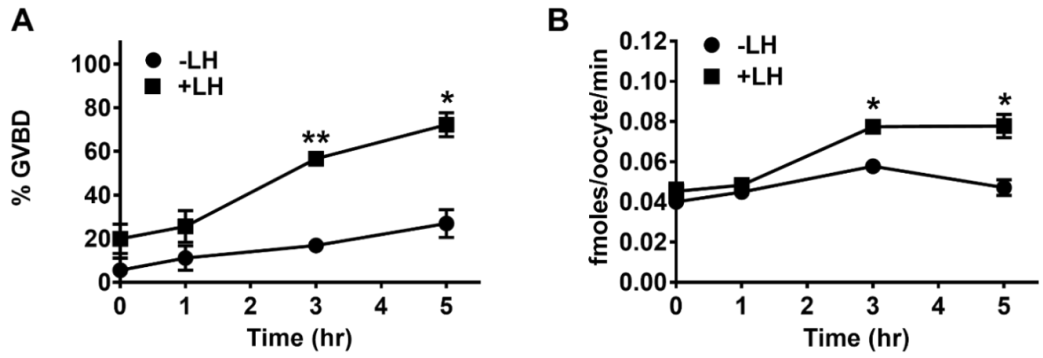

Figure 33. LH-stimulated meiotic resumption and GLYT1 activation in antral follicles. Intact antral follicles from P21 neonates were cultured overnight in antral follicle culture medium. After the culture period, follicles were cultured for an additional 0-5 hours with or without LH (350 nM) and oocytes were then examined for meiotic resumption (GVBD) and GLYT1 activity. (**A**) The percentage of oocytes which resumed meiosis is shown (% GVBD) in intact antral follicles cultured with (squares) or without (circles) LH (mean ± SEM, n=3). (**B**) The rate of GLYT1-mediated [^{3}H]-glycine uptake is shown in fmoles/oocyte/min in intact antral follicles cultured with (squares) or without (circles) LH (mean ± SEM, n=3). For both **A** and **B**, differences between means in follicles cultured with or without LH at various time points was measured by Student *t*-test (*P< 0.05, **P < 0.01). This figure was reproduced from the following publication: Richard S. & Baltz J.M. (2017). Preovulatory suppression of mouse oocyte cell volume-regulatory mechanisms is via signalling that is distinct from meiotic arrest. *Sci Rep*; 7(1):702. This article is licensed under a Creative Commons Attribution 4.0 International License. © Richard S. & Baltz J.M. 2017.

several other manipulations [Tartia et al. 2009]. In addition, I have shown above that GLYT1 is activated normally in cultured COCs that are maintained in meiotic arrest with NPPC and E_2 (Figure 30B). Despite the ability of GLYT1 to fully activate even in the absence of meiotic progression, it is possible that the signalling mechanisms inhibiting these two events in the antral follicle prior to ovulation are partly shared. The results previously discussed in the above sections have revealed many similarities between prophase-I arrest and GLYT1 suppression including the acquired competency of oocytes at the late stages of oogenesis to resume meiosis and activate GLYT1 (Figure 13 & Figure 15B), the release of inhibition of prophase I arrest and GLYT1 suppression in punctured antral follicles cultured greater than 4 hours (likely as a result of follicular fluid dilution, Figure 22 & Figure 32), and the stimulation of meiotic resumption and GLYT1 activation in response to LH in cultured intact antral follicles (Figure 33). Although NPPC was unable to maintain GLYT1 suppression in COCs, it is possible that sufficient cGMP was produced to only maintain meiotic arrest but that the concentration was too low to suppress GLYT1 activation. Alternatively, it is possible that prophase I arrest and GLYT1 suppression are indeed maintained by different signalling mechanisms within the antral follicle but that both rely on the secretion of inhibitory factors into the follicular fluid from mural granulosa cells and/or the presence of functional gap junctions to relay the inhibitory signal to the oocyte.

To further investigate whether NPPC-cGMP signalling is involved in GLYT1 suppression within the antral follicle, I cultured COCs in increasing concentrations of NPPC and in the presence of various agonists and antagonists of this signalling pathway to determine whether maximal GLYT1 activation could be prevented. Finally, since meiotic

arrest depends on gap junctional communication, I performed a detailed time course experiment of gap junction inhibition and comparing the resultant timing of GLYT1 activation to meiotic resumption.

4.1 Maintenance of GLYT1 suppression in the antral follicle is not dependent on NPPC-cGMP signalling.

Although GLYT1 suppression was not maintained when COCs were cultured in the presence of 100 nM NPPC, it was possible that enough cGMP was produced to maintain meiotic arrest but that insufficient cGMP was present under my culture conditions to also maintain GLYT1 suppression. To investigate this hypothesis, I first cultured COCs for 4 hours in the presence of increased concentrations (0-1 μM) of NPPC and then measured GLYT1 activity by [^{3}H]-glycine uptake. In the presence of all concentrations of NPPC tested, GLYT1 activated normally in cultured COCs, even at the highest concentration where meiotic maturation was previously shown to again resume, possibly due to toxicity (Figure 34A & Figure 21A). To further examine whether NPPC-cGMP signalling can suppress GLYT1 activity, various agonists of this signalling pathway were added to culture medium and COCs were cultured for 4 hours and then GLYT1 activity was measured by a [^{3}H]-glycine uptake experiment. In addition to NPPC and E_2, hypoxanthine, guanosine, and an oocyte-specific PDE9 inhibitor (BAY 73-6691) were also added to COC culture medium. Hypoxanthine has previously been shown to contribute to the maintenance of prophase-I arrest in mouse COCs at high concentrations possibly by the recovery of hypoxanthine to inosine monophosphate which is converted to GTP through a series of enzymatic reactions; hypoxanthine may also directly inhibit PDE3A thereby preventing

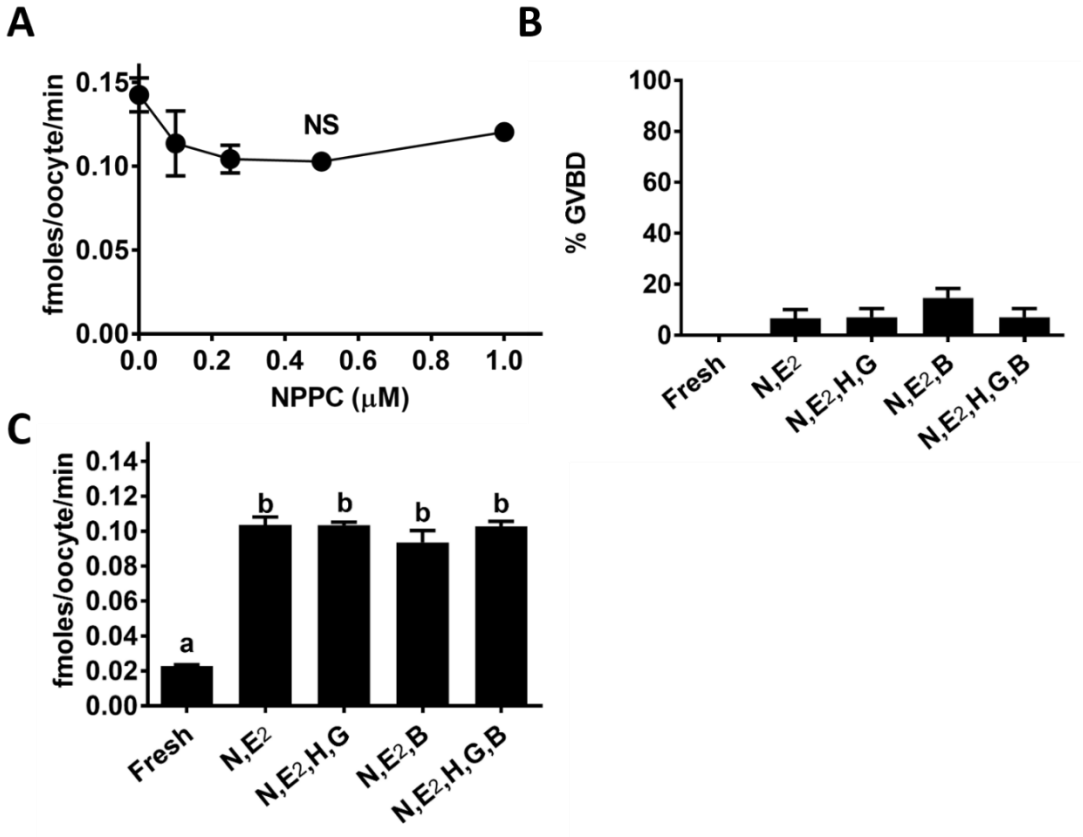

Figure 34. NPPC-cGMP signalling and GLYT1 activity in COCs. (A) COCs were cultured 4 hours in increased concentrations of NPPC (0-1 μM) and then GLYT1 activity was measured. Black circles represent the rate of GLYT1-mediated [^{3}H]-glycine uptake into oocytes (mean ± SEM, n=3-4). No significant difference between groups was measured by ANOVA and Tukey test. (**B, C**) COCs were cultured for 4 hours with various combinations of NPPC (N, 100 nM), estradiol (E_2, 100 nM), hypoxanthine (H, 4mM), guanosine (G, 50 μM), and BAY 73-6691 (B, 100 μM). (**B**) After the culture period, COCs were examined for meiotic resumption. Black bars represent the percentage of COCs which underwent GVBD. (**C**) After the culture period, GLYT1 activity was also measured. Black bars represent the rate of GLYT1-mediated [^{3}H]-glycine uptake as shown in

fmoles/oocyte/min. For both **B** and **C**, meiotic resumption and GLYT1 activity were also examined in freshly isolated COCs (fresh) as a control for meiotic arrest and GLYT1 suppression (mean ± SEM, n=3). Bars that do not share letters have significantly different means ($P < 0.05$ by ANOVA and Tukey test). (**C**) COCs were cultured 4 hours in increasing concentrations of NPPC (0-1 μM) and then GLYT1 activity was measured. Black circles represent the rate of GLYT1-mediated [^{3}H]-glycine uptake into oocytes (mean ± SEM, n=3-4). No significant difference between groups was measured by ANOVA and Tukey test. This figure was modified from the following publication: Richard S. & Baltz J.M. (2017). Preovulatory suppression of mouse oocyte cell volume-regulatory mechanisms is via signalling that is distinct from meiotic arrest. *Sci Rep*; 7(1):702.

cAMP degradation. Guanosine was added to culture medium since the presence of guanosine is essential to produce sufficient GMP to be converted to GTP and finally cGMP by NPR2 in the cumulus cells [Zhang et al. 2010; Wigglesworth et al. 2013]. PDE9A has been identified as the primary phosphodiesterase specific to cGMP in the mouse oocyte [Hanna et al. 2012]. The oocyte-specific PDE9A inhibitor BAY 73-6691 was therefore added to COC culture medium since this inhibitor was shown to augment the effects of synthetic cGMP on maintenance of meiotic arrest in denuded mouse oocytes, although BAY 73-6691 alone was unable to prevent spontaneous meiotic resumption in cultured oocytes [Hanna et al. 2012].

To maximize the production of cGMP to examine whether GLYT1 suppression could be maintained by the NPPC-cGMP signalling pathway, COCs were cultured for 4 hours in the presence of various combinations of the above-mentioned pharmacological agents that stimulate this pathway. After the culture period, oocytes were examined for the presence of meiotic resumption (GVBD) and GLYT1 activity was measured by [^{3}H]-glycine uptake. As a control for meiotic arrest and supressed GLYT1 activity, freshly isolated COCs were also examined for meiotic resumption and GLYT1 activity was measured. As expected, meiotic arrest was maintained in nearly all COCs under all culture conditions tested which did not significantly differ from freshly isolated COCs (Figure 34B). Low levels of GLYT1 activity were detected in freshly isolated COCs which became significantly increased over the 4-hour culture period even when COCs were cultured with any of the tested combinations of NPPC, E_2, hypoxanthine, guanosine, and BAY 73-6691 (Figure 34C).

4.2 Gap junction inhibition causes GLYT1 activation in cultured antral follicles but it is substantially delayed compared to meiotic resumption.

To examine the dependence of GLYT1 suppression on gap junctional communication, both COCs (0-4 hours) and punctured antral follicles (0-10 hours) were cultured with or without the general gap junction inhibitor AGA (150 µM) and oocytes were then examined for meiotic resumption (GVBD) and GLYT1 activation. Punctured antral follicles were used since I previously showed that gap junction inhibition was faster in punctured, compared to intact, antral follicles and I sought to inhibit gap junctions as quickly as possible to most accurately examine the timing of meiotic resumption and GLYT1 activation immediately after gap junction inhibition. COCs that were cultured 0-4 hours in the presence of AGA significantly resumed meiosis by 2 hours with the maximum percentage of COCs undergoing GVBD by 3 hours; meiotic arrest was maintained in nearly all COCs cultured without AGA for up to 4 hours (Figure 35A). Punctured follicles cultured 0-10 hours in the presence of AGA significantly resumed meiosis by 3 hours with ~80% of oocytes resuming meiosis compared to punctured antral follicles cultured in the absence of AGA which maintained meiotic arrest throughout the 10-hour culture period (Figure 35B). Therefore, meiotic resumption (GVBD) was delayed by ~1 hour in punctured antral follicles compared to COCs following gap junction inhibition, likely due to the additional time required for AGA to diffuse throughout the antral follicle.

As expected, when I measured GLYT1 activity in COCs cultured for 0-4 hours no significant difference was detected in COCs cultured with or without AGA (Figure 35C). As shown in the previous GLYT1 activity time-course (Figure 30B), GLYT1 became

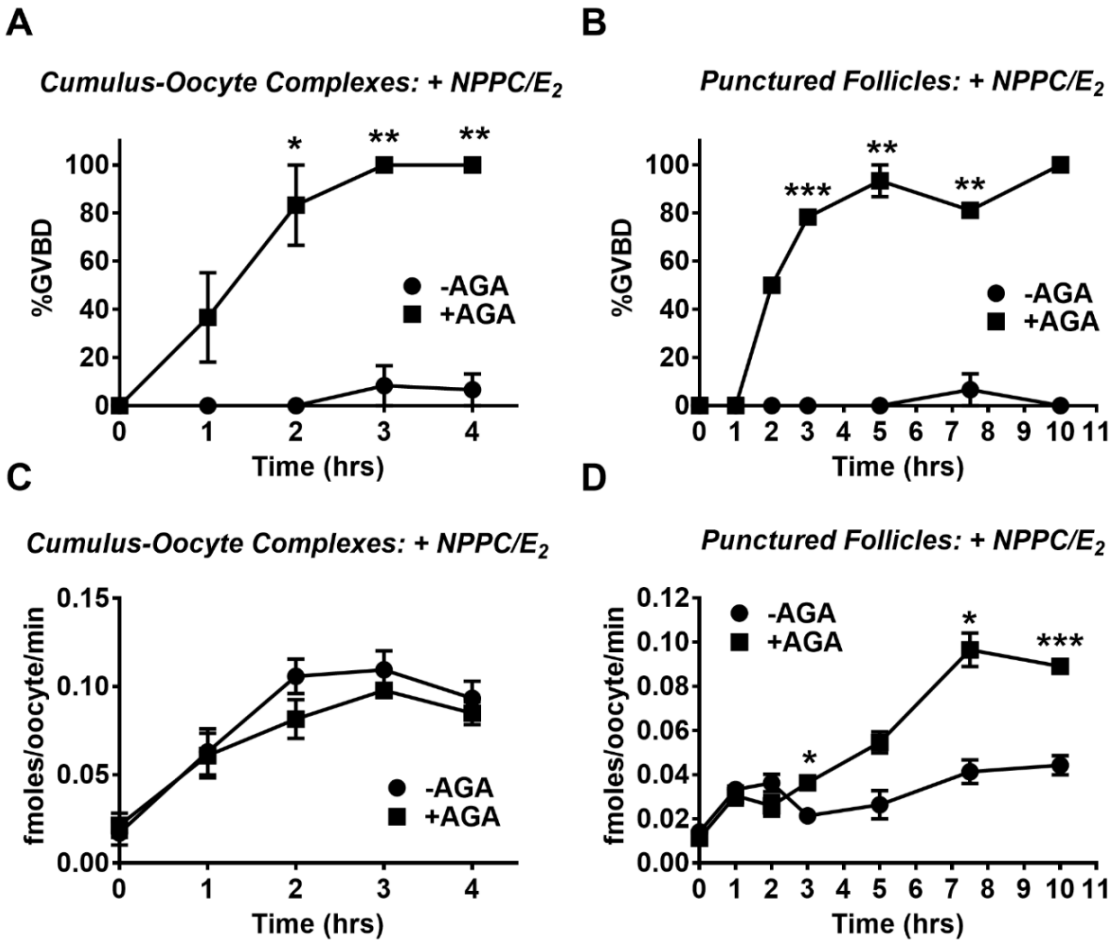

Figure 35. A time-course of general gap junction inhibition in COCs and punctured antral follicles: meiotic resumption and GLYT1 activity. (**A**) **Meiotic resumption in COCs.** COCs were cultured for 0-4 hours in the presence (squares) or absence (circles) of AGA (150 μM) and then meiotic resumption (% GVBD) was examined. COCs were maintained in meiotic arrest during culture with NPPC (100 nM) and E_2 (100 nM) (mean ± SEM, n=3). (**B**) **Meiotic resumption in punctured antral follicles.** Punctured antral follicles were cultured for 0-10 hours in the presence (squares) or absence (circles) of AGA and then examined for meiotic resumption (% GVBD). NPPC (100 nM) and E_2 (100 nM)

was added to medium for the duration of culture to maintain meiotic arrest (mean ± SEM, n=3). (**C**) **GLYT1 activation in COCs.** COCs were cultured for 0-4 hours in the presence (squares) or absence (circles) of AGA and then GLYT1 activity was measured as the rate of [^{3}H]-glycine uptake shown in fmoles/oocyte/min (mean ± SEM, n=3). (**D**) **GLYT1 activation in punctured antral follicles.** Punctured antral follicles were cultured for 0-10 hours in the presence (squares) or absence (circles) of AGA and then GLYT1 activity was measured as the rate of [^{3}H]-glycine uptake shown in fmoles/oocyte/min (mean ± SEM, n=3). For **A**-**D**, differences between means in the presence or absence of AGA for each time point was measured by Student *t*-test (*P< 0.05, **P < 0.01, ***P < 0.001). This figure was reproduced from the following publication: Richard S. & Baltz J.M. (2017). Preovulatory suppression of mouse oocyte cell volume-regulatory mechanisms is via signalling that is distinct from meiotic arrest. *Sci Rep*; 7(1):702. This article is licensed under a Creative Commons Attribution 4.0 International License. © Richard S. & Baltz J.M. 2017.

spontaneously activated in COCs and was fully active by ~2-3 hours. When punctured antral follicles were cultured in the absence of AGA, GLYT1 suppression was maintained for up to 10 hours. In contrast, GLYT1-mediated [^{3}H]-glycine uptake was significantly greater in punctured antral follicles cultured with AGA beginning at 7.5 hours, representing a delay of ~5 hours from when meiotic resumption occurred in punctured antral follicles cultured in the presence of the gap junction inhibitor (Figure 35D).

To further confirm the timing of meiotic resumption and GLYT1 activation following gap junction inhibition, punctured antral follicles were cultured in medium alone, with Cx43 CMP (600 µM), or with scrambled peptide (600 µM) for 0-20 hours and then isolated oocytes were examined for meiotic resumption (GVBD) and GLYT1-mediated [^{3}H]-glycine uptake was measured. Culture medium was supplemented with NPPC (100 nM) and E_2 (100 nM) to maintain meiotic arrest. Meiotic resumption of punctured follicles cultured with Cx43 CMP was significantly increased by 10 hours in culture with ~70% of oocytes undergoing GVBD which increased to ~80% by 12 hours and ~85% by 20 hours (Figure 36A). In contrast, GLYT1 activity was only slightly increased at 16 hours in punctured follicles cultured with Cx43 CMP compared to follicles cultured without CMP or with scrambled peptide (Figure 36B). GLYT1 activity continued to increase during culture and was greatest at 20 hours. Therefore, similar to general gap junction inhibitors, meiotic resumption and GLYT1 activation occurred in punctured follicles cultured with Cx43 CMP and again GLYT1 activation was delayed compared to meiotic resumption by at least 6 hours. These results further support the hypothesis that maintenance of GLYT1 suppression in ovarian follicles is not dependent on gap junctional communication between granulosa cells.

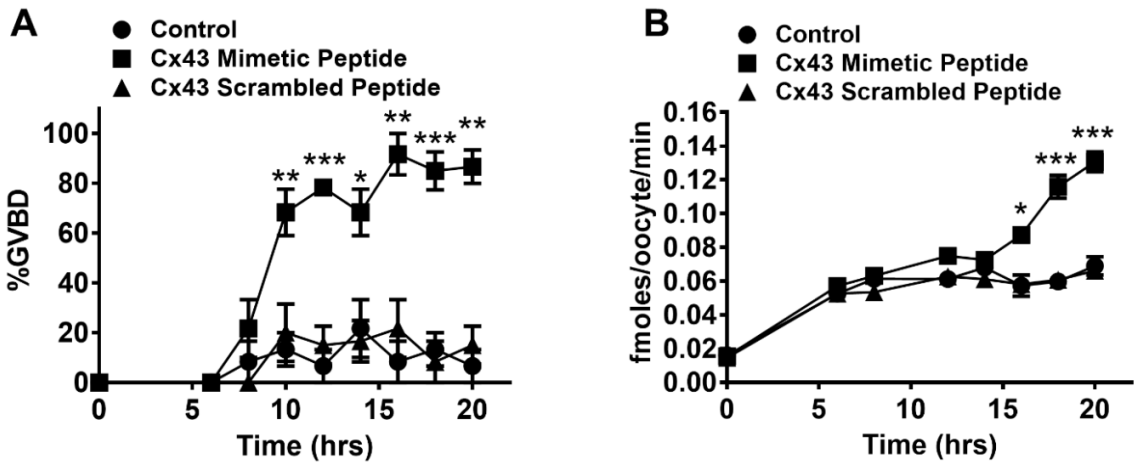

Figure 36. Isoform-specific gap junction inhibition in punctured antral follicles. (**A**) Punctured antral follicles were cultured 0-20 hours without CMP (circles), with Cx43 CMP (squares, 600 µM), or with Cx43 scrambled peptide (triangles, 600 µM) and then examined for meiotic resumption (% GVBD) (mean ± SEM, n=3). (**B**) Punctured antral follicles were cultured 0-20 hours without CMP (circles), with Cx43 CMP (squares, 600 µM), or with Cx43 scrambled peptide (triangles, 600 µM) and then the rate of [^{3}H]-glycine uptake was measured as shown in fmoles/oocyte/min. (mean ± SEM, n=3). For both **A** and **B**, differences between means for each time point were measured by Student *t*-test (*P< 0.05, **P < 0.01, ***P < 0.001). This figure was reproduced from the following publication: Richard S. & Baltz J.M. (2017). Preovulatory suppression of mouse oocyte cell volume-regulatory mechanisms is via signalling that is distinct from meiotic arrest. *Sci Rep*; 7(1):702. This article is licensed under a Creative Commons Attribution 4.0 International License. © Richard S. & Baltz J.M. 2017.

5. Mural granulosa cells (MGCs) or extracellular matrix are sufficient to maintain GLYT1 suppression in COCs.

Although GLYT1 suppression appears to be under the control of signalling distinct from the signalling pathway mediating meiotic arrest, I hypothesized that it is governed by an analogous inhibitory mechanism involving multiple cell types within the antral follicle. That GLYT1 suppression can be maintained in cultured antral follicles but not denuded oocytes or COCs suggests that mural granulosa cells (MGCs) may be required for putative GLYT1 inhibitory signalling within the follicle prior to ovulation. To further determine the involvement of MGCs on GLYT1 suppression, I sought to develop a MGC culture methodology with which COCs and denuded oocytes could be co-cultured on a monolayer of MGCs and GLYT1 activity subsequently measured. Interestingly, during the development of the MGC culture methodology, I discovered that in addition to MGCs, ECL Matrix isolated from Engelbreth-Holm-Swarm (EHS) mouse tumor (Millipore; EHS Matrix) and certain purified extracellular matrix components (EMs) alone could maintain transient GLYT1 suppression in cultured COCs. This effect allowed for manipulations to be performed to begin addressing questions regarding GLYT1 suppression including, but not limited to, which cell types participate in GLYT1 suppression and whether GLYT1 suppression can be sustained when meiotic resumption is allowed to proceed.

EMs and MGC monolayers allowed us for the first time to prevent the spontaneous GLYT1 activation in COCs that occurs after their isolation from ovarian follicles.

5.1 Mural granulosa cells (MGCs) maintain GLYT1 suppression in cultured COCs.

I found in the above experiments that GLYT1 spontaneously activates in denuded oocytes and COCs in culture but that GLYT1 suppression can be maintained in cultured antral follicles (Figure 30). This result suggests that MGCs may play a role in the inhibitory signalling mechanism preventing GLYT1 activation in antral follicles before ovulation.

To obtain a uniform MGC monolayer, plastic culture wells (96-well dish) were first pre-coated with purified collagen IV (50 µg/ml) for 2 hours prior to adding the MGC suspension to the well. As shown previously, MGCs formed aggregates when plated on plastic alone (Figure 37A) and lost their phenotype [Lee et al. 2013] and I found that normal GLYT1 activation occurred in COCs cultured on MGCs plated on plastic that were maintained in meiotic arrest with NPPC and E_2 (Figure 37C, D) [Carnegie et al. 1988; Ben-Rafael et al. 1988; Sites et al. 1996]. Collagen IV acts as an adhesive surface for cells to bind and has been used previously in cell culture [Fitzgerald et al. 1984; el Khoury et al. 1994; Warfield et al. 1997]. MGCs were isolated from ~50 antral follicles and the MGC suspension (~50µl) was plated over the pre-coated collagen IV culture well and incubated overnight. After the overnight incubation, a uniform MGC monolayer was observed. COCs were then added to the well and cultured 4 hours (Figure 37B).

Additional COCs were cultured on uncoated plastic culture wells or on collagen IV-coated wells without MGCs to determine whether collagen IV alone had an effect on GLYT1 activation. COCs were cultured on plastic alone (-), on collagen IV alone (CIV), or on the MGC monolayer (CIV+MGC), all in the presence of NPPC (100 nM) and E_2 (100 nM) to maintain meiotic arrest. After the culture period, COCs were tightly adhered to the

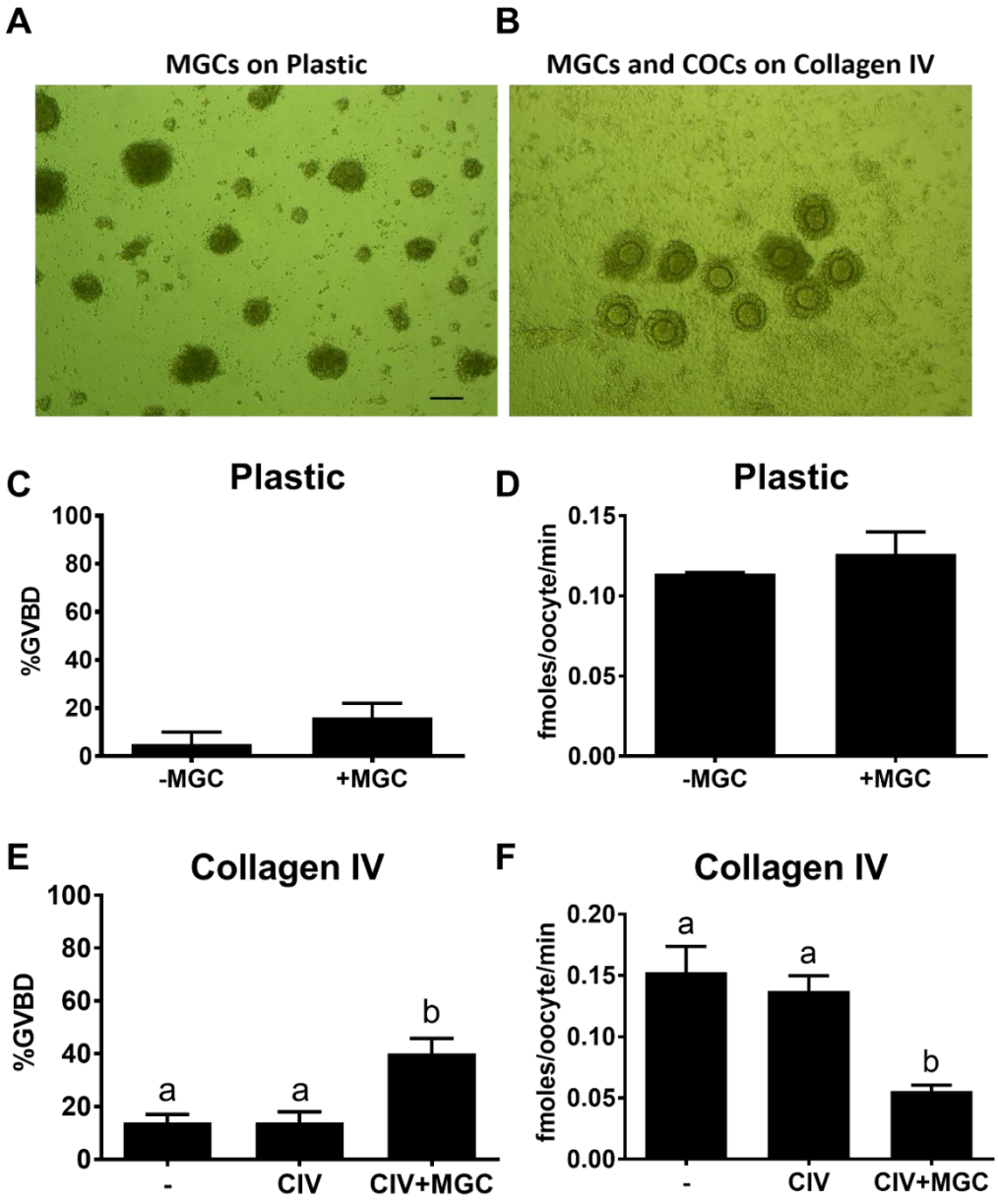

Figure 37. Mural granulosa cell (MGC) culture on plastic and EHS Matrix: the effect on GLYT1 activity in COCs. (**A**) A MGC suspension was plated in a plastic culture well (96-well dish) and incubated overnight. After the overnight culture, an image of the MGC culture was taken using a Nikon E4500 camera mounted on a Zeiss Axiovert microscope. (**B**) A MGC suspension was plated in a plastic culture well (96-well dish) pre-coated with

collagen IV and then incubated overnight. After the overnight culture COCs were added to the MGC monolayer and cultured for 4 hours. An image is shown of the MGC monolayer with COCs plated on top of the monolayer taken with a Nikon E4500 camera mounted on a Zeiss Axiovert microscope. The scale bar in **A** represents 100 µm and also applies to **B**. (**C, D**) COCs were cultured in an uncoated plastic culture well without MGCs (-MGC) or with MGCs (+MGC) and cultured 4 hours in the presence of NPPC (100 nM) and E_2 (100 nM) to maintain meiotic arrest. (**C**) Black bars represent the percentage of COCs that resumed meiosis (% GVBD) in the presence (+MGC) or absence (-MGC) of MGC aggregates (mean ± SEM, n=2). (**D**) Black bars represent the rate of GLYT1-mediated [^{3}H]-glycine uptake into oocytes cultured on plastic alone or with MGC aggregates as shown in fmoles/oocyte/min (mean ± SEM, n=2). (**E, F**) COCs were cultured 4 hours in a plastic culture well with no coating (-), in a well pre-coated with collagen IV (CIV), or in a well pre-coated with collagen IV and containing a MGC monolayer (CIV+MGC). NPPC (100 nM) and E_2 (100 nM) were added to culture medium to maintain meiotic arrest. (**E**) Black bars represent the percentage of COCs that resumed meiosis (% GVBD) (mean ± SEM, n=3). Bars that do not share letters have significantly different means ($P < 0.05$ by ANOVA and Tukey test). (**F**) Black bars represent the rate of GLYT1-mediated [^{3}H]-glycine uptake into oocytes as shown in fmoles/oocyte/min (mean ± SEM, n=3). Bars that do not share letters have significantly different means ($P < 0.05$ for **CIV** vs **CIV+MGC** and $P < 0.01$ for **–** vs **CIV+MGC** by ANOVA and Tukey test). This figure was reproduced from the following publication: Richard S. & Baltz J.M. (2017). Preovulatory suppression of mouse oocyte cell volume-regulatory mechanisms is via signalling that is distinct from

meiotic arrest. *Sci Rep*; 7(1):702.

MGC monolayer and had to be gently detached using a pulled Pasteur pipette; no obvious adherence of COCs to the plastic culture well was observed in the presence or absence (in the previous experiment) of MGCs.

Meiotic arrest was maintained in nearly all COCs cultured on plastic alone (-) or on collagen IV-coated wells (CIV) as determined by the presence of an intact GV (Figure 37E). Meiotic resumption occurred in ~40% of COCs cultured on the MGC monolayer (CIV+MGC) which was significantly greater than COCs cultured in the absence of MGCs. However, this effect was only slightly significant and may be attributable to high NPPC concentrations within the culture medium due to the combination of NPPC being added to medium and NPPC secretion by MGCs; I showed previously that COCs resumed meiosis in the presence of very high NPPC levels (Figure 21A). GLYT1 activation occurred normally in COCs cultured in uncoated plastic culture wells which did not significantly differ from GLYT1 activity in COCs cultured in culture wells pre-coated with collagen IV, suggesting that collagen IV has no effect on GLYT1 activity. In contrast, GLYT1 was significantly suppressed in COCs cultured in collagen IV-coated culture wells with the MGC monolayer (Figure 37F).

As discussed in the introduction to this thesis, NPPC is secreted by MGCs in the antral follicle into the follicular fluid where it binds its cognate NPR2 receptor on cumulus granulosa cells to increase the production of cGMP which maintains meiotic arrest within the oocyte [Zhang et al. 2010]. The mechanisms regulating the differential levels of *Nppc* mRNA in MGCs compared to cumulus granulosa cells remains unknown, however it is clear that *Nppc* expression is greatest in MGCs and is hormonally regulated [Lee et al. 2013]. Previous attempts to culture MGCs by John Eppig's laboratory in the absence of

extracellular matrix components showed decreasing *Nppc* expression levels detected in MGCs during culture which was hypothesized to occur due to MGCs being non-viable or lacking hormonal stimulation [Lee et al. 2013]. It was found that *Nppc* expression was increased 20-fold in cultured MGCs plated on extracellular matrix in the presence of E_2 (100 nM) and FSH (5 ng/ml) compared to MGCs plated on extracellular matrix in the absence of hormones [Lee et al. 2013].

My MGC culture methodology was based on the results obtained from the experiments by Lee et al [2013] and thus all culture medium was supplemented with E_2 (100 nM) and FSH (5 ng/ml). Since *Nppc* expression was shown to increase under these conditions, I sought to determine whether meiotic arrest and GLYT1 suppression could also be maintained when culture medium was not supplemented with additional NPPC. MGC isolation and COC culture was performed identically to the previous experiments except that NPPC was omitted from culture medium. Interestingly, although meiotic resumption occurred in COCs cultured in uncoated plastic culture wells (-) and in culture wells pre-coated with collagen IV (CIV), meiotic arrest was significantly maintained in COCs cultured in collagen IV-coated wells on a monolayer of MGCs (CIV+MGC) (Figure 38A). In addition, the effect of omitting NPPC from culture medium on GLYT1 activation in COCs was examined. Similar to COCs cultured in the presence of NPPC added to culture medium, spontaneous GLYT1 activation occurred in oocytes from COCs cultured in uncoated plastic culture wells (-) and in collagen IV-coated culture wells in the absence of NPPC while GLYT1 suppression was maintained when COCs were cultured in collagen IV-coated culture wells on a MGC monolayer in the absence of NPPC (Figure 38B).

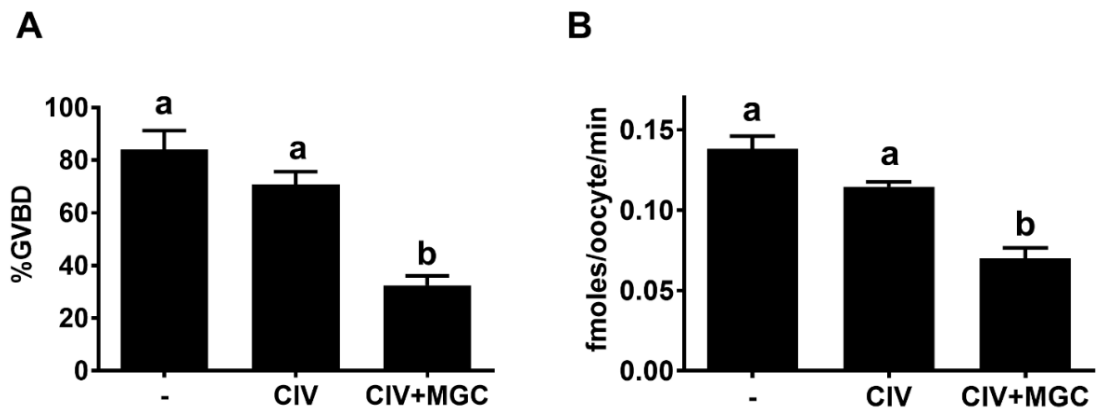

Figure 38. GLYT1 suppression and meiotic arrest by MGCs <u>without</u> NPPC added to culture medium. COCs were cultured 4 hours in uncoated plastic culture wells (-), in culture wells pre-coated with collagen IV (CIV), or in culture wells pre-coated with collagen IV and with MGCs (CIV+MGC). NPPC was <u>not</u> added to culture medium. (**A**) Meiotic resumption was examined in COCs after the culture period (mean ± SEM, n=5). Black bars represent the percentage of oocytes that resumed meiosis (% GVBD). Bars that do not share letters have significantly different means ($P < 0.001$ by ANOVA and Tukey test). (**B**) GLYT1 activity was measured in oocytes after removal from COCs (mean ± SEM, n=5). Black bars represent the rate of GLYT1-mediated [^{3}H]-glycine uptake as shown in fmoles/oocyte/min. Bars that do not share letters have significantly different means ($P < 0.001$ by ANOVA and Tukey test). This figure was reproduced from the following publication: Richard S. & Baltz J.M. (2017). Preovulatory suppression of mouse oocyte cell volume-regulatory mechanisms is via signalling that is distinct from meiotic arrest. *Sci Rep*; 7(1):702. This article is licensed under a Creative Commons Attribution 4.0 International License.

These results suggest that my MGC culture methodology maintains healthy MGCs in a monolayer culture capable of secreting the factors involved in the maintenance of meiotic arrest (i.e., NPPC) and GLYT1 suppression. Additionally, the ability of MGCs (but not plastic or collagen IV alone) to maintain GLYT1 suppression in cultured COCs for at least 4 hours supports my hypothesis that MGCs are required to maintain GLYT1 suppression in antral follicles prior to ovulation. To determine whether a soluble or secreted factor from MGCs is sufficient to maintain GLYT1 suppression in cultured COCs, culture medium was collected following a 24-hour culture period from plastic culture wells containing medium alone (-), collagen IV-coated culture wells containing medium (CIV), or collagen IV-coated wells containing medium and a MGC monolayer (CIV+MGC). Collected medium (~50 µl) was transferred to uncoated plastic culture wells and COCs were incubated in the various collected medium for 4 hours and then oocytes were examined for meiotic resumption (GVBD) and GLYT1 activity was measured; NPPC (and E_2) was present in all collected medium to maintain meiotic arrest in COCs during culture. As expected, meiotic arrest was maintained in ~80% of COCs regardless of the medium tested (Figure 39A). GLYT1 activation occurred normally in COCs cultured in medium collected from plastic culture wells alone (-) and from collagen IV-coated culture wells alone (CIV), however, GLYT1 activity was significantly suppressed in COCs cultured in conditioned medium collected from collagen IV-coated culture wells with a MGC monolayer (CIV+MGC) suggesting that a factor secreted into the culture medium from MGCs may be involved in maintaining suppressed GLYT1 activity in the ovarian follicle (Figure 39B).

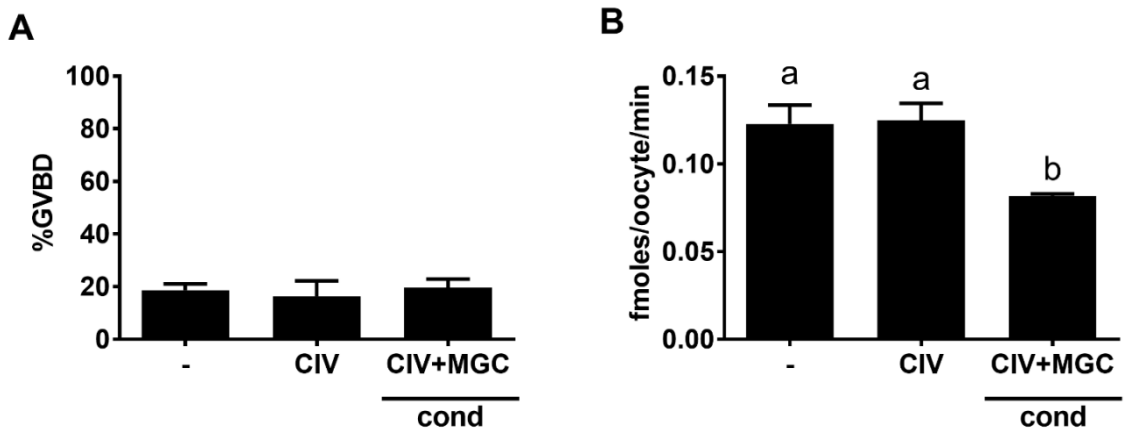

Figure 39. MGC-conditioned medium and GLYT1 suppression in COCs.

Medium was collected following a 24-hour culture period from plastic culture wells containing medium alone (-), from collagen IV-coated culture wells containing medium alone (CIV), or from collagen IV-coated culture wells containing a monolayer of MGCs (CIV+MGC). Collected medium was transferred to additional plastic culture wells and COCs were cultured in the various collected medium for 4 hours. (**A**) Meiotic resumption was examined in COCs after the culture period (mean ± SEM, n=3). Black bars represent the percentage of oocytes that resumed meiosis (% GVBD). No significant difference between groups was found by ANOVA and Tukey test (P=0.7648). (**B**) GLYT1 activity was measured in oocytes after removal from COCs (mean ± SEM, n=3). Black bars represent the rate of GLYT1-mediated [^{3}H]-glycine uptake as shown in fmoles/oocyte/min. Bars that do not share letters have significantly different means (*P < 0.05 by ANOVA and Tukey test). This figure was reproduced from the following publication: Richard S. & Baltz J.M. (2017). Preovulatory suppression of mouse oocyte cell volume-regulatory mechanisms is via signalling that is distinct from meiotic arrest. *Sci Rep*; 7(1):702. This

5.2 EHS Matrix suppresses GLYT1 activity in cultured COCs.

Preliminary experiments for the development of the MGC culture methodology involved using ECL Matrix© (Millipore Cat# 08-110) isolated from Engelbreth-Holm-Swarm (EHS) mouse (EHS Matrix) tumor as a coating surface based on the methodology by Lee and colleagues [Lee et al. 2013]. Prior to adding a MGC suspension to culture wells coated with EHS Matrix, COCs were first cultured with or without the EHS Matrix to determine whether EHS Matrix alone exerted any effect on GLYT1 activity. COCs were cultured for either 4 or 20 hours in uncoated plastic culture wells or in plastic culture wells pre-coated with EHS Matrix (50 μg/ml) in the presence of NPPC and E_2 to maintain meiotic arrest. After the specified culture period, maintenance of meiotic arrest was confirmed in COCs by examining GVBD and GLYT1 activity was measured by [^{3}H]-glycine uptake. As expected, meiotic arrest was maintained in nearly all COCs cultured 4 or 20 hours regardless of the coating material since NPPC and E_2 were present in medium (Figure 40A, C). Surprisingly however, GLYT1 activity was significantly suppressed in COCs cultured 4 hours on EHS Matrix-coated wells compared to COCs cultured on plastic alone (Figure 40B). This effect appeared to be somewhat transient since GLYT1 activity increased by 20 hours on EHS Matrix but was still significantly less than in COCs cultured without the EHS Matrix-coating (Figure 40D). It was possible that this effect of EHS Matrix on GLYT1 activity in COCs was merely an artifact. Therefore, additional experiments were performed to examine whether normal GLYT1 activation could occur in COCs after removal from the EHS Matrix and if additional EHS Matrix brands could exert the same effect on GLYT1 activity in COCs.

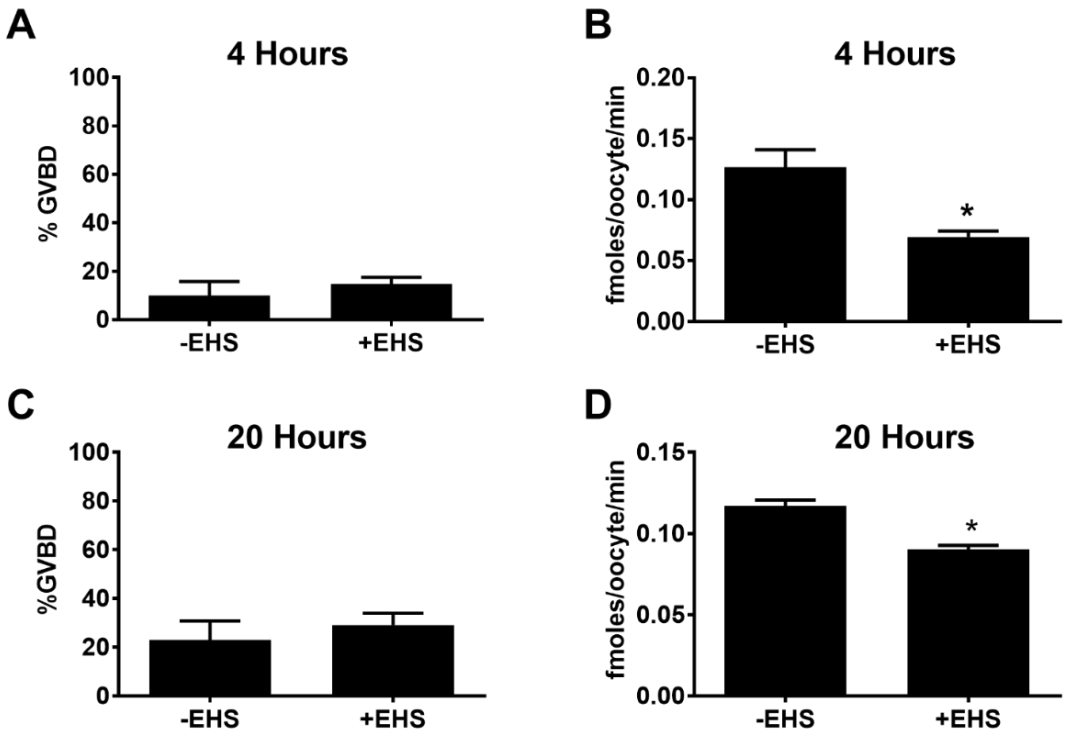

Figure 40. Suppression of GLYT1 in COCs cultured 4 or 20 hours on EHS Matrix.

COCs were cultured 4 or 20 hours in uncoated plastic culture wells (-EHS) or in plastic culture wells pre-coated with EHS Matrix (+ECL, 50 µg/ml) isolated from Engelbreth-Holm-Swarm (EHS) mouse tumor (Millipore). NPPC (100 nM) and E_2 (100 nM) were added to culture medium to maintain meiotic arrest in COCs. (**A**) Meiotic resumption of COCs cultured 4 hours with or without EHS Matrix. Black bars represent the percentage of COCs that underwent GVBD (mean ± SEM, n=3). No significant difference was found between means by Student *t*-test. (**B**) GLYT1 activity in COCs cultured 4 hours with or without EHS Matrix. Black bars represent the rate of GLYT1-mediated [^{3}H]-glycine uptake as shown in fmoles/oocyte/min (mean ± SEM, n=3). Differences between means were examined by Student *t*-test (*$P < 0.05$). (**C**) COCs were cultured 20 hours with or

without EHS Matrix. Black bars represent the percentage of COCs that underwent GVBD (mean ± SEM, n=3). No significant difference was found between means by Student *t*-test. (**D**) GLYT1 activity in COCs cultured 4 hours with or without EHS Matrix. Black bars represent the rate of GLYT1-mediated [^{3}H]-glycine uptake as shown in fmoles/oocyte/min (mean ± SEM, n=3). Differences between means were examined by Student *t*-test ($P < 0.05$).

To determine if normal GLYT1 activation could occur in COCs after culture on EHS Matrix, COCs were first cultured 4 hours in uncoated plastic culture wells (-EHS) or in EHS Matrix-coated wells (+EHS) and GLYT1 activity was measured in half of the COCs from each group by a [^{3}H]-glycine uptake experiment. The other half of the COCs cultured with or without EHS Matrix were cultured for an additional 4 hours in uncoated plastic culture wells (no EHS Matrix) and then GLYT1 activity was again measured. Meiotic arrest was maintained under all conditions throughout the culture period by NPPC and E_2.

Meiotic arrest was successfully maintained in nearly all COCs cultured with or without EHS Matrix coating for both culture periods (Figure 41A). For the initial 4-hour culture period, GLYT1 activity was again found to be suppressed in COCs cultured in EHS Matrix-coated culture (+EHS) wells compared to COCs cultured in uncoated plastic culture wells (-EHS) (Figure 41B). Normal GLYT1 activation occurred in COCs following transfer from EHS Matrix-coated plastic wells to uncoated plastic wells for the additional 4-hour culture period which did not significantly differ from COCs that were cultured in uncoated wells for the entire culture duration. Thus, normal GLYT1 activation occurs in COCs following EHS Matrix-mediated maintenance of GLYT1 suppression for at least 4 hours.

To further confirm the ability of EHS Matrix to maintain GLYT1 suppression in COCs, another EHS Matrix brand (Corning Matrigel©, Cat# 356234) also isolated from Engelbreth-Holm-Swarm (EHS) mouse tumor was used as a coating matrix. To determine whether growth factors present in EHS Matrix could be involved in the GLYT1 suppression measured in COCs, a growth factor-reduced (GFR) EHS Matrix (Corning

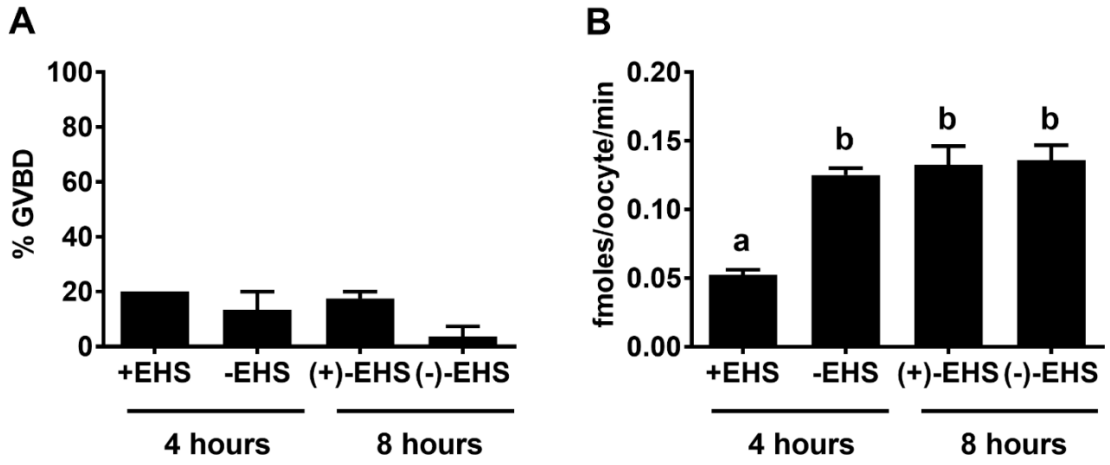

Figure 41. Reversibility of GLYT1 suppression by EHS Matrix in COCs. COCs were cultured 4 hours in EHS Matrix-coated culture wells (+EHS) or in uncoated plastic culture wells (-EHS). After the initial 4-hour culture period, meiotic resumption and GLYT1 activity were examined in half of COCs and the other half of COCs from each group were cultured an additional 4 hours in uncoated plastic culture wells. COCs cultured on EHS Matrix for the first culture period and plastic for the second culture period are labelled as (+)-EHS while COCs cultured for the first and second culture period on plastic alone are labelled as (-)-EHS. NPPC (100 nM) and E_2 (100 nM) were added to all culture groups to maintain meiotic arrest. (**A**) Black bars represent the percentage of COCs that resumed meiosis (% GVBD) (mean ± SEM, n=3). No significant difference between means of all groups was detected by ANOVA with Tukey test. (**B**) Black bars represent the rate of GLYT1-mediated [^{3}H]-glycine uptake as shown in fmoles/oocyte/min (mean ± SEM, n=3). Bars that do not share letters have significantly different means ($P < 0.01$ by ANOVA with Tukey test).

Matrigel©, Cat# 356230) was also used as a coating matrix. COCs were cultured 4 hours in uncoated plastic culture wells (-), in EHS Matrix-coated culture wells (Millipore, EHS), in Matrigel©-coated culture wells (Corning, Mat), or in growth factor-reduced Matrigel©-coated culture wells (Mat(GFR)). NPPC and E_2 were added to the culture medium in all groups to maintain meiotic arrest throughout the culture period.

Meiotic arrest was maintained in 80-90% of COCs in all culture groups as confirmed by the presence of an intact GV (Figure 42A). In the absence of any coating matrix, normal GLYT1 activation occurred in COCs over the 4-hour culture period (Figure 42B). In contrast, GLYT1 activity was significantly lower in COCs cultured in EHS Matrix-coated wells (Millipore) as shown in the previous experiments. Interestingly, GLYT1 was also significantly suppressed in COCs cultured on both normal Matrigel© and GFR Matrigel© from Corning, although somewhat less effectively than EHS Matrix from Millipore (Figure 42B). These results further support the ability of ECM from Engelbreth-Holm-Swarm (EHS) mouse tumor to maintain GLYT1 suppression in COCs and suggest that growth factors known to be present in EHS Matrix such as EGF, PDGF, and TGF-β are at least not solely responsible for the low GLYT1 activity measured [Vukicevic et al. 1992].

5.3 EHS Matrix does not maintain GLYT1 suppression in denuded oocytes in the presence or absence of COCs.

Since EHS Matrix (Millipore and Corning) maintained GLYT1 suppression in COCs, it was of interest to examine whether GLYT1 suppression in oocytes was possible

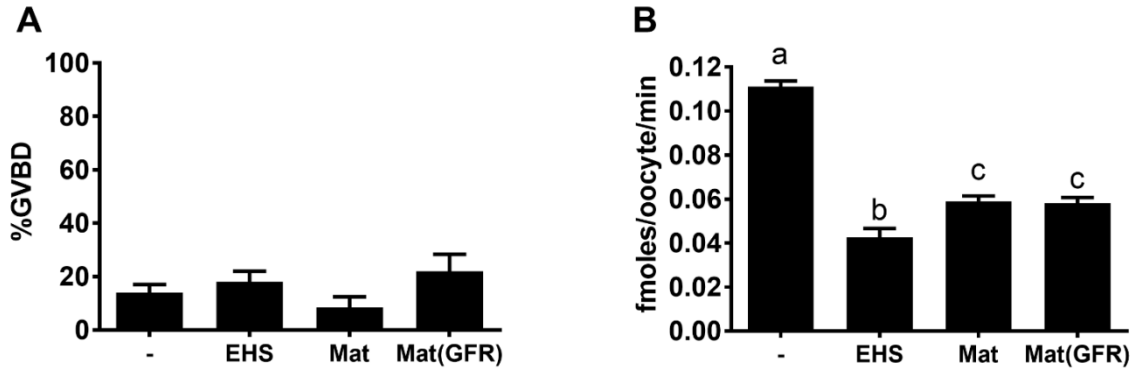

Figure 42. GLYT1 suppression by multiple brands of extracellular matrix derived from EHS cells. COCs were cultured 4 hours in uncoated plastic culture wells (-), in EHS Matrix-coated culture wells (EHS, Millipore), in Matrigel©-coated culture wells (Mat, Corning), or in growth factor-reduced Matrigel©-coated culture wells (Mat(GFR)). NPPC and E_2 were added to culture medium to maintain meiotic arrest. (**A**) Black bars represent the percentage of COCs that resumed meiosis (% GVBD) (mean ± SEM, n=3). No significant difference between means was measured under any conditions by ANOVA with Tukey test. (**B**) Black bars represent the rate of GLYT1-mediated [^{3}H]-glycine uptake as shown in fmoles/oocyte/min (mean ± SEM, n=3). Bars that do not share letters have significantly different means ($P < 0.0001$ for a vs b,c; $P < 0.05$ for b vs c).

without cumulus granulosa cells present. To determine whether EHS Matrix could maintain low GLYT1 activity in oocytes alone, denuded GV oocytes were cultured 4 hours in uncoated plastic culture wells (-EHS) or in EHS Matrix-coated culture wells (+EHS). No reagents to maintain meiotic arrest were added to the culture medium. Meiotic resumption occurred in ~80% of denuded oocytes when cultured in uncoated plastic culture wells (-EHS) or in EHS Matrix-coated culture wells (+EHS) (Figure 43A). This confirms that EHS Matrix alone does not prevent meiotic resumption from occurring in denuded GV oocytes. GLYT1 activation also occurred in denuded oocytes with no significant difference in the rate of [^{3}H]-glycine uptake in oocytes cultured in uncoated wells (-EHS) compared to EHS Matrix-coated wells (+EHS) (Figure 43B). This experiment was also performed with dbcAMP added to culture medium to maintain meiotic arrest and again GLYT1 suppression was not detected in denuded GV oocytes cultured with or without EHS Matrix (Figure 43C, D). Based on these results, EHS Matrix does not maintain meiotic arrest or GLYT1 suppression in denuded oocytes stripped of cumulus cells.

Since GLYT1 suppression was maintained in COCs, but not denuded oocytes, cultured on EHS Matrix I next sought to determine whether the introduction of cumulus cells into the culture medium could enable maintenance of GLYT1 suppression in denuded oocytes co-cultured with COCs. To examine this possibility, COCs and denuded oocytes were cultured alone or were co-cultured together for 4 hours in EHS Matrix-coated wells and then GLYT1 activity was measured for each culture condition by [^{3}H]-glycine uptake. NPPC, the physiological mediator of meiotic arrest, was added to culture medium to sustain meiotically-arrested COCs with functional gap junctions for the duration of culture. As

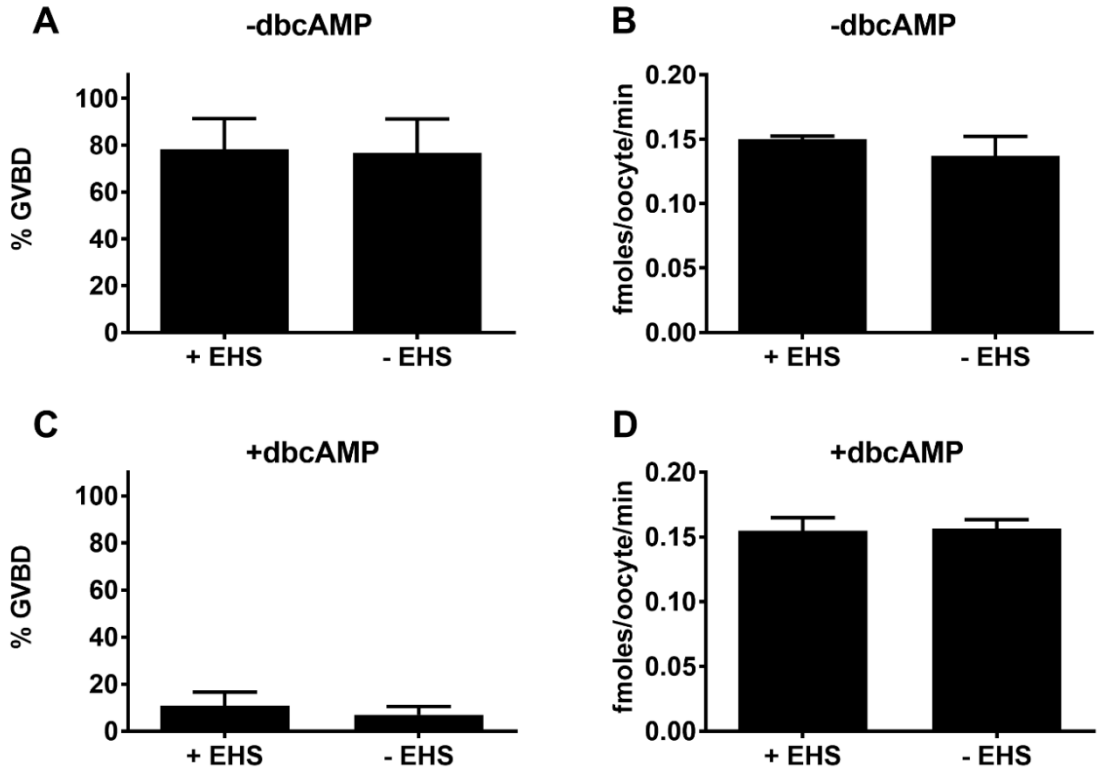

Figure 43. GLYT1 activity in denuded oocytes cultured on EHS Matrix.

Denuded GV oocytes were cultured 4 hours in uncoated plastic culture wells (-EHS) or in EHS Matrix-coated (Millipore) culture wells (+EHS) with or without dbcAMP (300 µM). (**A**) Black bars represent the percentage of oocytes that resumed meiosis in the absence of dbcAMP (% GVBD) (mean ± SEM, n=3). (**B**) Black bars represent the rate of GLYT1-mediated [^{3}H]-glycine uptake into oocytes cultured without dbcAMP as shown in fmoles/oocyte/min (mean ± SEM, n=3). (**C**) Black bars represent the percentage of oocytes that resumed meiosis in the presence of dbcAMP (% GVBD) (mean ± SEM, n=3). (**D**)Black bars represent the rate of GLYT1-mediated [^{3}H]-glycine uptake into oocytes cultured with dbcAMP as shown in fmoles/oocyte/min (mean ± SEM, n=3). For **A-D**, no significant difference between means in oocytes cultured with or without EHS Matrix or

with or without dbcAMP was measured by ANOVA with Tukey test for meiotic resumption or GLYT1 activity.

expected under these culture conditions, meiotic arrest was maintained in COCs characterized by the presence of an intact GV while meiotic resumption occurred in denuded oocytes which underwent GVBD (Figure 44A). When COCs were cultured alone (COC) or in the presence of denuded oocytes (COC(+D)), GLYT1 suppression was maintained on EHS Matrix (Figure 44B). In contrast, GLYT1 spontaneously activated in denuded oocytes when cultured alone (D) which did not significantly differ from GLYT1 activity measured in denuded oocytes cultured in the presence of COCs (D(+COC)) (Figure 44B). Therefore, the addition of cumulus cells in the form of COCs did not prevent GLYT1activation from occurring in denuded oocytes when cultured on EHS Matrix, while GLYT1 suppression was maintained in COCs cultured on EHS Matrix regardless of the presence of denuded oocytes.

5.4 Maintenance of meiotic arrest is necessary for GLYT1 suppression in COCs cultured on EHS Matrix.

All of the above experiments which describe GLYT1 suppression in COCs by EHS Matrix were performed with NPPC and E_2 present in culture medium to maintain meiotic arrest. Although it has previously been shown that GLYT1 activation occurs even when meiotic arrest is maintained, the reverse has never been demonstrated since it had not been possible to prevent GLYT1 from spontaneously activating in COCs or denuded oocytes [Tartia et al. 2009]. Here, for the first time, low GLYT1 activity can be sustained in cultured COCs for at least 4 hours, sufficient time for meiotic resumption to occur.

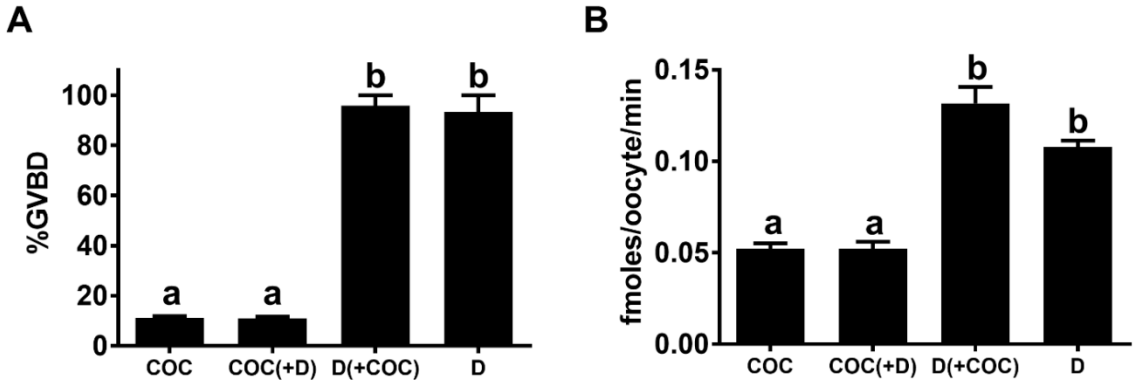

Figure 44. Co-culture of denuded oocytes and COCs on EHS Matrix: meiotic resumption and GLYT1 activity. COCs (COC) and denuded GV oocytes (D) were cultured alone or in combination for 4 hours on EHS Matrix-coated culture wells and then meiotic resumption and GLYT1 activity were examined. The specific culture groups are represented as follows: COCs alone (COC), COC cultured with denuded oocytes (COC(D)), denuded oocytes cultured with COCs (D(+COC)), and denuded oocytes alone (D). (**A**) Black bars represent the percentage of oocytes that resumed meiosis (% GVBD) (mean ± SEM, n=3). Bars that do not share letters have significantly different means ($P < 0.0001$ by ANOVA with Tukey test). (**B**) Black bars represent the rate of GLYT1-mediated [^{3}H]-glycine uptake into oocytes as shown in fmoles/oocyte/min (mean ± SEM, n=3). Bars that do not share letters have significantly different means ($P < 0.001$ by ANOVA with Tukey test).

To determine whether GLYT1 suppression can still be maintained in COCs cultured on EHS Matrix even when meiotic resumption is allowed to proceed, COCs were cultured in uncoated plastic culture wells (-M) or EHS Matrix-coated culture wells (+M) in medium that was either supplemented with NPPC and E_2 (+NE) or that did not contain any added NPPC and E_2 (-NE). After the 4-hour culture period, meiotic resumption was determined by the presence of GVBD and GLYT1 activity was measured as the rate of [^{3}H]-glycine uptake into oocytes. As expected, meiotic arrest was maintained in ~90% of COCs when NPPC and E_2 were present in culture medium regardless of whether the culture well was coated or uncoated (Figure 45A). In contrast, GVBD failed to occur in ~10% of COCs cultured in the absence of NPPC and E_2 which did not significantly differ when COCs were cultured in uncoated plastic wells or in EHS Matrix-coated wells (Figure 45A). When COCs were cultured in uncoated plastic culture wells, GLYT1 activation occurred normally in the presence or absence of NPPC and E_2 (Figure 45B). GLYT1 suppression was again found to be maintained in meiotically-arrested COCs when cultured in EHS Matrix-coated wells. However, GLYT1 activation occurred in COCs cultured in EHS Matrix-coated wells in the absence of NPPC and E_2 which did not significantly differ from GLYT1 activity in COCs cultured in uncoated plastic wells. Therefore, EHS Matrix-mediated GLYT1 suppression can only be sustained in COCs that are also maintained in meiotic arrest during culture.

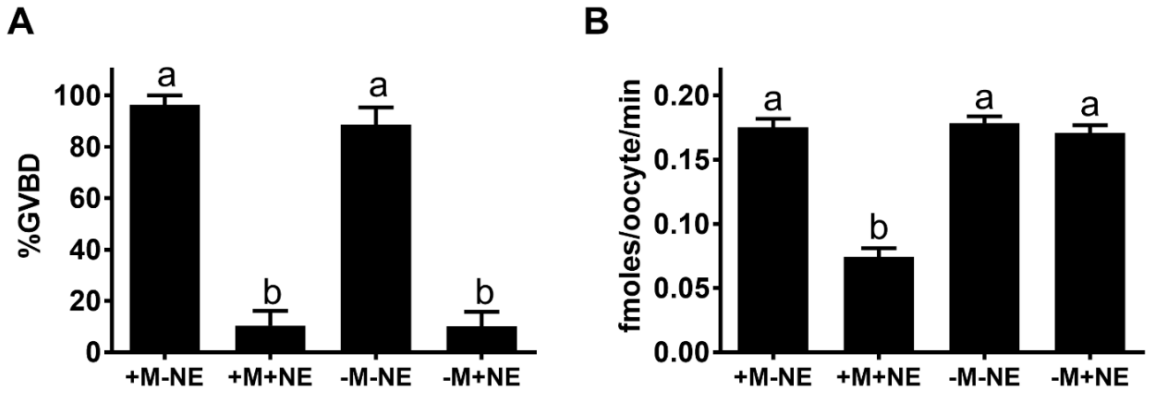

Figure 45. **Meiotic resumption in COCs cultured with or without EHS Matrix.** COCs were cultured 4 hours either in uncoated plastic culture wells (-M) or in EHS Matrix-coated culture wells (+M) and in the presence (+NE) or absence (-NE) of NPPC and E_2 in culture medium. (**A**) Black bars represent the percentage of COCs that resumed meiosis (% GVBD) under each culture condition (mean ± SEM, n=3). Bar that do not share letters have significantly different means ($P < 0.0001$ by ANOVA with Tukey test). (**B**) Black bars represent the rate of GLYT1-mediated [^{3}H]-glycine uptake in COCs cultured under each culture condition (mean ± SEM, n=3). Bar that do not share letters have significantly different means ($P < 0.0001$ by ANOVA with Tukey test).

5.5. Specific extracellular matrix components (EMs) can maintain GLYT1 suppression in COCs.

Since the growth factor-reduced EHS Matrix (GFR Matrigel©, Corning) maintained GLYT1 suppression as effectively as normal EHS Matrix (Matrigel©, Corning), I hypothesized that the extracellular matrix components (EMs) within the EHS Matrix rather than soluble growth factors or other low molecular weight factors could be involved in GLYT1 suppression in COCs. EHS Matrix is composed of many different EMs, especially laminin (~60%) and collagen IV (~30%), and contains multiple other factors that could be mediating GLYT1 suppression [Kleinman et al. 1986; Hughes et al. 2010]. To narrow the list of EMs which could be involved in sustaining low GLYT1 activity in COCs, I tested various purified EMs that have previously been shown to be expressed in ovaries and antral follicles. The most frequently studied EMs in ovaries and follicles included collagens (specifically collagen I and collagen IV), laminins, and fibronectin therefore these EMs were used as surface coatings on which COCs were cultured [Berkholtz et al. 2006a; Irving-Rodgers et al. 2010]. COCs were cultured 4 hours in uncoated plastic culture wells, EHS Matrix-coated culture wells, or culture wells coated with collagen I, collagen IV, laminin, or fibronectin and then GLYT1 activity was measured by [^{3}H]-glycine uptake. To rule out the possibility that the maintenance of GLYT1 suppression in COCs depends simply on adhesion, poly-lysine was tested as a coating surface. For all substrates tested, meiotic arrest was maintained in ~80% of COCs throughout the culture period by NPPC and E_2 (data not shown).

In all EM experiments performed, spontaneous GLYT1 activation occurred in COCs cultured in uncoated culture wells (-) while GLYT1 suppression was maintained in

COCs cultured in EHS Matrix-coated culture wells (EHS). GLYT1 activation occurred in COCs cultured in collagen IV-coated culture wells (Coll IV) which did not significantly differ from COCs cultured in uncoated wells, consistent with the results above (Figure 46A). As described prior to this section, purified collagen IV was used as a surface coating for MGC culture because no effect on GLYT1 activity was observed in COCs in this experiment. In contrast, COCs that were cultured on purified laminin (Lam) maintained GLYT1 suppression as effectively as COCs that were cultured on EHS Matrix (Figure 46B). When COCs were cultured in fibronectin-coated culture wells (Fibro), GLYT1 activity was lower compared to uncoated culture wells, but was significantly higher than in COCs cultured on laminin or EHS Matrix (Figure 46B). GLYT1 suppression was also maintained when COCs were cultured on collagen I (Coll I) which was not significantly different from COCs cultured on EHS Matrix (Figure 46C). GLYT1 activation also occurred normally in COCs cultured in poly-lysine-coated culture wells suggesting that adhesion of COCs to a non-specific surface alone is not sufficient to maintain GLYT1 suppression (Figure 46C). COCs tightly adhered to each surface coating tested (including poly-lysine) with no obvious qualitative differences observed between the different coatings. These results indicate that GLYT1 suppression in COCs is maintained most effectively by EHS Matrix, laminin, and collagen I while GLYT1 suppression is somewhat maintained by fibronectin and is not maintained by collagen IV or poly-lysine.

Since laminin is the major component of EHS Matrix and was able to maintain GLYT1 suppression in COCs as effectively as EHS Matrix, I sought to determine whether GLYT1 suppression is dependent on direct interaction of COCs with the laminin. An anti-

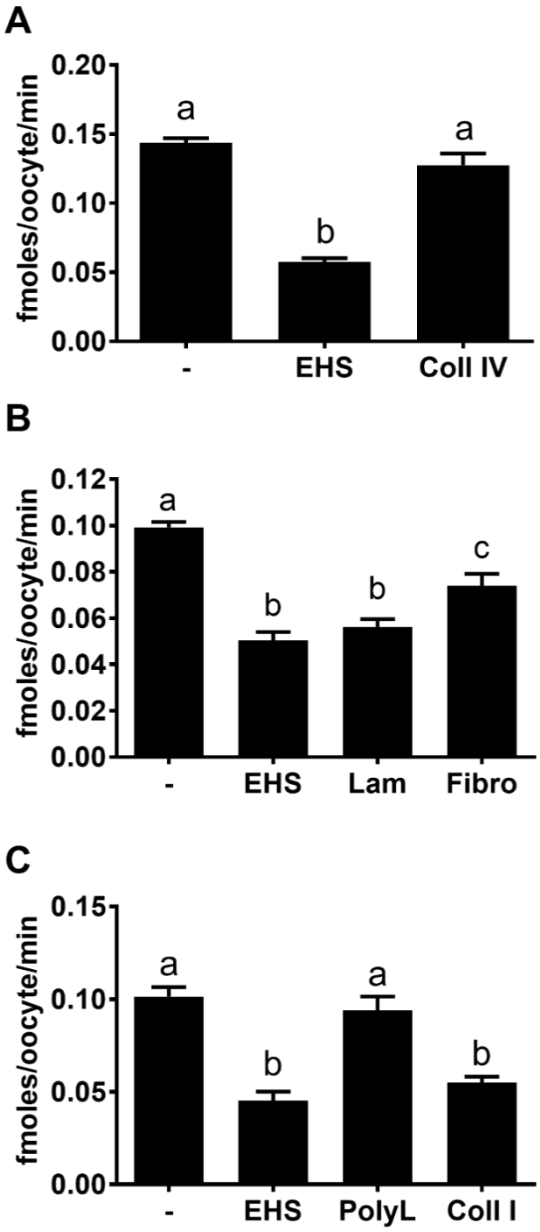

Figure 46. GLYT1 suppression in COCs by specific extracellular matrix components (EMs). For **A**-**C**, black bars represent the rate of GLYT1-mediated [^{3}H]-glycine uptake. (**A**) COCs were cultured 4 hours in uncoated culture wells (-), in EHS Matrix-coated culture wells (EHS), or in collagen IV-coated culture wells (Coll IV) (mean ± SEM, n=3). Bars that do not share letters have significantly different means (P <0.001 by ANOVA with

Tukey test). (**B**) COCs were cultured 4 hours in uncoated culture wells (-), in EHS Matrix-coated culture wells (EHS), in laminin-coated culture wells (Lam), or in fibronectin-coated culture wells (Fibro) (mean ± SEM, n=5). Bars that do not share letters have significantly different means ($P < 0.05$ for **Lam** vs **Fibro**, $P < 0.01$ for **EHS** vs **Fibro** and **–** vs **Fibro**, $P < 0.0001$ for **–** vs **EHS** and for **–** vs **Lam** by ANOVA with Tukey test). (**C**) COCs were cultured 4 hours in uncoated culture wells (-), in EHS Matrix-coated culture wells (EHS), in Poly-D-Lysine-coated culture wells (PolyL), or in collagen I-coated culture wells (Coll I) (mean ± SEM, n=3). Bars that do not share letters have significantly different means ($P < 0.01$ for **–** vs **Coll I** and **PolyL** vs **Coll I**, $P < 0.001$ for **–** vs **EHS** and **EHS** vs **PolyL** by ANOVA with Tukey test).

laminin antibody directed specifically against laminin isolated from EHS mouse tumor (the same laminin isoform found in EHS Matrix, laminin-111) was added to culture medium to block COCs from binding to laminin during culture. This specific antibody has previously been used to successfully block the ability of laminin to maintain pericytes in an undifferentiated state leading to differentiation of primary pericyte cultures plated on laminin [Yao et al. 2014]. To examine the effect of blocking functional laminin adhesion to COCs, COCs were cultured 4 hours in uncoated culture wells (-), in laminin-coated culture wells (L), in laminin-coated culture wells in the presence of anti-laminin antibody (L+Anti), or in laminin-coated culture wells in the presence of rabbit IgG (L+IgG) and then the rate of GLYT1-mediated [^{3}H]-glycine uptake was measured. Since I showed that GLYT1 suppression by EHS Matrix requires the maintenance of meiotic arrest, NPPC and E_2 were added to culture medium to maintain prophase-I arrest.

As observed above, COCs cultured on plastic alone did not adhere to the culture surface while COCs cultured on purified laminin tightly adhered to the laminin-coated surface; migration of cumulus cells along the laminin coating was also observed and appeared to be associated with adhesion (Figure 47A). When anti-laminin antibody was present during culture, the majority of COCs were not tightly attached to the laminin coating and minimal cumulus cell migration was visible following the 4-hour culture period (Figure 47A). In contrast, when COCs were cultured on laminin in the presence of rabbit IgG, tight adherence of COCs to the laminin coating was observed and extensive cumulus cell migration was visible (Figure 47A). As expected, meiotic arrest was maintained in nearly all COCs with only ~10% of COCs resuming meiosis (% GVBD) under all culture conditions (Figure 47B). GLYT1 activation occurred normally in COCs

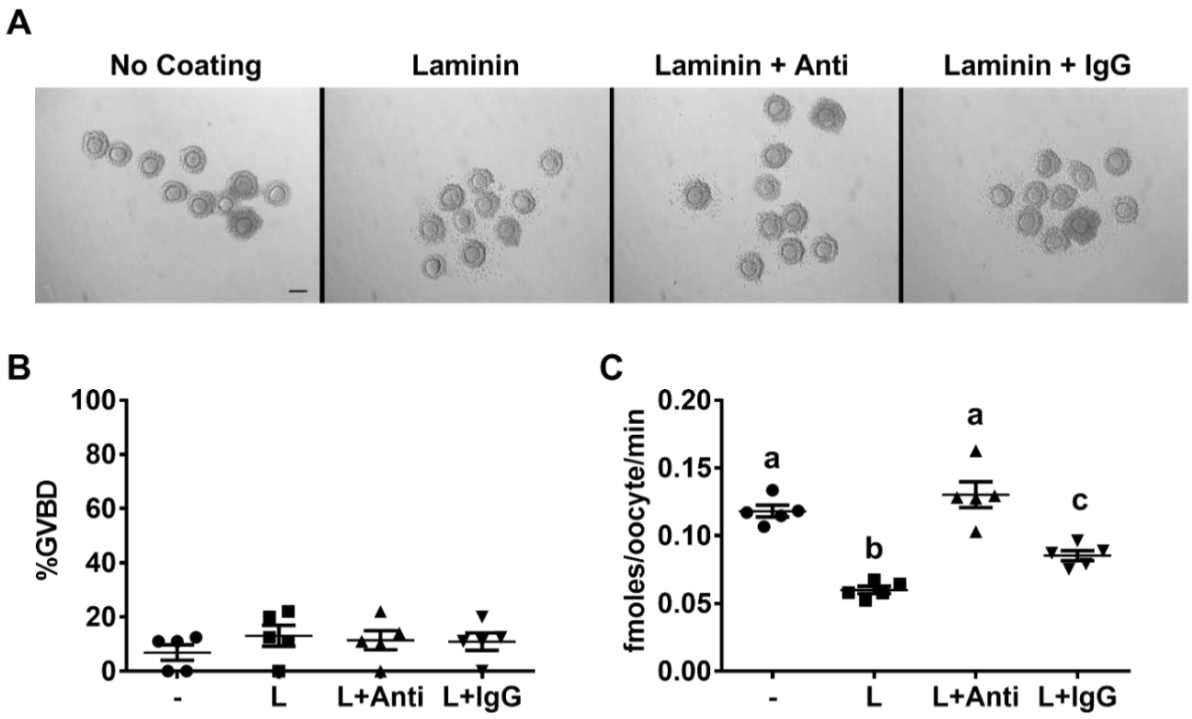

Figure 47. GLYT1 suppression by purified laminin: anti-laminin antibody. COCs were cultured 4 hours in uncoated culture wells (-), in laminin-coated culture wells (L), in laminin-coated culture wells in the presence of anti-laminin antibody (L+Anti, 50 µg/ml), or in laminin-coated culture wells with rabbit IgG (L+IgG, 50 µg/ml). Meiotic arrest was maintained in cultured COCs by NPPC and E_2. (**A**) Images of COCs following the 4-hour culture period taken with a Nikon E4500 camera mounted on a Zeiss Axiovert microscope. Various degrees of cumulus cell migration were visible which was often indicative of adhesion to the surface of the culture well. The scale bar in the first image represents 100 µm and applies to all images in **A**. (**B**) Individual replicates are shown which represent the percentage of COCs that resumed meiosis (% GVBD) when cultured 4 hours on plastic alone (circles), on laminin alone (squares), on laminin in the presence of anti-laminin antibody (triangles), or on laminin in the presence of control rabbit IgG (upside-

down triangles) (means for each condition are represented by a horizontal line ± SEM, n=5). No significant difference between means of each culture condition was detected by ANOVA with Tukey test. (**C**) Individual replicates are shown which represent the rate of GLYT1-mediated [^{3}H]-glycine uptake in COCs cultured 4 hours on plastic alone (circles), on laminin alone (squares), on laminin in the presence of anti-laminin antibody (triangles), or on laminin in the presence of control rabbit IgG (upside-down triangles) (means for each condition are represented by a horizontal line ± SEM, n=5). The rate of [^{3}H]-glycine uptake is shown in fmoles/oocyte/min. Groups that do not share letters have significantly different means ($P < 0.05$ for **L** vs **L+IgG**, $P < 0.01$ for **–** vs **L+IgG**, $P < 0.001$ for **L+Anti** vs **L+IgG**, and $P < 0.0001$ for **–** vs **L** and **L** vs **L+Anti** by ANOVA with Tukey test).

cultured in uncoated culture wells while GLYT1 suppression was maintained in COCs cultured on laminin (Figure 47C). When anti-laminin antibody was present in culture medium, GLYT1 activation occurred in COCs cultured on laminin with a rate of [^{3}H]-glycine uptake not significantly different than in COCs cultured on plastic alone. However, GLYT1 also became somewhat activated in COCs cultured on laminin in the presence of control rabbit IgG suggesting that interaction of IgG itself likely with COCs may be contributing to the observed GLYT1 activity increase in the presence of anti-laminin antibody, although GLYT1 activity was still significantly higher in the presence of the antibody compared to rabbit IgG (Figure 47C). This ability of the anti-laminin antibody to cause GLYT1 activation in COCs cultured on laminin helps to further validate that the maintenance of GLYT1 suppression in COCs is actually mediated by laminin, although it cannot be ruled out that a non-specific interaction with IgG itself was contributing to GLYT1 suppression; this hypothesis is supported by preliminary immunofluorescence data which showed bright fluorescent staining of COCs incubated with rabbit IgG alone (no primary antibody) followed by incubation with goat anti-rabbit-Alexa 594 secondary antibody (data not shown).

These results also suggest that GLYT1 suppression by EMs depends on the direct association of COCs to these EMs since blocking COC-laminin binding resulted in GLYT1 activation. However, further experiments are needed to determine the exact mechanism mediated this EM-induced GLYT1 suppression in COCs.

DISCUSSION

1. Oocyte-ZP detachment, GLYT1 activation, and meiotic resumption are acquired at a similar stage in oogenesis and occur simultaneously following the isolation of oocytes from the ovarian follicle.

1.1Oocytes acquire the ability to activate GLYT1 and detach from the ZP during the late stages of oogenesis.

GLYT1 activation and detachment of the oocyte from the ZP occurs spontaneously in fully grown oocytes following isolation from the ovarian follicle *in vitro* or in response to ovulatory stimulation *in vivo* [Tartia et al. 2009]. I found that oocytes removed from the follicles of adult mice first acquire the ability to activate high levels of GLYT1 activity and completely detach from the ZP near the end of oogenesis when oocytes are nearly fully grown, with the greatest level of GLYT1 activity and oocyte-ZP detachment occurring in fully-grown oocytes ~80 μm in diameter (Figure 12 & Figure 13). Interestingly, the acquisition of oocyte meiotic competence was also found to develop late during oogenesis although it seemed to be acquired somewhat earlier than the ability to activate GLYT1 and detach from the ZP. In adult mice, meiotic competence was first acquired when oocytes were ~70 μm in diameter, a stage in which GLYT1 activity was low and oocytes were unable to completely detach from the ZP (Figure 14 & Figure 15). Similarly, oocytes isolated during the initial wave of oogenesis from neonatal mice first acquired the ability to develop high GLYT1 activity levels near the end of oogenesis when oocytes were at least 75 μm in diameter (Figure 14A), after the acquisition of meiotic competence which

has previously been shown to occur at ~65-70 µm in diameter during the initial wave of oogenesis [Sorensen & Wassarman 1976; Erdogan et al. 2005]. Thus, I have demonstrated that oocytes acquire the ability to activate GLYT1 fully and detach from the ZP following removal from the ovarian follicle near the end of oogenesis when the oocyte is nearly fully grown, but slightly after oocytes become meiotically competent.

Although oocytes can activate GLYT1 to high levels and detach completely from the ZP when they approach the end of oogenesis, these processes are suppressed within the ovarian follicle and only proceed upon removal of the oocyte from the follicle or following an ovulatory stimulus *in vivo*. Therefore, it can be concluded that GLYT1 activation and oocyte-ZP detachment are prevented by unknown inhibitory mechanisms within the ovarian follicle, at least during the late stages of oogenesis, and that these are released following LH stimulation. Tight adhesion of the oocyte to the ZP by microvilli maintains oocyte volume within the ovarian follicle and eliminates the need for independent cell volume regulation [Tartia et al. 2009]. Although the reason for suppression of independent cell volume regulation within the ovarian follicle is currently unknown, it is thought that the oocyte maintains a tight adherence to the ZP and does not activate independent volume regulatory mechanisms to avoid disrupting intercellular communication between the oocyte and cumulus granulosa cells [Tartia et al. 2009; Richard et al. 2016]. The physical association of the oocyte to the ZP enables intercellular communication between the oocyte and surrounding cumulus granulosa cells via TZPs and is vital for maintenance of meiotic arrest and for healthy development of the oocyte and follicular granulosa cells (see Introduction) [Sugiura et al. 2005; FitzHarris & Baltz 2006; Pelland et al. 2009; Norris et al. 2009; Zhang et al. 2010]. Following ovulation, intercellular communication via TZPs

and gap junctions is lost and independent cell volume-regulatory mechanisms can be activated without compromising oocyte health or development.

1.2 GLYT1 activation and oocyte-ZP detachment follow a similar time-course following oocyte removal from the ovarian follicle.

I sought to further examine the timing of the oocyte transition from a passive ZP-dependent volume regulatory mechanism to the GLYT1-mediated independent mechanism of volume regulation which is activated following removal from the ovarian follicle. Fully grown oocytes were shown above to be capable of completely detaching from the ZP and activating high GLYT1 activity and thus were used to examine the timing of oocyte-ZP detachment after oocyte removal from ovarian follicles.

By 1.5 hours following isolation from ovarian follicles, ~30% of oocytes were completely detached from the ZP and nearly all oocytes were detached from the ZP by 2.5 hours *in vitro* (Figure 11). This timing is supported by previous experiments performed in our laboratory using transmission electron microscopy (TEM) which showed close apposition of the oocyte to the ZP immediately following isolation from ovaries with the formation of a small gap between the oocyte and ZP by 0.5 hours and complete PVS formation by 2-3 hours. In these TEM experiments, oocyte-ZP adhesion appeared to be maintained by a tight adherence of oocyte microvilli to the ZP matrix which is lost after isolation from ovarian follicles *in vitro* [Tartia et al. 2009]. My data are also consistent with studies that previously showed that mouse oocytes exhibit PVS formation within 60 minutes *in vitro* with maximal PVS formation by 120 minutes *in vitro* [Inoue et al. 2007].

In comparison, GLYT1 activity is essentially absent immediately following isolation from ovaries, increases to half-maximal activity by ~1.5 hours and is fully active by ~3-4 hours [Tartia et al. 2009]. A similar time course of GLYT1 activation was previously found to occur *in vivo* following hCG administration with maximal GLYT1 activity detected at ~3-4 hours post-hCG injection [Tartia et al. 2009]. The similar timing of oocyte-ZP detachment and GLYT1 activation following oocyte removal from the ovarian follicle likely represents the coordinated transition from dependent volume regulation mediated by the tight association of the oocyte to the ZP to the independent volume regulatory processes active throughout preimplantation embryo development. Interestingly, oocyte-ZP detachment appears to slightly precede GLYT1 activation which could suggest that detachment of the oocyte from the ZP matrix is required prior to GLYT1 activation. However, it has not been possible to test this theory since we are currently unable to specifically prevent or delay spontaneous oocyte-ZP detachment from occurring following oocyte isolation from ovaries and thus cannot determine whether GLYT1 activation occurs when oocyte-ZP detachment is prevented.

1.3 Oocyte-ZP detachment and GLYT1 activation occur independently from meiotic maturation in fully grown oocytes.

The similar timings of the development of independent volume regulatory mechanisms and the transition of meiotically-arrested GV oocytes to MI eggs following oocyte removal from ovaries *in vitro* or an ovulatory stimulus *in vivo* could suggest that these two processes are coupled [Donahue & Stern 1968; Tartia et al. 2009; Richard et al. 2016]. I showed above that oocyte acquisition of meiotic competence during oogenesis

slightly precedes the acquired ability of oocytes to fully activate GLYT1 and completely detach from the ZP which lends support to the hypothesis that GLYT1 activation and/or oocyte-ZP detachment is dependent on meiotic maturation. However, GLYT1 activation and oocyte-ZP detachment was previously shown to occur spontaneously in fully grown oocytes cultured *in vitro* that were maintained in meiotic arrest under conditions which sustained high intra-oocyte levels of cAMP [Inoue et al. 2007; Tartia et al. 2009]. As discussed in the introduction to this thesis, the physiological mechanism responsible for the maintenance of prophase I arrest has recently been a primary focus of many studies which has led to the identification of intra-follicular cyclic GMP (cGMP) concentrations as a critical factor for the maintenance of high intra-oocyte cAMP levels, a signalling mechanism which is dependent on NPPC binding to NPR2 on granulosa cells [Bornslaeger et al. 1984; Törnell et al. 1990; Norris et al. 2009; Vaccari et al. 2009; Zhang et al. 2010, 2011; Hanna et al. 2012; Wigglesworth et al. 2013]. Although cGMP maintains meiotic arrest by inhibiting the cAMP phosphodiesterase PDE3A, it was possible that GLYT1 suppression was maintained by divergent signalling pathways mediated by cGMP such as through cGMP-gated ion channels or cGMP-dependent protein kinases (PKG) [Biel 2009; Hofmann et al. 2009; Francis et al. 2010]. To address this possibility, COCs were maintained in meiotic arrest during culture with NPPC and GLYT1 activity measured following a 4-hour culture period. GLYT1 activation *in vitro* occurred at a similar rate in COCs maintained in meiotic arrest by NPPC and E_2 compared to denuded oocytes maintained in meiotic arrest by cell-permeant cAMP (dbcAMP), with maximal GLYT1 activity measured at ~3-4 hours for both COCs and denuded oocytes (Figure 30) suggesting

that an entirely different signalling mechanism mediates GLYT1 suppression in the ovarian follicle.

Although NPPC and E_2 alone were sufficient to maintain meiotic arrest in cultured COCs, it was possible that the cGMP concentration was too low under my culture conditions to additionally prevent spontaneous GLYT1 activation. In addition to the ability of cGMP to regulate the activity of phosphodiesterases (such as PDE3A), cGMP can also act via cGMP-dependent protein kinases (PKGs) and cGMP-regulated cation channels. Briefly, binding of cGMP to the serine-threonine kinase, PKG, induces a conformational change and an increase in PKG phosphorylating activity which has been shown to mediate a wide range of functions in various cell types including the modulation of intracellular calcium levels and the regulation of intracellular trafficking [Hofmann et al. 2009; Francis et al. 2010]. To examine whether increasing cGMP concentrations could maintain GLYT1 suppression by an alternative mechanism to PDE regulation, such as increasing PKG activity, I cultured COCs with various combinations of compounds previously shown to be capable of potentiating the NPPC-cGMP mediated mechanism of meiotic arrest by supporting cGMP production. Although prophase I arrest was maintained under all conditions tested, spontaneous GLYT1 activation proceeded normally regardless of the medium additions (Figure 36). Thus, despite the similar timings of both the initial acquisition of growing oocytes to complete these processes and the overall timing of the execution of these processes in fully grown oocytes following an ovulatory stimulus or isolation from ovaries, it appears that oocyte-ZP detachment and GLYT1 activation are regulated independently from the mechanisms mediating meiotic arrest and resumption. However, these conclusions did not rule out the possibility that these events are suppressed

within the ovarian follicle through shared general mechanisms including a requirement for gap junctional signalling or a dependence on communication between multiple cells types, which will be discussed below.

1.4 *Slc6a9a* mRNA and SLC6A9 protein expression increases throughout oogenesis.

I sought to determine when during oogenesis that *Slc6a9a* mRNA and SLC6A9 protein first appear as well as the cellular localization of this protein to further interpret the development of the minor GLYT1 activity level observed in isolated small growing oocytes and to determine whether the development of high levels of GLYT1 activity in isolated fully-grown oocytes was the result of a substantial increase in SLC6A9 protein at the plasma membrane. *Slc6a9a* expression increased with oocyte growth which plateaued in fully grown GV oocytes and persisted until at least the 1-cell stage and was absent by the 8-cell stage (Figure 16). This mRNA expression profile for *Slc6a9a* supports the hypothesis that SLC6A9 protein is present in oocytes throughout oogenesis which may account for the development of the low level of GLYT1 activity measured in small growing oocytes following isolation from ovaries.

SLC6A9 protein expression was shown to be present using immunofluorescence analysis in freshly isolated GV oocytes, MI eggs, 1-cell, 2-cell, and 8-cell embryos with no apparent expression in blastocyst stage embryos (Figure 18); this expression profile was confirmed by western blot analysis (Figure 17). This SLC6A9 expression profile is consistent with previously published data which measured GLYT1 activity throughout preimplantation embryo development. Tartia et al. previously showed that GLYT1 activity

is high in isolated MI eggs, MII eggs, 1-cell, and 2-cell embryos, is low in 4-cell and 8-cell embryos, and essentially absent in morula and blastocysts [Tartia et al. 2009]. Therefore, I have shown that SLC6A9 protein is indeed expressed in preimplantation embryos at the developmental stages where GLYT1-mediated glycine transport activity has previously been measured.

Examination of the total fluorescence intensity throughout oogenesis and preimplantation embryo development revealed that SLC6A9 expression significantly increased during oocyte growth with the highest expression level detected in oocytes isolated from P15 mice or older; maximal GLYT1 expression was present by P21 which did not significantly differ from fully grown oocytes isolated from adult (~4 weeks) mice (Figure 18A). If analyzed in the context of GLYT1 activity, this expression profile may indicate that only a low level of GLYT1 activity develops in isolated small growing oocytes due to the lower level of SLC6A9 protein expression and that the development of high levels of GLYT1 activity at the late stages of oogenesis depends on the expression of sufficient numbers of GLYT1 transporters capable of transporting glycine into oocytes. The half maximal GLYT1 activity level measured in isolated oocytes ranging from 75-79 μm in diameter (Figure 13 & Figure 14A) might be explained using my immunofluorescence results since oocytes of a similar size isolated from P15 mice widely ranged in SLC6A9 expression levels, with low expression in about half of oocytes and a high expression level in the other half of oocytes (Figure 18A). I hypothesize that the intermediate GLYT1 activity level measured in oocytes at this stage of development represents a combination of oocytes with a range of GLYT1 activity corresponding to SLC6A9 expression levels ranging from low to high.

1.5 SLC6A9 protein is localized to the oocyte plasma membrane throughout oogenesis and during GLYT1 activation.

Since I showed that *Slc6a9a* mRNA (Figure 16) and SLC6A9 protein levels (Figure17 & Figure 18) do not appear to differ in freshly-isolated GV oocytes compared to MI eggs, it seems unlikely that GLYT1 activation occurs because of an increase in SLC6A9 protein levels. My immunofluorescence data showed that SLC6A9 protein was localized to the plasma membrane throughout oogenesis which was maximal by P21 and did not appear to differ between fresh GV oocytes and MI eggs suggesting that the activation of high GLYT1 activity levels is not a result of an increase in trafficking of GLYT1 transporters to the oocyte surface. These results support previous experiments in our lab which indicated that the acute inhibition of SNARE proteins involved in protein insertion into the plasma membrane was unable to prevent the development of high levels of GLYT1 activity following isolation of oocytes from ovaries [Tartia 2009]. My immunofluorescence data instead suggests that SLC6A9 is ferried to the oocyte plasma membrane throughout oogenesis and is localized mainly at the plasma membrane (Figure 18). Taken together, these results favour a model in which the SLC6A9 protein that underlies GLYT1 activity is located in the plasma membrane before GLYT1 activation, and that the appearance of activity is due to activation of these pre-existing transmembrane proteins rather than increased insertion of SLC6A9 into the membrane.

In the CNS, the GLYT1 transporter is an essential regulator of both excitatory and inhibitory neurotransmission and thus it is essential that the activity of this transporter is tightly regulated in that context (see Introduction). GLYT1 activity has been shown to be controlled by mechanisms involving both the trafficking of the transporter to the plasma

membrane as well as by direct modification of transporters already present in the plasma membrane in glial and kidney cell lines [Gomeza et al. 1995; Sato et al. 1995; Geerlings et al. 2002; Fernandez-Sanchez et al. 2008; Mihalikova et al. 2014; Barrera et al. 2015]. Previous studies have shown that GLYT1 activity is downregulated by inhibition of calcium-dependent calmodulin signalling believed to be involved in regulating GLYT1 trafficking to the plasma membrane as well as by PKC-mediated endocytosis of transporters at the plasma membrane [Barrera et al. 2015; Mihalikova et al. 2014]. The presence of GLYT1 at the oocyte plasma membrane prior to activation and the inability of the PKC agonist PMA to prevent GLYT1 activation or downregulate GLYT1 activity in isolated oocytes [Tartia 2009] suggests that different mechanisms regulate GLYT1 activity in oocytes and early preimplantation embryos compared to the CNS. However, my immunofluorescence data cannot rule out the possibility that GLYT1 transporters reside on vesicles just below the plasma membrane prior to GLYT1 activation and become inserted into the membrane upon isolation from follicles. Ultrastructural analysis (e.g., immunogold electron microscopy) would have to be be performed to better visualize the exact localization of transporters during GLYT1 activation.

Since I showed GLYT1 transporters are localized at the plasma membrane prior to activation in the ovarian follicle and previous attempts to prevent GLYT1 activation following isolation of oocytes from follicles have failed [Tartia 2009], I hypothesized that GLYT1 is suppressed within the ovarian follicle by an unknown mechanism and that GLYT1 activation following removal of the oocyte from the follicle *in vitro* or an ovulatory trigger *in vivo* occurs indirectly due to a removal of inhibitory signalling, similar to the maintenance of meiotic arrest (see below).

2. Maintenance of prophase I arrest is dependent on both Cx43 and Cx37 gap junctions.

2.1 Isolated, intact antral follicles can maintain oocytes in meiotic arrest for extended culture periods.

To begin to study any signalling mechanisms mediating the maintenance of low GLYT1 activity and meiotic arrest in oocytes prior to an ovulatory stimulus, I sought to develop an antral follicle culture system capable of maintaining healthy, meiotically-arrested oocytes within antral follicles for extended culture periods. Since I showed above that the ability of oocytes to activate high GLYT1 activity and resume meiosis is acquired at the late stages of oogenesis when the oocyte is nearly fully grown, antral follicles were chosen as a culture model to ensure that the oocytes housed within follicles were capable of responding to manipulations aimed at stimulating intra-follicular GLYT1 activation or meiotic resumption.

Based on the previously validated intact antral follicle culture methodology developed by Dr. Steven Downs [2000], I isolated intact antral follicles from eCG-stimulated adult female mice and cultured these follicles for 20 hours. I found that at least 100 µl of medium was needed for antral follicles to effectively maintain meiotically-arrested oocytes (Figure 20). Volumes less than this may have cause meiotic resumption in oocytes due to the development of compromised health of the follicle possibly because of the depletion of nutrients from medium, a buildup of waste products, or the development of hypoxic conditions [Richard & Baltz 2014].

It has previously been shown that NPPC-cGMP signalling is the physiological mediator of meiotic arrest in the antral follicle and that inhibition of gap junctions using general pharmacological gap junction inhibitors causes meiotic resumption to occur in cultured antral follicles [Sela-Abramovich et al. 2006; Norris et al. 2008]. The ability of my intact antral follicle culture methodology to maintain meiotically arrested GV oocytes for up to 20 hours (Figure 22) suggests that within this culture system, antral follicles could sustain physiological NPPC-cGMP signalling and that normal paracrine and gap junctional communication were functional.

2.2 Punctured antral follicles maintain meiotically-arrested oocytes for extended culture periods when NPPC and E_2 are added to culture medium.

Downs [2000] had previously shown that intact antral follicles could be successfully cultured *in vitro*. However, I sought to determine whether meiotically-arrested GV oocytes could additionally be cultured within antral follicles in which the antral cavity was exposed directly to the culture medium. I hypothesized that this "open system" approach could potentially enable increased access of certain medium additions (see CMP section below) to the follicle interior which may otherwise have been prevented from reaching the COC contained within the intact antral follicle culture system. The outer wall of the antral follicles consists of multiple layers of cells including the theca cell layers, the follicular basal lamina, and the outer mural granulosa cell layer which collectively make up a semi-permeable barrier restricting the diffusion of certain compounds into or out of the follicle. The diffusion of molecules across the follicular wall appears to be dependent on molecular weight with high permeability to compounds that are <100 kDa, however,

molecular charge and the dynamic composition of the follicular basal lamina also seem to play a vital role [Rodgers & Irving-Rodgers 2010; Siu & Cheng 2012]. Therefore, I sought to increase the rate of diffusion of compounds into cultured antral follicles by puncturing the outer follicular wall, however, the reverse would also be true since compounds normally found within the follicular fluid could more rapidly diffuse out of the follicle via the puncture site.

Antral follicles were isolated and cultured identically to the intact antral follicle culture system described above except that a small hole was made in the outer follicular wall and thus was termed a "punctured" antral follicle. Punctured antral follicles cultured for up to 4 hours maintained meiotically-arrested GV oocytes similar to oocytes cultured within intact antral follicles. However, for culture periods longer than 4 hours, oocytes began to spontaneously resume meiosis by 20 hours in culture (Figure 22). Since prophase I arrest is dependent on the diffusion of NPPC through the antral fluid to access its cognate NPR2 receptor to produce cGMP, I hypothesized that the antral fluid was diluted over time in punctured antral follicles possibly due to increased diffusion out of the follicle through the puncture site, thus reducing the level of follicular NPPC and causing meiotic resumption to occur.

Since I hypothesized that the concentration of follicular NPPC was being diluted from punctured antral follicles, I supplemented the antral follicle culture medium with NPPC and E_2 at a concentration of 100 nM which I found to be sufficient to maintain meiotic arrest in COCs for up to 24 hours (Figure 21); this concentration of NPPC needed to maximally maintain meiotic arrest in COCs is consistent with previously reported results [Zhang et al 2010; Kawamura et al. 2011]. In the presence of additional exogenous NPPC

and E_2 in culture medium, meiotic arrest was maintained in oocytes within punctured antral follicles for up to 20 hours which was not significantly different from intact antral follicles (Figure 22). This is consistent with NPPC being diluted from the punctured follicle antrum during prolonged culture. Meiotically-arrested oocytes isolated after 20 hours in punctured antral follicles were subsequently able to resume meiosis and progress to MII eggs similarly to oocytes cultured in intact antral follicles indicating that my punctured antral follicle culture system can maintain healthy, meiotically-arrested oocytes when exogenous NPPC and E_2 are present in culture medium (Figure 23). Since the addition of exogenous NPPC (and E_2) prolonged the maintenance of oocyte meiotic arrest, it can be presumed that functional gap junctions were present within punctured antral follicles culture, since they are required for passage of cGMP between cumulus cells and into the oocyte.

2.3 Maintenance of meiotic arrest in intact and punctured follicles depends on gap junctional communication.

Previous studies have shown that general pharmacological inhibition of gap junctional communication in antral follicles does not change the concentration of cGMP within mural or cumulus granulosa cells, but that the concentration of cGMP in the oocyte decreases when gap junctions are blocked, resulting in meiotic resumption [Norris et al. 2008; Shuhaibar et al. 2015]. To examine whether meiotic resumption would occur as expected in my intact and punctured antral follicle culture systems following inhibition of all gap junctional communication, general pharmacological gap junction inhibitors were added to culture medium and then the effect on meiotic resumption of follicle-enclosed oocytes was examined. In the presence of the general gap junction inhibitor AGA, meiotic

resumption occurred in oocytes within both intact and punctured antral follicles with a faster effect observed in punctured antral follicles, possibly due to easier access for AGA to the follicle interior provided by the puncture site (Figure 24A, B); this effect was further confirmed using another general gap junction inhibitor, lindane (Figure 24C, D). These results highlight the vital role for gap junctional communication in the maintenance of prophase I arrest, although which specific gap junction isoforms are required to maintain meiotic arrest in the antral follicle are unclear from these experiments since all gap junctions were inhibited.

2.4 Meiotic resumption is stimulated in COCs and punctured follicles by Cx43 connexin mimetic peptides (CMPs).

The requirement for both GJA1 (connexin-43) and GJA4 (connexin-37) for normal folliculogenesis and oocyte development has previously been demonstrated by knockout mouse models and chimeric reaggregated ovaries (see Introduction) [Kidder & Mhawi 2002; Kidder 2005; Gershon et al. 2008]. Although both gap junction isoforms have clearly been shown to be essential in the developing follicle, the involvement of each gap junction isoform in the maintenance of meiotic arrest has not been directly demonstrated. The involvement of GJA1 (connexin-43) gap junctions between granulosa cells in the maintenance of meiotic arrest in the antral follicle has previously been inferred from studies which showed that LH-stimulation of cultured antral follicles resulted in phosphorylation of GJA1 gap junctions eventually culminating in a release of meiotic arrest [Norris et al. 2008]. Additionally, localization studies have revealed that gap junctions composed of connexin-43 were dominantly expressed between mural and cumulus granulosa cells thus

suggesting that these gap junctions are required for the diffusion of meiosis-inhibiting cGMP produced in the granulosa cells to the oocyte [Teilmann 2005; Simon et al. 2006; Norris et al. 2008]. To my knowledge, however, the requirement for functional GJA1 gap junctions for the maintenance of meiotic arrest in antral follicles has not previously been directly shown.

The general pharmacological gap junction inhibitors discussed in the previous section (AGA and lindane) exert their effects by disrupting cellular signalling mechanisms involved in sustaining functional gap junction communication and are unable to selectively inhibit specific gap junction isoforms and can have nonspecific effects [Juszczak & Swiergiel 2009; Brokamp et al. 2012]. I sought to more specifically inhibit gap junctions composed of connexin-43 and therefore used connexin-mimetic peptides (CMPs) which target specific short amino acid sequences unique to the extracellular loop domains of connexin hemi-channels thus allowing for inhibition of gap junctions composed of specific connexin isoforms [Evans & Leybaert 2007; Evans et al. 2012; Richard & Baltz 2014].

I cultured COCs meiotically-arrested with NPPC in the presence or absence of Cx43 CMP and found that meiotic resumption was significantly higher in COCs cultured with Cx43 CMP compared to COCs cultured with a scrambled version of the Cx43 CMP or without any CMP with the greatest effect observed at 20 hours in culture (Figure 25C). The ability of Cx43 CMP to cause significant meiotic resumption in COCs cultured with NPPC and E_2 is consistent with a role for GJA1 gap junctions between cumulus granulosa cells in the maintenance of oocyte meiotic arrest.

To further examine the ability of Cx43 CMP to stimulate meiotic resumption, both intact and punctured antral follicles were cultured in the presence of Cx43 CMP or the

scrambled version of the peptide and then oocyte GVBD was assessed. Meiotic resumption was significantly increased in both intact and punctured antral follicles in the presence of Cx43 CMP, although a greater effect was observed for punctured antral follicles (Figure 27 & Figure 28). The ability of Cx43 CMP to more effectively cause meiotic resumption in punctured follicles compared to intact follicles is consistent with an increase in the diffusion of compounds into punctured follicles through the puncture site in the follicle wall. Although entry of CMPs into punctured follicles bypasses the outer layers of the follicle resulting in faster gap junction inhibition, slower diffusion of Cx43 CMP into intact follicles still appears to be possible since meiotic resumption also occurred in intact follicles; this was expected since CMPs are small enough to traverse the layers of the semi-permeable follicle wall (~1.5 kDa) as discussed above [Rodgers & Irving-Rodgers 2010; Siu & Cheng 2012; Evans et al. 2012]. The previous identification of gap junctions composed of connexin-43 between both mural and cumulus granulosa cells within antral follicles and the ability of Cx43 CMP to cause meiotic resumption in COCs and antral follicles is suggestive of a vital role of GJA1 in the maintenance of meiotic arrest. These results are consistent with the model in which oocyte meiotic arrest depends on the secretion of NPPC from mural granulosa cells to stimulate cGMP production in the innermost mural granulosa cells and cumulus granulosa cells which diffuses through gap junctions between granulosa cells composed of connexin-43 to the oocyte.

2.5 Meiotic resumption is stimulated in COCs by Cx37 CMP when introduced to the site of their target gap junctions.

To determine more directly whether gap junctions composed of connexin-37 (GJA4) (previously found to be localized at the oocyte surface) are required to maintain oocyte meiotic arrest, COCs and punctured antral follicles were cultured with NPPC/E_2 and with or without Cx37 CMP or a scrambled version of the peptide and meiotic arrest was examined after 0-20 hours. Unexpectedly, meiotic arrest was maintained in COCs and punctured follicles despite the presence of Cx37 CMP which could either indicate that inhibition of Cx37 CMP was insufficient to prevent cGMP diffusion into oocytes and stimulate meiotic resumption or that the Cx37 CMP was not effectively able to inhibit GJA4 gap junctions in my culture system (Figure 25B & Figure 28).

Since it has previously been shown by a single study that specific inhibition of GJA4 gap junctions by antisera in antral follicle-enclosed oocytes caused meiotic resumption [Norris et al. 2008], I hypothesized that the Cx37 CMP was unable to access the GJA4 gap junctions located at the innermost cumulus granulosa cells. Indeed, I found that the diffusion of wheat germ agglutinin (WGA, ~38kDa; Molecular Probes Inc. 2009) to the oocyte ZP was hindered by the presence of granulosa cells, showing that cumulus cells present a barrier to diffusion of at least some proteins to the oocyte surface. Therefore, the lack of effect of Cx37 CMP when added to the medium may be due to its diffusion being similarly slowed or prevented by the cumulus barrier even though it is smaller (~1.5 kDa) than WGA (Figure 29A). CMP are thought to exert their effects by slowly intercalating between already formed gap junctions to inhibit this method of coupling [Evans & Leybaert 2007; Evans et al. 2012]. It was possible that longer culture periods

would permit Cx37 CMP to eventually reach GJA4 gap junctions at the oocyte surface, however, the health of COCs could be compromised over long duration culture due to nutrient depletion or the absence of mural granulosa cell-derived compounds leading to the indirect release of meiotic arrest.

To deliver Cx37 CMP more directly to the vicinity of the GJA4 gap junctions, Cx37 CMP was microinjected at the oocyte surface of COCs which were then subsequently cultured in the presence of medium supplemented with additional Cx37 CMP and NPPC/E_2; COCs were also microinjected with medium alone or scrambled peptide as controls. Interestingly, meiotic arrest was released in COCs microinjected at the oocyte surface with Cx37 CMP (Figure 29B). These data lend support to the hypothesis that Cx37 CMP were unable to reach the gap junctions located between the oocyte surface and innermost granulosa cells in my initial culture system. Since microinjection of GJA4-specific antisera into follicle-enclosed oocytes was previously shown to result in a decrease in GJA4 protein and connexin-37 gap junctions leading to meiotic resumption, I sought to confirm this effect in COCs maintained in arrest with NPPC and E_2 [Norris et al. 2008]. As expected, microinjection of GJA4 antisera into COCs also overcame NPPC-mediated meiotic arrest leading to meiotic resumption thus further demonstrating a requirement for gap junctions composed of connexin-37 for maintenance of meiotic arrest (Figure 29C).

Taken together, these results suggest a critical role for both GJA1 (connexin-43) and GJA4 gap junctions (connexin-37) in the maintenance of oocyte prophase I arrest by NPPC. To my knowledge, this is the first direct demonstration that CMP can be utilized to inhibit specific gap junction isoforms in follicles and COCs and that direct inhibition of either GJA1 or GJA4 gap junctions is sufficient to overcome NPPC-mediated meiotic

arrest in cultured COCs. The ability of Cx43 CMP in medium to readily induce meiotic resumption is consistent with the localization of GJA1 (connexin-43) gap junctions between granulosa cells throughout the follicle and cumulus cells of COCs while the inability of Cx37 CMP in medium alone (without microinjection at the oocyte surface) to cause meiotic resumption in COCs is consistent with GJA4 (connexin-37) gap junction expression strictly at the oocyte surface. These results support the model of meiotic arrest in the antral follicle in which NPPC stimulates cGMP production in granulosa cells which diffuses into the oocyte through gap junctions composed of both connexin-43 and connexin-37.

Whether gap junctions between the innermost cumulus granulosa cells and oocyte surface are composed of homotypic GJA4 gap junctions or heterotypic gap junctions composed of both connexin-37 (in the oocyte) and connexin-43 (in granulosa cells) remains controversial (see Introduction). My results were unable to distinguish between these differing scenarios since Cx37 CMP could have simply targeted the GJA4 (connexin-37) hemi-channels present at the oocyte surface without inhibiting the hemi-channels present at the inner granulosa cells thus preventing cGMP diffusion into the oocyte and releasing meiotic arrest. Despite this, it appears that functional GJA4 gap junctions, whether homotypic or heterotypic, are necessary to facilitate cGMP diffusion into the oocyte to maintain high levels of intra-oocyte cAMP and therefore meiotic arrest.

3. GLYT1 activity is suppressed in preovulatory cultured antral follicles.

3.1 GLYT1 activity is reversibly suppressed in cultured antral follicles.

GLYT1 activity has previously been shown to develop spontaneously following oocyte isolation from ovarian follicles which was not altered by the presence of adherent cumulus granulosa cells [Tartia et al. 2009]. It has not previously been determined, however, whether the presence of mural granulosa cells and/or follicular fluid is sufficient to maintain suppressed GLYT1 activity *in vitro*. I showed above that the ability of oocytes to activate high levels of GLYT1 activity was acquired during the late stages of oogenesis. Therefore, antral follicles were used as a model system in which oocytes were capable of activating GLYT1 but were enclosed within a physiologically relevant environment containing both mural and cumulus granulosa cells, functional gap junctional communication, and paracrine signalling mechanisms via follicular fluid.

To ascertain the involvement of mural granulosa cells in GLYT1 activity, I have compared GLYT1 activity levels in isolated denuded GV oocytes, COCs, and intact antral follicles (Figure 30). As expected, spontaneous GLYT1 activation occurred in denuded oocytes and COCs at a similar rate with maximal GLYT1 activity at ~3-4 hours. In contrast, GLYT1 activity was maintained at a low level in intact antral follicles for an extended culture period, an effect that was reversible following oocyte removal from cultured antral follicles (Figure 31). I further examined the ability of antral follicles to maintain GLYT1 suppression in punctured antral follicles and found that although GLYT1 activity remained low for short culture periods, GLYT1 activity increased over longer culture periods compared to intact antral follicles (Figure 32A). Interestingly, when NPPC and E_2 were added to culture medium, GLYT1 activity remained low in punctured antral follicles for

up to 20 hours which did not significantly differ from intact antral follicles (Figure 32B). These data could possibly indicate that NPPC-cGMP signalling is also directly involved in maintaining low GLYT1 activity in antral follicles since I showed above that meiotic arrest could only be maintained for long periods in punctured antral follicles when NPPC (and E_2) are added to culture medium, likely because of NPPC dilution from the follicular fluid into culture medium through the puncture site. This hypothesis is consistent with a requirement for mural granulosa cells since NPPC is exclusively secreted by mural, and not cumulus, granulosa cells. Alternatively, GLYT1 activity suppression may be mediated by signalling completely distinct from NPPC-cGMP signalling.

These results further confirm previous work that showed that the denuded oocyte and cumulus granulosa cells are insufficient to prevent spontaneous GLYT1 activation in culture [Tartia et al. 2009]. The ability of intact antral follicles to maintain low GLYT1 activity levels in culture however, suggests that mural granulosa cells may play a vital role in GLYT1 suppression within the antral follicle prior to an ovulatory stimulus. Although these data showed directly that at least mural granulosa cells are required to prevent GLYT1 activation, the mechanism of action remained unclear including whether cumulus granulosa cells were also involved and the requirement for gap junctional or paracrine signalling. These questions were further addressed in experiments discussed in the sections below.

3.2 LH-signalling can stimulate GLYT1 activation in intact antral follicles.

It has previously been shown that GLYT1 activation is stimulated *in vivo* by hCG administration in mice and that its activation is coincident with meiotic maturation and occurs at a similar rate as GLYT1 activation following oocyte isolation *in vitro* [Tartia et al. 2009]. To determine whether GLYT1 activation occurs in response to ovulatory LH-signalling *in vitro*, intact antral follicles were cultured with or without LH and GLYT1 activity was measured over 0-5 hours (Figure 33B). GLYT1 activity was significantly higher in intact antral follicles cultured with LH compared to follicles cultured without LH which occurred within a similar time-course as meiotic resumption (Figure 33A).

GLYT1 activation in antral follicles could be postulated to occur in response to LH-signalling either by activation of a signalling cascade within the antral follicle to "turn on" inactive GLYT1 or alternatively by disrupting an inhibitory signalling mechanism within the antral follicle constitutively suppressing GLYT1 activity at least during late-stage antral follicle development. The second scenario seems more likely since GLYT1 became rapidly activated in denuded oocytes and COCs following removal from the ovarian follicle and LH-stimulated GLYT1 activation occurred as quickly as meiotic maturation in intact follicles, which is known to occur because of a rapid decrease in NPPC-cGMP inhibitory signalling [Zhang et al. 2010; 2011; Norris et al. 2008; Jaffe & Egbert 2016]. Thus, from these results, I hypothesize that low GLYT1 activity is maintained in antral follicles by constitutively active inhibitory signalling originating from the mural granulosa cells and that LH-signalling leads to a disruption in this signalling mechanism leading indirectly to GLYT1 activation.

4. GLYT1 activation and meiotic maturation occur simultaneously but are mediated by distinct signalling mechanisms within the antral follicle.

4.1 GLYT1 suppression in the antral follicle is not acutely dependent on gap junctional communication.

The similarity in GLYT1 activation and meiotic resumption following both isolation from ovarian follicles *in vitro* and LH-stimulation *in vivo* and *in vitro* suggests that these two processes may share a common regulatory mechanism [Tartia et al. 2009]. The signalling mechanism mediating the maintenance of prophase I arrest has been elucidated and found to depend on gap junctional communication between granulosa cells and between the oocyte and innermost granulosa cells, as further confirmed in the above experiments [Norris et al. 2008; Richard & Baltz 2014; Jaffe & Egbert 2016].

To rapidly inhibit gap junctional communication, AGA was added to culture medium and the timing of meiotic resumption compared to GLYT1 activation was examined in response to general gap junction inhibition. I would expect GLYT1 activation to occur as quickly as meiotic resumption if GLYT1 suppression is dependent on gap junctional communication. In COCs meiotically arrested with NPPC, gap junction inhibition rapidly stimulated meiotic resumption reflecting the disruption in cGMP diffusion to the oocyte (Figure 35A), while GLYT1 was spontaneously activated in COCs regardless of whether gap junctions were inhibited (Figure 35C). This lack of effect on GLYT1 activation by AGA was expected since I previously showed that cumulus cells alone are insufficient to maintain low GLYT1 activity in culture.

Similarly, rapid meiotic resumption was observed in oocytes cultured within intact antral follicles in the presence of AGA (Figure 35B). However, GLYT1 activation was delayed by ~5 hours compared to meiotic resumption indicating that a gap junction-independent mechanism remained active within the follicle to prolong the suppression of GLYT1 activity after gap junctional communication was disrupted, leading to the timing of meiotic resumption and GLYT1 activation becoming decoupled (Figure 35D). This same effect was observed in punctured antral follicles in which Cx43 CMPs were used to specifically inhibit gap junctions between mural granulosa cells with an even longer delay in GLYT1 activation observed (~6-8 hours) compared to meiotic resumption (Figure 36).

Although delayed compared to meiotic resumption, GLYT1 activity did eventually increase in intact and punctured antral follicles in the presence of AGA or Cx43 CMP. I hypothesize that the delayed GLYT1 activation is not a direct result of gap junction inhibition but rather a secondary effect that occurs in response to an altered physiology of the antral follicle following long-term gap junctional inhibition. Disruption of intercellular signalling via gap junctions could possibly lead to altered MGC function over time and therefore a reduction in a GLYT1-inhibitory signal normally originating from these cell types in the follicle; however, further experiments are required to both identify this possible inhibitory signal and determine whether prolonged gap junction inhibition alters MGC physiology.

These results point to a GLYT1-inhibitory mechanism propagated by signalling that is independent of gap junctional communication. Previous studies have shown that following LH stimulation, the concentration of cGMP in MGCs is reduced leading to a rapid diffusion of cGMP out of cumulus granulosa cells and the oocyte through gap

junctions leading to an overall decrease in oocyte cGMP and meiotic resumption [Shuhaibar et al. 2015; Jaffe & Egbert 2016]. Therefore, gap junctional communication appears to be involved in both the maintenance of prophase I arrest and meiotic resumption following LH-stimulation by regulating the diffusion of cGMP into and out of the oocyte. Since gap junction inhibition did not appear to directly cause GLYT1 activation in antral follicles, it is likely that the maintenance of GLYT1 suppression prior to ovulation and GLYT1 activation following LH-stimulation instead relies on paracrine signalling between granulosa cells and/or the oocyte and not gap junctional communication as in the maintenance of meiotic arrest.

4.2 Low GLYT1 activity in the antral follicle is maintained by mechanisms which are distinct from NPPC-cGMP signalling.

I showed above that GLYT1 activation occurs spontaneously in COCs maintained in meiotic arrest with NPPC and E_2 and that maintenance of low GLYT1 activity within the antral follicle is not acutely dependent on gap junctional communication. These results suggest that GLYT1 suppression is not maintained by the NPPC-cGMP signalling known to mediate meiotic arrest. However, it was possible that although the concentration of NPPC in my culture system was sufficient to maintain meiotic arrest in COCs, the level was too low to additionally maintain low GLYT1 activity. To examine whether a higher concentration of NPPC was required for GLYT1 suppression in COCs, increased concentrations of NPPC were added to COC culture medium and the effect on GLYT1 activity was examined. Although all tested concentrations of NPPC successfully maintained meiotic arrest in COCs (except for the highest concentration due to possible

toxicity or downregulation of NPR2), spontaneous GLYT1 activation occurred under all culture conditions (Figure 34A). Since hypoxanthine and guanosine contribute to cGMP production in granulosa cells downstream of NPPC signalling, these compounds were added together to COC culture medium (with NPPC and E_2) but were unable to prevent GLYT1 activation [Wigglesworth et al. 2013] (Figure 34B, C). The oocyte-specific cGMP phosphodiesterase PDE9 inhibitor, BAY 73-6691, has previously been shown to contribute to cGMP-mediated meiotic arrest. Therefore, this inhibitor was added to culture medium containing NPPC and E_2 and GLYT1 activity was measured in cultured COCs [Hanna et al. 2012]. Similar to the previous culture conditions, GLYT1 was again spontaneously activated despite the maintenance of meiotic arrest in nearly all COCs (Figure 34B, C). Finally, in an attempt to maximize NPPC-cGMP signalling, hypoxanthine, guanosine, BAY73-6691, and NPPC/E_2 were added to culture medium together. However, once again GLYT1 was spontaneously activated to high activity levels (Figure 34B, C).

The inability of NPPC-cGMP signalling to maintain low GLYT1 activity in cultured COCs despite meiotic arrest maintenance, and the delay in GLYT1 activation compared to meiotic resumption in antral follicles following gap junction inhibition together suggested that the maintenance of low GLYT1 activity in the antral follicle is distinct from the mechanisms mediating meiotic arrest. Since meiotic (nuclear) maturation occurs in response to a disruption in the propagation of inhibitory NPPC-cGMP signalling, it is likely that GLYT1 activation is mediated by different signalling mechanisms active during oocyte maturation. Although meiotic, or “nuclear”, maturation has been a primary focus of study in the past, more recently “cytoplasmic” maturation has also been shown to occur in the oocyte following LH-signalling. Studies have emerged which demonstrate the

essential role in embryo development for cytoplasmic maturation which includes events such as cytoskeletal reorganization, the redistribution of organelles, and chromatin remodelling [Luciano et al. 2012; Dalton & Carroll 2013; Coticchio et al. 2015]. These extensive cytoplasmic maturation processes appear to be diversely regulated and it is possible that one or more of the regulatory signalling mechanisms controlling components of cytoplasmic maturation are involved in GLYT1 activation or suppression. However, further studies are required to elucidate the signalling cascades mediating cytoplasmic maturation and any connection to GLYT1 suppression or activation remains to be determined [Coticchio et al. 2015]. What is clear from the above experiments is that GLYT1 activity is regulated by a mechanism that appears to be independent of NPPC-mediated meiotic arrest, demonstrating a significant physiological event occurring during oocyte maturation which is not controlled by the mechanisms mediating meiotic (nuclear) maturation.

5. A putative inhibitory signalling mechanism in the antral follicle responsible for maintaining low GLYT1 activity likely originates from MGCs and may be mediated by components of the ECM.

5.1 MGCs maintain GLYT1 suppression in isolated COCs.

The observation that low GLYT1 activity could be maintained in cultured antral follicles but not COCs or denuded oocytes suggests that MGCs play a role in GLYT1 suppression prior to ovulation. To further examine this hypothesis, I cultured MGCs as a monolayer and examined the effect on GLYT1 activity in COCs cultured on the MGC

monolayer. I found that low GLYT1 activity was indeed maintained for at least 4 hours in COCs when cultured on a monolayer of MGCs pre-plated on collagen IV (Figure 37F & Figure 38B); this was the first time that spontaneous GLYT1 activation was prevented from occurring in isolated COCs. The MGCs appeared morphologically normal and seemed to function like those *in vivo* within the follicle since meiotic arrest was maintained in the absence of additional NPPC added to medium indicating that sufficient NPPC was produced by the MGC monolayer alone to prevent spontaneous meiotic resumption in isolated COCs (Figure 38A) [Lee et al. 2013].

These results combined with the ability of GLYT1 suppression to be maintained in cultured antral follicles, but not COCs, suggests that MGCs are required to maintain low GLYT1 activity within the antral follicle. Since I showed above that the maintenance of low GLYT1 activity in antral follicles was not directly dependent on gap junctional communication, I hypothesized that paracrine signalling may play a role in GLYT1 suppression. NPPC is secreted from MGCs and diffuses through the antral fluid to bind its cognate NPR2 receptor in granulosa cells and increases cGMP production. It is only after this point in this signalling pathway that diffusion of cGMP through gap junctions is essential to deliver sufficient cGMP to the oocyte to inhibit the cAMP phosphodiesterase [Zhang et al. 2010; Norris et al. 2008]. Similar to the upstream NPPC signalling mechanism in the meiotic arrest pathway, I hypothesized that the putative GLYT1-inhibitory signalling cascade within the antral follicle originates from a factor secreted from MGCs which is propagated via paracrine signalling to the cumulus cells or oocyte. To examine this, culture medium was collected following an overnight incubation of MGCs on a collagen IV matrix and COCs (maintained in meiotic arrest with NPPC and E_2) were then added to the

conditioned medium and GLYT1 activity was examined after a 4-hour period. Compared to medium from plastic wells alone or collagen IV alone, GLYT1 activity was significantly lower when COCs were cultured in conditioned medium from MGCs (Figure 39). This data supports the hypothesis that MGCs are involved in maintaining low GLYT1 activity in the antral follicle possibly by secreting a factor into the follicular fluid. However, the identity of this inhibitory factor remains to be determined.

5.2 Engelbreth-Holm-Swarm mouse tumor (EHS) matrix maintains low GLYT1 activity in cultured COCs, but not denuded oocytes.

Interestingly, when EHS Matrix was used as a coating matrix, lower GLYT1 activity was measured in COCs cultured on the EHS Matrix compared to plastic alone, even in the absence of MGCs (Figure 40). This effect was found to be reversible since GLYT1 activity was increased to normal levels following removal of COCs from the EHS Matrix (Figure 41). EHS Matrix has previously been shown to contain endogenous growth factors known to influence cell differentiation including transforming growth factor β (TGF-β) and epidermal growth factor (EGF), as well as insulin-like growth factor 1 (IGF-1), and platelet-derived growth factor (PDGF) [Vukicevic et al. 1992]. It was possible that the maintenance of low GLYT1 activity measured in COCs cultured on EHS Matrix was influenced by one or more of these endogenous growth factors. Therefore, a growth factor-reduced (GFR) EHS Matrix was used as a coating surface and compared to "normal" EHS Matrix for the ability to prevent the development of high GLYT1 activity in COCs. Following a 4-hour culture period, however, GLYT1 activity remained low in COCs cultured on the GFR EHS Matrix which was not significantly different from normal EHS

Matrix suggesting that endogenous growth factors within the EHS Matrix were not directly responsible for maintaining low GLYT1 activity (Figure 42). Although growth factor concentrations are reduced in the GFR EHS Matrix, these growth factors are not completely absent and therefore I could not completely rule out their possible involvement in suppressing full GLYT1 activation in COCs based on this experiment alone.

The involvement of each cell type within the ovarian follicle for the maintenance GLYT1 suppression has not previously been determined and the above experiments provide the first evidence that at least MGCs are likely required for the propagation of a putative GLYT1-inhibitory signal in the pre-ovulatory follicle. The isolation and culture of MGCs is a time-consuming and difficult process and the ability of EHS Matrix alone to prevent the development of high GLYT1 activity in isolated COCs provided a simple model with which to examine the conditions surrounding this maintenance of GLYT1 suppression, such as the requirement for cumulus granulosa cells. Meiotically arrested and meiotically maturing denuded oocytes cultured on EHS Matrix were found to spontaneously activate GLYT1 normally, suggesting that cumulus granulosa cells are needed for the maintenance of low GLYT1 activity (Figure 43). Somewhat surprisingly, when COCs were co-cultured with denuded oocytes, GLYT1 again was activated normally despite the maintenance of GLYT1 suppression in the co-cultured COCs (Figure 44). If paracrine signalling, and not gap junctional communication, was involved in the maintenance of low GLYT1 activity in the antral follicle, I would expect the addition of cumulus cells to enable the maintenance of a similarly low level of GLYT1 activity in denuded oocytes. It is possible that a paracrine factor from the cumulus cells is secreted and involved in GLYT1 suppression in the oocyte but that it becomes too diluted within

the culture medium and therefore insufficient concentrations are available to prevent spontaneous GLYT1 activation in denuded oocytes. Alternatively, other intercellular signalling mechanisms could be involved in this putative inhibitory pathway within the COC such as signal transduction pathways which are mediated by direct cell-to-cell interactions; this hypothesis would be consistent with my observations that COCs, but not denuded oocytes, are stably adhered to the EHS Matrix during culture (discussed below).

5.3 EHS matrix-mediated GLYT1 suppression is only maintained in meiotically-arrested COCs.

My results and previous work have demonstrated that spontaneous GLYT1 activation proceeds in isolated COCs and oocytes regardless of whether oocytes are maintained in meiotic arrest or allowed to resume meiosis [Tartia et al. 2009]. However, it has not previously been possible to prevent spontaneous GLYT1 activation in cultured COCs and therefore whether GLYT1 suppression can be maintained even during meiotic maturation has not previously been explored. Since I have determined that EHS Matrix can prevent the development of high GLYT1 activity in COCs without impeding meiotic resumption, I sought to examine whether these two events could remain uncoupled with GLYT1 suppression being maintained during meiotic maturation. Surprisingly, although low GLYT1 activity was maintained in COCs cultured on EHS Matrix when oocytes were maintained in prophase I arrest by NPPC, high GLYT1 activity developed in COCs cultured on EHS Matrix when meiotic maturation occurred (Figure 45). This result was unexpected since all previous work has shown distinct regulatory mechanisms mediating these two processes. Therefore, it appears that the maintenance of prophase I arrest in

oocytes is necessary but not sufficient to maintain low GLYT1 activity in COCs which could explain the above co-culture results in which denuded oocytes which resumed meiosis during culture were unable to maintain suppressed GLYT1 activity even in the presence of COCs. Since GLYT1 suppression appears to require the maintenance of meiotic arrest, it is also possible that the eventual GLYT1 activation measured in antral follicles following extended culture with gap junction inhibitors could have been a secondary effect of the release of oocytes from meiotic arrest (Figures 35& Figure 36). Since meiotic resumption occurred rapidly in response to gap junction inhibition in intact and punctured antral follicles, oocytes in which the uptake of [^{3}H]-glycine was measured following gap junction inhibition had already resumed meiosis which could explain the GLYT1 activation observed in follicles exposed to gap junction inhibitors since GLYT1 suppression does not appear to be maintained under conditions where meiosis is allowed to resume.

5.4 Certain extracellular matrix components (EMs) suppress GLYT1 activation in COCs.

The composition of EHS Matrix is complex and contains many growth factors, proteases, and proteins in varying amounts which makes it difficult to narrow down the element(s) involved in the maintenance of low GLYT1 activity in COCs [Kleinman & Martin 2005; Hughes et al. 2010]. Predominant proteins known to be present in EHS Matrix include laminin (60%), type IV collagen (30%), nidogen (5%), heparan sulfateproteoglycans (<3%), and entactin (<1%) [Kleinman & Martin 2005; Kleinman et al, 1986]. Studies of the ovarian extracellular matrix (ECM) *in vivo* have primarily focused

on its role in the regulation of folliculogenesis and the distribution of extracellular matrix components (EMs) during follicle growth and development. The most commonly examined ECM proteins in the ovary include laminin, fibronectin, collagen I, and collagen IV with differing expression patterns observed within specific cellular compartments within the ovarian follicle and throughout follicle growth. In the mouse, collagen I is expressed throughout the ovarian follicle at all stages of folliculogenesis and within all cellular compartments including minimal expression within the follicular fluid of antral follicles. In contrast, collagen IV and laminin are most heavily expressed in the theca compartment and basement membrane (basal lamina) with some expression in granulosa cells and with expression increasing within the ovarian follicle at later stages of folliculogenesis. Finally, fibronectin is expressed in the follicle basement membrane with the heaviest expression in follicular fluid increasing in intensity as folliculogenesis progresses [Berkholtz et al. 2006a].

Based on these ECM expression patterns in mouse ovaries and the major components of EHS Matrix, COCs were cultured on isolated preparations of EMs and the ability of each EM to maintain GLYT1 suppression was examined compared to EHS Matrix. Laminin and collagen I were the most effective at maintaining low GLYT1 activity in COCs, fibronectin was somewhat effective, while collagen IV was unable to maintain GLYT1 suppression in cultured COCs (Figure 46). Since laminin was as effective as EHS Matrix in maintaining GLYT1 suppression in COCs and since EHS Matrix is largely comprised of laminin (~60% [Kleinman et al. 1986]), laminin isolated from EHS was used as a coating surface for COCs and the ability of an anti-laminin antibody to overcome laminin-mediated GLYT1 suppression in isolated COCs was examined. Interestingly, in

the presence of the anti-laminin antibody, adhesion of COCs to the laminin surface coating was reduced and GLYT1 activity was significantly increased compared to COCs cultured on laminin in the absence of anti-laminin antibody (Figure 47).

The laminin isolated from EHS is laminin-111, which was the first identified laminin protein and is named for the combined subunits α1, β1, and γ1. The laminin isoform used as the purified laminin coating surface in the above experiments was laminin-111 also isolated from EHS [Irving-Rodgers et al. 2010]. Laminins are large ECM heterotrimeric proteins consisting of an α, β, and γ subunit of which there are five α, four β, and three γ subunits identified allowing for vast diversity in the possible laminin proteins (50+), however only ~16 have previously been predicted or identified in tissues [Aumailley 2013]. Although laminin-111 is widely expressed throughout preimplantation embryo development, the expression of this laminin isoform is rare in adults. In the mouse, various laminin subunits have been identified which differ in their expression patterns throughout folliculogenesis. Interestingly, the laminin subunits α1, β1, and γ1 are expressed throughout all stages of folliculogenesis at the basement membrane (basal lamina) and in larger aggregates deposited between granulosa cells termed the "focimatrix". The laminin subunit α2 is expressed only in some preantral and some antral follicles at the basal lamina while other laminin subunits including α4 and α5 have not been detected at any stage of folliculogenesis [Irving-Rodgers et al. 2004; 2010; Irving-Rodgers & Rodgers 2005].

Folliculogenesis is a dynamic process in the ovary requiring continuous tissue remodelling as follicles develop and eventually become atretic or ovulate. Reorganization of the extracellular matrix (ECM) is essential to accommodate the growing follicles and to mediate cellular processes involved in folliculogenesis including but not limited to

maintenance of normal cell morphology, cell survival, differentiation, and steroidogenesis [Berkholtz et al. 2006b]. As discussed above, laminin and collagen IV are heavily expressed in the ovarian basal lamina (and focimatrix) throughout folliculogenesis as well as in EHS Matrix with these two proteins often bound together in ECM. The ability of laminin alone, but not collagen IV alone, to maintain low GLYT1 activity in cultured COCs suggests that if the basal lamina or focimatrix participate in the signalling mechanism maintaining suppressed GLYT1 in the follicle, the effect may be predominantly mediated by a laminin-specific mechanism in these structures (Figure 46). Collagen I was also shown to maintain GLYT1 suppression in COCs and is expressed throughout the ovarian follicle at all stages of folliculogenesis, therefore the involvement of this EM in a putative GLYT1 inhibitory mechanism cannot be ruled out (Figure 46).

Laminin's effect on cells is accomplished by C-terminal binding to cell surface receptors on neighbouring cells with binding specificity often determined by the type of α subunit present in the laminin isoform [Aumialley 2013]. The interaction of cumulus cells with laminin was confirmed in the above experiments by the tight adhesion of COCs to the laminin surface coating. Since GLYT1 activation of COCs cultured on laminin by the laminin antibody was accompanied by a reduced adhesion (and migration) of cumulus cells on the laminin surface, it is tempting to hypothesize that maintenance of low GLYT1 activity in the follicle is at least partly mediated by ECM-cell and/or cell-cell adhesion-dependent signalling, propagated through granulosa cells to the oocyte possibly via the stalk connecting the outer mural granulosa cells with the inner cumulus granulosa cells; however, this remains to be investigated. It is important to note that COC adhesion was

observed regardless of the coating surface used (including poly-lysine) and therefore adhesion alone was not sufficient to maintain low GLYT1 activity in isolated COCs.

A major mechanism in laminin-mediated transmission of mechanical and biochemical signalling involves binding of laminin to integrins. Integrins are heterodimeric transmembrane proteins consisting of an α and β subunit associated by non-covalent bonds that are mainly expressed extracellularly with short cytoplasmic tails. Binding of ligands (such as laminin) induces conformational changes in the integrin structure enabling the propagation of signalling into the cell (outside-in signalling) or even extracellularly (inside-out signalling) [Harburger & Calderwood 2009]. There are currently 18 α subunits and 8 β subunits identified which can combine to form 24 different integrin isoforms all of which bind with varying affinity to specific EMs. Integrin-mediated signalling has previously been shown to influence granulosa cell survival, proliferation, and differentiation through various signalling cascades which could potentially be involved in maintaining GLYT1 suppression in follicles and several integrin isoforms have previously been identified in oocytes and MII eggs, however the potential role of this complex signalling mechanism in GLYT1 activity requires further study [Evans et al. 1995; Oktay et al. 2000; Le Bellego et al. 2002, 2005; Berkholtz et al. 2006b; Rolaki et al. 2007].

The ability of fibronectin to somewhat maintain low GLYT1 activity in cultured COCs adds further complexity to the above hypothesis since fibronectin was previously found to be mostly expressed as a soluble factor in the follicular fluid (Figure 46) [Berkholtz et al. 2006a]. It is possible that EMs secreted from MGCs into follicular fluid also contribute to GLYT1 suppression in the follicle to further propagate laminin/collagen I intercellular signalling; this could explain the ability of conditioned medium from

cultured MGCs to maintain low GLYT1 activity in COCs. Although future studies are required to identify the exact mechanism(s) mediating GLYT1 activity before and after an ovulatory trigger, the above data supports the hypothesis that a factor from the MGCs is required to transmit an intra-follicular inhibitory signal involving cumulus granulosa cells to maintain GLYT1 suppression in the oocyte independent of gap junctional communication, possibly by ECM-integrin intercellular and intracellular signalling.

CONCLUSIONS

The results presented in my thesis have revealed aspects of the mechanism(s) mediating suppression of the GLYT1 transporter within the ovarian follicle prior to the LH-induced ovulatory stimulus or removal of oocytes from antral follicles *in vitro*. My experimental data has shown that MGCs are required to maintain suppressed GLYT1 activity, possibly by the release of an inhibitory factor into follicular fluid which acts on the cumulus granulosa cells and/or oocyte to propagate inhibitory signalling which does not require gap junctional communication (Figure 48A1). The ability of specific extracellular matrix components (EMs) to maintain GLYT1 suppression in cultured COCs further suggests that low GLYT1 activity in the ovarian follicle may be mediated by ECM-cell and/or cell-cell adhesion-dependent signalling, propagated through granulosa cells to the oocyte possibly via the stalk connecting the outer mural granulosa cells with the inner cumulus granulosa cells (Figure 48A2) or by the actions of EMs present in follicular fluid (Figure 48A3). Despite the predicted similarity in the mechanisms mediating maintenance of meiotic arrest and GLYT1 suppression, such as the requirement of MGCs and the propagation of an inhibitory signal within the ovarian follicle, I have shown that these two processes are likely mediated by distinct signalling components. Based on my results, I hypothesize that GLYT1 activation following LH-stimulation occurs indirectly due to a loss of this putative GLYT1-inhibitory signal either by a decrease in a MGC-derived inhibitory signal (Figure 48B1) and/or possibly a change in the composition of the extracellular matrix (Figure 48B2, 3), however this remains to be investigated. At ovulation, the COC is extruded from the ovarian follicle and therefore any connection of

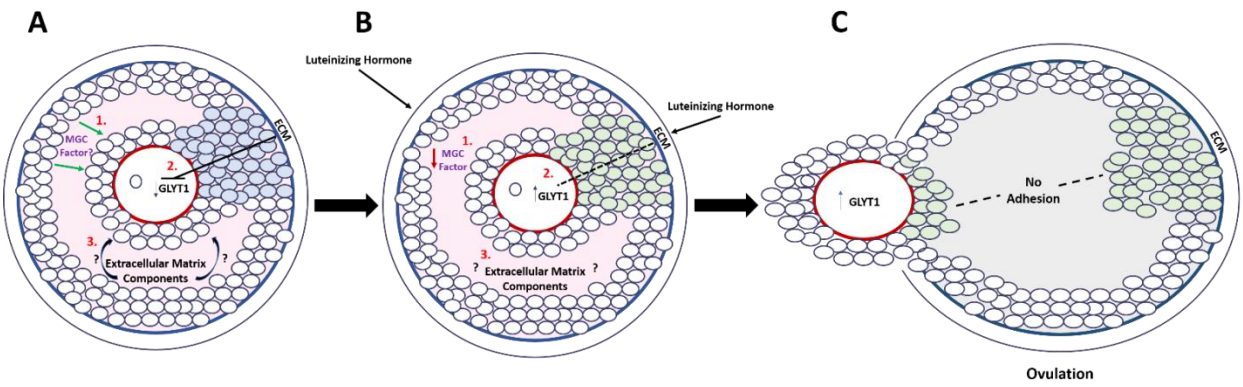

Figure 48. **GLYT1 suppression in the ovarian follicle and GLYT1 activation following an ovulatory stimulus.** Hypothetical illustration of the mechanism(s) mediating GLYT1 suppression within the ovarian follicle and GLYT1 activation following LH-stimulation. (**A**) **GLYT1 suppression in the ovarian follicle**. (**1.**) A putative inhibitory signal is released from the MGCs into follicular fluid and acts at the cumulus cells and/or oocyte to maintain GLYT1 suppression. (**2.**) Extracellular matrix (ECM) components (blue circles) contribute to maintenance of GLYT1 suppression in the ovarian follicle via cell-cell or cell-ECM signalling. (**3.**) Soluble extracellular matrix components found in follicular fluid contribute to maintenance of GLYT1 suppression in the ovarian follicle. (**B**) **GLYT1 activation following LH-stimulation.** (**1.**) LH binding to LH-receptors on outer mural granulosa cells decreases the release of a MGC-derived GLYT1 inhibitory factor. (**2.**) Following LH-binding to LH receptors on outer mural granulosa cells, changes in ECM composition (green circles) or adhesion occur leading to changes in GLYT1-inhibitory signalling mechanisms. (**3.**) Following LH-binding to LH receptors on outer mural granulosa cells, secretion of components (such as soluble extracellular matrix components) into follicular fluid is decreased leading to changes in GLYT1-inhibitory signalling. (**C**) **GLYT1 activity at ovulation**. At ovulation, the COC is extruded from the ovarian follicle

and therefore any connection of cumulus cells with MGCs is lost and the COC is no longer bathed in follicular fluid likely ensuring the prolonged maintenance of high GLYT1 activity for volume regulation in the absence of an inhibitory signal.

cumulus cells with MGCs is lost and the COC is no longer bathed in follicular fluid likely ensuring the prolonged maintenance of high GLYT1 activity for volume regulation in the absence of an inhibitory signal (Figure 48C).

My thesis work has also demonstrated that GLYT1 is expressed throughout oogenesis with the ability of small growing oocytes to activate GLYT1 to low levels and nearly fully-grown oocytes to activate high levels of GLYT1 activity following removal from the follicle. My immunofluorescence data has shown that GLYT1 is primarily localized to the oocyte plasma membrane during development and prior to GLYT1 activation in fully grown oocytes. Thus, the putative inhibitory signalling mechanism(s) involved in the maintenance of GLYT1 suppression within the ovarian follicle is likely present throughout oogenesis to prevent spontaneous activation of GLYT1 transporters at the plasma membrane from occurring in the follicle prior to LH-stimulation.

The results of my thesis work have revealed the existence of another major intra-follicular signalling mechanism involving multiple cell types within the follicle which is distinct from signalling involved in the maintenance of meiotic arrest. The identity of this signalling mechanism might be utilized in the development of human IVM practices capable of supporting complete oocyte competence acquisition and maturation *in vitro* to produce fertilizable and healthy oocytes and preimplantation embryos. The maintenance of GLYT1 suppression may be required to maintain intercellular communication between the oocyte and cumulus granulosa cells thereby ensuring the completion of both cytoplasmic and nuclear maturation processes. It is possible that certain EMs could be used as a coating surface for the culture of COCs in human IVM procedures since I showed that GLYT1 could at least temporarily be suppressed when COCs were cultured on these

surfaces and may therefore be able to prolong physiological oocyte development *in vitro* to produce fully competent oocytes. Therefore, my results presented in this thesis have answered basic physiological questions regarding the regulation of GLYT1-mediated volume regulatory mechanisms within the ovarian follicle throughout oogenesis and have provided a base upon which future work can be performed to identify the exact components of this putative intra-follicular GLYT1 inhibitory signal to be applied to the improvement of ART technologies and to the overall body of scientific knowledge regarding volume regulatory mechanisms in oocytes and preimplantation embryos.

LITERATURE CITED

Abel M.H. et al. (2000). The effect of a null mutation in the follicle-stimulating hormone receptor gene on mouse reproduction. *Endocrinology*; 141(5):1795-803.

Ackert C.L et al. (2001). Intercellular communication via connexin43 gap junctions is required for ovarian folliculogenesis in the mouse. *Dev Biol*; 233:258-270.

Adhikari D. et al. (2012). Cdk1, but not Cdk2, is the sole Cdk that is essential and sufficient to drive resumption of meiosis in mouse oocytes. *Hum Mol Genet*; 21(11):2476-84.

Al-Habori M. (2001). Macromolecular crowding and its role as intracellular signalling of cell volume regulation. *Int J Biochem Cell Biol*; 33(9):844-64.

Alexander R.T. & Grinstein S. (2006). Na^+/H^+ exchangers and the regulation of volume. *Acya Physiol (Oxf);* 187(1-2):159-67.

Alexandre H. (2001). A history of mammalian embryological research. *Int J Dev Biol*; 45(3):457-67.

Ali A.A. et al. (2003). Antioxidant requirements for bovine oocytes varies during in vitro maturation, fertilization and development. *Theriogenology*; 59(3-4):939-49.

Alper S.L. (2006). Molecular physiology of SLC4 anion exchangers. *Exp Physiol*; 91(1):153-61.

Anas M.K. et al. (2007). The organic osmolytes betaine and proline are transported by a shared system in early preimplantation mouse embryos. *J Cell Physiol*; 210(1):266-77.

Anas M.K. et al. (2008). SIT1 is a betaine/proline transporter that is activated in mouse eggs after fertilization and functions until the 2-cell stage. *Development*; 135(24):4123-30.

Anderson E.& Albertini D.F. (1976). Gap junctions between the oocyte and companion follicle cells in the mammalian ovary. *J Cell Biol*; 71(2):680-6.

Aragón M.C. et al. (1987). Stoichiometry of sodium- and chloride-coupled glycine transport in synaptic plasma membrane vesicles derived from rat brain. *FEBS Lett*; 212(1):87-90.

Aumailley M. (2013). The laminin family. *Cell Adh Migr*; 7(1):48-55.

Baltz J.M. (2001). Osmoregulation and cell volume regulation in the preimplantation embryo. *Curr Top Dev Biol*; 52:55-106.

Baltz J.M.& Tartia A.P. (2010). Cell volume regulation in oocytes and early embryos: connecting physiology to successful culture media. *Hum Reprod Update*; 16(2):166-76.

Baltz J.M. (2012). Media composition: salts and osmolality. *Methods Mol Biol*; 912:61-80.

Baltz J.M.& Zhou C. (2012). Cell volume regulation in mammalian oocytes and preimplantation embryos. *Mol Reprod Dev*; 79(12):821-31.

Baltz J.M et al. (2013). Measuring transport and accumulation of radiolabeled substrates in oocytes and embryos. *Meth Molec Biol*;957:163-78.

Barrera S.P. et al. (2015). PKC-dependent GlyT1 ubiquitination occurs independent of phosphorylation: inespecificity in lysine selection for ubiquitination. *PLoS One*; 10(9):e0138897.

Ben-Rafael Z. et al. (1988). Collagen matrix influences the morphologic features and steroid secretion of human granulosa cells. *Am J Obstet Gynecol*; 159(6):1570-4.

Berkholtz C.B. et al. (2006a). Distribution of extracellular matrix proteins type I collagen, type IV collagen, fibronectin, and laminin in mouse folliculogenesis. *Histochem Cell Biol*; 126(5):583-92.

Berkholtz C.B. et al (2006b). Extracellular matrix functions in follicle maturation. *Semin Reprod Med*;24(4):262-9.

Beyer E.C., Paul D.L., & Goodenough D.A. (1990). Connexin family of gap junction proteins. *J Membr Biol*; 116(3):187-94.

Biel M. (2009). Cyclic nucleotide-regulated cation channels. *J Biol Chem*; 284(14):9017-21.

Biggers J.D. et al. (1967). The pattern of energy metabolism in the mouse oocyte and zygote. *PNAS*; 58(2):560-7.

Biggers J.D. et al. (1988). Mammalian blastocyst: transport functions in a developing epithelium. *Am J Physiol*; 255(4 Pt 1):C419-32.

Biggers J.D. (1998). Reflections on the culture of the preimplantation embryo. *Int J Dev Biol*; 42(7):879-884.

Biggers J.D. et al. (1993). The protective action of betaine on the deleterious effects of NaCl on preimplantation mouse embryos in vitro. *Mol Reprod Dev*; 34(4):380-90.

Bliel J.D. &Wassarman P.M. (1980a). Structure and function of the zonapellucida: identification and characterization of the proteins of the mouse oocyte's zona pellucida. *Dev Biol*; 76(1):185-202.

Bliel J.D. &Wassarman P.M. (1980b). Synthesis of zonapellucida proteins by denuded and follicle-enclosed mouse oocytes during culture in vitro. *PNAS*; 77(2):1029-33.

Boja E.S. et al. (2003). Structural characterization of native mouse zonapellucida proteins using mass spectrometry. *J Biol Chem*; 278(36):34189-202.

Bolton V.N. et al. (1989). Development of spare human preimplantation embryos in vitro: an analysis of the correlations among gross morphology, cleavage rates, and development to the blastocyst. *J In Vitro Fertil Embryo Transfer*; 6(1):30-5.

Borgnia M. et al. (1999). Cellular and molecular biology of the aquaporin water channels. *Annu Rev Biochem*; 68:425-58.

Bork E.S.& Sander C. (1992). A large domain common to sperm receptors (Zp2 and Zp3) and TGF-beta type III receptor. *FEBS Lett*; 300(3):237-40.

Borland R.M. et al. (1977). The elemental composition of the environments of the gametes and preimplantation embryo during the initiation of pregnancy. *Biol Reprod*; 16(2):147-57.

Bornslaeger E.A. et al. (1984). Regulation of mouse oocyte maturation: involvement of cyclic AMP phosphodiesterase and calmodulin. *Dev Biol*; 105(2):488-99.

Borowsky B. et al. (1993). Two glycine transporter variants with distinct localization in the CNS and peripheral tissues are encoded by a common gene. *Neuron*; 10(5):851-63.

Borowsky B.& Hoffman B.J. Analysis of a gene encoding two glycine transporter variants reveals alternative promoter usage and a novel gene structure. *J Biol Chem*; 273(44):29077-85.

Bortner C.D.& Cidlowski J.A. (1996). Absence of volume regulatory mechanisms contributes to the rapid activation of apoptosis in thymocytes. *Am J Physiol*; 271(3 Pt 1):C950-61.

Brachet A. (1912). Développement in vitro de blastodermes et de jeunes embryons de Mammifères. *C R Acad Sci Paris*; 155:1191-1193.

Brokamp C. et al. (2012). Electrophysiology of single and aggregate Cx43 hemichannels. *PLoS One;* 7:e47775.

Browe D.M.& Baumgarten C.M. (2006). EGFR kinase regulates volume-sensitive chloride current elicited by integrin stretch via PI-3K and NADPH oxidase in ventricular myocytes. *J Gen Physiol*; 127(3):237-51.

Brown H.M. et al. (2010). ADAMTS1 cleavage of versican mediates essential structural remodeling of the ovarian follicle and cumulus-oocyte matrix during ovulation in mice. *Biol Reprod*; 83(4):549-57.

Buccione R. et al. (1990a). FSH-induced expansion of the mouse cumulus oophorus in vitro is dependent upon a specific factor(s) secreted by the oocyte. *Dev Biol*; 138(1):16-25.

Buccione R., Schroeder A.C., & Eppig J.J. (1990b) Interactions between somatic cells and germ cells throughout mammalian oogenesis. *Bio Reprod*; 43(4):543-7.

Burg M.B. (2000). Macromolecular crowding as a cell volume sensor. *Cell Physiol Biochem*; 10(5-6):251-6.

Burg M.B. et al. (2007). Cellular response to hyperosmotic stresses. *Physiol Rev*; 87(4):1441-74.

Burg M.B.& Ferraris J.D. (2008). Intracellular organic osmolytes: function and regulation. *J Biol Chem*; 283(12):7309-13.

Bussolati O. et al. (2001). The role of system A for neutral amino acid transport in the regulation of cell volume. *Mol Membr Biol*; 18(1):27-38.

Cakmak H et al. (2016). Dynamic secretion during meiotic reentry integrates the function of the oocyte and cumulus cells. *PNAS*; 113(9):2424-9.

Camous S. et al. (1984). Cleavage beyond the block stage and survival after transfer of early bovine embryos cultured with trophoblastic vesicles. *J Reprod Fertil*; 72(2):479-85.

Caon M. (2008). Osmoles, osmolality and osmotic pressure: clarifying the puzzle of solution concentration. *Contemp Nurse*; 29(1):92-9.

Carabatsos M.J et al. (2000). Oocyte-granulosa cell heterologous gap junctions are required for the coordination of nuclear and cytoplasmic meiotic competence. *Dev Biol*; 226(2):167-79.

Carnegie J.A. et al. (1988). Culture of granulosa cells in collagen gels: the influence of cell shape on steroidogenesis. *Biol Reprod*; 38(4):881-90.

Cecconi S.& Colonna R. (1996). Influence of granulosa cells and of different somatic cell types on mammalian oocyte development in vitro. *Zygote*; 4(4):305-7.

Cetica P. et al. (2002). Activity of key enzymes involved in glucose and triglyceride catabolism during bovine oocyte maturation in vitro. *Reproduction*; 124(5):675-81.

Cha J.H. et al. (2001). Hydration status affects nuclear distribution of transcription factor tonicity responsive enhancer binding protein in rat kidney. *J Am Soc Nephrol*; 12(11):2221-30.

Chatot C.L. et al. (1989). An improved culture medium supports development of random-bred 1-cell mouse embryos in vitro. *J Reprod Fertil*; 86(2):679-88.

Chen L. et al. (1993). Functional significance of cumulus expansion in the mouse: roles for the preovulatory synthesis of hyaluronic acid within the cumulus mass. *Mol Reprod Dev*; 34(1):87-93.

Chen N.H. et al. (2004). Synaptic uptake and beyond: the sodium- and chloride-dependent neurotransmitter transporter family SLC6.*Pflugers Arch*; 447(5):519-31.

Cho W.K. et al. (1974). Inhibitory effect of dibutyryl cAMP on mouse oocyte maturation in vitro. *J Exp Zool*; 187(3):383-6.

Cockburn K., & Rossant J. (2010). Making the blastocyst: lessons from the mouse. *The Journal of Clinical Investigation*; 120:995-1003.

Collins J.L. & Baltz J.M. (1999). Estimates of mouse oviductal fluid tonicity based on osmotic responses of embryos. Biol Reprod 1999; 60(5):1188-93.

Conaghan J. et al. (1993). Effects of pyruvate and glucose on the development of human preimplantation embryos in vitro. *J Reprod Fertil*; 99(1):87-95.

Conti M. et al. (2002). Role of cyclic nucleotide signaling in oocyte maturation. *Molecular and Cellular Endocrinology*; 187:153-159.

Copp J. et al. (2005a). Hypertonic shock inhibits growth factor receptor signaling, induces caspase-3 activation, and causes reversible fragmentation of the mitochondrial network. *Am J Physiol Cell Physiol*; 288(2):C403-15.

Corbett H.E. et al. (2014). Uptake of betaine into mouse cumulus-oocyte complexes via the SLC7A6 isoform of y+L transporter. *Biol Reprod*; 90(4):81.

Corbett S. et al. (2014). The prevention of ovarian hyperstimulation syndrome. *J Obstet Gynaecol Can*; 36(11):1024-36.

Coticchio G. et al. (2012). Human oocyte maturation in vitro. *Int J Dev Biol*; 56(10-12):909-18.

Coticchio G. et al. (2015). Oocyte maturation: gamete-somatic cells interactions, meiotic resumption, cytoskeletal dynamics and cytoplasmic reorganization. *Hum Reprod Update*; 21(4):427-54.

Coyle J.T. (2006). Glutamate and schizophrenia: beyond the dopamine hypothesis. *Cell Mol Neurobiol*; 26(4-6):365-84.

Cubelos B. et al. (2005a). Localization of the GLYT1 glycine transporter at glutamatergic synapses in the rat brain. *Cereb Cortex*; 15(4):448-59.

Cubelos B. et al. (2005b). The scaffolding protein PSD-95 interacts with the glycine transporter GLYT1 and impairs its internalization. *J Neurochem*; 95(4):1047-58.

Da Silva-Buttkus, P. et al. (2008). Effect of cell shape and packing density on granulosa cell proliferation and formation of multiple layers during early follicle development in the ovary.*J Cell Sci*; 121(Pt 23):3890-900.

Dall'Asta V. et al. (1999). Amino acids are compatible osmolytes for volume recovery after hypertonic shrinkage in vascular endothelial cells. *Am J Physiol*; 276(4 Pt 1):C865-72.

Dalton C.M. & Carroll J. (2013). Biased inheritance of mitochondria during asymmetric cell division in the mouse oocyte. *J Cell Sci*; 126(Pt 13):2955-64.

Dawson K.M.& Baltz J.M. (1997). Organic osmolytes and embryos: substrates of the Gly and beta transport systems protect mouse zygotes against the effects of raised osmolarity. *Biol Reprod*; 56(6):1550-8.

Dawson K.M. et al. (1998). Osmolarity-dependent glycine accumulation indicates a role for glycine as an organic osmolyte in early preimplantation mouse embryos. *Biol Reprod*; 59(2):225-32.

de Vantery C. et al. (1997). Acquisition of meiotic competence in growing mouse oocytes Is controlled at both translational and posttranslational levels. *Dev Biol*; 187:43–54.

Demeestere I. et al. (2012). Follicle-stimulating hormone accelerates mouse oocyte development in vivo. *Biol Reprod*; 87(1):3, 1-11.

Devreker F. et al. (1999). Effects of taurine on human embryo development in vitro. *Hum Reprod*; 14(9):2350-6.

DiLuigi A. et al. (2008). Meiotic arrest in human oocytes is maintained by a Gs signaling pathway. *Biol Reprod*; 78(4):667-72.

Donahue R.P. & Stern S. (1968). Follicular cell support of oocyte maturation: production of pyruvate in vitro. *J Reprod Fertil*; 17(2):395-8.

Dong J. et al. (1996). Growth differentiation factor-9 is required during early ovarian folliculogenesis. *Nature*; 383(6600):531-5.

Downs S.M., Daniel S.A.J.& Eppig J.J. (1988). Induction of maturation in cumulus cell-enclosed mouse oocytes by follicle-stimulating hormone and epidermal growth factor:

evidence for a positive stimulus of somatic cell origin. *The Journal of Experimental Zoology*; 245:86-96.

Downs S.M. et al. (1996). Glucose utilization during gonadotropin-induced meiotic maturation in cumulus cell-enclosed mouse oocytes. *Mol Reprod Dev*; 44(1):121-31.

Downs S.M. et al. (1998). Meiotic induction in cumulus cell-enclosed mouse oocytes: involvement of the pentose phosphate pathway. *Biol Reprod*; 58(4):1084-94.

Downs S.M. (2000). Adenosine blocks hormone-induced meiotic maturation by suppressing purine de novo synthesis. *Mol Reprod Dev*; 56(2):172-9.

Downs S.M. et al. (2002). Pyruvate utilization by mouse oocytes is influenced by meiotic status and the cumulus oophorus. *Mol Reprod Dev*; 62(1):113-23.

Durkin J.T. et al. (2011). Amino-terminal isoforms of the human glycine transporter GlyT1 exhibit similar pharmacology. *Brain Res*; 1374:1-7.

Egbert J.R. et al. (2014). Dephosphorylation and inactivation of NPR2 guanylyl cyclase in granulosa cells contributes to the LH-induced decrease in cGMP that causes resumption of meiosis in rat oocytes. *Development*; 141(18):3594-604.

Egbert J.R. et al. (2016). Luteinizing hormone causes phosphorylation and activation of the cyclic GMP phosphodiesterase PDE5 in rat ovarian follicles, contributing, together with PDE1 activity, to the resumption of meiosis. *Biol. Reprod*; 94:110, 1–11.

el Khoury J. et al. (1994). Macrophages adhere to glucose-modified basement membrane collagen IV via their scavenger receptors. *J Biol Chem*; 269(14):10197-200.

El-Fouly M.A et al. (1970). Role of the ovum in follicular luteinization. *Endocrinology*; 87(2):286-93.

Emma F. et al. (1997). Intracellular electrolytes regulate the volume set point of the organic osmolyte/anion channel VSOAC. *Am J Physiol*; 272(6 Pt 1):C1766-75.

Emori C.& Sugiura K. (2014). Role of oocyte-derived paracrine factors in follicular development. *Anim Sci J*; 85(6):627-33.

Epifano O. et al. (1995). Coordinate expression of the three zonapellucida genes during mouse oogenesis. *Development*; 121(7):1947-56.

Eppig J.J.& Schroeder A.C. (1989). Capacity of mouse oocytes from preantral follicles to undergo embryogenesis and development to live young after growth, maturation, and fertilization in vitro. *Biol Reprod*; 41(2):268-76.

Eppig J.J.& Telfer E.E. (1993). Isolation and culture of oocytes. *Methods in Enzymology*; 225:77-84.

Eppig J.J. et al. (2000). Conditions that affect acquisition of developmental competence by mouse oocytes in vitro: FSH, insulin, glucose, and ascorbic acid. *Mol Cell Endocrinol*; 163(1-2):109-16.

Eppig J.J. (2001). Oocyte control of ovarian follicular development and function in mammals. *Reproduction*; 122(6):829-38.

Eppig J.J. et al. (2002). The mammalian oocyte orchestrates the rate of ovarian follicular development. *PNAS*; 99(5):2890-4.

Eppig J.J. et al. (2005). Mouse oocytes regulate metabolic cooperativity between granulosa cells and oocytes: amino acid transport. *Biol Reprod*; 73(2):351-7.

Erbach G.T. et al. (1994). Differential growth of the mouse preimplantation embryo in chemically defined media. *Biol Reprod*; 50(5):1027-33.

Erdogan S. et al. (2005). Mechanisms regulating intracellular pH are activated during growth of the mouse oocyte coincident with acquisition of meiotic competence. *Dev Biol*; 286(1):352-60.

Erdogan S. et al. (2011). Changes in the activity of defense mechanisms against induced acidosis during meiotic maturation in mouse oocytes. *Theriogenology*; 75(6):1057-66.

Eulenberg V. et al. (2005). Glycine transporters: essential regulators of neurotransmission. *Trends Biochem Sci*; 30(6):325-33.

Evans J.P. et al. (1995). Identification and localization of integrin subunits in oocytes and eggs of the mouse. *Mol Reprod Dev*; 40(2):211-20.

Evans J.P. (2002). The molecular basis of sperm-oocyte membrane interactions during mammalian fertilization. *Hum Reprod Update*; 8(4):297-311.

Evans J.P. & Robinson D.N. (2011). The spatial and mechanical challenges of female meiosis. *Mol Reprod Dev*; 78(10-11):769-77.

Evans W.H.& Martin P.E.M. (2002). Gap junctions: structure and function (review). *Molecular Membrane Biology;* 19:121-136.

Evans W.H. & Leybaert L. (2007). Mimetic peptides as blockers of connexin channel-facilitated intercellular communication. *Cell Commun Adhes*; 14:265–273.

Evans W.H. et al. (2012). Manipulating connexin communication channels: use of peptidomimetics and the translational outputs. *J Membr Biol*; 245:437–449.

Fadini R. et al. (2009). Effect of different gonadotrophin priming on IVM of oocytes from women with normal ovaries: a prospective randomized study. *Reprod Biomed Online*; 19(3):343-51.

Fadini R. et al. (2011). Anti-mullerian hormone as a predictive marker for the selection of women for oocyte in vitro maturation treatment. *J Assist Reprod Genet*; 28(6):501-8.

Fernández-Sánchez E. et al. (2008). Mechanisms of endoplasmic-reticulum export of glycine transporter-1 (GLYT1). *Biochem J*; 409(3):669-81.

Ferraris J.D. et al. (2002). Activity of the TonEBP/OREBP transactivation domain varies directly with extracellular NaCl concentration. *PNAS*; 99(2):739-44.

Fiorenza M.T. et al. (2004). Early transcriptional activation of the hsp70.1 gene by osmotic stress in one-cell embryos of the mouse. *Biol Reprod*; 70(6):1606-13.

Fitzgerald T.J. (1984). Attachment of Treponema pallidum to fibronectin, laminin, collagen IV, and collagen I, and blockage of attachment by immune rabbit IgG.*Br J Vener Dis*;60(6):357-63.

FitzHarris G. & Baltz J.M. (2006). Granulosa cells regulate intracellular pH of the murine growing oocyte via gap junctions: development of independent homeostasis during oocyte growth. *Development*; 133:591–599.

FitzHarris G. et al. (2007). Granulosa cells regulate oocyte intracellular pH against acidosis in preantral follicles by multiple mechanisms. *Development*; 134(23):4283-95.

Franciosi F. et al. (2016). FSH regulates mRNA translation in mouse oocytes and promotes developmental competence. *Endocrinology*; 157(2):872-82.

Francis S.H. et al. (2010). cGMP-dependent protein kinases and cGMP phosphodiesterases in nitric oxide and cGMP action.*Pharmacol Rev*; 62(3):525-63.

Fulop C. et al. (2003). Impaired cumulus mucification and female sterility in tumor necrosis factor-induced protein-6 deficient mice. *Development*; 130(10):2253-61.

Gabernet L. et al. (2005). Enhancement of the NMDA receptor function by reduction of glycine transporter-1 expression. *Neurosci Lett*; 373:79-84.

Gagnon K.B. et al. (2006). Volume sensitivity of cation-Cl-cotransporters is modulated by the interaction of two kinases: Ste20-related proline-alanine-rich kinase and WNK4. *Am J Physiol Cell Physiol*; 290(1):C134-42.

Galloway S.M. et al. (2000). Mutations in an oocyte-derived growth factor gene (BMP15) cause increased ovulation rate and infertility in a dosage-sensitive manner. *Nat Genet*; 25(3):279-83.

Garcia-Perez A. & Burg M.B. (1991). Renal medullary organic osmolytes. *Physiol Rev*; 71(4):1081-115.

Gardner D.K.& Lane M. (1993). Amino acids and ammonium regulate mouse embryo development in culture. *Biol Reprod*; 48(2):377-85.

Garner M.M.& Burg M.B. (1994). Macromolecular crowding and confinement in cells exposed to hypertonicity. *Am J Physiol*; 266(4 Pt 1):C877-92.

Garnovskaya N.M. et al. (2003). Hypertonicity activates Na^+/H^+ exchange through Janus kinase 2 and calmodulin. *J Biol Chem*; 278(19):16908-15.

Gatsios P. et al. (1998). Activation of the Janus kinase/signal transducer and activator of transcription pathway by osmotic shock. *J Biol Chem*; 273(36):22962-8.

Gautier J. et al. (1989). Dephosphorylation and activation of Xenopus p34cdc2 protein kinase during the cell cycle. *Nature*; 339(6226):626-9.

Geerlings A. et al. (2000). Characterization of the interactions between the glycine transporters GLYT1 and GLYT2 and the SNARE protein syntaxin 1A. *FEBS Lett*; 470(1):51-4.

Geerlings A. et al. (2001). Calcium- and syntaxin 1-mediated trafficking of the neuronal glycine transporter GLYT2. *J Biol Chem*; 276(20):17584-90.

Geerlings A. et al. (2002). Glycine transporter isoforms show differential subcellular localization in PC12 cells. *J Neurochem*; 82(1):58-65.

Gershon E., Plaks V., & Dekel N. (2008). Gap junctions in the ovary: expression, localization and function. *Mol Cell Endocrinol*; 282(1-2):18-25.

Gershon E. et al. (2008). Oocyte-directed depletion of connexin43 using the Cre-LoxP system leads to subfertility in female mice. *Dev Biol*; 313(1):1-12.

Giepmans B.N. et al. (2001). Interaction of c-Src with gap junction protein connexin-43. Role in the regulation of cell-cell communication. *J Biol Chem*; 276(11):8544-9.

Gittens J.E.& Kidder G.M. (2005). Differential contributions of connexin37 and connexin43 to oogenesis revealed in chimeric reaggregated mouse ovaries. *J Cell Sci*; 118(Pt 21):5071-8.

Gomeza J. et al. (1995). Regulation by phorbol esters of the glycine transporter (GLYT1) in glioblastoma cells. *Biochim Biophys Acta*;1233(1):41-6.

Gomeza J. et al. (2003a). Inactivation of the glycine transporter 1 gene discloses vital role of glial glycine uptake in glycinergic inhibition. *Neuron*; 40(4):785-96.

Gomeza J. et al. (2003b). Deletion of the mouse glycine transporter 2 results in a hyperekplexia phenotype and postnatal lethality. *Neuron*; 40(4):797-806.

Goodenough D.A., Simon A.M.& Paul D.L. (1999). Gap junctional intercellular communication in the mouse ovarian follicle. *Novartis Found Symp*; 219:226-35.

Grinstein S. et al. (1992). Activation of the Na^+/H^+ antiporter during cell volume regulation. Evidence for a phosphorylation-independent mechanism. *J Biol Chem*; 267(33):23823-8.

Grunder S. et al. (1992). Regions involved in the opening of ClC-2 chloride channel by voltage ad cell volume. *Nature*; 360(6406):759-62.

Guastella J. et al. (1992). Cloning, expression, and localization of a rat brain high-affinity glycine transporter. *PNAS*; 89(15):7189-93.

Haddad A.& Nagai M.E. (1977). Radioautographic study of glycoprotein biosynthesis and renewal in the ovarian follicles of mice and the origin of the zona pellucida. *Cell Tissue Res*; 177(3):347-69.

Hadi T. et al. (2005). Similar effects of osmolarity, glucose, and phosphate on cleavage past the 2-cell stage in mouse embryos from outbred and F1 hybrid females. *Biol Reprod*; 72(1):179-87.

Haghighat N. & Van Winkle L.J. (1990). Developmental change in follicular cell-enhanced amino acid uptake into mouse oocytes that depends on intact gap junctions and transport system Gly.*J Exp Zool*; 253(1):71-82.

Hammer M.A. et al. (2000). Glycine transport by single human and mouse embryos. *Hum Reprod*;15(2):419-26.

Hammer M.A. & Baltz J.M. (2002). Betaine is a highly effective organic osmolyte but does not appear to be transported by established organic osmolyte transporters in mouse embryos. *Mol Reprod Dev*; 62(2):195-202.

Hammer M.A. & Baltz J.M. (2003). Beta-alanine but not taurine can function as an organic osmolyte in preimplantation mouse embryos cultured from fertilized eggs. *Mol Reprod Dev*; 66(2):153-61.

Han L. et al. (2010). Insights into egg coat assembly and egg-sperm interaction from the X-ray structure of full-length ZP3. *Cell*; 143(3):404-15.

Handler J.S.& Kwon H.M. (1996). Regulation of the myo-inositol and betaine cotransporters by tonicity. *Kidney Int*; 49(6):1682-3.

Hanley J.G. et al. (2000). GABA receptor rho1 subunit interacts with a novel splice variant of the glycine transporter, GLYT-1. *J Biol Chem*; 275(2):840-6.

Hanna C.B. et al. (2012). Identification of phosphodiesterase 9A as a cyclic guanosine monophosphate-specific phosphodiesterase in germinal vesicle oocytes: a proposed role in the resumption of meiosis. *Fertil Steril*; 98(2):487-95.e1.

Harburger D.S. & Calderwood D.A. (2009). Integrin signalling at a glance. *J Cell Sci*; 122(Pt 2):159-63.

Harding E.A. et al. (2002). Developmental stages in the management of acid loads during preimplantation mouse development. *Biol Reprod*; 67(5):1419-29.

Harris A.L. (2001). Emerging issues of connexin channels: biophysics fills the gap. *Q Rev Biophys;* 34(3):325-472.

Harris S.E. et al. (2005). Nutrient concentrations in murine reproductive fluid and the female reproductive tract. *Theriogenology*; 64(4):992-1006.

Harris S.E. et al. (2007). Carbohydrate metabolism by murine ovarian follicles and oocytes grown in vitro. *Reproduction*; 134(3):415-24.

He D.S. et al. (1999). Formation of heteromeric gap junction channels by connexins 40 and 43 in vascular smooth muscle cells. *PNAS*; 96(11):6495-500.

Hebert S.C. (2004). Molecular physiology of cation-coupled of Cl- cotransport: the SLC12 family. *Eur J Physiol*; 447:580-593.

Heller D.T. & Shultz R.M (1980). Ribonucleoside metabolism by mouse oocytes: metabolic cooperativity between the fully grown oocyte and cumulus cells. *J Exp Zool*;214(3):355-64.

Heller D.T. et al. (1981). Biochemical studies of mammalian oogenesis: metabolic cooperativity between granulosa cells and growing mouse oocytes. *Dev Biol*; 84(2):455-64.

Hinckley M. et al. (2005). The G-protein-coupled receptors GPR3 and GPR12 are involved in cAMP signaling and maintenance of meiotic arrest in rodent oocytes. *Dev Biol*; 287:249-261.

Hirshfield A.N. (1989). Rescue of atretic follicles in vitro and in vivo. *Biol Reprod*; 40(1):181-90.

Hirshfield A.N. (1991). Development of follicles in the mammalian ovary. *Int Rev Cytol*; 124:43-101.

Hoffmann E.K.& Dunham P.B. (1995). Membrane mechanisms and intracellular signalling in cell volume regulation. *Int Rev Cytol*; 161:173-262.

Hoffmann E.K. (2001). The pump and leak steady-state concept with a variety of regulated leak pathways. *J Membr Biol*; 184(3):321-30.

Hoffmann E.K. et al. (2009). Physiology of cell volume regulation in vertebrates. *Physiol Rev*; 89(1):193-277.

Hofmann F. et al. (2009). cGMP regulated protein kinases (cGK). *Handb Exp Pharmacol*; (191):137-62.

Hogan B., Beddington R., Costantini F., & Lacy E. (1994). Manipulating the Mouse Embryo: A Laboratory Manual; United States of America: Cold Spring Harbor Laboratory Press.

Hoodbhoy T. et al. (2006). ZP2 and ZP3 traffic independently within oocytes prior to assembly into the extracellular zonapellucida. *Mol Cell Biol*; 26(21):7991-8.

Horner K. et al. (2003). Rodent oocytes express an active adenylyl cyclase required for meiotic arrest. *Dev Biol*; 258:385-396.

Houghton F.D. (2012). Media composition: amino acids and cellular homeostasis. *Embryo Culture*; 912:97-106.

Howard A.&Hirst B.H. (2011). The glycine transporter GLYT1 in human intestine: expression and function. *Biol Pharm Bull*; 34(6):784-8.

Huang E.J. et al. (1993). The murine steel panda mutation affects kit ligand expression and growth of early ovarian follicles. *Dev Biol*; 157(1):100-9.

Hughes C.S. et al. (2010). Matrigel: a complex protein mixture required for optimal growth of cell culture.*Proteomics*; 10(9):1886-90.

Hunzicker-Dunn M. & Maizels E.T. (2006). FSH signalling pathways in immature granulosa cells that regulate target gene expression: branching out from protein kinase A. *Cell Signal*; 18(9):1351-9.

Inoue A. et al. (2007). The perivitelline space-forming capacity of mouse oocytes is associated with meiotic competence. *J Reprod Dev*; 53(5):1043-52.

Irving-Rodgers H.F. et al. (2004). A novel basal lamina matrix of the stratified epithelium of the ovarian follicle. *Matrix Biol*; 23(4):207-17.

Irving-Rodgers H.F. & Rodgers R.J. (2005). Extracellular matrix in ovarian follicular development and disease. *Cell Tissue Res*; 322(1):89-98.

Irving-Rodgers H.F. et al. (2010). Dynamics of extracellular matrix in ovarian follicles and corpora lutea of mice. *Cell Tissue Res*; 339(3):613-24.

Jaffe L.A. & Egbert J.R. (2016). Regulation of mammalian oocyte meiosis by intercellular communication within the ovarian follicle. *Annu Rev Physiol;* 79:237-260.

Jagarlamudi K. et al. (2009). Oocyte-specific deletion of Pten in mice reveals a stage-specific function of PTEN/PI3K signaling in oocytes in controlling follicular activation. *PLoS One*; 4(7):e6186.

Jamshidi M.B.& Kaye P.L. (1995). Glutamine transport by mouse inner cell masses. *J Reprod Fertil*; 104(1):91-7.

Jentsch T.J. (2016). VRACs and other ion channels and transporters in the regulation of cell volume and beyond. Nat Rev Mol Cell Biol 2016; 17(5):293-307.

Jiang L. et al. (1997). Secondary regulatory volume increase conferred on Xenopus oocytes by expression of AE2 anion exchanger. *Am J Physiol*; 272(1 Pt 1):C191-202.

Jiminez-Movilla M. & Dean J. (2011). ZP2 and ZP3 cytoplasmic tails prevent premature interactions and ensure incorporation into the zona pellucida. *J Cell Sci*; 124(Pt 6):940-50.

Johnson M.H.& Ziomek C.A. (1981). The foundation of two distinct cell lineages within the mouse morula. *Cell*; 24(1):71-80.

Johnson J.W.& Asher P. (1987). Glycine potentiates the NMDA response in cultured mouse brain neurons. *Nature*; 325(6104):529-31.

Johnson Z.I. et al. (2014). Extracellular osmolarity regulates matrix homeostasis in the intervertebral disc and articular cartilage: evolving role of TonEBP. *Matrix Biol*; 40:10-6.

Jovine L. et al. (2002). The ZP domain is a conserved module for polymerization of extracellular proteins. *Nat Cell Biol*; 4(6):457-61.

Jovine L. et al. (2004). A duplicated motif controls assembly of zona pellucida domain proteins. *PNAS*; 101(16):5922-7.

Jovine L. et al. (2005). Zona pellucida domain proteins. *Annu Rev Biochem*; 74:83-114.

Jursky F.& Nelson N. (1996). Developmental expression of the glycine transporters GLYT1 and GLYT2 in mouse brain. *J Neurochem*; 67(1):336-44.

Juszczak G.R. & Swiergiel A.H. (2009). Properties of gap junction blockers and their behavioural, cognitive and electrophysiological effects: animal and human studies. *Prog Neuropsychopharmacol Biol Psychiatry*; 33:181–198.

Kahle K.T. et al. (2010). Phosphoregulation of the Na-K-2Cl and K-Cl cotransporters by the WNK kinases. *Biochim Biophys Acta*; 1802(12):1150-8.

Kanatsu-Shinohara M. et al. (2000). Acquisition of meiotic competence in mouse oocytes: absolute amounts of p34(cdc2), cyclin B1, cdc25C, and wee1 in meiotically incompetent and competent oocytes. *Biol Reprod*; 63(6):1610-6.

Kaplan J.H. (2002). Biochemistry of Na,K-ATPase. *Annu Rev Biochem*; 71:511-35.

Kawamura K. et al. (2011). Pre-ovulatory LH/hCG surge decreases C-type natriuretic peptide secretion by ovarian granulosa cells to promote meiotic resumption of pre-ovulatory oocytes. *Hum Reprod*; 26(11):3094-101.

Ke F.C. et al. (2005). Lindane, a gap junction blocker, suppresses FSH and transforming growth factor fbetag1-induced connexin43 gap junction formation and steroidogenesis in rat granulosa cells. *J Endocrinol*; 184:555–566.

Kidder G.M & Mhawi A.A. (2002). Gap junctions and ovarian folliculogenesis. *Reproduction*; 123:613–620.

Kidder G.M (2005). Roles of gap junctions in ovarian folliculogenesis: implications for female infertility. *In: Winterhager E (ed.), Gap Junctions in Development and Disease. Berlin: Springer-Verlag*; 223–237.

Kidder G.M.& Vanderhyden B.C. (2010). Bidirectional communication between oocytes and follicle cells: ensuring oocyte developmental competence. *Can J Physio Pharmacol*; 88(4):399-413.

Kim K.M. et al. (1994). Cloning of the human glycine transporter type 1: molecular and pharmacological characterization of novel isoform variants and chromosomal localization of the gene in the human and mouse genomes. *Mol Pharmacol*; 45(4):608-17.

King L.S.& Agre P. (1996). Pathophysiology of the aquaporin water channels. *Annu Rev Physiol*; 58:619-48.

Kishi J. et al. (1991). Block to development in cultured rat 1-cell embryos is overcome using medium HECM-1. *Hum Reprod*; 6(10):1445-8.

Kleinman H.K. et al. (1986). Basement membrane complexes with biological activity. *Biochemistry*; 25(2):312-8.

Kleinman H.K. & Martin G.R. (2005). Matrigel: basement membrane matrix with biological activity. *Semin Cancer Biol*; 15(5):378-86.

Krebs H.A.& Henseleit K. (1932). Untersuchen über die Harnstoffbildung im Tierkörper. *Z Phys Chem*; 210:33-66.

Kreeger P.K. et al. (2005). Regulation of mouse follicle development by follicle-stimulating hormone in a three-dimensional in vitro culture system is dependent on follicle stage and dose. *Biol Reprod*; 73(5):942-50.

Kwon H.M.& Handler J.S. (1995). Cell volume regulated transporters of compatible osmolytes. *Curr Opin Cell Biol*; 7(4):465-71.

Lam X. et al. (2000). Assay and importance of adhesive interaction between hamster (Mesocricetus auratus) oocyte-cumulus complexes and the oviductal epithelium. *Biol Reprod*; 62(3):579-88.

Lambert I.H. et al. (2008). Cell volume regulation: physiology and pathophysiology. *Acta Physiol (Oxf);* 194(4):255-82.

Lampe P.D. et al. (2000). Phosphorylation of connexin43 on serine368 by protein kinase C regulates gap junctional communication. *J cell Biol*; 149(7):1503-12.

Lane M. & Gardner D.K. (1994). Increase in postimplantation development of cultured mouse embryos by amino acids and induction of fetal retardation and exencephaly by ammonium ions. *J Reprod Fertil*; 102(2):305-12.

Lane M. & Gardner D.K. (1997). Differential regulation of mouse embryo development and viability by amino acids. *J Reprod Fertil*; 109(1):153-64.

Lang F. et al. (1998). Functional significance of cell volume regulatory mechanisms. *Physiol Rev*; 78(1):247-306.

Lang F. (2007). Mechanisms and significance of cell volume regulation. *J Am Coll Nutr*; 26(5 Suppl):613S-623S.

Lawitts J.A.& Biggers J.D. (1992). Joint effects of sodium chloride, glutamine, and glucose in mouse preimplantation embryo culture media. *Mol Reprod Dev*; 31(3):189-94.

Lawitts J.A. & Biggers J.D. (1993). Culture of preimplantation embryos. *Methods Enzymol*; 225:153-64.

Le Bellego F. et al. (2002). Laminin-alpha6beta1 integrin interaction enhances survival and proliferation and modulates steroidogenesis of ovine granulosa cells. *J Endocrinol*; 172(1):45-59.

Le Bellego F. et al. (2005). Cytoskeleton reorganization mediates alpha6beta1 integrin-associated actions of laminin on proliferation and survival, but not on steroidogenesis of ovine granulosa cells. *Reprod Biol Endocrinol*; 16;3:19.

Lechner S.M. (2006). Glutamate-based therapeutic approaches: inhibitors of glycine transport. *Curr Opin Pharmacol*; 6(1):75-81.

Ledent C. et al. (2005). Premature ovarian aging in mice deficient for Gpr3. *PNAS*; 102:8922-8926.

Lee S.D. et al. (2011). TonEBP stimulates multiple cellular pathways for adaptation to hypertonic stress: organic osmolyte-dependent and -independent pathways. *Am J Physiol Renal Physiol*; 300(3):F707-15.

Lee K.B. et al. (2013). Hormonal coordination of natriuretic peptide type C and natriuretic peptide receptor 3 expression in mouse granulosa cells. *Biol Reprod*; 88(2):42.

Lee G.T. et al. (2014). Increased trophoblast expression of NFAT5/TonEBP in pre-eclamptic placentas and hyperosmolar-treated BeWo cells. *Eur J Obstet Gynecol Reprod Biol*; 183:37-43.

Lewis W.H.& Hartmann C.G. (1933). Early cleavage stages of the egg of the monkey (Macacus rhesus). *Contrib Embyrol (Carnegie Inst Wash)*; 24:187-201.

Lewis A.M. & Kaye P.L. (1992). Characterization of glutamine uptake in mouse two-cell embryos and blastocysts. *J Reprod Fertil*; 95(1):221-9.

Lezama R. et al. (2005). Epidermal growth factor receptor is a common element in the signaling pathways activated by cell volume changes in isosmotic, hyposmotic, or hyperosmotic conditions. *Neurochem Res*; 30(12):1589-97.

Li R. & Mathur J.P. (1997). Lindane, an inhibitor of gap junction formation, abolishes oocyte directed follicle organizing activity in vitro. *Endocrinology*; 138:4477–4480.

Li T.Y. et al. (2007). Rescue of oogenesis in Cx37-null mutant mice by oocyte-specific replacement with Cx43.*J Cell Sci*; 120:4117–4125.

Liang L.F. et al. (1990). Oocyte-specific expression of mouse Zp-2: developmental regulation of the zonapellucida genes. *Mol Cell Biol*; 10(4):1507-15.

Lincoln A.J. et al. (2002). Cdc25b phosphatase is required for resumption of meiosis during oocyte maturation. *Nat Genet*; 30(4):446-9.

Lira S.A. et al. (1990). An upstream region of the mouse ZP3 gene directs expression of firefly luciferase specifically to growing oocytes in transgenic mice. *PNAS*; 87(18):7215-9.

Liu Q.R. et al. (1992). Cloning and expression of a glycine transporter from mouse brain. *FEBS Lett*; 305(2):110-4.

Liu Q.R. et al. (1993). Cloning and expression of a spinal cord- and brain-specific glycine transporter with novel structural features. *J Biol Chem*; 268(30):22802-8.

Liu Z. et al. (1995). Development of early bovine embryos in co-culture with KSOM and taurine, superoxide dismutase insulin. *Theriogenology*;44(5):741-50.

Liu C. et al. (1996). Targeted disruption of the mZP3 gene results in production of eggs lacking a zonapellucida and infertility in female mice. *PNAS*; 93(11):5431-6.

Liu X. et al. (2014). Multiple pathways mediate luteinizing hormone regulation of cGMP signaling in the mouse ovarian follicle. *Biol Reprod*; 91(1):9.

Llorca O. et al. (2007). Structural model of human endoglin, a transmembrane receptor responsible for hereditary hemorrhagic telangiectasia. *J Mol Biol*; 365(3):694-705.

Luciano A.M. (2012). Large-scale chromatin morpho-functional changes during mammalian oocyte growth and differentiation. *Eur J Histochem*; 56(3):e37.

Maeno E. et al. (2000). Normotonic cell shrinkage because of disordered volume regulation is a prerequisite to apoptosis. *PNAS*; 97(17):9487-92.

Magnusson M. et al. (1982). Comparison between the progestin secretion responsiveness to gonadotrophins of rat cumulus and mural granulosa cells in vitro. *Cta Endocrinol*; 101(4):611-6.

Makowski L. et al. (1977). Gap junction structures. II. Analysis of the x-ray diffraction data. *J Cell Biol*; 74(2):629-45.

Mamo S. et al. (2007). Quantitative evaluation and selection of reference genes in mouse oocytes and embryos cultured in vivo and in vitro.*BMC Dev Biol;* 7:14.

Maouyo D. et al. (2001). Mouse TonEBP-NFAT5: expression in early development and alternative splicing. *Am J Physiol Renal Physiol*; 282(5):F802-9.

Markadieu N.& Delpire E. (2014). Physiology and pathophysiology of SLC12A1/2 transporters. *Pflugers Arch*; 466(1):91-105.

Martinez-Maza R. et al. (2001). The role of N-glycosylation in transport to the plasma membrane and sorting of the neuronal glycine transporter GLYT2. *J Biol Chem*; 276(3):2168-73.

Masciarelli S. et al. (2004). Cyclic nucleotide phosphodiesterase 3A-deficient mice as a model of female infertility. *J Clin Invest*; 114(2):196-205.

McClatchie T. et al. (2017). Betaine is accumulated via transient choline dehydrogenase activation during mouse oocyte meiotic maturation. *J Biol Chem*; 292(33):13784-13794.

McLaren A.& Biggers J.D. (1958). Successful development and birth of mice cultivated in vitro as early as early embryos. *Nature*; 182(4639):877-8.

Melhmann L.M et al. (2004). The Gs-linked receptor GPR3 maintains meiotic arrest in mammalian oocytes. *Science*; 306:1947-1950.

Mehlmann L.M. (2005). Stops and starts in mammalian oocytes: recent advances in understanding the regulation of meiotic arrest and oocyte maturation. *J Reprod Fertil*; 130:791–799.

Mezler M. et al. (2008). Inhibitors of GlyT1 affect glycine transport via discrete binding sites. *Mol Pharmacol*; 74(6):1705-15.

Mihalikova A. et al. (2014). Calcium dependent interaction of calmodulin with the GlyT1 C-terminus. *Neurochem Res*; 39(11):2225-33.

Mikkelsen A.L. & Lindenberg S. (2001). Benefit of FSH priming of women with PCOS to the in vitro maturation procedure and the outcome: a randomized prospective study. *Reproduction*; 122(4):587-92.

Millan M.J. (2005). N-Methyl-D-aspartate receptors as a target for improved antipsychotic agents: novel insights and clinical perspectives. *Psychopharmacology*; 179(1):30-53.

Mittal S. et al. (2015). Macromolecular crowding: macromolecules friend or foe. *Biochim Biophys Acta*; 1850(9):1822-31.

Miyakawa H. et al. (1999). Tonicity-responsive enhancer binding protein, a rel-like protein that stimulates transcription in response to hypertonicity. *PNAS*; 96(5):2538-42.

Mohler H. et al. (2011). Glycine transporter 1 as a potential therapeutic target for schizophrenia-related symptoms: evidence from genetically modified mouse models and pharmacological inhibition. *Biochem Pharmacol*; 81:1065-1077.

Molecular Probes Inc. (2009). Wheat germ agglutinin conjugates. *Invitrogen User Manual*; MP 00831. https://tools.thermofisher.com/content/sfs/manuals/mp00831.pdf.

Moore-Hoon M.L.& Turner R.J. (2000). The structural unit of the secretory Na+-K+-2Cl- cotransporter (NKCC1) is a homodimer. *Biochemistry*; 39(13):3718-24.

Morita Y. et al. (1999). Requirement for phosphatidylinositol-30-kinase in cytokine-mediated germ cell survival during fetal oogenesis in the mouse. *Endocrinology*; 140(2):941-9.

Mueller P.R. et al. (1995a). Myt1: a membrane-associated inhibitory kinase that phosphorylates Cdc2 on both threonine-14 and tyrosine-15. *Science*; 270(5233):86-90.

Mueller P.R. et al. (1995b) Cell cycle regulation of a Xenopus Wee1-like kinase. *Mol Biol Cell*; 6(1):119-34.

Nelson N. (1998). The family of Na^+/Cl^- neurotransmitter transporters. *J Neurochem*; 71(5):1785-803.

Nielsen M.B. et al. (2008). Effects of osmotic stress on the activity of MAPKs and PDGFR-beta-mediated signal transduction in NIH-3T3 fibroblasts. *Am J Physiol Cell Physiol*; 294(4):C1046-55.

Nilius B. et al. (1994). Volume activated Cl- currents in different mammalian non-excitable cell types. *Pflugers Arch*; 428(3-4):364-71.

Norris R.P. et al. (2008). Luteinizing hormone causes MAPK-dependent phosphorylation and closure of Cx43 gap junctions in mouse ovarian follicles: one of two paths to meiotic resumption. *Development*; 135:3229–38.

Norris R.P. et al. (2009). Cyclic GMP from the surrounding somatic cells regulates cyclic AMP and meiosis in the mouse oocyte. *Development*; 136(11):1869-78.

Norris R.P, Freudzon M., Nikolaev V.O., &Jaffe L.A. (2010). Epidermal growth factor receptor kinase activity is required for gap junction closure and for part of the decrease in ovarian follicle cGMP in response to LH. *J Reprod Fertil*; 140:655–662.

Okada Y. (1997). Volume expansion-sensing outward-rectifier Cl- channel: fresh start to the molecular identity and volume sensor. *Am J Physiol*; 273(3 Pt 1):C755-89.

Okada Y. et al. (2001). Receptor-mediated control of regulatory volume decrease (RVD) and apoptotic volume decrease (AVD). *J Physiol*; 532(Pt 1):3-16.

Okada Y. (2004). Ion channels and transporters involved in cell volume regulation and sensor mechanisms. *Cell Biochem Biophys*; 41(2):233-58.

Oktay K. et al. (2000). Interaction of extracellular matrix and activin-A in the initiation of follicle growth in the mouse ovary. *Biol Reprod*; 63(2):457-61.

Olivares L. et al. (1994). Carboxyl terminus of the glycine transporter GLYT1 is necessary for correct processing of the protein. *J Biol Chem*; 269(45):28400-4.

Olivares L. et al. (1995). The role of N-glycosylation in the targeting and activity of the GLYT1 glycine transporter. *J Biol Chem;* 270(16):9437-42.

Olivares L. et al. (1997). Analysis of the transmembrane topology of the glycine transporter GLYT1. *J Biol Chem*; 272(2):1211-7.

Orlowski J.& Grinstein S. (2004). Diversity of the mammalian sodium/proton exchanger SLC9 gene family. *Pflugers Arch*; 447(5):549-65.

Packer A.I. et al. (1994). The ligand of the c-kit receptor promotes oocyte growth. *Dev Biol*; 161(1):194-205.

Panigone S. et al. (2008). Luteinizing hormone signaling in preovulatory follicles involves early activation of the epidermal growth factor receptor pathway. *Mol Endocrinol*; 22(4):924-36.

Park J.Y. (2004). EGF-like growth factors as mediators of LH action in the ovulatory follicle. *Science*; 303:682-684.

Pasantes-Morales H. et al. (2006). Tyrosine kinases and osmolyte fluxes during hyosmotic swelling. *Acta Physio (Oxf);* 187(1-2):93-102.

Pedersen S.F. et al. (2006). Physiology and pathophysiology of Na+/H+ exchange and Na+-K+-2Cl- cotransport in the heart, brain, and blood. *Am J Physiol Regul Integr Comp Physiol*; 291(1):R1-25.

Pederson S.F. et al. (2011). Osmosensory mechanisms in cellular and systemic volume regulation. *J Am Soc Nephrol*; 22(9):1587-97.

Pelland A.M. et al. (2009). Amino acid transport mechanisms in mouse oocytes during growth and meiotic maturation. *Biol Reprod*; 81(6):1041-54.

Peng X.R. et al. (1991). Localization of luteinizing hormone receptor messenger ribonucleic acid expression in ovarian cell types during follicle development and ovulation. *Endocrinology*; 129(6):3200-7.

Pepin D. et al. (2013). The imitation switch ATPase Snf2l is required for superovulation and regulates Fgl2 in differentiating mouse granulosa cells. *Biol Reprod*; 88(6):142.

Perez-Armendariz E.M. et al. (2003). Connexin43 is expressed in mouse fetal ovary. *Anat Rec A Discov Mol Cell Evol Biol*; 271(2):360-7.

Persani L. et al. (2014). The fundamental role of bone morphogenetic protein 15 in ovarian function and its involvement in female fertilitydisorders. *Hum Reprod Update*; 20(6):869-83.

Piechotta K. et al. (2002). Cation chloride cotransporters interact with the stress-related kinases Ste20-related proline-alanine-rich kinase (SPAK) and oxidative stress response 1 (OSR1). *J Biol Chem*; 277(52):50812-9.

Pincus G.& Enzmann E.V. (1935). The comparative behavior of mammalian eggs in vivo and in vitro: I. the activation of ovarian eggs. *J Exp Med*; 62(5):665-75.

Planells-Cases R. et al. (2015). Subunit composition of VRAC channels determines substrate specificity and cellular resistance to Pt-based anti-cancer drugs. *EMBO J*; 34(24):2993-3008.

Poyatos I. et al. (1997). The glycine transporter GLYT2 is a reliable marker for glycine-immunoreactive neurons. *Brain Res Mol Brain Res*; 49(1-2):63-70.

Qi H. et al. (2002). Secretion and assembly of zonapellucida glycoproteins by growing mouse oocytes microinjected with epitope-tagged cDNAs for mZP2 and mZP3.*Mol Biol Cell*; 13(2):530-41.

Qiu Z. et al. (2014). SWELL1, a plasma membrane protein, is an essential component of volume-regulated anion channel. *Cell*; 157(2):447-58.

Rankin T.L. et al. (1996). Mice homozygous for an insertional mutation in the Zp3 gene lack a zonapellucida and are infertile. *Development*; 122(9):2903-10.

Rankin T.L. et al. (1999). Abnormal zonaepellucidae in mice lacking ZP1 result in early embryonic loss. *Development*; 126(17):3847-55.

Rankin T.L. et al. (2001). Defective zonaepellucidae in Zp2-null mice disrupt folliculogenesis, fertility and development. *Development*; 128(7):1119-26.

Reaume A.G. et al. (1995). Cardiac malformation in neonatal mice lacking connexin43. *Science*; 267(5205):1831-4.

Reddy P. et al. (2008). Oocyte-specific deletion of Pten causes premature activation of the primordial follicle pool. *Science*; 319(5863):611-3.

Reinehr R. et al. (2004). The Src family kinase Yes triggers hyperosmotic activation of the epidermal growth factor receptor and CD95. *J Biol Chem*; 279(23):23977-87.

Richard S.& Baltz J.M. (2014). Prophase I arrest of mouse oocytes mediated by natriuretic peptide precursor C requires GJA1 (connexin-43) and GJA4 (connexin-37) gap junctions in the antral follicle and cumulus-oocyte complex. *Biol Reprod*; 90(6):137.

Richard S. et al. (2016). Mouse oocytes acquire mechanisms that permit independent cell volume regulation at the end of oogenesis. *J Cell Physiol*; 232(9): 2436-2446.

Richards J.S. (1980). Maturation of ovarian follicles: actions and interactions of pituitary and ovarian hormones on follicular cell differentiation. *Physiol Rev*; 60(1):51-89.

Richards J.S. et al. (2002). Novel signalling pathways that control ovarian follicular development, ovulation, and luteinization. *Recent Prog Horm Res*; 57:195-220.

Robinson J.W. et al. (2012). Luteinizing hormone reduces the activity of the NPR2 guanylyl cyclase in mouse ovarian follicles, contributing to the cyclic GMP decrease that promotes resumption of meiosis in oocytes. *Dev Biol*; 366(2):308-16.

Rodgers R.J. & Irving-Rodgers H.F. (2010). Formation of the ovarian follicular antrum and follicular fluid. *Biol Reprod*; 82(6):1021-9.

Rolaki A. et al. (2007). Luteogenic hormones act through a vascular endothelial growth factor-dependent mechanism to up-regulate alpha 5 beta 1 and alpha v beta 3 integrins, promoting the migration and survival of human luteinized granulosa cells. *Am J Pathol*; 170(5):1561-72.

Roller R.J.&Wassarman P.M. (1983). Role of asparagine-linked oligosaccharides in secretion of glycoproteins of the mouse egg's extracellular coat. *J Biol Chem*; 258(21):13243-9.

Rose-Hellekant T.A. et al. (1998). Energy substrates and amino acids provided during in vitro maturation of bovine oocytes alter acquisition of developmental competence. *Zygote*; 6(4):285-94.

Roux M.J. & Supplisson S. (2000). Neuronal and glial glycine transporters have different stoichiometries. *Neuron*; 25(2):373-83.

Roux M.J. et al. (2001). The glial and the neuronal glycine transporters differ in their reactivity to sulfhydryl reagents. *J Biol Chem*; 276(21):17699-705.

Rudnick G. (1998). Bioenergetics of neurotransmitter transport. *J Bioenerg Biomembr*; 30(2):173-85.

Russell D.L. et al. (2003). Processing and localization of ADAMTS-1 and proteolytic cleavage of versican during cumulus matrix expansion and ovulation. *J Biol Chem*; 278(43):42330-9.

Russell D.L.& Robker R.L. (2007). Molecular mechanisms of ovulation: co-ordination through the cumulus complex. *Hum Reprod Update*; 13(3):289-312.

Saito T. et al. (1994). Development of glucose utilization studied in single oocytes and preimplantation embryos from mice. *Biol Reprod*; 50(2):266-70.

Salustri A. et al. (1990). Mouse oocytes regulate hyaluronic acid synthesis and mucification by FSH-stimulated cumulus cells. *Dev Biol*; 138(1):26-32.

Salustri A. et al. (1992). Localization and synthesis of hyaluronic acid in the cumulus cells and mural granulosa cells of the preovulatory follicle. *Dev Biol*; 151(2):541-51.

Sato K. et al. (1995). Modulation of a recombinant glycine transporter (GLYT1b) by activation of protein kinase C.*J Neurochem*; 65(5):1967-73.

Schini S.A. & Bavister B.D. (1988). Two-cell block to development of cultured hamster embryos is caused by phosphate and glucose. *Biol Reprod*; 39(5):1183-92.

Sela-Abramovich S. et al. (2006). Disruption of gap junctional communication within the ovarian follicle induces oocyte maturation.*Endocrinology*; 147:2280–2286.

Shmorgun D. & Claman P. (2011). The diagnosis and management of ovarian hyperstimulation syndrome. *J Obstet Gynaecol Can*; 33(11):1156-62.

Shimizu S. et al. (1983). In vitro biosynthesis of three sulfated glycoproteins of murine zonaepellucidae by oocytes grown in follicle culture. *J BiolChem*; 258(9):5858-63.

Shin J.A. et al. (2012). TonEBP and SMIT expression in human placenta. *Anat Cell Biol*; 45(3):155-9.

Shuhaibar L.C. et al. (2015). Intercellular signaling via cyclic GMP diffusion through gap junctions restarts meiosis in mouse ovarian follicles. *PNAS*; 112:5527-5532.

Shuhaibar L.C. et al. (2016). Dephosphorylation of juxtamembrane serines and threonines of the NPR2 guanylyl cyclase is required for rapid resumption of oocyte meiosis in response to luteinizing hormone. *Dev Biol*; 409(1):194-201.

Simon A.M. et al. (1997). Female infertility in mice lacking connexin 37. *Nature*; 385(6616):525-9.

Simon A.M. et al. (2006). Cx37 and Cx43 localize to zona pellucida in mouse ovarian follicles. *Cell Commun Adhes*; 13: 61–77.

Singer P. (2007). Enhanced recognition memory following glycine transporter 1 deletion in forebrain neurons. *Behav Neurosci*; 121(5):815-25.

Sirard M.A et al. (2007). In vivo and in vitro effects of FSH on oocyte maturation and developmental competence. *Theriogenology*; 68 Suppl 1:S71-6.

Sites C.K. et al. (1996). Adhesion proteins increase cellular attachment, follicle-stimulating hormone receptors, and progesterone production in cultured porcine granulosa cells. *Proc Soc Exp Biol Med*; 212(1):78-83.

Siu M.K. & Cheng C.Y. (2012). The blood-follicle barrier (BFB) in disease and in ovarian function. *Adv Exp Med Biol*; 763:186-92.

Siyanov V.&Baltz J.M. (2013). NHE1 is the sodium-hydrogen exchanger active in acute intracellular pH regulation in preimplantation mouse embryos. *Biol Reprod*; 88(6):157.

Smith K.E. et al. (1992). Cloning and expression of a glycine transporter reveal colocalization with NMDA receptors. *Neuron*; 8(5):927-35.

Solc P. et al. (2008). CDC25A phosphatase controls meiosis I progression in mouse oocytes. *Dev Biol*; 317(1):260-9.

Solc P. et al. (2010). Prophase I arrest and progression to metaphase I in mouse oocytes: comparison of resumption of meiosis and recovery from G2-arrest in somatic cells. *Mol Hum Reprod*; 16(9):654-64.

Sorensen R.A.& Wassarman P.M. (1976). Relationship between growth and meiotic maturation of the mouse oocyte. *Dev Biol*; 50:531-536.

Spears N. et al. (1996). The establishment of follicular dominance in co-cultured mouse ovarian follicles. *J Reprod Fertil*; 106(1):1-6.

Spike R.C. et al. (1997). An ultrastructural study of the glycine transporter GLYT2 and its association with glycine in the superficial laminae of the rat spinal dorsal horn. *Neurosci*; 77(2):543-51.

Steeves T.E.& Gardner D.K. (1999). Metabolism of glucose, pyruvate, and glutamine during the maturation of oocytes derived from pre-pubertal and adult cows. *Mol Reprod Dev*; 54(1):92-101.

Steeves C.L. et al. (2003). The glycine neurotransmitter transporter GLYT1 is an organic osmolyte transporter regulating cell volume in cleavage-stage embryos. *PNAS*; 100(24):13982-7.

Steeves C.L.&Baltz J.M. (2005). Regulation of intracellular glycine as an organic osmolyte in early preimplantation mouse embryos. *J Cell Physiol*; 204(1):273-9.

Stetson I. et al. (2012). Rabbit zonapellucida composition: a molecular, proteomic and phylogenetic approach. *J Proteomics*; 75(18):5920-35.

Strange K. et al. (1996). Cellular and molecular physiology of volume-sensitive anion channels. *Am J Physiol*; 270(3 Pt 1):C711-30.

Sugiura K. et al. (2005). Oocyte control of metabolic cooperativity between oocytes and companion granulosa cells: energy metabolism. *Dev Biol*; 279(1):20-30.

Sung U. et al. (2003). A regulated interaction of syntaxin 1A with the antidepressant-sensitive norepinephrine transporter establishes catecholamine clearance capacity. *J Neurosci*; 23(5):1697-709.

Supplisson S.& Bergman C. (1997). Control of NMDA receptor activation by a glycine transporter co-expressed in Xenopus oocytes. *J Neurosci*; 17(12):4580-90.

Sutton-McDowall M.L. et al. (2010). The pivotal role of glucose metabolism in determining oocyte developmental competence. *Reproduction*; 139(4):685-95.

Syeda R. et al. (2016). LRRC8 proteins form volume-regulated anion channels that sense ionic strength. *Cell*; 164(3):499-511.

Szybek K. (1972). In-vitro maturation of oocytes from sexually immature mice. *J Endocrinol*; 54(3):527-8.

Talbot P.&Dandekar P. (2003). Perivitelline space: does it play a role in blocking polyspermy in mammals? *Microsc Res Tech*; 61(4):349-57.

Tartia A.P. et al. (2009). Cell volume regulation is initiated in mouse oocytes after ovulation. *Development*; 136(13):2247-54.

Tartia A.P. (2009). Cell volume regulation is initiated in oocytes at ovulation (Doctoral dissertation). Retried from Proquest dissertations and theses (Publication number NR59508).

Teilmann S.C. (2005). Differential expression and localisation of connexin-37 and connexin-43 in follicles of different stages in the 4-week-old mouse ovary. *Mol Cell Endocrinol*; 234(1-2):27-35.

Thomas F.H. et al. (2005). Follicle-stimulating hormone regulates oocyte growth by modulation of expression of oocyte and granulosa cell factors. *Endocrinology*; 146(2):941-9.

Törnell J. et al. (1990). Resumption of rat oocyte meiosis is paralleled by a decrease in guanosine 3',5'-cyclic monophosphate (cGMP) and is inhibited by microinjection of cGMP.*Acta Physiol Scand*; 139(3):511-7.

Tosteson D.C.& Hoffmann J.F. (1960). Regulation of cell volume by active cation transport in high and low potassium sheep red cells. *J Gen Physiol*; 44:169-94.

Trama J. et al. (2000). The NFAT-related protein NFATL1 (TonEBP/NFAT5) is induced upon T cell activation in a calcineurin-dependent manner. *J Immunol*; 165(9):4884-94.

Trounson A. et al. (1994). In vitro maturation and the fertilization and developmental competence of oocytes recovered from untreated polycystic ovarian patients. *Fertil Steril*; 62(2):353-62.

Tsafrifi A. et al. (1996). Oocyte maturation involves compartmentalization and opposing changes of cAMP levels in follicular somatic and germ cells: studies using selective phosphodiesterase inhibitors. *Dev Biol*; 178(2):393-402.

Tsai T.T. et al. (2006). TonEBP/OREBPis a regulator of nucleus polposus cell function and survival in the intervertebral disc. *J Biol Chem*; 281(35):25416-24.

Unwin P.N.& Zampighi G. (1980). Structure of the junction between communicating cells. *Nature*; 283(5747):545-9.

Vaccari S. et al. (2008). Generation of mouse oocytes defective in cAMP synthesis and degradation: endogenous cyclic AMP is essential for meiotic arrest. *Dev Biol*; 316(1):124-34.

Vaccari S. et al. (2009). Cyclic GMP signaling is involved in the luteinizing hormone-dependent meiotic maturation of mouse oocytes. *Biol Reprod*; 81(3):595-604.

Van Winkle L.J. et al. (1985). Na+-dependent transport of basic, zwitterionic, and bicyclic amino acids by a broad-scope system in mouse blastocysts. *J Biol Chem*; 260(22):12118-23.

Van Winkle L.J. et al. (1988a). Glycine transport in mouse eggs and preimplantation conceptuses. *Biochim Biophys Acta*; 941(2):241-56.

Van Winkle L.J. et al. (1988b). Na+-independent transport of basic and zwitterionic amino acids in mouse blastocysts by a shared system and by processes which distinguish between these substrates. *J Biol Chem*; 263(7):3150-63.

Van Winkle L.J. et al. (1990a). Development of system $B^{0,+}$ and a broad-scope $Na(^{+})$-dependent transporter of zwitterionic amino acids in preimplantation mouse conceptuses. *Biochim Biophys Acta;* 1025(2):225-33.

Van Winkle L.J. et al. (1990b). Transport of benzenoid amino acids by system T and four broad scope systems in preimplantation mouse conceptuses. *Biochim Biophys Acta*; 1027(3):268-77.

Van Winkle L.J. et al. (1990c). Glycine protects preimplantation mouse conceptuses from a detrimental effect on development of the inorganic ions in oviductal fluid. *J Exp Zool*; 253(2):215-9.

Van Winkle L.J. et al. (1994). Osmotic regulation of taurine transport via system beta and novel processes in mouse preimplantation conceptuses. *Biochim Biophys Acta*; 1191(2):244-55.

Van Winkle L.J.& Dickinson H.R. (1995). Differences in amino acid content of preimplantation mouse embryos that develop in vitro versus in vivo: in vitro effects of five amino acids that are abundant in oviductal secretions. *Biol Reprod*; 52(1):96-104.

Van Winkle L.J. & Campione A.L. (1996). Amino acids transport regulation in preimplantation mouse embryos: effects on amino acid content and pre- and peri-implantation development. *Theriogenology*; 45:69-80.

Van Winkle L.J. (2001). Amino acid transport regulation and early embryo development. *Biol Reprod*; 64(1):1-12.

Vandenberg R.J. et al. (2007). Molecular basis for substrate discrimination by glycine transporters. *J Biol Chem*; 282(19):14447-53.

Vanderhyden B.C. et al. (1990). Developmental pattern of the secretion of cumulus expansion-enabling factor by mouse oocytes and the role ofoocytes in promoting granulosa cell differentiation. *Dev Biol*; 140(2):307-17.

Vanderhyden B.C. et al. (2003). Evaluation of members of the TGFbeta superfamily as candidates for the oocyte factors that control mousecumulus expansion and steroidogenesis. *Reprod Suppl*; 61:55-70.

Vargas-Medrano J. et al. (2011). PKCβ-dependent phosphorylation of the glycine transporter 1. *Neurochem Int*; 59(8):1123-32

Veitch G.I et al. (2004). Selective assembly of connexin37 into heterocellular gap junctions at the oocyte/granulosa cell interface. *Journal of Cell Science*; 117(13):2699-2707.

Verselis V.K., Ginter C.S., & Bargiello T.A. (1994). Opposite voltage gating polarities of two closely related connexins. *Nature*; 368(6469):348-51.

Voets T. et al. (1999). Reduced intracellular ionic strength as the initial trigger for activation of endothelial-volume regulated anion channels. *PNAS*; 96(9):5298-303.

Voss F.K. et al. (2014). Identification of LRRC8 heteromers as an essential component of the volume-regulated anion channel VRAC. *Science*; 344(6184):634-8.

Vukicevic S. et al. (1992). Identification of multiple active growth factors in basement membrane Matrigel suggests caution in interpretation of cellular activity related to extracellular matrix components. *Exp Cell Res*; 202(1):1-8.

Warfield P.R. et al. (1997). Adhesion of human breast carcinoma to extracellular matrix proteins is modulated by galectin-3. *Invasion Metastasis*; 17(2):101-12.

Wassarman P.M. et al. (1979). Meiotic maturation of mouse oocytes in vitro. *Adv Exp Med Biol*;112:251-68.

Wassarman P.M. (1988). Zona pellucida glycoproteins. *Annu Rev Biochem*; 57:415-42.

Wassarman P.M. & Mortillo S. (1991). Structure of the mouse egg extracellular coat, the zona pellucida. *Int Rev Cytol*; 130:85-110.

Wassarman P.M. (2008). Zona pellucida glycoproteins. *J Biol Chem*; 283(36):24285-9.

Wassarman P.M. & Litscher E.S. (2013). Biogenesis of the mouse egg's extracellular coat, the zona pellucida. *Curr Top Dev Biol*; 102:243-66.

Wehner F. et al. (2003). Cell volume regulation: osmolytes, osmolyte transport, and signal transduction. *Rev Physiol Biochem Pharmacol*; 148:1-80.

Whitten W.K. (1956). Culture of tubal mouse ova. *Nature*; 177(4498):96.

Whitten W.K. (1957). Culture of tubal ova. *Nature*; 179(4569):1081-2.

Whittingham D.G. & Biggers J.D. (1967). Fallopian tube and early cleavage in the mouse. *Nature*; 213(5079):942-3.

Whittingham D.G. (1971). Culture of mouse ova. *J Reprod Fertil Suppl*; 14:7-21.

Wigglesworth K. et al. (2013). Bidirectional communication between oocytes and ovarian follicular somatic cells is required for meiotic arrest of mammalian oocytes. *PNAS*; 110(39):E3723-9.

Williams Z.&Wassarman P.M. (2001). Secretion of mouse ZP3, the sperm receptor, requires cleavage of its polypeptide at a consensus furin cleavage-site. *Biochemistry*; 40(4):929-37.

Woo S.K. et al. (2002). TonEBP transcriptional activator in the cellular response to increased osmolality. *Pflugers Arch*; 444(5):579-85.

Wright C.S. et al. (2001). Stage-specific and differential expression of gap junctions in the mouse ovary: connexin-specific roles in follicular regulation. *Reproduction*; 121(1):77-88.

Yamashita A. et al. (2005). Crystal structure of a bacterial homologue of Na^+/Cl^--dependent neurotransmitter transporters. *Nature*; 437(7056):215-23.

Yancey P.H. et al. (1982). Living with water stress: evolution of osmolyte systems. *Science*; 217(4566):1214-22.

Yancey P.H. (2005). Organic osmolytes as compatible, metabolic and counteracting cytoprotectants in high osmolarity and other stresses. *J Exp Biol*; 208(Pt 15):2819-30.

Yao Y. et al. (2014). Astrocytic laminin regulates pericyte differentiation and maintains blood brain barrier integrity. *Nat Commun*; 5:3413.

Yeager M.& Gilula N.B. (1992). Membrane topology and quaternary structure of cardiac gap junction ion channels. *J Mol Biol*; 223(4):929-48.

Yee B.K. et al. (2006). Disruption of glycine transporter 1 restricted to forebrain neurons is associated with a procognitive and antipsychotic phenotypic profile. *J Neurosci*; 26(12):3169-81.

Yonezawa N. (2014). Posttranslational modifications of zonapellucida proteins. *Adv Exp Med Biol*; 759:111-40.

Young J.M.& McNeilly A.S. (2010). Theca: the forgotten cell of the ovarian follicle. *Reproduction*; 140(4):489-504.

Zafra F. et al. (1995a). Glycine transporters are differentially expressed among CNS cells. *J Neuorsci*; 15(5 Pt 2):3952-69.

Zafra F. et al. (1995b). Regional distribution and developmental variation of the glycine transporters GLYT1 and GLYT2 in the rat CNS.*Eur J Neurosci*; 7(6):1342-52.

Zafra F. et al. (1997). Neuronal dependency of the glycine transporter GLYT1 expression in glial cells. *Glia*; 20(2):155-62.

Zafra F.&Giménez C. (2008). Glycine transporters and synaptic function. *IUMBM Life*; 60(12):810-7.

Zhang Z. et al. (2003). Expression of osmotic stress-related genes in tissues of normal and hyposmotic rats. *Am J Physiol Renal Physiol*; 285(4):F688-93.

Zhang M. et al. (2010). Granulosa cell ligand NPPC and its receptor NPR2 maintain meiotic arrest in mouse oocytes. *Science*; 330(6002):366-9.

Zhang M. et al. (2011). Estradiol promotes and maintains cumulus cell expression of natriuretic peptide receptor 2 (NPR2) and meiotic arrest in mouse oocytes in vitro. *Endocrinology*; 152(11):4377-85.

Zhao M. et al. (2002). Conserved furin cleavage site not essential for secretion and integration of ZP3 into the extracellular egg coat of transgenic mice. *Mol Cell Biol*; 22(9):3111-20.

Zhao M. et al. (2003). Mutation of a conserved hydrophobic patch prevents incorporation of ZP3 into the zonapellucida surrounding mouse eggs. *Mol Cell Biol*; 23(24):8982-91.

Zhou C. et al. (2009). HCO_3^-/Cl^- exchange activation inactivation and reactivation during mouse oocyte meiosis correlates with MEK/MAPK-regulated Ae2 plasma membrane localization. *PLoS One;* 4(10):e7417.

Zhou C. & Baltz J.M. (2013). JAK2 mediates the acute response to decreased cell volume in mouse preimplantation embryos by activating NHE1. *J Cell Physiol*; 228(2):428-38.

Zhou C. et al. (2013). Na^+/H^+ exchange is inactivated during mouse oocyte meiosis, facilitating glycine accumulation that maintains embryo cell volume. *J Cell Physiol*; 228(10):2042-53.

Zimmer D.B. et al. (1987). Topological analysis of the major protein in isolated intact rat liver gap junctions and gap junction-derived single membrane structures. *J Biol Chem*; 262(16):7751-63.